A Legionella pneumophila type IV-secreted effector suppresses human Argonaute activities and promotes pathogenicity in macrophages

Justine Toinon

Thèse de doctorat de Sorbonne Université

École doctorale Complexité du vivant (ED515)

Présentée et soutenue publiquement le 30 septembre 2021
par Justine TOINON

A *Legionella pneumophila* type IV-secreted effector suppresses human Argonaute activities and promotes pathogenicity in macrophages

---

Sous la direction de Lionel NAVARRO

Préparée à l'Institut de Biologie de l'École Normale Supérieure
CNRS UMR8197 - Inserm U1024

Composition du jury :

Pr Patricia DOUBLET	CIRI, Lyon	Rapporteure et présidente du jury
Dr Sébastien PFEFFER	IBMC, Strasbourg	Rapporteur
Dr Carla SALEH	Institut Pasteur, Paris	Examinatrice
Dr Sarah GALLOIS MONTBRUN	Institut Cochin, Paris	Examinatrice
Dr Clément CARRE	IBPS, Paris	Examinateur
Dr Lionel NAVARRO	IBENS, Paris	Directeur de thèse
Dr Antoine ALAM	Evotec, Lyon	Membre invité

REMERCIEMENTS

La rédaction de mon manuscrit de thèse fut un challenge auquel je ne m'attendais pas. Après de longs jours d'écriture, j'ai retardé jusqu'au dernier moment celle des remerciements. Maintenant je me rends compte que cette aventure incroyable prend fin. J'espère que mes remerciements seront à la hauteur de la gratitude que je ressens pour toutes les personnes qui ont, de près ou de loin, permis à ce travail de voir le jour.

Avant tout, j'aimerai remercier très chaleureusement l'ensemble de mon jury d'avoir accepté d'évaluer mon travail. Merci au Pr Patricia Doublet et Dr Sébastien Pfeffer de me faire l'honneur d'être rapporteurs de ma thèse. Dr Carla Saleh, Dr Sarah Gallois Montbrun et Dr Clément Carré, je vous remercie pour votre contribution et votre implication en qualité d'examinateurs. Je remercie également Dr Alice Lebreton et Dr Carmen Buchrieser, qui ont accepté de faire partie de mon comité de thèse et qui m'ont prodigué de précieux conseils pendant ces quatre années. Je voudrais également remercier l'Association Nationale de la Recherche et de la Technologie (ANRT) ainsi que la Fondation pour la Recherche Médicale (FRM), dont les financements ont rendu ce travail possible.

Je tiens à remercier tout particulièrement Dr Lionel Navarro, qui m'a encadré tout au long de cette thèse. Merci, Lionel, de m'avoir confié ce projet et accompagné dans sa réalisation. Tes conseils, ta rigueur et tes encouragements m'ont permis d'arriver au bout de cette aventure inoubliable. Merci de la confiance que tu m'as accordée, d'avoir écouté toutes mes idées et de m'avoir laissé une liberté dans la conduite de ce projet.

Je souhaite remercier Antoine Alam et Michael Mourez pour cette belle opportunité via cette collaboration. Merci pour votre participation scientifique et votre enthousiasme pour ce projet.

Ma gratitude s'adresse également à Stéphane Renard et Nadège Moreno, sans qui, je n'aurai jamais franchi le pas d'aller jusqu'au doctorat. Je vous remercie d'avoir autant cru en moi.

Je remercie vivement Lionel Schiavolin et Isabelle Barbosa pour votre aide précieuse, pour les expériences, ainsi que pour votre soutien moral. J'ai grâce à vous énormément appris tant sur le plan pratique que théorique. Merci d'avoir toujours été à mon écoute. Ce fut un réel plaisir de travailler avec vous.

Cette thèse s'est déroulée dans de bonnes conditions grâce à l'ensemble des membres passés et présents de l'équipe. Merci à vous tous : Odon, Angélique, Martin, Thierry, Alvaro, Lionel, Khadeeja, Magali, Antonio, Antinéa, Gersende, Marc, Delase, Diep, Didier, Chi, Brice. Je remercie tout particulièrement Jérôme pour son écoute et son aide de tout instant.

J'ai passé la majorité de mon temps au sein de la section « génomique fonctionnelle » de l'IBENS, avec des collègues géniaux. L'accueil que j'ai reçu a été très chaleureux. Je voudrais spécifiquement remercier Martine pour sa gestion, le maintien du bon fonctionnement de la section et son sourire quotidien. Plus que des collègues, j'ai aussi noué de belles amitiés. Merci Isa pour ta bonne humeur et ton soutien à chaque instant. Merci à Oh Sung Know pour ton oreille attentive et tes conseils avisés. Merci Olivier (OB) pour tes belles histoires de sciences. Merci aussi aux nombreuses personnes que j'ai rencontrées à tous les étages. Ensemble, nous avons passé de belles soirées et séances de sport. Merci à Souraya, Jérôme, Vinko, Hind, Bérénice, Valentin, Basile, Quentin, Nadia, Lucia, Morgane, Bertrand, Suzanne, Caroline. Bien évidemment, merci au meilleur cafetier du coin, Youcef. Ta terrasse a été un vrai lieu de rencontre et d'échange entre amis et collègues.

Merci à mes amis qui me sont restés fidèles depuis toutes ces années. Vous avez participé à ce projet par votre soutien continu.

Enfin, je tiens à remercier en particulier ma famille, sans qui rien n'aurait été possible. Merci à mes parents pour leur amour inconditionnel et leur soutien sans faille. Vous m'avez toujours encouragée et donnée tous les moyens pour que je puisse arriver jusqu'ici. Merci à ma sœur adorée Doriane et sa compagne Aurore pour votre appui et vos encouragements. Mes derniers remerciements vont à Clément. Je n'aurai pas suffisamment de mots pour te remercier à la hauteur que tu mérites. Ta présence, ton amour, ton écoute et ton soutien m'ont énormément apporté, surtout pendant ces dernières années. Merci de m'avoir accompagnée tout au long de ce voyage. J'ai hâte de voir quelles seront nos prochaines aventures et je les espère plus merveilleuses encore que celles que nous avons vécues.

ABSTRACT

Title: A *Legionella pneumophila* type IV-secreted effector suppresses human Argonaute activities and promotes pathogenicity in macrophages

Keywords: *Legionella pneumophila*, RNA interference, RNA silencing suppressor, Argonaute, Argonaute-binding platform

Abstract:

RNA interference (RNAi) is a post-transcriptional gene regulatory mechanism directed by short-interfering RNAs (siRNAs) or microRNAs (miRNAs). MicroRNAs are present in a wide range of eukaryotic organisms and have been characterized in diverse fundamental biological processes. During the past decade, plant and mammalian miRNAs have emerged as major regulators of host-bacteria interactions by controlling multiple steps of bacterial infections. As a counter-defense mechanism, type III-secreted effectors from a phytopathogenic *Pseudomonas syringae* strain were found to suppress different steps of the plant miRNA pathway to enable disease. However, it remains unknown whether mammalian pathogenic bacteria could have evolved similar strategies to promote pathogenesis in host cells.

Here, we report that the *Legionella pneumophila* type IV-secreted effector LegK1 efficiently suppresses siRNA- and miRNA- activities in human cells. This phenomenon requires both its known serine/threonine kinase activity and an identified tryptophan (W)-based Argonaute (Ago)-binding platform. In addition, we found that LegK1 makes use of its Ago-binding platform to physically associate with Ago1, Ago2, Ago4 but also PABPC1 and DDX6, which are part of active and assembled RNA-Induced Silencing Complexes (RISCs). We show that two conserved W-motifs embedded in the kinase domain of LegK1 are responsible for the ability of this effector to bind human Ago proteins. Importantly, LegK1 was found to promote *L. pneumophila* growth in both amoeba and human macrophages, highlighting its biological relevance in pathogenesis. Finally, we provide evidence that human Ago4 is a central genetic target of LegK1, which might be inactivated in infected macrophages to promote *L. pneumophila* intracellular replication at an early stage of the infection. Overall, these findings provide the first evidence indicating that a secreted effector from a human pathogenic bacterium can directly target the host RNAi machinery to promote pathogenicity. They also unveil a common virulence strategy employed by both plant and mammalian pathogenic bacteria.

RESUME

Titre : Une protéine effectrice de type IV de *Legionella pneumophila* supprime les activités des Argonautes humaines et favorise la pathogénicité en macrophages

Mots clés : *Legionella pneumophila*, ARN interférence, suppresseur d'ARN interférence, Argonaute, plateforme de liaison aux Argonautes

Résumé :

L'ARN interférence (ARNi) est un mécanisme de régulation génique post-transcriptionnel dirigé par des petits ARN interférent (siARN) ou des microARN (miARN). Les miARN sont présents chez un grand nombre d'organismes eucaryotes et ont été caractérisés dans divers processus biologiques fondamentaux. Au cours de la dernière décennie, les miARN des plantes et des mammifères sont apparus comme des régulateurs majeurs des interactions hôte-bactérie en contrôlant de multiples étapes des infections bactériennes. En contre-défense, la bactérie *Pseudomonas syringae* phytopathogène sécrète des protéines effectrices de type III qui suppriment différentes étapes de la voie des miARN chez les plantes pour entraîner la maladie. Cependant, nous ignorons encore si les bactéries pathogènes des mammifères auraient pu développer des stratégies similaires pour favoriser la pathogénie bactérienne.

Nous montrons ici que la protéine effectrice de type IV LegK1 produite par *Legionella pneumophila* supprime les activités des siARN et des miARN en cellules humaines. Ce phénomène nécessite à la fois son activité sérine/thréonine protéine kinase et une plateforme de liaison aux Argonautes (Ago), composée de résidus tryptophane (W). De plus, nous avons découvert que LegK1 utilise cette plateforme de liaison aux Ago pour interagir avec Ago1, Ago2, Ago4 mais aussi avec PABPC1 et DDX6, qui font partie des complexes RISC actifs et assemblés. Nous avons montré que deux motifs W, conservés et intégrés dans le domaine kinase de LegK1, jouent un rôle crucial dans l'interaction avec les protéines Ago humaines. Nous avons aussi découvert que LegK1 favorise la croissance de *L. pneumophila* à la fois chez les amibes et en macrophages humains, ce qui souligne son importance dans la pathogénie bactérienne. Enfin, nous démontrons que la protéine Ago4 humaine est une cible génétique majeure de LegK1, qui pourrait être inactivée en macrophages infectés pour favoriser la réplication intracellulaire de *L. pneumophila* à un stade précoce de l'infection. Dans l'ensemble, ces résultats fournissent la toute première preuve indiquant qu'une protéine effectrice sécrétée par une bactérie pathogène de l'homme peut cibler directement la machinerie de l'ARNi de

l'hôte pour promouvoir la pathogénicité. Aussi, ils dévoilent une stratégie de virulence commune utilisée à la fois par les bactéries pathogènes des plantes et des mammifères.

Contents

LIST OF ABBREVIATIONS

2′OMe: 2′O-methylation
3’UTR: Three prime Untranslated Transcribed Region
4E-T: eIF4E transporter
5’UTRs: Five prime Untranslated Transcribed Region

A

Å: ångström
A. castellanii: *Acanthamoeba castellanii*
a.a.: amino acid
ABD: Ago-binding domain
ACES: N-(2-acetamido)-2-aminoethanesulfonic acid
ADAR1: Adenosine Deaminase Acting on RNA 1
Ago: Argonaute
Ago2-PD: Ago2 pocket-dead
AIM2: Absent In Melanoma 2
AKT2: RAC-beta serine/threonine-protein kinase
ALR: AIM2-like receptor
ASC: Apoptosis-associated speck-like protein
ATP: Adenosine triphosphate
aviD: antiviral Dicer

B

BCG: *Bacillus Calmette Guérin*
BCYE: Buffered charcoal-yeast extract
BLAST: Basic Local Alignment Search Tool
BLI: Bio-Layer Interferometry
bp: base pair
BPSSM: Bidirectional Position-Specific Scoring Matrix
BSA: Bovine Serum Albumin
BSR: Bacterial Suppressor of RNA silencing

C

C. elegans: *Caenorhabditis elegans*
CBP: Calmodulin-Binding Protein
CCR4: Carbon Catabolite Repressor 4
Cdc42: Cell division control protein 42
cDNA: coding DNA
CFU: colony-forming units
cGAS: cyclic GMP-AMP synthase
CLR: C-type Lectin Receptor
CMV: *Cytomegalovirus*
CR: Complement receptor
CTL: Control

D

D: Aspartic acid
D. discoideum: *Dictyostelium discoideum*
D. melanogaster: *Drosophila melanogaster*
DAMP: Damage-associated molecular pattern
DCL: Dicer-like
DCP1: Decapping protein 1
DCP2: Decapping protein 2
DDA: Data-dependent acquisition
DDX58: DExD/H-box helicase
DDX6: DEAD-Box RNA Helicase 6

DGCR8: DiGeorgesyndrome Critical Region gene 8
DMEM: Dulbecco's Modified Eagle's Medium
DMSO: Dimethylsulfoxide
DNA: Deoxyribonucleic acid
DNase: desoxyribonuclease
dsRNA: double-stranded RNA
DTT: Dithiothréitol

E

E: glutamic acid
E. coli: *Escherichia coli*
EBV: *Epstein-Barr virus*
ECDC: European Centre for Disease Prevention and Control
eGFP: enhanced Green Fluorescent Protein
eIF4G: eukaryotic Initiation Factor 4 gamma
EMCV: *encephalomyocarditis virus*
endo-siRNAs: endogenous siRNAs
eNOS: endothelial Nitric Oxide Synthase
ER: Endoplasmic recticulum
ETI: Effector-triggered immunity
EV: Extracellular Vesicle
EXP5: Exportin-5

F

FBS: Fetal Bovine Serum
FHV: *Flock house virus*

G

G: Glycin
Gal/GalNAc: Galactose/N-acetylgalactosamine-inhibitable lectin
gDNA: genomic DNA
GEF-H1: Guanine Exchange Factor H1
GFP: Green Fluorescent Protein
GSK3β: Glycogen synthase kinase 3 beta
GST: Glutathione S-transferase
GW: Glycine-tryptophan

H

H. vermiformis: *Hartmannella vermiformis*
HAMP: Homeostasis-altering molecular process
HcPro: Helper component proteinase
HEK293T: Human embryonic kidney 293T
HEPES: 4-(2-hydroxyethyl)-1-piperazineethanesulfonic acid
hetsiRNA: heterochromatic siRNA
HEV71: *Human enterovirus 71*
HFMD: Hand-Foot-and-Mouth Disease
HLA: α-Hemolysin
HMW-RISC: high molecular weight-RNA-induced silencing complex
hNPC: human Neural Progenitor Cell
HopT1-1: Hrp outer protein T1-1
HPA: Human Protein Atlas
HR: Hypersensitive response
HSC70: Heat Shock Cognate protein 70
Hsp70: 70-kDa heat shock proteins
HSP90: Heat Shock Protein 90
HSV-1: *Herpes simplex virus-1*

I

IAV: *Influenza A virus*
IBENS: Institutit de Biologie de l'Ecole Normale Supérieure
IBPC: Institut de Biologie Physico-Chimique

IFN: Interferon
IKK: I-kappa-B kinase
IL: Interleukin
IP: Immunoprecipitation
IPTG: Isopropyl-β-D-thiogalactopyranoside
IRAK1: Interleukin-1 receptor-associated kinase 1
IRF: Interferon Regulatory Factor
ISG: Interferon-Stimulated Genes

K

KLF4: Krüppel-like factor 4

L

L. bozemanae: Legionella bozemanae
L. longbeachae: *Legionella longbeachae*
L. micdadei: *Legionella micdadei*
L. norrlandica: Legionella norrlandica
L. pneumophila: Legionella pneumophila
L. quateirensis: Legionella quateirensis
L. waltersii: Legionella waltersii
LC-MS/MS: Liquid Chromatography-Mass Spectrometry/Mass Spectrometry
LCV: *Legionella*-containing vacuole
LGALS8: Galectin-8
LGP2: Laboratory of Genetics and Physiology 2
LIMD1: LIM domain-containing protein 1
LLO: Lysteriolysin O
LM: Lipomannan
LnaB: *Legionella* NF-κB activator B
LPS: Lipopolysaccharide
LRR: Leucine-rich repeat

M

M. tuberculosis: *Mycobacterium tuberculosis*
MAPK: Mitogen-Activated Protein Kinase
MDA5: Melanoma-differentiation-associated gene 5
mESC: murine Embryonic Stem Cell
MHC: Major Histocompatibility Complex
miRISC: miRNA-induced silencing complex
miRNA: microRNA
miRNP: miRNA ribonucleoprotein
mirtron: miRNA-intron
MKK: MAPK kinase kinase
MOB1A: MOB Kinase Activator 1A
MOI: Multiplicity of infection
MRE: miRNA Response Elements
mRNA: messenger RNA
MS: mass spectrometry
MST1/2: STE20-like serine/threonine kinases MST1 and MST2
MX1: MX dynamin-like GTPase 1
MyD88: Myeloid differentiation primary response protein

N

N-WASP: Neural Wiskott-Aldrich syndrome protein
N: asparagine
Naip: NLR family apoptosis inhibitory protein
NBD: Nucleotide-binding domain
NCBI: National Center for Biotechnology Information
Nef: Negative Regulatory Factor
NF-κB: nuclear factor Kappa B

NIK: NF-κB-inducing kinase
NLR: Nod-Like Receptor
NLRC4: NLR Family CARD Domain Containing 4
NLRP1B: NLR family pyrin domain containing 1 B
NLRP3: Nucleotide-binding oligomerization domain-like receptor pyrin domain-containing protein 3
NOD1: Nucleotide binding oligomerization domain containing 1
NoV: *Nodamura virus*
NS1: Non-Structural 1
nt: nucleotide
NX: Normalized eXpression

O

OAS1: 2'-5'-oligoadenylate synthetase 1
OD600: Optical density at 600 nm

P

P-bodies: Processing bodies
PABP: poly(A)-binding protein
PABPC1: Polyadenylate-binding protein 1
PACT: Protein kinase R-activating protein
PAMP: Pathogen-Associated Molecular Pattern
PBS1X: Phosphate Buffered Saline 1 X
PCR: Polymerase Chain Reaction
PDCD4: Programmed cell death protein 4
PFK-M: Phosphofructokinase muscle
PI: Phosphoinositide
piRNA: PIWI-interacting RNA
PKR: Protein Kinase R
PMA: Phorbol 12-Myristate 13-Acetate
PNG: Peptidoglycan
pre-miRNA: miRNA precursor
pri-miRNA: primary miRNA
PRM: Parallel Reaction Monitoring
PRR: Pattern Recognition Receptor
PSSM: Position-Specific Scoring Matrix
PTEN: Phosphatidylinositol 3,4,5-trisphosphate 3-phosphatase and dual-specificity protein phosphatase
PTI: PAMP-triggered immunity
PTM: Post-translational modification
Pto DC3000: *Pseudomonas syringa* pv. tomato strain DC3000

R

RAC1: Rac family small GTPase 1
RAN-GTP: RAs-related Nuclear protein
RDE-1: RNA Interference-deficient 1
RdRP: RNA-dependent RNA polymerase
rER: rough endoplasmic reticulum
RGS2: Regulator of G-protein signaling 2
RIG-I: Retinoic acid inducible gene I
RIN4: RPM1-interacting protein 4
RIPA: Radio-Immunoprecipitation Assay
RIPK1: Receptor-interacting serine-threonine kinase 1
RISC: RNA-Induced Silencing Complex
RLR: RIG-I-Like Receptor
RNA-seq: RNA sequencing
RNA: Ribonucleic acid
RNAi: RNA interference
RNase: ribonuclease
ROS: Reactive oxygen species
Rpm: Revolutions per minute
RPMI: Roswell Park Memorial Institute

RPS: NLR resistance to *Pseudomonas syringae*

RRE: Rev-Response Element

RSS: RNA silencing suppressors

RT-qPCR: Reverse transcription quantitative polymerase chain reaction

S

S: serine

S. enteritidis: *Salmonella enteritidis*

S. flexneri: *Shigella flexneri*

S. Typhimurium: *Salmonella Typhimurium*

SARS-CoV-2: *Severe acute respiratory syndrome coronavirus 2*

SD: Standard Deviation

SDS-PAGE: Sodium dodecyl sulphate–polyacrylamide gel electrophoresis

SEM: Standard Error of Mean

SG: Stress granule

SHIP1: SH-2 containing inositol 5' polyphosphatase 1

siRNA: short-interfering RNA

snoRNA: small nucleolar RNA

SOCS1: Suppressor of cytokine signaling 1

SPMMV: *Sweet potato mild mottle virus*

ssRNA: single-stranded RNA

T

T1SS: Type-I secretion systems

T6B: TNRC6B-derived peptide

TAB2: TGF-beta-activated kinase 1 and MAP3K7-binding protein 2

Tav2b: Tomato *aspermy cucumovirus* 2b protein

TB: Terrific Broth

TE: Transposable Element

TIR: Toll–interleukin 1 receptor

TLR: Toll-Like Receptor

TMV: *Tobacco mosaic tobamovirus*

TNFα: Tumor Necrosis Factor α

TNFAIP3: TNF-α-induced protein 3

TNRC6: Trinucleotide repeat-containing gene

TP53: Tumor protein P53

TPM: Transcripts Per Million

TRAF6: TNF receptor-associated factor 6

TRBP: Transactivation Response element RNA-Binding Protein

TRIF: Toll/IL-1R domain-containing adaptor-inducing IFN-β

tRNA: transfert RNA

TSN: Translin

U

UNC5C: Unc-5 Netrin Receptor C

V

v-miRNA: viral miRNA

vsiRNA: virus-derived siRNA

VSR: viral suppressors of RNA silencing

W

W-motif: tryptophan-containing motif

WT: wild-type

X

XRN1: 5'-3' Exoribonuclease 1exonuclease

Z

ZIKV: *Zika virus*

CHAPTER I: GENERAL INTRODUCTION

I. SMALL RNA PATHWAYS IN MAMMALS

I.I. OVERVIEW OF RNA INTERFERENCE: AN ANCESTRAL GENE REGULATORY MECHANISM TRIGGERED BY SMALL NON-CODING RNA SPECIES

RNA silencing has been discovered fortuitously in 1990, by a Dutch and an American research teams (van der Krol *et al.*, 1990; Napoli *et al.*, 1990). These two research groups were looking for ways to accentuate the purple color of Petunia petals. For this purpose, they have introduced by genetic transformation an additional copy of the chalcone synthase gene, an enzyme involved in the biosynthesis of the red pigment anthocyanin. Among the transformants obtained, some exhibited white petals, depigmented either totally or in sectors. The molecular analysis of these transformants showed that the depigmentation resulted from the silencing of the transgene and the endogenous chalcone synthase. Thus, it was shown for the first time that the introduction of an extra copy of a gene could lead to its inactivation as well as that of the endogenous gene. This phenomenon has been named co-suppression. In the late 1990s, a similar phenomenon called quelling, RNA interference (RNAi) or post-transcriptional gene silencing, was demonstrated in the filamentous fungus *Neurosporacrassa* (Cogoni *et al.*, 1996), in *Caenorhabditis elegans*, with the discovery of the first microRNA (miRNA) (Fire *et al.*, 1998; Lee *et al.*, 1993) and in plants through the detection of small interfering RNAs (siRNAs) in the context of viral infection (Hamilton and Baulcombe, 1999), respectively. Later, RNAi was found to be an evolutionarily conserved gene regulatory mechanism in mammals (Elbashir *et al.*, 2001), that operate in a wide range of organisms, including protozoa, algae, invertebrates and vertebrates (Agrawal *et al.*, 2003; Tarver *et al.*, 2012; Bartel, 2018). The central actors of RNAi are small regulatory RNAs that are divided into three major classes in mammals, namely miRNAs, siRNAs and PIWI-interacting RNAs (piRNAs) (Ghildiyal and Zamore, 2009; Kim *et al.*, 2009). In plants, the latter class is lacking, but a subclass of siRNAs, referred to as heterochromatic siRNAs (hetsiRNAs), orchestrate similar functions. They trigger gene silencing of transposable elements (TEs) as well as some genes carrying TEs or remnant TEs in their vicinity (Borges and Martienssen, 2015). These small RNA classes differ in many ways, including their origin, their biogenesis, their size, the mechanism of target regulation and their

biological functions. In humans, the majority of the endogenous small RNAs that have been reported are composed of miRNAs, which control the expression of a large repertoire of human protein-coding genes. These miRNAs post-transcriptionally regulate diverse fundamental biological processes, including development, differentiation, proliferation, and stress responses.

Endogenous miRNAs are produced from miRNA precursors transcripts, which are either transcribed from intergenic regions or embedded in intronic sequences (Borges and Martienssen, 2015). MicroRNAs can also be generated exogenously from viral genomes, a phenomenon which has been initially reported in human cells infected by the DNA virus Epstein-Barr virus (EBV) (Pfeffer *et al.*, 2004). Small interfering RNAs originate from double-stranded RNA (dsRNA) precursors, whereas piRNAs originate from single-stranded transcripts (Bartel, 2018). Compared to siRNAs and miRNAs, piRNAs are produced through alternative biogenesis mechanisms implicating, in the first place, the transcription and processing of piRNA precursor transcripts, and then primary piRNAs enter the ping-pong amplification loop to generate secondary piRNAs (Brennecke *et al.*, 2007). The piRNAs were first found to function towards TEs regulation and transgene silencing in the germline, but other functions in the soma have now been reported, implicating mRNA deadenylation and decay through the piRNA-guided targeting of 3'UTR transcript regions (Weick and Miska, 2014; Ernst *et al.*, 2017). Short interfering RNAs were thought to be primarily exogenous in origin, derived directly from viral genome or its replicative intermediates. Nevertheless, endogenous siRNAs (endo-siRNAs) were reported in embryonic stem cells and oocytes in mammals, where they are notably produced from TEs (Piatek and Werner, 2014; Tam *et al.*, 2008; Watanabe *et al.*, 2008). It is noteworthy that endo-siRNAs can mediate mRNA decay and act as major regulators of the mouse oocyte-to-zygote transition (Dallaire and Simard, 2016).

I.II. MICRORNA AND SIRNA BIOGENESIS IN MAMMALS

The human genome encodes more than 2500 miRNAs that regulate a wide range of biological processes. The biogenesis of human miRNAs starts with the transcription of miRNA loci typically transcribed by the RNA polymerase II to produce stem-loop-structured primary miRNA (pri-miRNA) transcripts (Figure 1.1A) (Bartel, 2018; Cullen, 2004). A subset of miRNA loci can also be transcribed by the RNA polymerase III (Lee *et al.*, 2004; Borchert *et al.*, 2006). Accordingly, the majority of pri-miRNAs are both capped and polyadenylated (Cai *et al.*, 2004). Then, the processing of miRNAs involves Drosha and Dicer III-type RNase enzymes. The first cleavage of the pri-miRNA transcripts by the microprocessor complex is performed by Drosha and its co-factor DiGeorgesyndrome Critical Region gene 8 (DGCR8) in the nucleus to release a ~ 60-70 bp miRNA precursor (pre-miRNA) hairpin structure (Lee *et al.*, 2003; Nguyen *et al.*, 2015). However, an alternative pathway of microprocessor complex-mediated cleavage has been reported, using splicing of pri-miRNA transcripts, thereby releasing introns sharing structural features of pre-miRNAs (Ruby *et al.*, 2007). This class of miRNAs generated from a short-spliced intron is called mirtrons (miRNA-introns). The hairpin is then exported from the nucleus to the cytoplasm by the Exportin-5 (EXP5), with the involvement of RAs-related Nuclear protein (RAN-GTP) (Yi *et al.*, 2003; Bohnsack *et al.*, 2004; Lund *et al.*, 2004). Once inside the cytoplasm, the second cleavage step of the pre-miRNA is achieved. The RNase III-type enzyme Dicer further processes the pre-miRNA into mature ~ 20-22 bp miRNA duplex with 5’ phosphates and 2-nucleotide 3’ overhangs (Hutvágner *et al.*, 2001; Zhang *et al.*, 2004). This step requires the Dicer partners Transactivation response element RNA-binding protein (TRBP) and Protein kinase R-activating protein (PACT), allowing the sensing of the pre-miRNA and the regulation of the Dicing processing events (Heyam *et al.*, 2015). Dicer is also able to process other types of RNA molecules such as hairpin RNAs, small nucleolar RNA (snoRNA), which in turn exert miRNA-like repressive functions (Ender *et al.*, 2008).

Endo-siRNAs are synthesized from dsRNAs such as hairpins with a long, perfect stem or sense-antisense transcript hybrids, while exogenous siRNAs are mainly derived from viral dsRNAs. The biogenesis of siRNA bypass nuclear processing and is produced by Dicer to form ~ 20-23 bp dsRNA (Figure 1.1B).

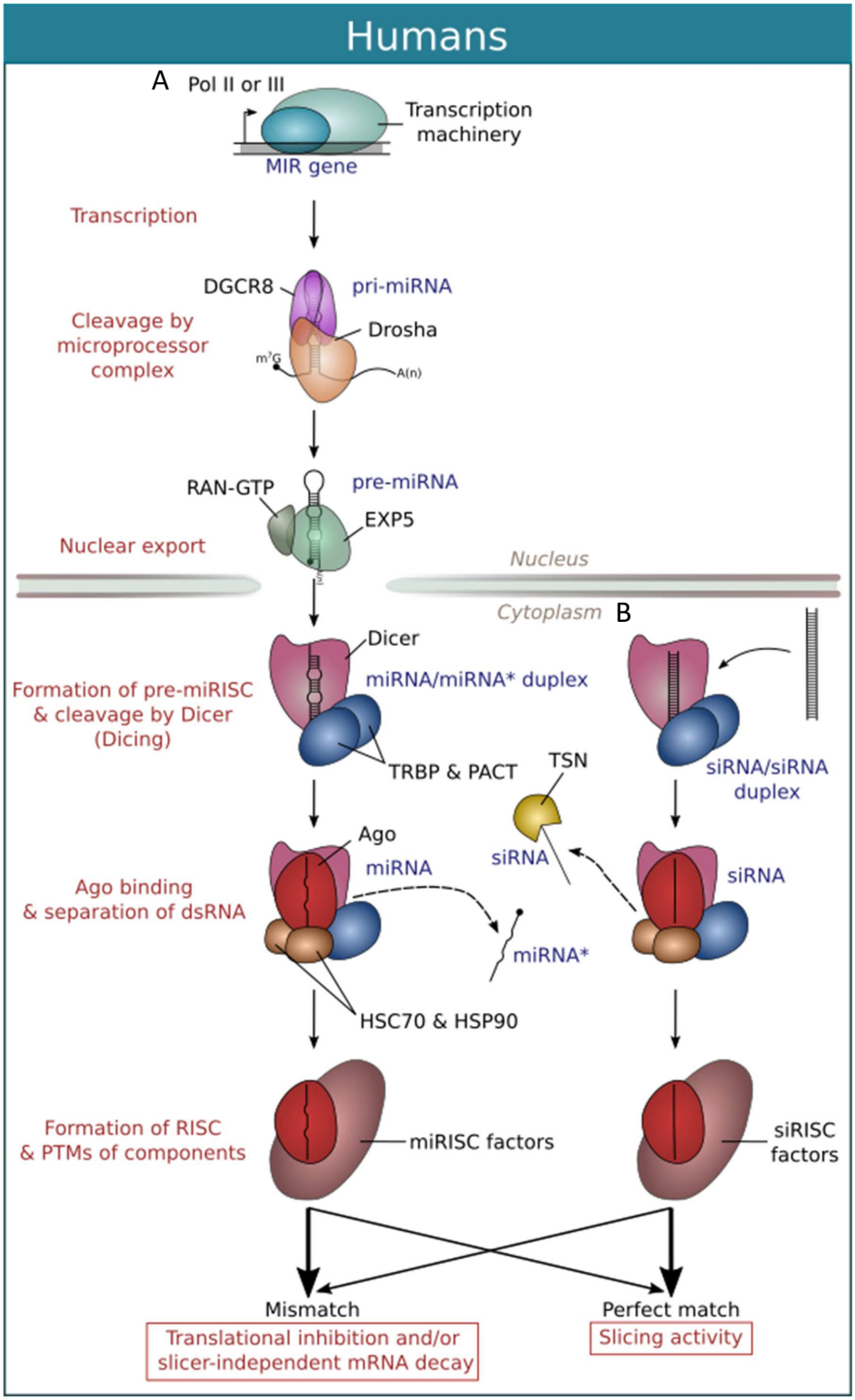

Figure 1.1. Biogenesis of miRNAs and siRNAs in humans.
(A) Once transcribed by RNA Polymerase II or III, the primary microRNA (pri-miRNA) containing imperfectly base-paired stem loop is cleaved by microprocessor, comprised of Drosha and DiGeorge syndrome critical region 8 (DGCR8). This process releases a ~70-nucleotide hairpin known as precursor miRNAs (pre-miRNAs). The pre-miRNA is then exported from nucleus to the cytoplasm through Exportin 5 (EXP5) and RAs-related Nuclear protein (RAN–GTP), where it is cleaved by Dicer to produce a ~ 20 bp miRNA duplex with a 5' phosphate and a 2 nt 3' overhang on each end. Transactivation response RNA-binding protein (TRBP) and protein activator of PKR (PACT) are important regulatory factors that facilitate recognition and processing of dsRNA through the interaction of dsRNA-binding protein. One selected strand is incorporated into Ago (Ago1-4), a process which requires the heat shock cognate protein 70 (Hsc70)/ heat shock protein 90 (Hsp90) chaperone machinery, while the other strand is degraded. In some instances, the passenger miRNA (miRNA*) can also be incorporated into Ago proteins and guide RNA silencing. Following these steps of processing, the miRNA is assembled into miRNA-mediated RNA-induced silencing complex (miRISC), which direct slicing, translational repression and/or mRNA decay. **(B)** Exogenous or endogenous double-stranded RNAs (dsRNAs) from cytoplasm are also processed in the canonical pathway by Dicer enzyme associated with its partners. Ago and accessory proteins assemble and form the RISC, where one siRNA is transferred to Ago. The passenger siRNA is degraded by the endonuclease Translin (TSN). The siRNA guides RISC to perfectly complementarity sequence of its target mRNAs and induces gene silencing, with a prevalence for mRNA cleavage.

I.III. RNA-INDUCED SILENCING COMPLEX ASSEMBLY AND SILENCING ACTIVITIES IN MAMMALS

Once small RNA duplexes are produced, they are further loaded onto an Argonaute (Ago)-containing RNA-induced silencing complex (RISC) with the help of the chaperone proteins Heat shock cognate protein 70 (HSC70) and Heat shock protein 90 (HSP90) (Figure 1.1) (Iwasaki *et al.*, 2010; Nakanishi, 2016). The HSC70/HSP90 chaperone machinery is required to load small RNA duplexes into Ago2 through ATP hydrolysis (Iwasaki *et al.*, 2010). The duplex is composed of the mature miRNA or siRNA called the guide strand- and of the "passenger" strand or miRNA*. The siRNA passenger strand is cleaved by Ago2, a process which facilitates RISC assembly (Matranga *et al.*, 2005; Leuschner *et al.*, 2006; Wang *et al.*, 2009), and is further degraded by the endonuclease Translin (TSN, also known as C3PO) (Ye *et al.*, 2011). In some cases, the miRNA* was shown to be loaded in Ago proteins and to silence sequence-specific targets (Bhayani *et al.*, 2012). Finally, mature miRNA and siRNA direct RISCs to the sequence complementary mRNA target and recognize it by Watson-Crick base pairing through its 5' seed region (2-8 nucleotides of miRNA) (Figure 1.1). Due to the initial identification and characterization of *C. elegans* miRNAs targeting the 3'UTR regions of mRNA targets (Lee *et al.*, 1993; Reinhart *et al.*, 2000), miRNA-binding sites were thought to be mainly located at 3'UTRs. However, using unbiased experimental approaches, a substantial number of miRNA interactions were additionally found in 5'UTRs and coding regions (Helwak *et al.*, 2013; Ni and Leng, 2015).

I.IV. MECHANISMS OF ARGONAUTE-DIRECTED GENE SILENCING IN HUMANS

Four Ago proteins (Ago1 to 4) are expressed from the human genome. These proteins are composed of four core domains (Figure 1.2A): the PAZ domain that binds to the 3' termini of small RNAs, the PIWI domain, which carries the endonucleolytic activity, the N domain, which notably contributes to the loading of small RNAs as well as the unwinding of RNA duplexes, and the MID domain, which binds the 5'end of small RNAs (Meister, 2013). Structural studies on human Ago2 unveiled a bi-lobed structure, which influences how the protein interacts with the guide and target molecules (Figure 1.2B) (Elkayam *et al.*, 2012; Schirle and MacRae, 2012). More specifically, the central cleft enables the binding of guide and target RNAs. A kink has been identified, which may function in miRNA target recognition or in the release of sliced RNA products. Finally, these studies put forward the presence of tandem tryptophan binding pockets in the PIWI domain, which define an interaction surface for recruitment of W-rich cofactors of Ago proteins. Among the four human Ago proteins, Ago2 has been extensively characterized and shown to participate, with the help of accessory proteins, in various RNA regulatory processes, including RNA cleavage, decapping, deadenylation-related or unrelated RNA degradation, as well as translational repression (Li *et al.*, 2020). The target specificity of miRISC is due to its interaction with complementary sequences on target mRNA, termed miRNA response elements (MREs). The degree of MRE complementarity notably determines whether the mRNA target will undergo Ago-dependent slicing or miRISC-mediated translational inhibition and/or degradation (Jo *et al.*, 2015; O'Brien *et al.*, 2018). A fully complementary miRNA:MRE interaction results in Ago2-directed slicing of the miRNA target transcripts. In mammals, these interactions are usually not fully complementary an therefore more prone for slicing-independent regulation through translational repression and mRNA decay (Jonas and Izaurralde, 2015). It is also noteworthy that some endogenous miRNAs that are fully complementary to their targets can engage RISC towards slicing, and can have potent silencing effects in different mammalian cell types (Guo *et al*., 2010; Eichhorn *et al*., 2014; Subtelny *et al*., 2014).

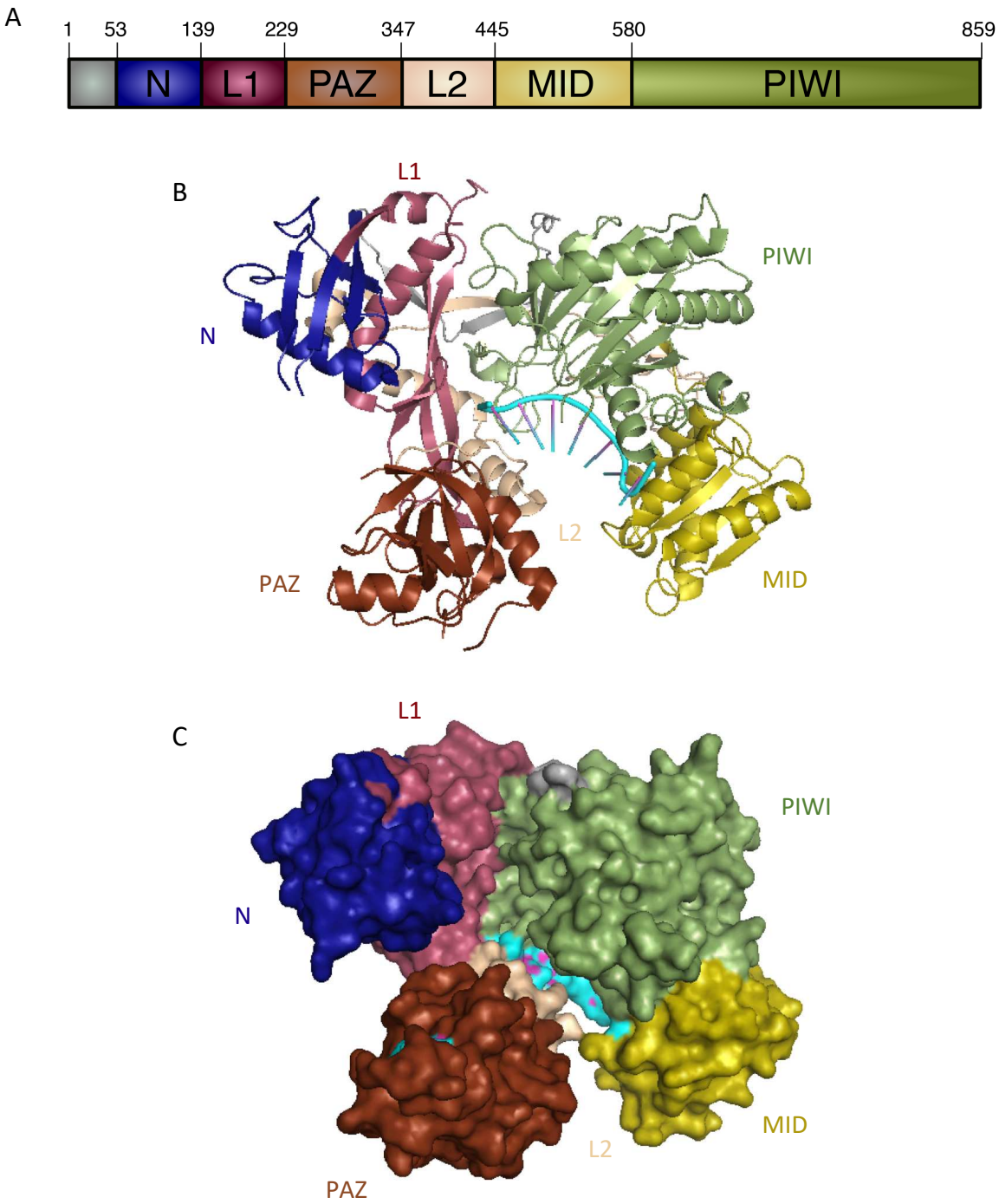

Figure 1.2. Structure of human Ago2.
(A) Schematic representation of the Ago2 primary sequence. The N (navy), PAZ (brown), MID (yellow), PIWI (green) domains and linkers L1 (purple) and L2 (pink) are indicated. **(B)** Cartoon representation of Ago2 (PDB ID: 4OLA). A generic guide RNA (teal) can be traced for nucleotides 1–8 and 21. **(C)** Surface representation of Ago2.

I.V. AGO2-DIRECTED SLICER ACTIVITY

The slicer activity of human Ago2 is mediated by a well-defined catalytic tetrad (Liu *et al.*, 2004; Meister *et al*., 2004, Nakanishi *et al.*, 2012). Whereas it was initially thought that only human Ago2 possesses an endonuclease activity, a recent report provides evidence that human Ago3 is also capable of triggering the slicing of some miRNA targets, although with distinct substrate requirements (Park *et al.*, 2017, 2020b). The slicer activity of Ago2 typically consists on the cleavage of the phosphodiester linkage positioned at siRNA/miRNA residues 10 and 11 from the 5' end, which releases a 5'-phosphomonoester and a 3'-hydroxyl group (Martinez and Tuschl, 2004) (Figure 1.3). Once the mRNA target is cleaved, degradation is promoted by cellular exonucleases to complete mRNA degradation (Orban and Izaurralde, 2005). The 5' mRNA fragment was notably shown to be degraded by the exosome in *Drosophila* cells, while the 3' fragment was shown to be degraded by 5'-3' Exoribonuclease 1 (XRN1) (Bartel, 2018; Orban and Izaurralde, 2005).

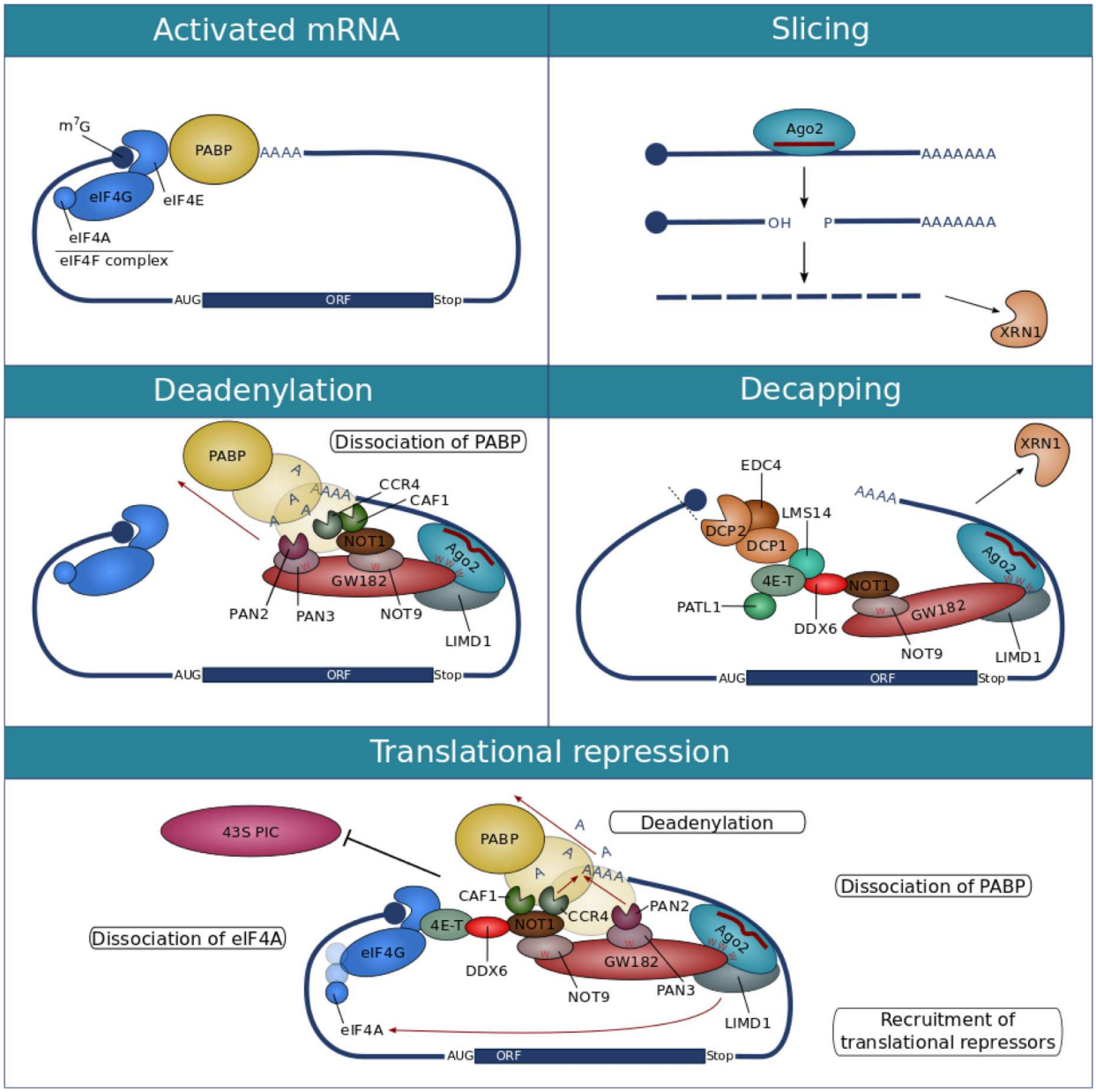

Figure 1.3. siRNA- and miRNA-mediated slicing, translational repression and mRNA decay in humans.
When small RNAs bind Argonaute (Ago) protein in RNA-induced silencing complex (RISC), there are four main steps orchestrating siRNA- and miRNA-mediated gene silencing. One is a cleavage of fully complementarity target mRNA by slicing activity, which is mainly directed the catalytic activity of Ago2. The Ago2 slicing activity is highly specific, and concerned the phosphodiester linkage that joins the residues positioned to siRNA nucleotides 10 and 11 from 5' end to 5′-monophosphate and 3′-hydroxyl termini. For non-endonucleolytic gene silencing, three mechanisms are important and involve deadenylation, decapping and translational repression. Ago2 recruits GW182 family member protein (TNRC6A, B or C) through multiple glycine–tryptophan (GW)-repeats. Three tryptophan-binding pockets (W in red) are located at the surface of Ago2. LIM domain-containing protein 1 (LIMD1) coordinates the interaction between Ago2 and TNRC6/proteins. In turn, GW182 serves as a platform, which associates with poly(A)-binding protein (PABP) protein, the deadenylase complexes poly(A)-specific ribonuclease 2 (PAN2)–PAN3 or carbon catabolite repressor 4 (CCR4)–negative regulator of transcription (NOT). The deadenylation involves two consecutive steps, one of which is with the PAN2-PAN3 complex cutting the long poly(A) tails, and the second with the CCR4–NOT complex shortening the poly(A) tails. After deadenylation, RISC can induce either degradation in the 5'-to-3' mRNA decay pathway or mRNA decapping following by mRNA decay. Indeed, CCR4-NOT transcription complex subunit 1 (NOT1) interacts with DEAD-Box RNA Helicase 6 (DDX6), and recruits decapping factors such as catalytic subunit of decapping complex (DCP2), or decapping activators including DCP1, enhancer of mRNA decapping protein 4 (EDC4) and decapping factors such as protein PAT1 homolog 1 (PATL1) and U6 snRNA-associated Sm-like protein (LSM1). All these proteins are recruited to the 5′ end of the mRNA and remove the 7-methylguanylate (m7G) cap (black circle). Finally, the unprotected mRNA is degraded by the 5′–3′ exoribonuclease 1 (XRN1) or 3'-to-5' exonucleolytic mRNA decay by exoribonuclease exosome. Another way is the translational repression, where three major mechanisms have been proposed, including a GW182-mediated PABP displacement, a recruitment of the translational repressors via GW182 or a dissociation of Eukaryotic initiation factor 4A (eIF4A) from the cap-binding complex eIF4F. These mechanisms seem not to be exclusive and, can overlap with each other. The first model proposes that GW182 displaces PABP from the target mRNA through interaction with the CCR4–NOT complex, breaking the "closed-loop" structure formed by the interaction between eIF4G and PABP. The second model implies the recruitment of translational repressors. The association of GW182 with chromatin assembly factor-1 (CAF1) through CCR4–NOT complex induces repression of the target mRNAs in a deadenylation-dependent or –independent manner. It is also thought that eIF4A2 is required for translational repression through interaction with component of CCR4-NOT complex, NOT1 or with DDX6. DDX6 is a crucial coordinator in translation repression and mRNA decay, since it connects the processes of deadenylation and decapping. Moreover, eIF4E-binding protein (4E-T) is also recruited to repress translation. The last model is the dissociation of eIF4A component from the eIF4F complex. This factor is released on the target mRNA, which is suggested to inhibit ribosome binding and scanning. These mechanisms could probably prevent the recruitment of the 43S preinitiation complex (PIC) through the action of initiation factors (eIF4s). Many of these gene-silencing processes, deadenylation and mRNA decay, appear to be dependent on GW182, and suggesting that GW182 is responsible for a strong localized association of factors on the target mRNA. However, it is also proposed that other miRNA-directed gene silencing mechanisms are GW182-independent.

I.VI. MICRORNA-DIRECTED TRANSLATIONAL REPRESSION AND MRNA DECAY

Argonautes are key components involved in miRNA-directed translational inhibition and mRNA degradation, and are assisted by a dozen of other proteins in these processes. This occurs through the recruitment of downstream accessory proteins by proteins containing glycine-tryptophan (GW)-repeats, such as the human paralogs TNRC6A, -B or -C (Figure 1.3) (Behm-Ansmant *et al*., 2006; Bridge *et al*., 2017; Chekulaeva *et al*., 2011; Horman *et al*., 2013; La Rocca *et al*., 2015; Lian *et al*., 2009; Liu *et al.*, 2005). These GW-proteins are characterized by multiple GW-repeats, where the tryptophan residues mediate the direct interaction with Ago proteins. Given that they are multidomain proteins, they act as scaffolds to organize supramolecular complexes (Hicks *et al*., 2017; Niaz and Hussain, 2018). The recruitment of diverse accessory proteins coordinates all downstream steps for deadenylation and translational inhibition processes (Eulalio *et al.*, 2008; Horman *et al*., 2013; Till *et al*., 2007; Wakiyama *et al.*, 2007). More specifically, upon phosphorylation of Ago2 at serine 387, the adapter protein LIM domain-containing protein 1 (LIMD1) binds to this silencing effector, thereby recruiting TNRC6 proteins and its associated downstream accessory proteins (Bridge *et al*., 2017; Horman *et al.*, 2013). This post-translational modification of human Ago2 is crucial to trigger a rapid repression of miRNA targets (Bridge *et al*., 2017; Horman *et al.*, 2013). The interaction between human LIMD1 and Ago2 can also interfere with the silencing function of other Ago proteins. For example, the loss of LIMD1 was found to abolish Ago2-mediated miRNA silencing, resulting in a switch towards Ago3-guided miRNA silencing (Bridge *et al*., 2017).

TNRC6 proteins ensure miRISC assembly by recruiting to Ago2 several factors including poly(A)-binding protein (PABP) and two deadenylase complexes, CCR4–NOT and PAN2–PAN3 complexes (Braun *et al*., 2011; Chekulaeva *et al.*, 2011; Fabian *et al.*, 2011; Horman *et al*., 2013; Huntzinger *et al.*, 2010; Wahle and Winkler, 2013). The deadenylation involves two consecutive steps, one of which is mediated by the PAN2-PAN3 complex cutting the long poly(A) tails, while the second one is directed by the CCR4–NOT complex shortening the poly(A) tails (Yamashita *et al.*, 2005). Following deadenylation, miRNA targets are decapped and then degraded through mRNA decay (Pillai *et al*., 2005; Braun *et al.*, 2012). The decapping process occurs through the recruitment of the decapping activator DEAD-Box RNA Helicase 6 (DDX6) (also termed RCK or p54), which promotes the removal of cap structure via the decapping DCP1/DCP2 complex (Chen *et al*., 2014; Mathonnet *et al.*, 2007). This is

followed with a 5'-to-3' degradation by exoribonuclease XRN1 or 3'-to-5' exonucleolytic mRNA decay by exoribonuclease exosome (Ghosh and Jacobson, 2010). It is thought that decapping is a consequence of miRNA-mediated deadenylation, however these two processes can also operate independently (Badis *et al.*, 2004).

Translational repression and deadenylation are two processes interconnected since TNRC6 proteins direct both effects through their interaction with the CCR4–NOT deadenylase complex (Huntzinger *et al.*, 2013; Chen *et al.*, 2014; Mathys *et al.*, 2014). Several mechanisms of miRNA-mediated translational repression have been proposed (Huntzinger and Izaurralde, 2011; Fabian and Sonenberg, 2012; Jonas and Izaurralde, 2015; Iwakawa and Tomari, 2015). The first models postulated that mammalian miRNAs could interfere with either the post-initiation, the initiation or the elongation steps of translation. However, recent ribosome profiling approaches revealed that miRNAs primarily trigger silencing by altering translational initiation (Eichhorn *et al.*, 2014; Guo *et al.*, 2010; Ricci *et al.*, 2013; Subtelny *et al.*, 2014). At least two major mechanisms are retained for the repression of translational initiation. In *Drosophila,* Ago2 containing RISC recruits GW182 and promotes the release of PABP from miRNA transcript targets (Zekri *et al.*, 2013). This phenomenon further removes the protection of the poly(A) tail of mRNAs. It also breaks the loop structure formed by the interaction between PABP and Eukaryotic translation initiation factor 4G (eIF4G), thereby repressing translation initiation and triggering mRNA degradation (Figure 1.3) (Zekri *et al.*, 2013). The second proposed mechanism occurs at the level of ribosomal pre-initiation complexes. In particular, the decapping activator DDX6 was shown to associate with eIF4E transporter (4E-T), which competes with component of eIF4E complex and promotes both the decay and translational repression of miRNA targets (Figure 1.3) (Kamenska *et al.*, 2016; Kuzuoğlu-Öztürk *et al.*, 2016). Although TNRC6 proteins play an essential role in translational repression, some studies conducted in *Drosophila* have reported that miRNAs can also repress translation in the absence of GW182 (Bawankar *et al.*, 2013; Fukaya and Tomari, 2012). Additional in-depth studies are needed to examine whether such TNRC6-independent mechanisms could function in mammals. Alternative models have also provided evidence that deadenylation was not necessary for miRNA-directed translational inhibition. For instance, miRISC was shown to induce the dissociation of eIF4A from the mRNA target and its partner eIF4G (Fukao *et al.*, 2014), or associate with and elF6, thereby inhibiting ribosomal scanning (Chendrimada *et al.*, 2007).

I.VII. CANONICAL FEATURES OF FUNCTIONAL W-MOTIFS

It has been well-established that GW182/TNRC6 family members proteins in both mammalian and *Drosophila* cells bind Ago proteins through multiple binding sites (El-Shami *et al.*, 2007; Lian *et al*., 2009; Pfaff *et al.*, 2013; Takimoto *et al*., 2009; Till *et al.*, 2007). Indeed, the N-terminal regions of human TNRC6A, TNRC6B, and TNRC6C interact with all four human Ago proteins, and W-repeats are critical for these interactions (Lazzaretti *et al.*, 2009; Lian *et al.*, 2009; Takimoto *et al.*, 2009; Till *et al.*, 2007; Zipprich *et al.*, 2009). Specifically, it has been determined that the conserved motifs I and II, and Ago-hook, present in some members, in the N-terminal region of GW182/TNRC6 proteins mediate an interaction with human Ago2 *in vitro* (Eulalio *et al*., 2009a; Till *et al.*, 2007). The W-motifs within these three domains are divergent, and computer analyses have uncovered consensus features surrounding these W-domains (El-Shami *et al*., 2007). Indeed, an excessive length polymorphism is observed due to variation in the number and size of W-repeats, that vary considerably among Ago-binding platforms (from 2 to up to 40). However, residues surrounding the tryptophan show a biased, but common amino-acid composition, which includes a strong positive tendency towards small, polar and non-hydrophobic amino acids such as glycine (G), asparagine (N), aspartic acid (D), glutamic acid (E), serine (S) (Zielezinski and Karlowski, 2015). Moreover, the tryptophan residues are embedded in hyper-variable low complexity sequences that fall into locally disordered regions with low overall hydropathy and high net charge.

Importantly, it was reported that not all W-repeats contribute equally to the interaction and might have different functional preferences (Chekulaeva *et al.*, 2010; Eulalio *et al*., 2009b; Sheu-Gruttadauria and MacRae, 2018; Takimoto *et al*., 2009; Yao *et al*., 2011). First, it was determined that the individual deletion of motifs I and II in TNRC6A, TNRC6B, and TNRC6C do not prevent them from interacting with Ago2, whereas the binding is impaired when both of these motifs are deleted from TNRC6C, and further abrogated when the Ago-hook is additionally deleted from TNRC6B (Lazzaretti *et al*., 2009). Second, within an Ago-binding domain, it was also shown that single tryptophan to alanine substitutions can either affect partly, strongly or unalter the interaction with Ago2, highlighting that some W-repeats are crucial for Ago-binding, while others are not or less important for this process (Takimoto *et al.*, 2009). Finally, it has been reported that the mutations in the 36 tryptophan residues of the N-terminal Ago-binding domain (ABD) of the TNRC6B protein abolished its interaction with human Ago2

(Sheu-Gruttadauria and MacRae, 2018). Importantly, when only two or three tandemly tryptophan residues found receptively in the motif I or motif II of TNRC6B were adding back to this mutant, the binding was restored (Sheu-Gruttadauria and MacRae, 2018). These findings highlight that a few specific tryptophan residues from the ABD domain of TNRC6B are critical for Ago-binding and that their tandem-based organization is also essential for this process.

I.VIII. COMPARTMENTALIZATION OF MIRNA-MEDIATED GENE REPRESSION

The cellular compartmentalization for miRNA repression is an emerging research area. Early studies have provided evidence indicating that human Ago2 is associated with Processing bodies (P-bodies in mammals), and that this recruitment is linked with RNA degradation (Eulalio *et al.*, 2007a; Parker and Sheth, 2007; Luo *et al.*, 2018). However, miRNA-mediated repression is functional in cells lacking detectable microscopic P-bodies, indicating that P-bodies are not essential for miRNA activity (Eulalio *et al.*, 2007a, 2007b). Stress granules (SG), which contain common components with P-bodies and many translation initiation components (Protter and Parker, 2016), were also proposed to be the site of human Ago2 action (Leung *et al.*, 2006; Pare *et al.*, 2009). Upon different types of stresses, a subpopulation of miRNAs, mRNA targets, Ago proteins and miRNA-protein complex components become enriched in SG (Leung *et al.*, 2006). Many RNA regulators have also been found, that can modulate miRNA activity (Anderson and Kedersha, 2008). However, these studies showed that the recruitment of human Ago2 to SGs during stress-signaling is accompanied by a decreased RNAi efficacy, which in turn suppresses SG formation (Detzer *et al.*, 2011; Lou *et al.*, 2019). The localization of RNAi factors is dynamic and suggests that the silencing machinery can be distributed in different compartments, particularly under stress conditions. Hence, a mRNA cycle has been proposed between polysomes, P-bodies, and SGs (Decker and Parker, 2012; Stoecklin and Kedersha, 2013). Moreover, human Ago2 and TNRC6 proteins were retrieved at multivesicular bodies (MVBs), which are specialized late endosomal compartments (Gibbings *et al.*, 2009). Other studies have shown that the central nucleation site of miRNA assembly and their interaction with target mRNAs appear to occur on polysome-associated rough endoplasmic reticulum (rER) membranes (Figure 1.4) (Barman and Bhattacharyya, 2015; Stalder *et al.*, 2013). Although miRNA-mediated translation repression was found to operate at these rER

membranes, deadenylation, decapping, and mRNA degradation have not been shown to function at these cellular compartments (Bose *et al.*, 2017). Instead, repressed mRNAs are thought to shuttle to early and late endosome, and then to MVBs, where they are released from miRISC and undergo degradation (Bose *et al.*, 2017, 2020). Subsequently, free miRNA ribonucleoprotein (miRNP) might be recycled back to the rER for further cycles of miRNA-mediated repression.

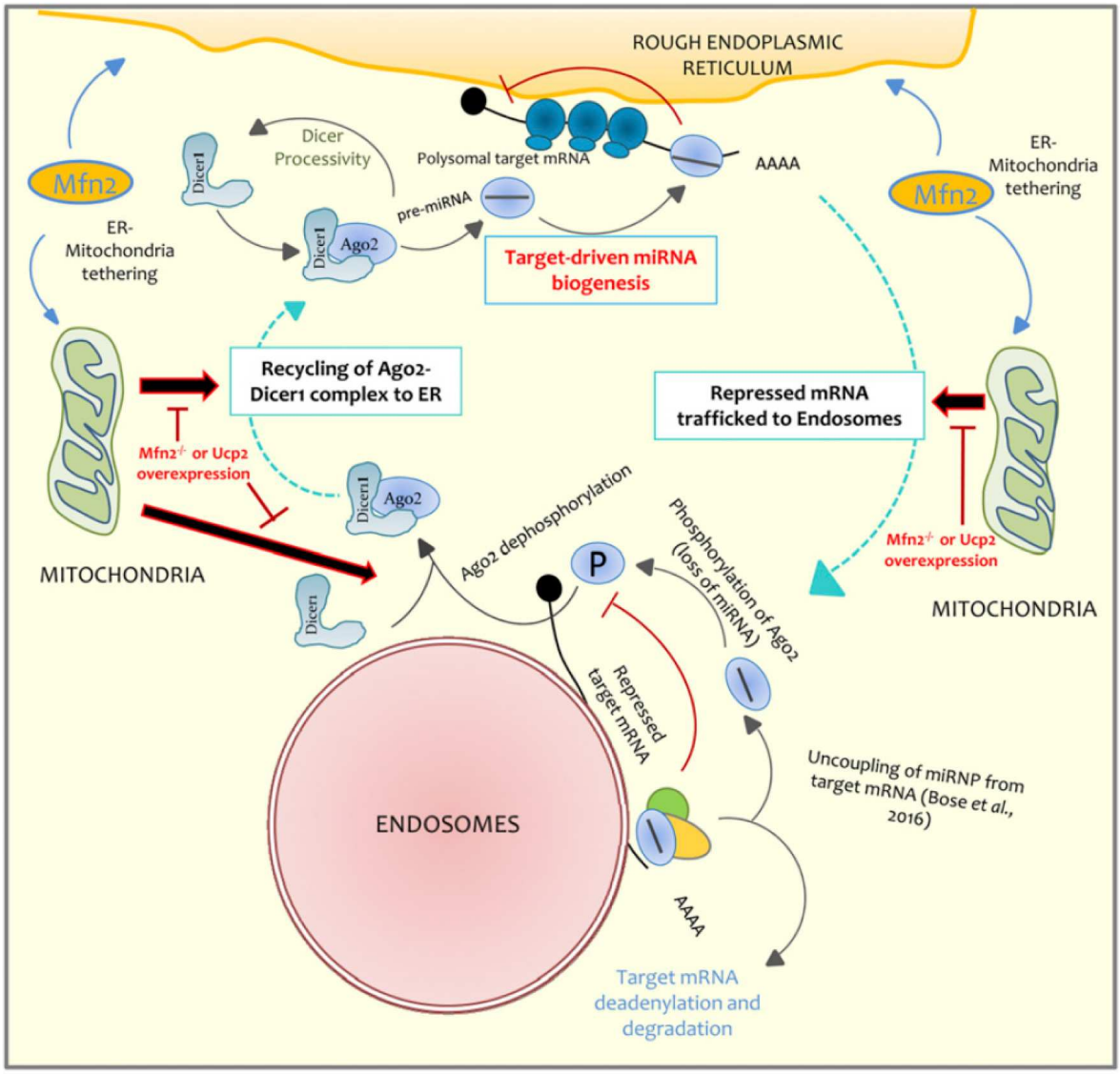

Figure 1.4. Proposed model of internal exchange of Ago2 between compartments by mitochondria-driven inter-organellar interaction controls. Polysomes associated to the rough endoplasmic reticulum (rER) appear to serve as the cellular sites for miRNA assembly and their interaction with target mRNAs. First, the newly synthesized target mRNA is directed at the rER and then binds miRISC, followed by translation repression. The repressed mRNAs are shuttled to early and late endosomes and then to multivesicular bodies (MVBs), where they are released from the bound miRISC and further subjected to degradation. The free miRISC may recycle back to the rER for new cycles of repression. The mitochondrial tethering with rER seems to control miRISC recycling and regulates Ago2 trafficking at the subcellular level. This acts as a rate-limiting step in the miRNA biogenesis process. The overall schematic representation is derived from Bose M. *et al*., 2020.

II. RNA SILENCING: A CONSERVED HOST ANTIVIRAL RESPONSE

II.I. ANTIVIRAL RNA SILENCING IN PLANTS AND INVERTEBRATES

Short interfering RNAs were first detected in plants, and more particularly in the context of viral infection (Hamilton and Baulcombe, 1999). It is now well-established that virus-derived siRNAs (vsiRNAs) accumulate in plants and invertebrates infected with viruses (Ding, 2010; Jin *et al.*, 2021). The dsRNAs from the viral genome (*i.e.* from dsRNA viruses), RNA virus replicative intermediates or DNA virus-encoded transcripts are recognized and processed by plant Dicer-like (DCL) endonuclease to produce vsiRNAs (Wu *et al.*, 2019). They are subsequently incorporated into Ago-RISCs, which in turn specifically induce translational repression and/or degradation of cognate viral RNA transcripts in a sequence-specific manner (Hamilton and Baulcombe, 1999; Jin *et al.*, 2021). The use of genetically tractable model organisms such as *A. thaliana*, *C. elegans* or *D. melanogaster* has been instrumental to provide genetic evidence for a central role of RNAi components in antiviral resistance. For example, loss-of-function in *Arabidopsis DCL2*, *DCL4, AGO1* or *AGO2* was shown to increase the replication of various phytopathogenic viruses (Deleris *et al.*, 2006; Harvey *et al.*, 2011; Morel *et al.*, 2002). Similar observations were also made in *C. elegans*, whereby inactivation of the *Argonaute RNA Interference-deficient 1* (*RDE-1*) was found to enhance viral replication from a transgenic-based viral RNA expression system, but also during infection of a natural virus of nematodes (Félix *et al.*, 2011; Lu *et al.*, 2005). The central role of RNAi in antiviral resistance has also been demonstrated in *D. melanogaster*, because the Dicer-2 and Ago2-defective mutants were shown to exhibit increased viral load during infections of major fruit fly viral pathogens (Galiana-Arnoux *et al.*, 2006; van Rij *et al.*, 2006; Wang *et al.*, 2006a). As a counter-defense, plant and invertebrate viruses encode proteins that interfere with host RNAi pathways, termed RNA silencing suppressors (RSSs) or viral suppressors of RNA silencing (VSRs), further highlighting a major role of RNAi in antiviral resistance. Many VSRs have been identified from phytopathogenic viruses (Diaz-Pendon *et al.*, 2007; Jin *et al.*, 2021; Kasschau *et al.*, 2003; Mallory *et al.*, 2002; Voinnet *et al.*, 1999), and we know now that most, if not all, plant viruses encode VSR proteins (see section VI of this thesis chapter for further details). VSRs from natural and non-adapted viral pathogens of *D. melanogaster* have also been reported and play a major role in promoting viral replication (Berry *et al.*, 2009; Li *et al.*, 2002; van Rij *et al.*, 2006; Wang *et al.*, 2006a).

II.II. INTERFERON AND ANTIVIRAL SIRNA-MEDIATED GENE SILENCING IN MAMMALS

RNAi is a well-established antiviral defense mechanism in plants and invertebrates, however its role in mammalian antiviral defense has just recently emerged and is still under debate (Berkhout, 2018a; Ding *et al.*, 2018). The mammalian antiviral defense relies on an innate immune response implicating the production of type I IFNs (mainly IFNα and IFNβ) and type III IFNs (IFNλ) through the sensing of viral dsRNAs (Figure 1.5). More specifically, the dsRNAs are recognized by Pattern Recognition Receptors (PRRs), including Toll-like receptor 3 (TLR3) or RIG-I-like receptors (RLRs) family, such as retinoic acid inducible gene I (RIG-I; also known as DDX58), melanoma-differentiation-associated gene 5 (MDA5; also known as IFIH1) and Laboratory of genetics and physiology 2 (LGP2) (Schlee and Hartmann, 2016). The recognition of dsRNAs typically results in the activation of Interferon regulatory factor 3 (IRF-3), IRF-7 and NF-κB transcription factors, and ultimately triggers the production of IFN. The IFN production is detected by specific receptors (*i.e.* IFNAR, IL-28R), from the stimulated cells or the surrounding and distal cells, which in turn trigger the activation of the JAK-STAT pathway and the transcriptional activation of hundreds of interferon-stimulated genes (ISGs) (Crosse *et al.*, 2018; Lee and Ashkar, 2018). ISGs encode antiviral proteins that inhibit viral replication and enhance adaptive immune response against the targeted virus (Crosse *et al.*, 2018; Schneider *et al.*, 2014). It is noteworthy that viral dsRNAs are also recognized by a group of ISGs, including Protein Kinase R (PKR; also known as eIF2AK2), 2'-5'-oligoadenylate synthetase 1 (OAS1), and Adenosine Deaminase Acting on RNA 1 (ADAR1).

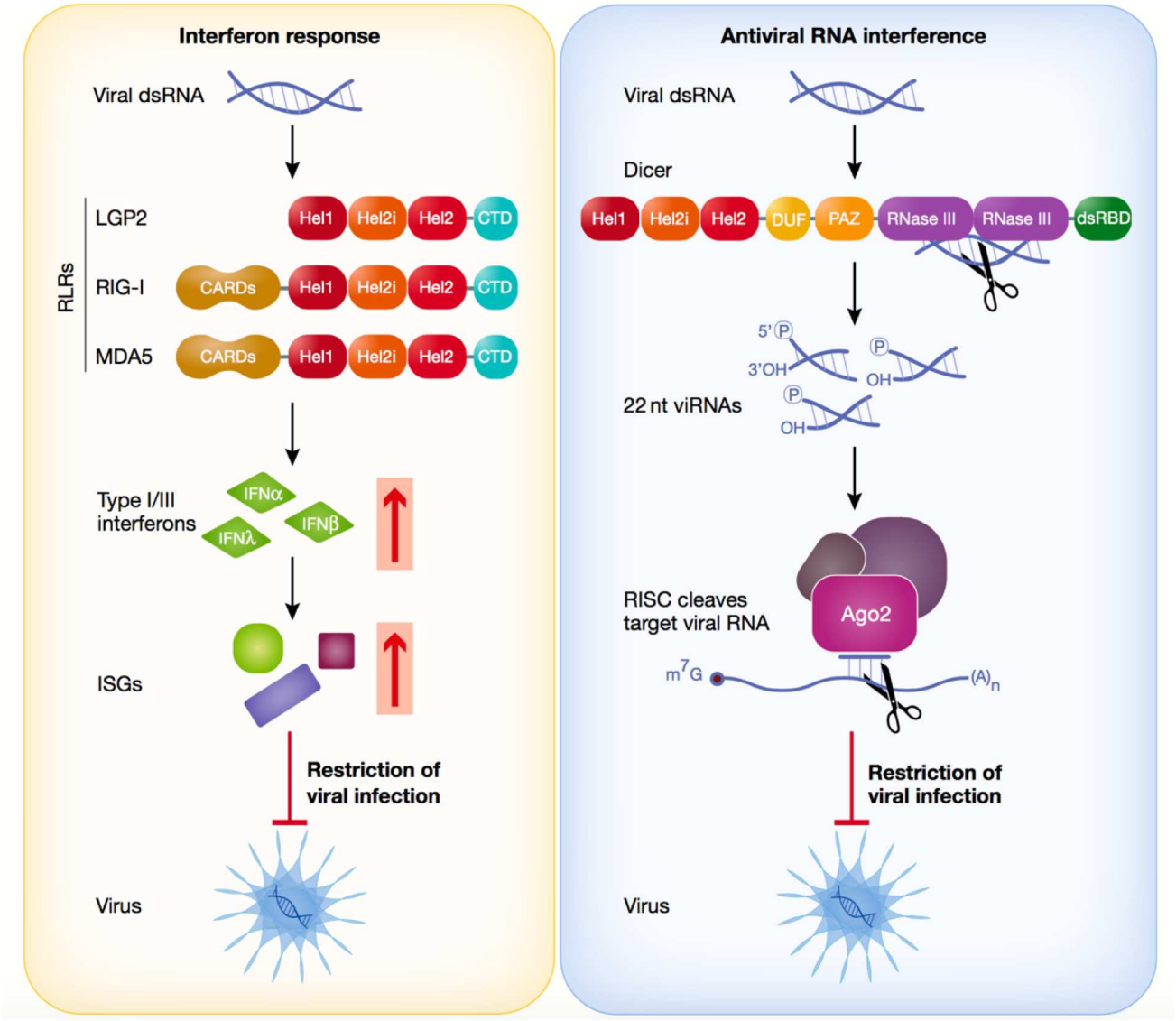

Figure 1.5. Mammalian IFN response and antiviral RNAi triggered by viral double-stranded RNA.
On the left, the interferon (IFN) response is illustrated. Three RIG-I-like receptors (RLRs), laboratory of genetics and physiology 2 (LGP2), retinoic acid inducible gene I (RIG-1) and melanoma-differentiation-associated gene 5 (MDA5) recognize double-stranded RNAs (dsRNA) in the cytoplasm of human cells to initiate antiviral innate immune responses. The caspase recruitment domain (CARD) of RIG-1 and MDA5 transduces the signal leading to the transcriptional activation of type I or III IFNs (IFNα, β for type I IFN and λ for type III). LGP2, which is not competent for signaling, regulates RIG-1 and MDA5 by acting as a dominant-negative inhibitor. IFNs induce signaling in a paracrine and autocrine manner via their recognition by interferon-α/β receptor (consisting of two subunits, IFNAR1 and IFNAR2). This activates the Janus Kinase/Signal Transducers and Activators of Transcription (JAK-STAT) pathway that triggers the induction of a broad range of interferon-stimulated genes (ISGs), which encode proteins capable of restricting viral infection. On the right, the antiviral RNA interference (RNAi) is shown. Antiviral RNAi is initiated by the sensing and cleavage of dsRNAs into duplexes of viral-derived siRNAs (vsiRNAs) by Dicer through its two RNase III domains. The vsiRNA are then loaded into Argonaute (Ago)-containing RNA silencing-induced complex (RISC), which can target complementary viral RNAs, thereby inhibiting viral replication. The three RLRs and Dicer share a common DExD/Helicase domain refers to Asp-Glu-x-Asp/His, where "x" can be any amino acid. The conserved helicase core consists of two highly similar tandem helicase domains (Hel1 and Hel2) separated by a unique insertion (Hel2i). The overall schematic representation is derived from Maillard *et al*., 2019.

Several VSRs characterized to date are dsRNA-binding proteins essential for the suppression of RNAi, and which can therefore sequester viral dsRNAs to prevent Dicer-mediated processing. However, such activity can also be coupled with a suppression of the canonical antiviral IFN pathway. This is notably the case of *Influenza A virus* NS1 and *Vaccinia virus* E3L, which act as both suppressors of RNAi and IFN (Chinnappan *et al.*, 2014; Li *et al.*, 2004). Therefore, it was for a long time unclear whether the pathogenicity of viruses was due to their abilities to suppress the production of vsiRNAs or to inhibit the IFN response. Early studies were conducted to test the effects of dsRNAs on RNAi and siRNA production. It was notably shown that long dsRNAs were not competent in triggering RNAi in somatic differentiated cells (Caplen *et al.*, 2000; Elbashir *et al.*, 2001). By contrast, in oocytes, embryos, embryonic stem cells or embryonal carcinoma cell lines, long dsRNAs were competent for triggering RNAi (Wianny and Zernicka-Goetz, 2000; Yang *et al.*, 2001; Billy *et al.*, 2001; Paddison *et al.*, 2002). Because these pluripotent and multipotent cells are known to be hypo-responsive to IFN (D'Angelo *et al.*, 2016), it was hypothesized that dsRNA-triggered RNAi is effective in cells exhibiting an attenuated IFN response.

The RNAi and IFN responses present some similarities, since Dicer and RLRs are cytosolic RNA helicase family proteins sensing dsRNAs. In particular, the amino acid sequences of the ATPase/helicase domains of Dicer and to the RLRs LGP2, RIG-I and MDA5 were found to exhibit strong similarities (Figure 1.5) (Takahashi and Ui-Tei, 2020). Hence, the antagonism hypothesis between IFN and RNAi was further investigated in somatic differentiated cells deficient for IFN receptor. Interestingly, the expression of dsRNAs was found processed in a Dicer-dependent manner in this IFN-deficient cell lines, suggesting that dsRNA-triggered RNAi is effective in differentiated somatic cells lacking IFN (Maillard *et al.*, 2016). Subsequently, IFN signaling was shown to inhibit RNAi activity through an interaction of LPG2 with Dicer, which prevents the processing of dsRNAs into siRNAs (Figure 1.6) (van der Veen *et al.*, 2018). During *Theiler's murine encephalomyelitis virus* or *encephalomyocarditis virus* infections, it was also shown that LPG2 binds TRBP and PACT, two modulators of Dicer activity, thus inhibiting the processing of pre-miRNAs into miRNA duplexes (Takahashi *et al.*, 2018; David *et al.*, 2019; Miyamoto and Komuro, 2017). A more recent study reported that LPG2 can enhance apoptosis by upregulating apoptosis-regulatory genes through repression of TRBP-bound pre-miR-106b during *Sendai virus* infection (Takahashi *et al.*, 2020). Therefore, these findings demonstrate that the IFN pathway can modulate both siRNA- and miRNA-mediated silencing in somatic differentiated cells.

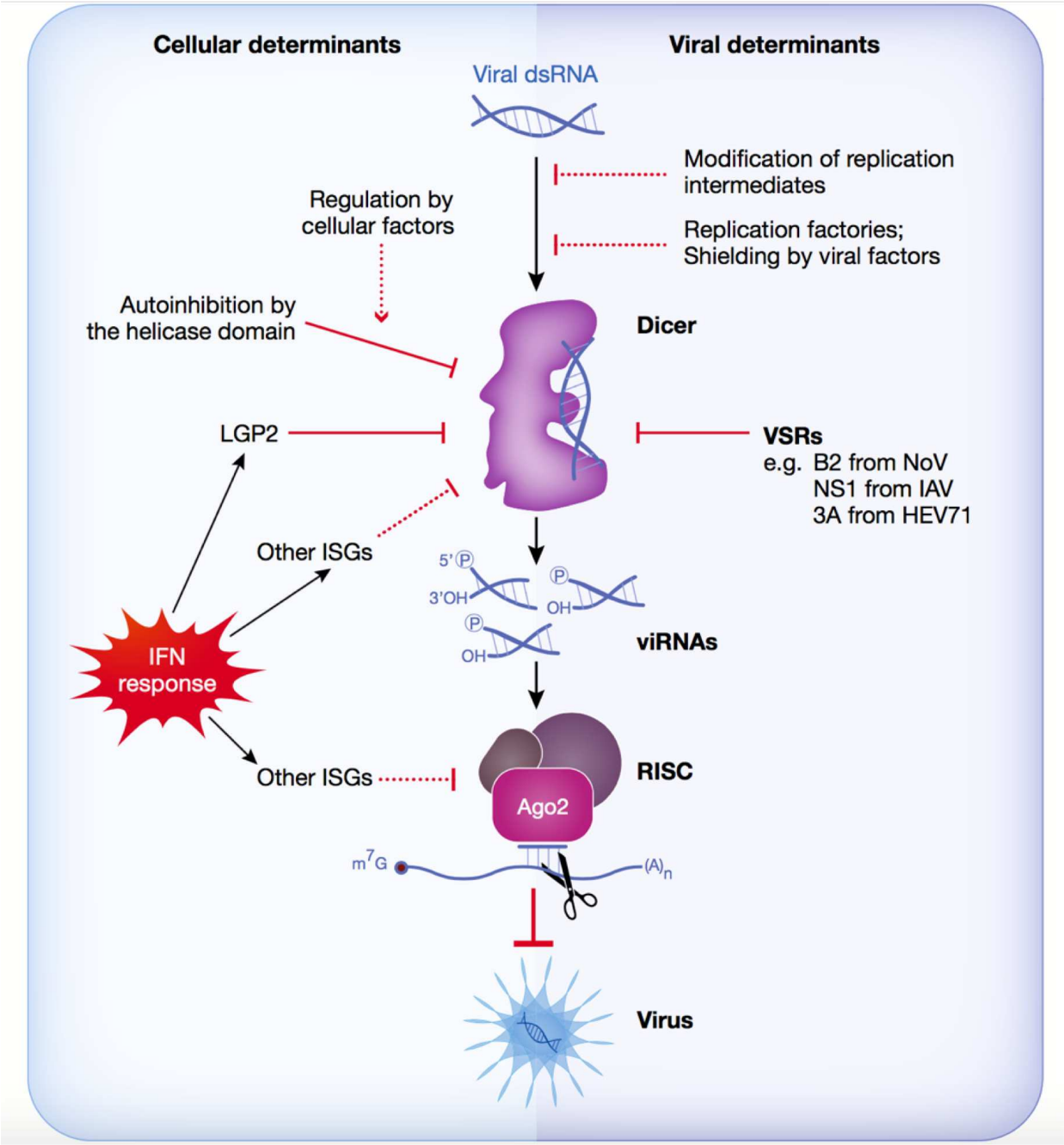

Figure 1.6. Impact of viral and cellular determinants on mammalian antiviral RNAi.
Antiviral RNA interference (RNAi) is functionally active in mammalian differentiated cells. Long viral double-stranded RNA (dsRNA) is processed into virus-derived siRNAs (vsiRNAs) that can restrict viral infection. However, mammalian-specific interferon (IFN) pathway inhibits this more ancient mechanism of antiviral defense. The catalytic activities of Dicer and RNA-induced silencing complex (RISC) are influenced by various cellular determinants. Several studies have reported that Dicer possesses an autoinhibitory activity and that the IFN pathway inhibits RNAi through induction of laboratory of genetics and physiology 2 (LGP2), which binds and negatively regulates Dicer. Putative mechanisms that can counteract RNAi have been suggested and correspond to dashed reference line. Viral determinants can also affect host RNAi at the level of dsRNA recognition and Dicer activity. One mechanism proposed is that the 5' extremities of certain viral genomes and replication intermediates can display modifications, including the cap structure, highly structured regions or 2–3 phosphates. The other determinants are the shielding of replication products from positive-sense RNA viruses often occurring in membranous structures (replication factories) or from negative-sense RNA viruses which are associated with nucleocapsid. Numerous viral suppressors of RNA silencing (VSRs) have been characterized, with only a few examples illustrated above. The overall schematic representation is derived from Maillard *et al*., 2019.

Reciprocally, PACT was determined to stimulate ATPase activity of RIG-I, which enhances IFN production during *Sendai virus* or *Ebola virus* infections (David *et al.*, 2019; Kok *et al.*, 2011). Furthermore, the complexity of crosstalk between the two signaling pathways was illustrated by the regulation the IFN-inducible PKR by three modulators of RNA silencing, TRBP, ADAR-1 and PACT (Haase *et al.*, 2005; Ota *et al.*, 2013; Patel and Sen, 1998). It has also more recently been illustrated in the context of infection of human cells by the *Sindbis virus* and *Semliki forest virus* (Montavon *et al.*, 2021). More specifically, Dicer was found to interact with several dsRNA-binding proteins and RNA helicases during infection, including PKR, through its helicase domain. Importantly the deletion of Dicer helicase domain triggered an antiviral defense response that was found dependent on PKR but not on RNAi. Finally, RNAi activity was also shown to be repressed shortly after viral infection through poly-ADP-ribosylation of Ago2 and its associated proteins, which led to an increased expression of ISGs (Seo *et al.*, 2013). This work therefore suggests that the inhibition of RISC activity could be a trigger of IFN signaling. Collectively, these studies suggest that a bi-directional crosstalk between RNAi and the IFN response seems to operate with mutual regulation through protein-protein interactions (Takahashi and Ui-Tei, 2020).

II.III. Occurrence and relevance of antiviral RNAi in mammals

The debate on the occurrence and relevance of antiviral RNAi in mammals persisted because several studies failed to detect vsiRNAs in mammalian somatic cells infected with RNA viruses (Backes *et al.*, 2014; Bogerd *et al.*, 2014; Girardi *et al.*, 2013; Parameswaran *et al.*, 2010). Furthermore, it was shown that Dicer-deficient cells did not exhibit enhanced viral titers during infection, further arguing against a role for antiviral RNAi in mammalian somatic cells (Bogerd *et al.*, 2014). One model to explain these observations was that Dicer could lack the ability to produce siRNAs from long dsRNAs in somatic differentiated cells. Consistent with this hypothesis, several studies reported that the N-terminal helicase domain of Dicer displays an autoinhibitory role on its ability to process dsRNAs into siRNAs (Figure 1.6) (Ma *et al.*, 2008; Flemr *et al.*, 2013). It was for instance shown that mouse oocytes express a Dicer isoform that lacks a N-terminal helicase domain, which results in an enhanced dsRNA-triggered processing activity of this truncated Dicer compared to the full-length Dicer (Flemr *et al.*,

2013). In addition, it was reported that vsiRNAs do accumulate upon ectopic expression of a N-terminally truncated human Dicer in somatic cells infected with IAV (Kennedy *et al.*, 2015). Despite these evidences arguing against a role for antiviral RNAi in mammals, a seminal study reported the accumulation of vsiRNAs during infection of murine embryonic stem cells (mESCs) with the *encephalomyocarditis virus* (EMCV), a positive-sense single-stranded RNA (ssRNA) which naturally infects pigs (Maillard *et al.*, 2013a). Importantly, these vsiRNAs were produced from viral dsRNA replication intermediates and exhibited hallmarks of antiviral siRNAs (*i.e*. they were Dicer-dependent, mostly 21 to 23 nt in size, displayed 2-nt 3 overhangs and were loaded in Ago2). By contrast, canonical vsiRNAs were not detected during infection of mouse differentiated mESC with EMCV (Maillard *et al.*, 2013a). Interestingly, infection of human neural progenitor cells (hNPCs) with the authentic human pathogenic *Zika virus* (ZIKV), was also subsequently shown to trigger the accumulation of vsiRNAs, exhibiting typical features or antiviral siRNAs (Xu *et al.*, 2019). Furthermore, knocking-down *Dicer* or *Ago2* in hNPCs led to an enhanced ZIKV load, while challenging hNPCs and brain organoids with the RNAi enhancer enoxacin significantly reduced viral replication (Xu *et al.*, 2019). Although these studies suggested that embryonic stem cells and progenitor cells are more prone for antiviral RNAi than differentiated somatic cells, the underlying mechanisms remained ill-defined. A very recent report has however filled the gap by showing that a Dicer isoform, which lacks a part of the N-terminal helicase segment, was found preferentially expressed in mouse and human stem cells (Poirier *et al.*, 2021). Importantly, this truncated Dicer version, named antiviral Dicer (aviD), exhibited an enhance dsRNA processing activity compared to the full-length Dicer protein, and was found required for antiviral RNAi against ZIKV and *severe acute respiratory syndrome coronavirus 2* (SARS-CoV-2) in brain organoids. Altogether, these studies suggest that pluripotent, multipotent and progenitor mammalian cells are probably the major site of antiviral RNAi, possibly to compensate for the hypo-responsiveness of these cells to IFN.

Another explanation for why vsiRNAs are not readily detectable in differentiated mammalian somatic cells infected with viruses, resides in their ability to suppress the biogenesis of siRNAs through VSRs (Figure 1.6). This phenomenon has been initially discovered during infection of rodent somatic cells and suckling mice with a *Nodamura virus* mutant that does not express B2, a VSR that suppresses dsRNA processing and incorporation of vsiRNAs into Ago proteins (Li *et al.*, 2013; Maillard *et al.*, 2013a). Similar findings were subsequently made during infection of human somatic cells with VSR-defective *human*

enterovirus 71 (HEV71) and *Influenza A virus* (IAV), which are responsible for hand-foot-and-mouth disease (HFMD) and influenza, respectively (Li *et al.*, 2016; Qiu *et al.*, 2017). In these conditions, the slicing activity of human Ago2 was found necessary to target and degrade viral RNAs, and to restrict viral replication in host cells in an IFN-dependent manner. These findings provided evidence that antiviral RNAi can also operate in somatic cells, but solely upon infection with VSR-defective viruses. However, a few very recent reports indicate that vsiRNAs could additionally accumulate *in vivo* in differentiated tissues. For example, somatic vsiRNAs were detected in murine muscle tissues that cannot respond to IFN-α/β and from the murine central neuron system (Zhang *et al.*, 2020). Furthermore, one study demonstrated that the NS2A protein of *dengue virus-2* acts as a *bona fide* VSR in the context of infection to evade antiviral activity in mice and also in the natural vector of this virus, *Aedes* mosquito cells (Qiu *et al*., 2020). The involvement of other RNAi components than antiviral Dicer and Ago2 has also been reported. For example, the catalytically inactive mouse Ago4 was recently shown to promote antiviral resistance against different RNA viruses (Adiliaghdam *et al.*, 2020). This function was independent of, and complementary to, the IFN-dependent immune pathway. Furthermore, Ago4 was found to limit disease symptoms as well as viral titers in mouse lungs infected with *influenza virus* (Adiliaghdam *et al.*, 2020). Therefore, although cell-based studies have revealed that somatic differentiated cells are not competent for antiviral RNAi, *in vivo* studies suggest that some differentiated tissues can still mount antiviral RNAi. Nevertheless, additional *in vivo* studies are needed to challenge the latter possibility.

II.IV. BIOGENESIS AND FUNCTIONS OF VIRAL-DERIVED MIRNAS

In recent years, the role of miRNAs in the establishment of antiviral immune responses has been a subject of intense research interest. The first miRNAs of viral origin –also referred to as v-miRNAs– have been described during infection of the DNA virus *Epstein-Barr virus* (EBV) (Pfeffer *et al.*, 2004). Subsequently, other viral-encoded miRNAs were detected during lytic infection with *herpes simplex virus-1* (HSV-1), and were found loaded into RISC (Cui *et al.*, 2006; Flores *et al.*, 2013). Several studies have investigated the mechanism by which v-miRNAs are produced (Zhan *et al.*, 2020). It has notably been shown that Drosha and Dicer are required for this process (Mishra *et al.*, 2020). Most v-miRNAs were identified following infections with DNA viruses whereas the production of v-miRNAs during infection of RNA

viruses remains controversial. In addition, some miRNA-like RNA fragments have been detected through non-canonical processing processes (Shapiro *et al.*, 2010; Varble *et al.*, 2010). The host cellular functions that are targeted by v-miRNAs include immune evasion, autoregulation of the viral life cycle and tumorigenesis (Mishra *et al.*, 2020; Sullivan *et al.*, 2005; Umbach *et al.*, 2008; Vojtechova and Tachezy, 2018; Zhan *et al.*, 2020). Additionally, host miRNAs also contribute to the regulation of antiviral immunity. Several reports have characterized individual miRNAs which directly target virus and restrict viral production in human cells and mouse (Girardi *et al.*, 2018). Conversely, some cellular miRNAs can positively regulate viral replication and pathogenicity (Gottwein and Cullen, 2008; Trobaugh and Klimstra, 2017). The expression of host miRNAs can also be regulated through the IFN pathway, which points to the existence of some IFN-regulated miRNAs. This kind of IFN-modulated miRNAs inhibit specific viruses, but one, miR-342-5p exhibited broad antiviral resistance by regulating the sterol pathway, known to be an integral part of the macrophage IFN response (Robertson *et al.*, 2016). There is now growing evidence that multiple host miRNAs directly modulate the production of type-I IFN (Forster *et al.*, 2015), thereby modulating viral infections.

III. SMALL RNAS ACT AS FUNDAMENTAL REGULATORS OF HOST-BACTERIA INTERACTIONS

III.I. ROLE AND REGULATION OF MAMMALIAN MIRNAS DURING INNATE IMMUNITY AND HOST-BACTERIA INTERACTIONS

Although mammalian miRNAs were initially characterized in cell proliferation, apoptosis and various pathologies, including cancer and cardiovascular diseases, they have also been extensively studied in the context of host-pathogen interactions (Adams *et al.*, 2014; Aguilar *et al.*, 2019; Bueno *et al.*, 2008; Jovanovic and Hengartner, 2006; Quiat and Olson, 2013). In particular, the regulation of miRNAs have been initially characterized upon stimulation of human cells with lipopolysaccharide (LPS) or lipomannan (LM), which are major components of outer membrane of Gram negative bacteria or mycobacterium cell wall, respectively (Taganov *et al.*, 2006; Tili *et al.*, 2007; Rajaram *et al.*, 2011). The regulation of miRNA expression were subsequently investigated during infections with diverse human pathogenic bacteria, such as *Helicobacter pylori*, *Salmonella enterica*, *Pseudomonas aeruginosa*, *Mycobacterium*, *Listeria monocytogenes* and *Staphylococcus aureus* (Maudet *et al*., 2014a; Das *et al*., 2016; Zhou *et al.*, 2018). The use of different human pathogens was instrumental to establish the specific profiling of host miRNAs expression in response to these microbes (Jin *et al.*, 2014).

The recognition of pathogen components is carried out by distinct classes of Pattern Recognition Receptors (PRRs) in humans, including Toll-like receptors (TLRs), RIG-I-like receptors (RLRs), Nod-like receptors (NLRs), AIM2-like receptors (ALRs), C-type lectin receptors (CLRs), and intracellular DNA sensors such as cGAS (Gulati *et al.*, 2018). In particular, TLRs are the most characterized PRRs and ensure the sensing of many different pathogens. Pathogen-Associated Molecular Patterns (PAMPs) recognition can induce two pathways, one of them depends on the TLR adapter Myeloid differentiation primary response protein (MyD88), while the other one relies on Toll/IL-1R domain-containing adaptor-inducing IFN-β (TRIF). As an example, the TRIF-dependent signaling pathway is specifically triggered by TLR3, whereas TLR4 activates both pathways (Kawasaki and Kawai, 2014). Once activated, these pathways trigger either nuclear factor Kappa B (NF-κB), mitogen-activated protein kinases (MAPK) or interferon regulatory factor 3 (IRF3) signaling culminating in the secretion

of pro-inflammatory cytokines and IFN (Kawasaki and Kawai, 2014). Interestingly, the deletion of *dicer1* in human macrophages, which results in the depletion of a large set of miRNAs, reduces the production of inflammatory cytokines during innate immune activation (Gantier *et al*., 2012). This observation suggests that miRNAs could act as modulators of inflammatory responses. Consistent with this hypothesis, many TLR-responsive miRNAs have been identified, including miR-21, miR-29, miR-146, miR-155 and let-7 families, and were found to play critical roles in the regulation of innate immune responses (Aguilar *et al.*, 2019; Androulidaki *et al.*, 2009; Nejad *et al.*, 2018; Taganov *et al.*, 2006). More specifically, these miRNAs, and many others, were shown to regulate different steps of the TLR signaling, such as TLR expression, downstream signaling components, TLR-induced genes like cytokines and transcription factors (Figure 1.7) (O'Neill *et al.*, 2011). The in-depth functional characterization of these miRNAs indicates that a subset of them act either as anti-inflammatory and/or pro-inflammatory factors.

III.II. TLR-DEPENDENT MIRNAS

Among TLR-dependent miRNAs, miR-155 was found up-regulated in the presence of different pathogens. This miRNA was notably shown to positively regulate antibacterial resistance since miR155-deficient mice are more susceptible to *Citrobacter rodentium* compared to wild-type infected mice (Clare *et al.*, 2013). MicroRNA-155 can act as a pro-inflammatory modulator by silencing different targets of TLR signaling, such as the suppressor of cytokine signaling 1 (SOCS1) and the critical negative regulator of immune cell activation, SH-2 containing inositol 5' polyphosphatase 1 (SHIP1) (Lu *et al.*, 2009; O'Connell *et al.*, 2009; Rodriguez *et al.*, 2007). In turn, this miR-155-dependent regulation activates tumor necrosis factor α (TNF-α), interleukin-6 (IL-6), and IL-12 pro-inflammatory cytokines production and reduces the expression of the anti-inflammatory cytokine IL-10 (Billeter *et al.*, 2014). In addition, miR-155 was found to regulate humoral response, by allowing antigen-driven B cell maturation, T and B cell immunity, germinal center formation, and the persistence and/or differentiation of immunoglobulin class switched plasma cells (Clare *et al.*, 2013; Rodriguez *et al.*, 2007; Vigorito *et al.*, 2007). However, miR-155 has also been reported to negatively regulate TLR-signaling because this miRNA was found to repress TGF-beta-activated kinase 1 and MAP3K7-binding protein 2 (TAB2), NF-κB-inducing kinase (NIK), I-kappa-B kinase

epsilon (IKKε), Myd88, receptor-interacting serine-threonine kinase 1 (RIPK1), endothelial nitric oxide synthase (eNOS) and NF-κB subunit p65, which are all key signaling molecules required for the expression of type I IFN and some interleukins (Thai *et al.*, 2007; Tili *et al.*, 2007; Ceppi *et al.*, 2009; Zhou *et al.*, 2010; Tang *et al.*, 2010; Tili *et al.*, 2007; Wu *et al.*, 2014). Overall, miR-155 exerts both pro- and anti-inflammatory effects during innate immune induction.

Another extensively studied TLR-dependent miRNA is the miR-146 family, composed of miR-146a and miR-146b. MicroRNA-146a is the first PAMP-induced human miRNA that has been described in the literature (Taganov *et al.*, 2006). This miRNA locus is transcriptionally activated in response to various PAMPs including bacterial-derived LPS and flagellin (Taganov *et al.*, 2006). Both miR-146a and -146b act mainly as anti-inflammatory modulator, as they were shown to repress Interleukin-1 receptor-associated kinase 1 (IRAK1), IRAK2 and TNF receptor-associated factor 6 (TRAF6) transcripts, required for the activation of NF-κB signaling (Taganov *et al.*, 2006; Schulte *et al.*, 2013; Hou *et al.*, 2009). Moreover, miR-146b was also shown to silence MyD88 and TLR4 (Curtale *et al.*, 2013). Interestingly, miR-146 and miR-155 are responsive to different environmental stimuli, and act non-redundantly on TLR4 response through functional specialization (Schulte *et al.*, 2013). First of all, LPS triggers the transcriptional activation of miR-146a, while it does not alter miR-155 expression, a regulatory mechanism which was proposed to maintain endotoxin tolerance in macrophages (Doxaki *et al.*, 2015). Reciprocally, one NLR, the nucleotide-binding oligomerization domain 2 (NOD2) receptor, recognizes bacterial peptidoglycan (PNG) of intracellular bacteria, and enhances miR-155 expression, while it does not regulate miR-146 (Schulte *et al.*, 2013). This regulatory mechanism ultimately limits pro-inflammatory signaling. This sophisticated regulation allows macrophages to adjust their inflammatory responses upon pathogen detection.

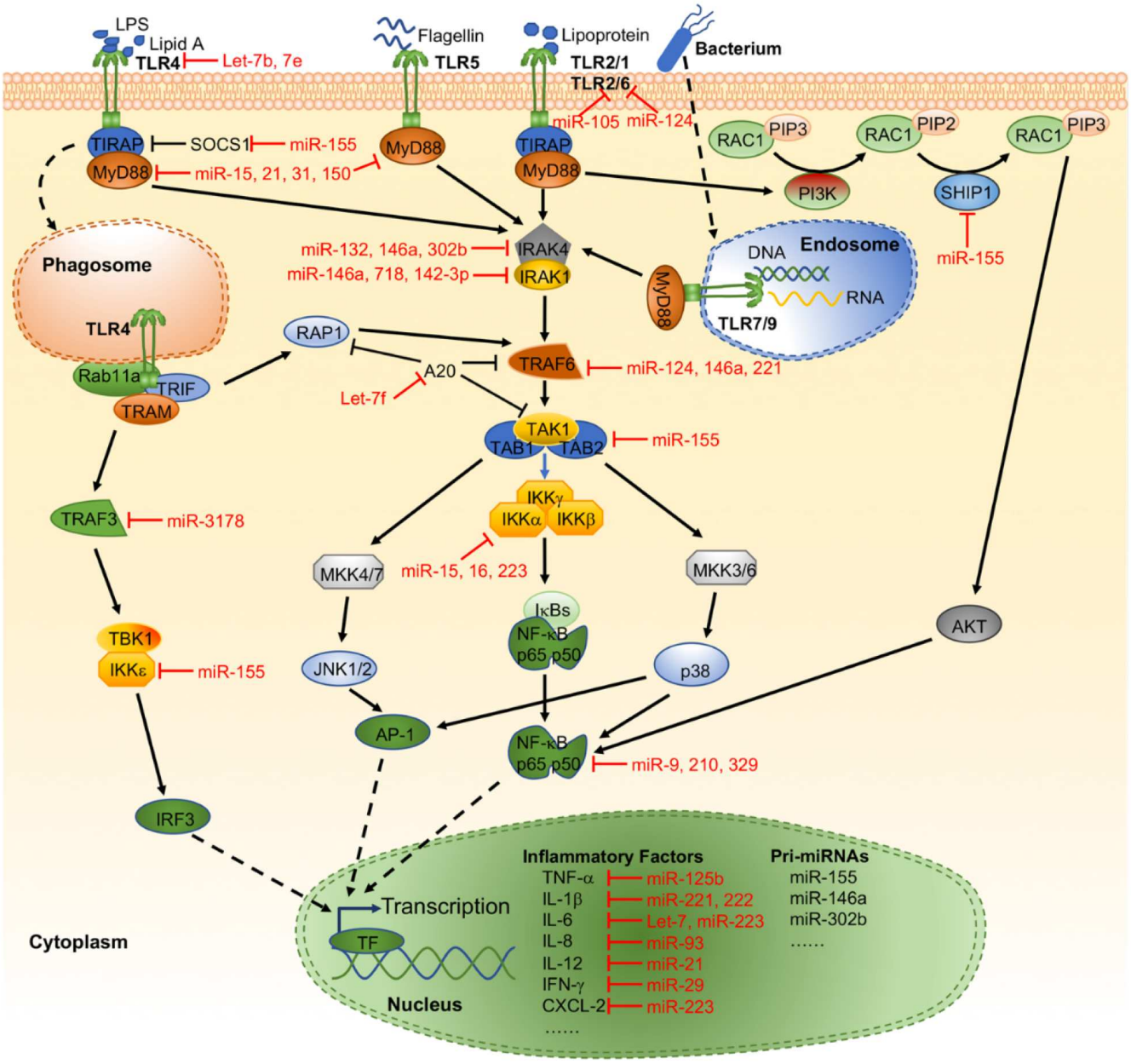

Figure 1.7. Roles of human miRNAs in the regulation of TLR signaling upon bacterial elicitations.
Different bacterial components are recognized by Toll-like receptors (TLRs) and lead to the activation of intracellular immune signaling pathways. Various inflammatory factors are subsequently produced by different transcription factors. TLR-mediated signaling can profoundly reprogram miRNA expression, and some individual miRNAs have been characterized in the modulation of inflammatory responses. Among the most studied miRNAs, miR-146 and miR-155 were found to act mainly as negative feedback regulators of TLR signaling. In addition, miR-125b was shown to inhibit Tumor Necrosis Factor α (TNF-α) production, while Let-7 miRNA and miR-21 were found to repress TLR4 activation. LPS, lipopolysaccharide; TF, transcription factor. The overall schematic representation is derived from Zhou *et al.*, 2018.

The miR-21 is one of the most highly expressed miRNAs in many tissues. This miRNA also negatively regulates inflammatory responses and acts as a central repressor of the anti-inflammatory response in macrophages (Sheedy, 2015). Several studies reported that miR-21 silences phosphatidylinositol 3,4,5-trisphosphate 3-phosphatase and dual-specificity protein phosphatase (PTEN), glycogen synthase kinase 3 β (GSK3β) and programmed cell death protein 4 (PDCD4), which collectively decrease the production of TNF-α in response to LPS (Das *et al*., 2014; Sheedy *et al*., 2010). Moreover, miR-21 prevents the up-regulation of vitamin D-dependent antimicrobial pathway (Liu *et al.*, 2012). On the other hand, avirulent mycobacterial strain BCG or *Mycobacterium leprae*, induces an up-regulation of miR-21 to escape immune responses or to promote disease development (Liu *et al*., 2012; Wu *et al.*, 2012).

The let-7 miRNAs (let-7a/c/d/f/g/i) represent another well-characterized family of immune regulators. This family is repressed upon bacterial infections in a NF-κB-dependent manner (Iliopoulos *et al.*, 2009; Hayashi *et al.*, 2013). The let-7 miRNAs family was shown to control several immune-modulatory targets, including cytokines IL-6 and IL-10, TLR4, the feedback inhibitor of the NF-κB pathway deubiquitinating enzyme A20 (also known as TNF-α-induced protein 3 [TNFAIP3]) or some components of the mTOR pathway (Iliopoulos *et al.*, 2009; Schulte *et al.*, 2011; Teng *et al.*, 2013; Marcais *et al.*, 2014; Kumar *et al.*, 2015). MicroRNA-29 is an another known miRNA involved in the regulation of innate immune responses, and was shown to target IFN-γ production, which is essential to control the replication of intracellular bacteria (Ma *et al.*, 2011). Upon infections of natural killer cells during systemic infection of mice by *Listeria monocytogenes* and *Mycobacterium bovis bacillus Calmette Guérin* (BCG), this miRNA was notably found to be down-regulated, thereby leading to IFN-γ production and antibacterial resistance (Ma *et al.*, 2011). Finally, the miR-125b was shown to be induced during *Mycobacterium tuberculosis* infection, which results in the silencing of TNF-α mRNA, followed by a reduction in TNF-α biosynthesis (Tili *et al.*, 2007).

Numerous other inflammatory-related miRNAs have been recently identified (Chandan *et al.*, 2019). For instance, a genome-wide miRNA profiling has been characterized in human dendritic cells infected with various mycobacterium pathogens, *Staphylococcus epidermidis*, *Salmonella typhimurium* or *Yersinia pseudotuberculosis*. This study revealed that 49 miRNAs were differently expressed by all bacterial challenges and represent a core of generally stress-

responsive miRNAs (Siddle *et al.*, 2015). By contrast, other miRNAs were differentially expressed during specific bacterial pathogen infection, including an induction of miR-132/212 family in response to mycobacterial infection. In addition, the authors observed that bacterial infections modulate the relative abundance of miRNA hairpin arms as well as miRNA isoforms, highlighting another level of miRNA regulation during host-bacteria interactions.

III.III. MICRORNAS MODULATE DIVERSE INFLAMMATORY PROCESSES

TLR-dependent signaling is strongly controlled by miRNA activities, but other inflammatory mechanisms are also regulated by these small non-coding RNAs (Rebane and Akdis, 2013; Chandan *et al.*, 2019). For example, all stages of macrophage life cycle, from the production to the differentiation, were found to be regulated by miRNAs. One example of such miRNA-dependent regulation occurs at the level of macrophage polarization, which is a crucial step for *M. tuberculosis* pathogenesis. Macrophage polarization refers to the process by which they produce distinct functional phenotypes, into classically activated (M1) and alternatively activated (M2) macrophages. Upon *M. tuberculosis* infection, miR-26a is down-regulated which in turn increases expression of its target, the transcription factor Krüppel-like factor 4 (KLF4), and further favors M2 polarization linked to the persistence of bacterial pathogens (Sahu *et al.*, 2017). Conversely, down-regulation of miR-20b upon infection prevents M1 to M2 macrophage polarization through repression of nucleotide-binding oligomerization domain-like receptor pyrin domain-containing protein 3 (NLRP3) (Lou *et al.*, 2017). Another inflammatory mechanism affected by miRNAs are antigen presentation of macrophages or dendritic cells (Martinez-Nunez *et al.*, 2009). Upon *H. pylori* infection, a down-regulation of miR-4270 has been detected, which in turn alters macrophage ability to express and expose major histocompatibility complex class II (MHC class II) molecules, thereby preventing their recognition and activation by T cells (Pagliari *et al.*, 2017). The antigen-presenting ability is also impacted by miR-381-3p in *M. tuberculosis* infected dendritic cells (Wen *et al.*, 2016). In addition, the recruitment of immune cells to infection site, such as macrophages or neutrophils, was found to be regulated by some miRNAs, such as miR-223 and miR-128 during *M. tuberculosis* and *S. enterica* infections, respectively (Dorhoi *et al.*, 2013; Zhang *et al.*, 2014). Other types of immune cells are controlled by specific miRNAs, like the differentiation of granulocytes towards neutrophils and then their activation, which are critical for the first line

of defense against bacteria (Johnnidis *et al.*, 2008). Some miRNAs were also found required for dendritic cells differentiation from monocytes (Hashimi *et al.*, 2009). These cells exert a key role as a bridge of innate and adaptive immune responses. The adaptive immunity is achieved through activation and clonal expansion of T- and B-cells. A set of miRNAs was extensively associated with the regulation of adaptive immune response by modulating the development, activation, survival, and proliferation of T- and B-cells (Chandan *et al.*, 2019).

III.IV. MICRORNAS AS MODULATORS OF AUTOPHAGY AND APOPTOSIS IN THE CONTEXT OF HOST-BACTERIA INTERACTIONS

Autophagy is a major process involved in the recycling of damaged macromolecules and cytosolic organelles (Dikic and Elazar, 2018). Hence, autophagy is also an important component of innate immune response against bacterial infection to capture and degrade intracellular bacteria (Huang and Brumell, 2014). Different Mycobacterium species illustrate the importance of this regulatory mechanism. During infection with *M. tuberculosis* and BCG, bacteria evade host protective immune responses using miRNA-dependent mechanisms to suppress autophagy (Duan *et al.*, 2015; Kumar *et al.*, 2016; Kim *et al.*, 2017). The roles of miRNAs in the regulation of autophagy have been well-characterized (Figure 1.8A) (Zhou *et al*., 2018; Aguilar *et al*., 2019; Silwal *et al*., 2020). A recent study focused on the activation of miRNAs in human macrophages upon *Legionella pneumophila* infection. The authors found that a trio of miRNAs affect intracellular *L. pneumophila* replication in a cooperative manner (Herkt *et al.*, 2020). Among these three miRNAs, miR-579 targets galectin-8 (LGALS8), known to be an anti-bacterial restriction factor, by targeting damaged vesicles for autophagy to protect cells against bacterial invasion (Thurston *et al.*, 2012). Finally, host cell death is often triggered as part of the immune defense. Pathogens employ diverse strategies to regulate apoptosis for their own benefit, and numerous miRNAs participate in the control of bacteria-mediated apoptosis (Figure 1.8B) (Zhou *et al*., 2018; Aguilar *et al*., 2019).

Overall, these studies, among many others that are not described here, highlight the critical role of miRNAs in fine-tuning the host immune responses. This post-transcriptional regulation is notably essential to clear bacterial infection, while protecting the organism from deleterious effects that would be caused by a sustained inflammation. There are also emerging

evidence indicating that pathogens have developed strategy to exploit miRNA-mediated repression of inflammatory immune signaling to subvert host defense and to promote bacterial survival in infected cells.

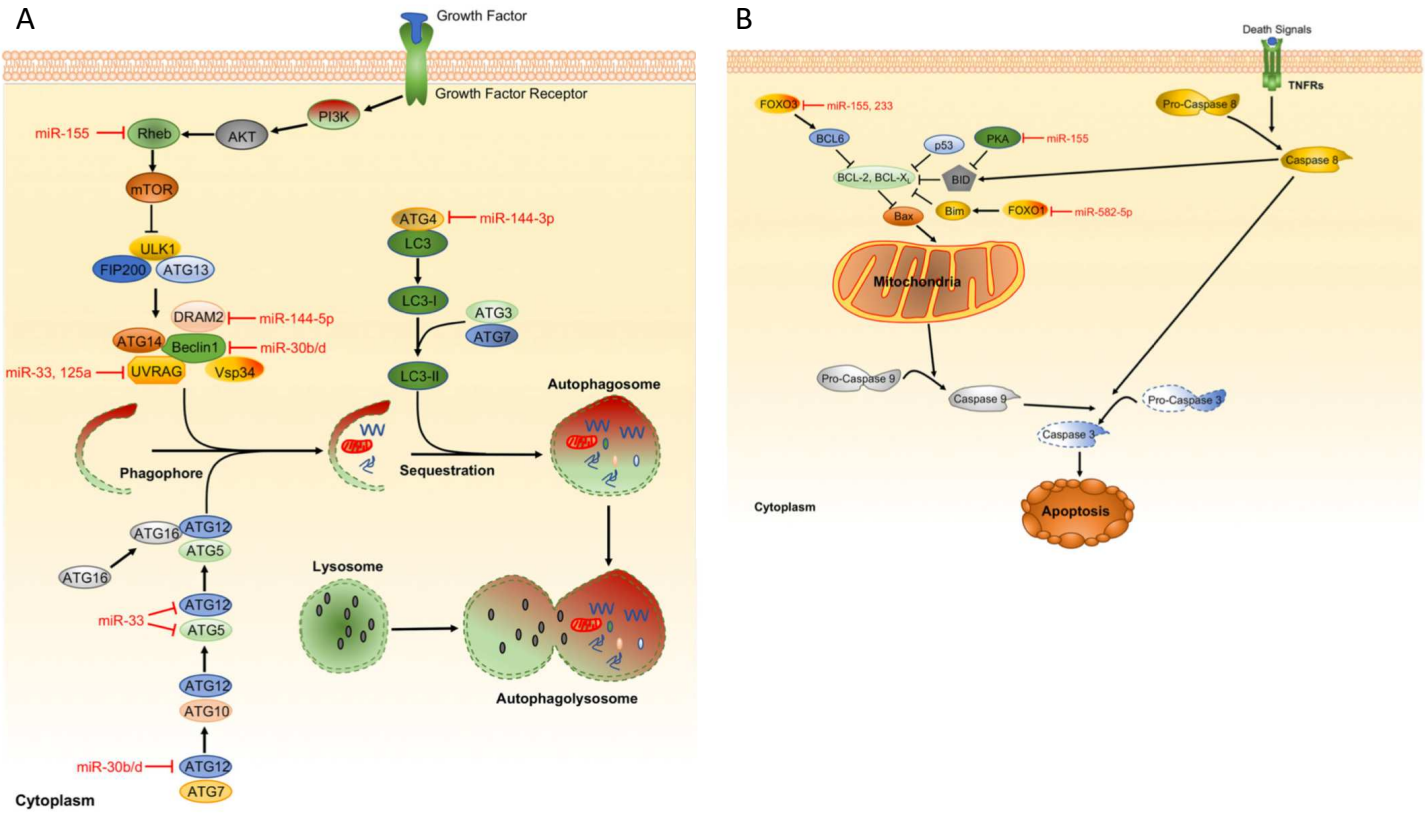

Figure 1.8. Roles of human miRNAs in the regulation of autophagy and apoptosis signaling
Autophagy and apoptosis are important responses that eliminate a wide range of bacterial pathogens. **(A)** As a counter-defense, bacteria have developed the ability to interfere with host autophagy. Some miRNAs target autophagy-related gene transcripts, which encode specialized immune effectors and effectively modulate host innate immune responses. **(B)** Bacteria can also activate several host proapoptotic proteins and miRNAs to induce apoptosis. Upon infection, some miRNAs were shown to be involved in signaling networks that control innate immunity and apoptosis pathways. The overall schematic representation is derived from Zhou *et al.*, 2018.

IV. ROLES OF SMALL RNAS ON CELLULAR PROCESSES DURING HOST-BACTERIA INTERACTIONS

IV.I. ROLES OF HOST SMALL RNAS DURING SYMBIOSIS

There are emerging studies describing the differential regulation of mammalian miRNAs in response to commensal bacteria. For example, host miRNAs were found differentially expressed in response to the gut microbiota in mice. One study using germ-free mice colonized with gut microbiota revealed nine differentially expressed miRNAs in the ileum and the colon (Dalmasso *et al.*, 2011). One of these miRNAs was shown to regulate a multidrug resistance-associated protein, which is involved in the metabolism of xenobiotic and endogenous toxins, an intestinal function dysregulated in response to colonization of mice. Another study reporting the miRNA profiling of murine caecal revealed that 16 miRNAs were differentially expressed in the presence of commensal bacteria (Singh *et al.*, 2011). In addition, a comparison between intestinal epithelial cells from conventional and germ-free mice reported the up-regulation of miR-21-5p by the gut microbiota, which regulates cellular permeability (Nakata *et al.*, 2017). All these reports shed light on a host miRNA regulation by the gut microbiota and further in-depth characterization are needed to determine the possible relevance of such miRNA-dependent regulation in the control of bacterial infections in the gut and of the gut homeostasis.

IV.II. CROSS-KINGDOM RNAI DURING HOST-BACTERIA INTERACTIONS

During the last decade, it became evident that small RNAs can be transferred between two eukaryotic partners to impact their relationship, through the regulation of complementary target genes. This general process, referred to as "cross-kingdom RNAi" (Liu *et al.*, 2017; Zeng *et al.*, 2019), constitutes a key mechanism of communication between organisms. In plant-parasitic and plant-fungi interactions, like Arabidopsis infections by the oomycete *Phytophtora capsica* and the fungi *Botrytis cinerea* or *Verticillium dahliae*, host miRNAs and/or secondary siRNAs have been shown to trigger silencing of virulence and/or of essential genes from these pathogens (Cai *et al.*, 2018; Hou *et al.*, 2019; Huang *et al.*, 2019; Hudzik *et al.*, 2020; Wang *et al.*, 2016). The transfer of such sRNAs from plant cells towards *P. capsica* and *B. cinerea* cells

was found to be orchestrated by extracellular vesicles (EVs) (Cai *et al.*, 2018; Hou *et al.*, 2019). Even though eubacteria have no "classical" RNAi machinery, there are increasing evidences for eukaryote-prokaryote trans-kingdom RNAi. For instance, mice fecal miRNAs have previously been shown to enter bacteria, such as *Fusobacterium nucleatum* and *Escherichia coli*, thereby modulating their gene expression and growth (Liu *et al.*, 2016) . In addition, ginger exosome-like nanoparticles containing miRNAs have recently been shown to selectively silence the expression of genes from the gut commensal bacterium *Lactobacillus reuteri* (Teng *et al.*, 2018). Importantly, this regulatory mechanism is functionally relevant because it was found to modulate the gut microbiota composition, metabolites production, and growth, thereby reducing mouse colitis (Teng *et al.*, 2018). Ginger exosome-like nanoparticles carrying miRNAs were also recently found to be taken-up by the oral bacterial pathogen *Porphyromonas gingivalis*, thereby reducing the expression of specific virulence factors (Sundaram *et al.*, 2019). A very recent study provides also solid evidence of cross-kingdom RNAi between host alveolar epithelial cells and *Pseudomonas aeruginosa*. More specifically, it was shown that human alveolar epithelial cells produce EV-embedded miRNAs that are transferred to *P. aeruginosa* cells (Koeppen *et al.*, 2021). Among these endogenous cargo, let7b-5p was retrieved in *P. aeruginosa* cells and found to reduce the abundance of bacterial proteins that are essential for biofilm formation, including PpkA and ClpV1-3 (Koeppen *et al.*, 2021). The transferred miRNA was also determined to increase the ability of beta-lactam antibiotics to reduce biofilm formation through the targeting of the beta-lactamase AmpC (Koeppen *et al.*, 2021) . Overall, these findings indicate that both human miRNAs and exogenous plant miRNAs can directly and selectively modulate the expression of genes from commensal or pathogenic bacteria.

IV.III. ROLE OF MAMMALIAN MIRNAS ON CELL-DIVISION CYCLE

It is now well-established that mammalian miRNAs act as crucial regulators of cellular processes during host-bacteria interactions (Aguilar *et al.*, 2019). Mammalian pathogenic bacteria can, for instance, interfere with cell-division cycle, the cytoskeleton, iron homeostasis or post-translational modifications (Das *et al.*, 2016; Aguilar *et al.*, 2019). Apoptosis and autophagy, which are processes related to immunity, are also tightly controlled by miRNAs and were discussed in the previous section. The control of cell-division cycle by human pathogenic bacteria has also emerged as an important miRNA-dependent regulatory process (Figure 1.9). The differential regulation of mammalian miRNAs regulating gastric epithelial cell cycle during *Helicobacter pylori* infection is one of the best characterized examples. In particular, this bacterium was found to up-regulate a subset of human miRNAs, which represses the expression of known regulators of cell cycle, thereby promoting bacterial proliferation and invasion (Aguilar *et al.*, 2019). Other human cell-cycle-regulating miRNAs were found down-regulated during *H. pylori* infection, such as miR-372 and miR-373 (Belair *et al.*, 2011). This regulatory mechanism led to the derepression of large tumor suppressor homolog 2 (LATS2), which results in a cell cycle arrest at the G1/S transition (Belair *et al.*, 2011). In some cases, the transcriptional dysregulation of these miRNAs is caused by DNA methylation of their promoters, as reported at the miR-210 and let-7 miRNA loci (Hayashi *et al.*, 2013; Kiga *et al.*, 2014). Additionally, a recent study demonstrated that the most up-regulated miRNAs in *Helicobacter*-positive gastric cancer tissues, including miR-143-3p, are able to attenuate cell growth, apoptosis, migration and invasion through the direct targeting of RAC-beta serine/threonine-protein kinase (AKT2) gene (Wang *et al.*, 2017). Although there are conflicting results on cell cycle promotion or blockage in the context of *H. pylori* infection, it is suggested that a balance between cell proliferation and inhibition of epithelial cell renewal is necessary to maintain the intracellular niche of this bacterium. As observed for *H. pylori*, *Salmonella enterica* serova Typhimurium can exploit host miRNAs to control cell division cycle. The level of miR-15 family is down-regulated by this pathogen, which in turn promotes G1/S transition, a cell cycle transition that was found favorable for bacterial intracellular replication (Maudet *et al.*, 2014b). This strategy is also employed by *Citrobacter rodentium*, which deregulates Wnt/β-catenin signaling, thereby increasing cell proliferation and crypt hyperplasia (Roy *et al.*, 2015).

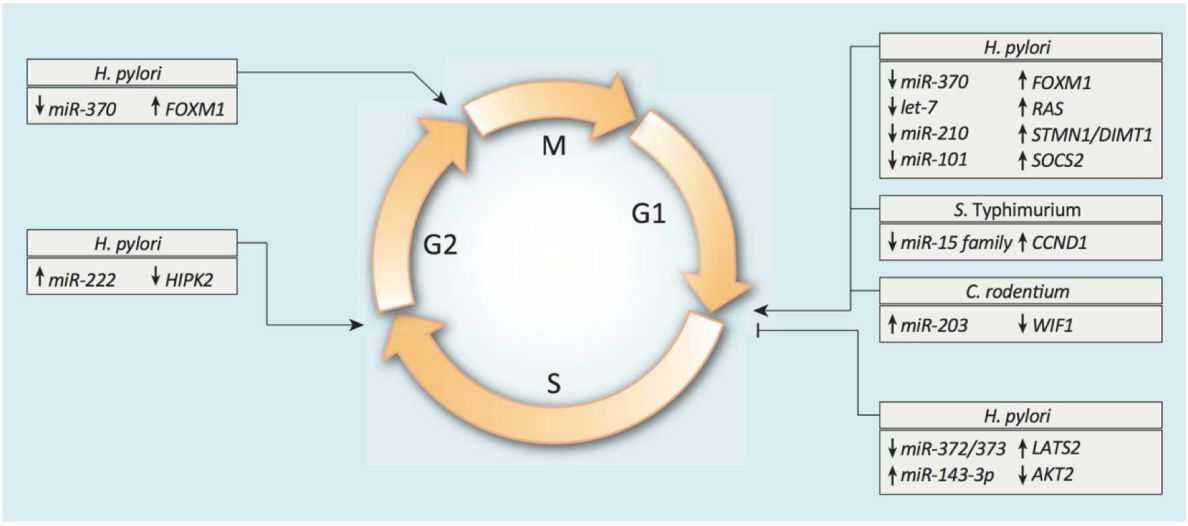

Figure 1.9. Human pathogenic bacteria differentially regulate miRNAs that control host cell-division cycle.
The modulation of miRNA expression caused by bacterial infections contributes to survival and/or proliferation of pathogens by maintaining their proliferative niche. Representative miRNAs are shown in this scheme. *H. pylori*, *Helicobacter pylori*; *S.* Typhimurium, *Salmonella* enterica serovar Typhimurium; *C. rodentium*, *Citrobacter rodentium*. The scheme is derived from Aguilar *et al*., 2019.

IV.IV. ROLE OF MAMMALIAN MIRNAS ON CYTOSKELETON

In order to facilitate bacterial entry and/or spreading, intracellular bacteria can also interfere with host cytoskeleton. This virulence strategy has been extensively described in response to bacterial effectors, which are delivered in the host cytosol through secretion systems. The remodeling of host cytoskeleton by miRNAs has also emerged as an important virulence mechanism. Using a piglet model system, a study showed that *S. Typhimurium* can up-regulate miR-29a, which in turn represses Caveolin 2 (Hoeke *et al.*, 2013). This miRNA-dependent regulation modulates the activation of cell division control protein 42 (Cdc42), thereby impacting focal adhesion and organization of actin cytoskeleton and favoring bacterial uptake by host cells. By contrast, some miRNAs were shown to prevent bacterial uptake and invasion. Following challenge with *S. Typhimurium* bacteria, an up-regulation of miR-331-3p was observed, which impairs bacterial uptake by host cells (Bao *et al.*, 2015). Another example is provided by miR-142-3p, which is induced in response to *M. tuberculosis* and targets an actin-binding protein crucial for phagocytosis, namely neural Wiskott-Aldrich syndrome protein (N-WASP) (Bettencourt *et al*., 2013). *Shigella flexneri* is another intracellular bacterium that modulates the expression of human miRNA during infection, notably miR-29b-2-5p (Sunkavalli *et al.*, 2017). This miRNA exerts a dual role during *S. flexneri* infection. MicroRNA-29b-2-5p is well expressed at an early stage of infection and plays an essential function in the binding of *S. flexneri* to host cells. This phenomenon involves the miR-29b-2-5p-directed repression of Unc-5 Netrin receptor (UNC5C), which in turn promotes the formation of filopodia, corresponding to slender cytoplasmic projections used by *S. flexneri* to bind host cells (Valencia-Gallardo *et al.*, 2015). At later stages of infection, *S. flexneri* triggers the repression of miR-29b-2-5p, which contributes to intracellular replication and to the dampening of host cell death, thereby favoring spreading to adjacent cells (Sunkavalli *et al.*, 2017). In a subsequent study, the same research group has performed a screening of human miRNAs for their ability to module the intracellular replication of *S. Typhimurium* and/or *S. flexneri* (Aguilar *et al.*, 2020). This study revealed that a largely non-overlapping subset of miRNAs regulates infection by these two pathogens, probably reflecting their distinct intracellular lifestyles. The authors report two examples that illustrate the complexity of miRNA-regulated host–bacterial interactions (Figure 1.10). They notably discovered that three miRNAs, namely miR-3668, miR-4732-5p and miR-6073, impair *S. flexneri* actin-based motility and intracellular spreading through the targeting of N-WASP, a strategy similar to the

one used by *M. tuberculosis* (see above). This response was specific to *S. flexneri* because these miRNAs did not alter actin-based motility of *Listeria monocytogenes* during infection. In addition, they found that Let-7i-3p miRNA can inhibit *S. Typhimurium* and *S. flexneri* binding to host cells. Let-7i-3p exerts also another specific effect on *S. Typhimurium* replication via modulation of endolysosomal trafficking and the vacuolar environment by targeting the host regulator of G-protein signaling 2 (RGS2). Finally, a link between miRNAs and integrin/actin dynamics regulation in *Klebsiella pneumoniae*-infected pulmonary epithelial cells has also been established (Teng *et al.*, 2016). Enhanced expression of miR-155 and miR-23a accelerates the bacterial adhesion. This observation was partially explained by miR-155 that promotes integrin α5β1 function and results in the increased actin polymerization. Overall, these results indicate that host miRNAs are critical regulators of bacterial infections, and highlight a selectivity of miRNA action towards a specific bacterial pathogen.

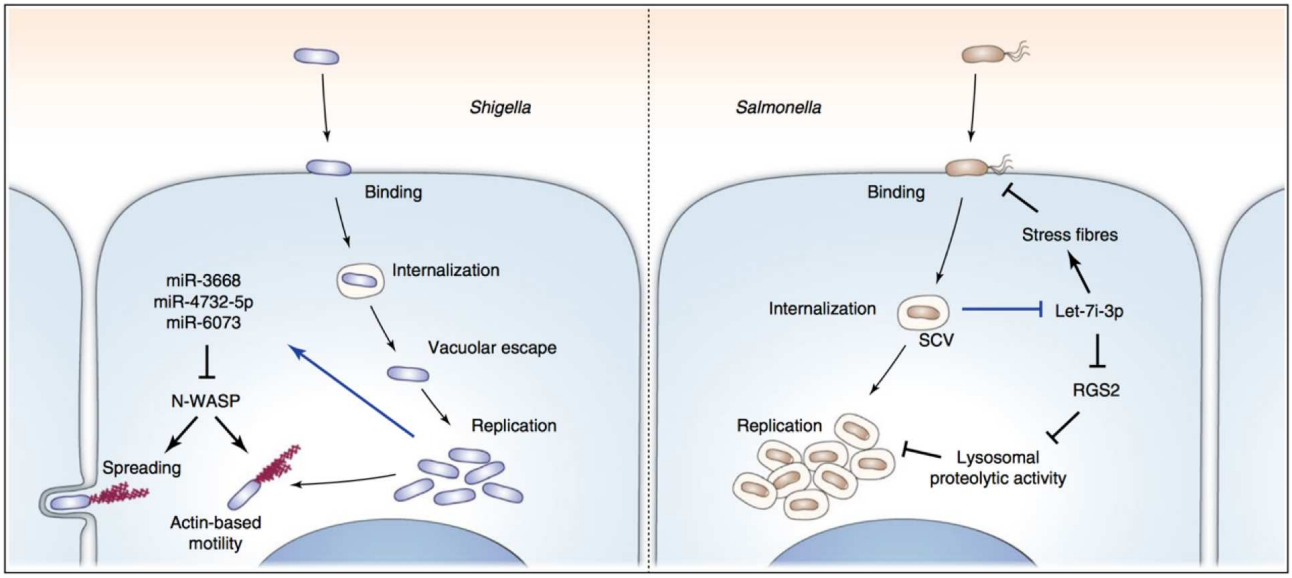

Figure 1.10. Model depicting the selective effects of miRNAs on the life cycle of *Shigella* and *Salmonella*.
On the left panel, miR-3668, miR-4732-5p and miR-6073 target neural Wiskott-Aldrich syndrome protein (N-WASP), thereby inhibiting *Shigella* actin-based motility, intercellular spreading and *Shigella* infection. The expression of endogenous miR-4732-5p and miR-6073 is induced over the course of *Shigella* infection, which is correlated with a progressive reduction of N-WASP expression. On the right panel, let-7i-3p miRNA acts on two distinct steps of *Salmonella* infection, namely the binding to host cells and the intracellular replication. On the one hand, let-7i-3p induces actin stress fibers. On the other hand, this miRNA acts through modulation of endolysosomal trafficking, via regulator of G-protein signaling 2 (RGS2), modifying the vacuolar environment and thus, inhibiting *Salmonella* intracellular replication. Let-7i-3p miRNA expression is reduced during *Salmonella* infection. The scheme is derived from Aguilar *et al.*, 2020.

IV.V. ROLE OF MAMMALIAN MIRNAS ON METABOLISM PATHWAY AND POST-TRANSLATIONAL MODIFICATION

The reprogramming of cellular metabolism is essential for controlling antibacterial responses, and has been recently shown to be controlled by mammalian miRNAs. In particular, the profiling and characterization of miRNAs from the whole blood of pigs upon *Salmonella* challenge revealed that miR-214 positively regulates intracellular iron homeostasis (Bao *et al.*, 2015). This miRNA silences *SLC11A1* expression, which in turn controls *Salmonella* replication by actively removing iron from the phagosomal space. Additionally, miR-21 was found to be involved in host glycolytic metabolism during *M. tuberculosis* infection (Hackett *et al.*, 2020). Indeed, macrophages were shown to display an increased reliance on the glycolytic pathway during the activation of inflammation, since increased glycolysis is critical for *M. tuberculosis* infection of macrophages, at an early stage of infection. The authors demonstrated that *M. tuberculosis* represses phosphofructokinase muscle (PFK-M) expression and its cognate protein activity at the rate-limiting and committed step of glycolysis through miR-21-mediated regulation, ensuring bacterial survival and replication. The last cellular process found to be modulated by miRNAs is the SUMOylation (Verma *et al.*, 2015). SUMOylation is a post-translational modification (PTM) that can rapidly and reversibly affect the cellular proteome. Several pathogens have been reported to use PTMs to achieve successful infection. For example, *S. Typhimurium* was found to up-regulate miR-30c and miR-30e, which was necessary and sufficient for the down-regulation of the SUMO pathway enzyme Ubc-9, and for successful infection (Verma *et al*., 2015).

IV.V. ROLE OF MAMMALIAN MIRNAS DURING LEGIONELLA PNEUMOPHILA INFECTION

Another miRNA-dependent regulatory network was shown to restrict *Legionella pneumophila* replication in human macrophages. As mentioned above, the trio miR-125b, miR221 and miR579, which targets repressors of *L. pneumophila* intracellular growth, were found co-repressed during infection of human macrophages (Herkt *et al.*, 2020). In more details, miR-125b, miR-221 and miR579 were shown to directly target tumor protein P53 (TP53), DExD/H-box helicase 58 (DDX58, encoding the RIG-I receptor), and galectin-8 (LGALS8),

respectively (Herkt *et al.*, 2020). MX dynamin-like GTPase 1 (MX1), which is not directly targeted by these miRNAs and known to possess an antiviral activity, was also found down-regulated by both miR-125b and miR-221 targets, resulting in an enhanced *L. pneumophila* replication. The third target, LGALS8, has already been characterized as a repressor of bacterial replication. Overall, this study suggests that human macrophages orchestrate the transcriptional shut-down of these miRNAs to negatively regulate *L. pneumophila* intracellular replication.

Taken together, these studies provide evidence that intracellular bacterial pathogens can reprogram miRNA expression during infections, and that some of them play essential functions in modulating bacterial infections. These miRNAs were found to impact multiple host cellular functions, including immune response, cell cycle progression, cytoskeleton organization, cell death and autophagy. Given that more than 2500 mature human miRNAs are currently annotated in the miRNA database miRBase, many additional miRNAs are expected to be relevant for host-bacteria interactions and await in-depth characterization.

V. ROLE OF THE RNAI MACHINERY IN HOST-BACTERIA INTERACTIONS

V.I. BIOLOGICAL RELEVANCE OF THE RNAI MACHINERY IN PLANT-BACTERIA INTERACTIONS

The biological relevance of the RNAi machinery in host-bacteria interactions is now well-established in plants. It has been initially shown that non-pathogenic bacteria, which mount a potent PAMP-triggered immunity (PTI) in wild-type plants, were able to grow on Arabidopsis miRNA-defective mutants (Navarro *et al.*, 2008). This study suggested that the miRNA pathway likely plays a central role in PTI. Consistent with this hypothesis, mutations in Arabidopsis *Dicer-Like 1* (*DCL1*), which is the main Dicer-like enzyme responsible for the processing of miRNA precursors in plants, and in Arabidopsis AGO1, which is the central component of plant miRISC, led to impaired PAMP-triggered production of reactive oxygen species (ROS), gene activation and callose deposition (Li et al., 2010b; Thiébeauld et al., 2021). A loss-of-function mutation in *Serrate*, which encodes a zinc-finger domain-containing protein that assists DCL1 in the processing of miRNA precursors, was also found compromised in PAMP-triggered ROS production and in basal resistance against *Pseudomonas syringa* pv. *tomato* strain DC3000 (*Pto* DC3000) (Niu *et al.*, 2016; Thiébeauld *et al.*, 2021). By contrast, the overexpression of *Serrate* in Arabidopsis was shown to restrict the growth of *Pto* DC3000 (Niu *et al.*, 2016), indicating that this miRNA biogenesis factor promotes basal resistance against this bacterium. Altogether, these data indicate that the Arabidopsis miRNA pathway plays a central role in antibacterial immunity. Arabidopsis mutants defective in the biogenesis of endogenous siRNAs required for post-transcriptional gene silencing were also found to exhibit enhanced disease susceptibility towards *Pto* DC3000 expressing AvrRpt2, a type III-secreted effector. This effector is sensed by the NLR Resistance to *Pseudomonas syringae* 2 (RPS2) protein, resulting in Effector-triggered immunity (ETI) (Huang *et al.*, 2019). Collectively, these data indicate that both the miRNA and siRNA pathways are central components of the plant immune system. The role of the RNAi machinery is not restricted to the control of the plant immune system but can also be hijacked by bacteria for their own benefit. As an example, a report provides evidence that small RNAs derived from *Bradyrhizobium japonicum* tRNA maturation can enter soybean nodule host cells, where they are loaded into AGO1 to trigger the silencing of specific host target genes, thus controlling the establishment of symbiosis (Ren *et al.*, 2019).

V.II. BIOLOGICAL RELEVANCE OF THE MAMMALIAN RNAI MACHINERY IN HOST-BACTERIA INTERACTIONS

So far, very little is known about the involvement of mammalian miRNA factors in antibacterial resistance. The role of Dicer, and of its isoform, has been mostly studied in the context of antiviral defense but not antibacterial defense. However, one study has shown that a specific ablation of Dicer in the intestinal epithelial cells resulted in an enhanced susceptibility to colitis (Liu *et al.*, 2016). Importantly, the authors also observed an increase in the gut microbiota dissimilarity in these mutant mice, suggesting that miRNAs can regulate the gut microbiota composition. As mentioned previously, primary bone marrow-derived macrophages isolated from *dicer1*-defective mice exhibit defect in pro-inflammatory cytokine production after TLR agonists stimulation (Gantier *et al.*, 2012). This suggests that the mouse Dicer positively regulates pro-inflammatory cytokine production in response to TLR activation. Despite these seminal studies on the role of Dicer in host-bacteria interactions and on mammalian innate immunity, there is currently not evidence indicating that any of the mammalian Ago could contribute to antibacterial resistance. However, some studies have reported that human Ago2 could be highjacked by bacteria to promote pathogenesis. The first evidence has been reported during *Salmonella enteritidis* infection. More specifically, bacterial-derived RNAs corresponding to the *S. enteritidis* genome were retrieved in host cells during infection (Gu *et al.*, 2017; Zhao *et al.*, 2017). Sal-1 was the most enriched RNA fragment recovered, and exhibited a length typical for a miRNA. Interestingly, Sal-1 was specifically detected in infected host cells but not in *S. enteritidis* cells alone, suggesting that this bacterial RNA fragment must be processed by host cells. Accordingly, the Sal-1 precursors, termed Pri-Sal-1, were processed by the host Ago2 but not Dicer (Diederichs and Haber, 2007; Cifuentes *et al.*, 2010; Cheloufi *et al.*, 2010). Importantly, Sal-1 miRNA-like fragment was found to facilitate bacterial intracellular replication and survival in infected cells (Gu *et al.*, 2017), supporting a positive role of Sal-1 in bacterial pathogenesis. The authors also found that Sal-1 silences host inducible nitric oxide synthase, thus reducing the production of nitric oxide, which serves as a critical anti-microbial mechanism (Zhao *et al.*, 2017). Interestingly, the Sal-1 fragment is conserved across *Salmonella enterica*, *Escherichia coli* and *Shigella spp*, suggesting a potential widespread virulence mechanism. Therefore, *Salmonella* is able to exploit Ago2 to produce a biologically relevant miRNA-like fragment in host cells, which can directly regulate host gene expression.

Another recent study pointed out an important role of human Ago2 in the *Shigella flexneri* infection cycle (Filopon, Schiavolin, Bonnet *et al., in preparation*). *Shigella* induces its host cell internalization in a macropinocytic-like process, and rapidly escapes from its vacuole to reach the cytosol, which represents its main replicative niche (Valencia-Gallardo *et al.*, 2015). Importantly, *Shigella* was found to trigger a rapid and transient recruitment of human Ago2 at bacterial invasion sites and at the phagocytic vacuole prior to its rupture (Filopon, Schiavolin, Bonnet *et al.*, *in preparation*). This phenotype was associated with a pronounced delay in *Shigella*-induced vacuole rupture during infection of *ago2*-deficient cells, indicating that human Ago2 positively regulates vacuolar rupture. A similar phenotype was found in human cells depleted of other miRNA factors, including TNRC6A and Drosha, supporting a role for the human miRNA pathway in this process. Furthermore, the miRNA-mediated translation inhibition activity of Ago2, and its ability to interact with GW-containing TNRC6 proteins, were found essential for this phenotype. Collectively, these data suggest that an assembled Ago2-miRISC likely orchestrates vacuolar rupture. Importantly, specific Ago2-loaded miRNAs were found to directly target *ARHGDIA* mRNAs, which encodes a negative regulator of RhoGTPases, namely RhoGDIα. This presumably releases the negatively effect of RhoGDIα towards RhoGTPases, including Cdc42, which has recently been shown to promote *Shigella*-induced vacuolar rupture (Kühn *et al.*, 2020; Mellouk *et al.*, 2014). Hence, this work suggests that *Shigella* likely hijacks human Ago2 function at early steps of the infection, to promote the rupture of its vacuole (Figure 1.11).

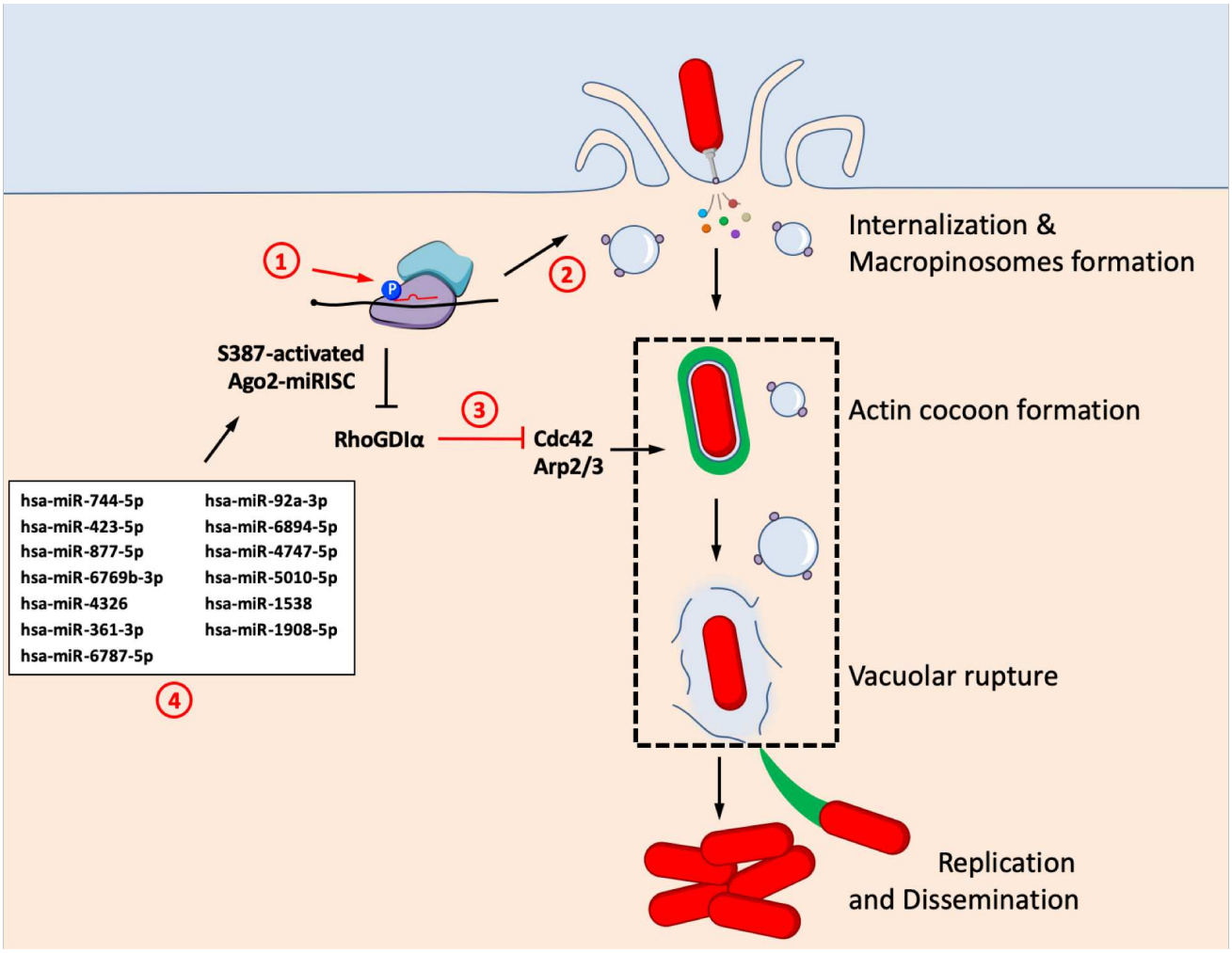

Figure 1.11. *Shigella* recruits human Ago2 at macropinosomes to silence RhoGDIα and promote vacuolar rupture.
Shigella induces its host cell internalization in a macropinocytic-like process. It further rapidly escapes from its phagocytic vacuole to reach the cytosol. For this process, *Shigella* triggers a rapid and transient recruitment of human Ago2 at bacterial invasion sites as well as at macropinosomes. **(1)** The miRNA-mediated translation inhibition activity of Ago2, and its ability to interact with GW-containing TNRC6 proteins, are essential for *Shigella*-induced vacuolar rupture. Accordingly, the serine 387 of Ago2 is phosphorylated, which is essential for miRISC assembly, is also required for *Shigella*-induced vacuolar rupture. **(3)** The Ago2-miRISC was found to repress the translation of RhoGDIα mRNAs, thereby reducing the abundance of cognate proteins. This Ago2-mediated repression of RhoGDIα no longer inhibits Cdc42 activity, which in turn results in a rapid Cdc42-dependent vacuolar rupture. **(4)** List of miRNAs that were found loaded in Ago2, some of which directly target RhoGDIα mRNAs. Schematic representation derived from Filopon, Schiavolin, Bonnet, *et al*., *in preparation.*

VI. VIRAL AND BACTERIAL SUPPRESSORS OF RNAi

VI.I. VIRAL SUPPRESSORS OF RNA SILENCING (VSRs)

The ability of viruses to suppress RNAi has been initially described in plant-viral interactions, whereby the Helper component proteinase (HcPro) encoded by *potyviridae* genomes, and the 2b protein of *cucumber mosaic virus*, were characterized as *bona fine* VSRs (Diaz-Pendon *et al.*, 2007; Kasschau *et al.*, 2003; Mallory *et al.*, 2002). This VSR-based phenomenon has been subsequently extended to a wide range of phytopathogenic RNA viruses, (Figure 1.12, left) (Jin *et al.*, 2021; Voinnet *et al.*, 1999), and was found essential for viral replication in plant cells. The occurrence and relevance of VSRs has also been reported in insect-viral interaction. The B2 protein, produced by *Flock house virus* (FHV), is for instance the first VSR from animal virus identified. This viral protein was found to suppress RNAi in both *Drosophila* and plants (Li *et al.*, 2002). FHV is a member of the *Nodaviridae* family, including insect pathogens, and also *Nodamura virus* (NoV), which can reduce not only insect, but also, mammalian survival. A B2 homolog has been identified in NoV. This VSR was found to bind long dsRNAs and siRNAs *in vitro,* and to potently suppress RNAi in insect cells (Chao *et al*., 2005; Sullivan and Ganem, 2005; Wang *et al.*, 2006a). Consistently, the ability of a B2-deficient NoV to replicate in insect cells, in mammalian cells, but also in suckling mice, is strongly compromised, supporting a critical role for this VSR in viral pathogenicity (Li *et al.*, 2013; Maillard *et al.*, 2013b).

Many VSRs of mammalian pathogenic RNA viruses have now been identified (Figure 1.12, right). Most of the VSRs characterized can bind dsRNAs, thereby preventing their Dicer-dependent processing into siRNAs. This ability to bind dsRNAs is biologically relevant because mutations in VSRs that alter this function abrogate RNAi suppression activity (Ding *et al.*, 2018). As dsRNAs are also known to trigger IFN signaling, some VSRs can additionally act as IFN antagonists, as described with the *Influenza A virus* NS1 and *Vaccinia virus* E3L (Chinnappan *et al.*, 2014; Li *et al.*, 2004). Other VSRs can interfere directly with the processing activity of Dicer. For example, the core protein of *Hepatitis C virus* directly binds to, and inhibits the activity of, the Dicer enzyme (Wang et al., 2006c; Chen et al., 2008), while VP35 protein from *Ebola virus* associates with Dicer co-factors TRBP and PACT (Fabozzi *et al.*, 2011). Although several VSRs from phytopathogenic RNA viruses have evolved to directly

suppress plant AGO1 activity (Azevedo *et al.*, 2010; Baumberger *et al.*, 2007; Bortolamiol *et al.*, 2007; Michaeli *et al.*, 2019; Pazhouhandeh *et al.*, 2006; Watt *et al.*, 2020; Zhang *et al.*, 2006), only a few VSRs from human pathogenic virus were found to act downstream of small RNA biogenesis. One example is the *human immunodeficiency virus-1* (HIV-1) Negative Regulatory Factor (Nef) protein, which interacts with human Ago2 through two conserved glycin/tryptophan motifs (GW-motifs, also known as W-containing motifs) (Aqil *et al.*, 2013). Importantly, this phenomenon is notably required for the dampening of miRNA-dependent Ago2-directed slicing activity, and appears to be relevant for viral replication in host cells (Aqil *et al.*, 2013). As mentioned previously, W-motifs are critical for the binding between Argonaute proteins and RNAi-related components, and form evolutionarily and functionally conserved Ago-binding platforms (El-Shami *et al.*, 2007; Till *et al.*, 2007). One another example is NS3 from the *dengue virus*, which was found to interact with the human heat shock cognate 70 (HSC70) (Kakumani *et al.*, 2015). This interaction perturbs the formation of miRISC, probably by displacing TRBP and possibly impairing the downstream activity of miRNAs. Interestingly, *vaccinia virus* protein VP55 has also been shown to mediate the non-templated addition of 2-7 adenosines specifically to the miRNAs associated with the miRISC (Backes *et al.*, 2012). This results in a rapid degradation of these miRNA species. In contrast, siRNAs, which are protected by 2′O-methylation (2′OMe) in mammals, were not targeted by VP55. Finally, small structured RNAs from human pathogenic virus may also act as a VSR. For instance, *Adenovirus* VAI RNA inhibits shRNA-induced RNAi by acting as a decoy substrate for Dicer (Lu and Cullen, 2004; Andersson *et al.*, 2005). Other examples include two highly structured RNA regions of HIV-1, TAR and Rev-Response Element (RRE), which were shown to bind TRBP, thereby displacing siRNA bound to TRBP (Bennasser *et al*., 2006; Daniels *et al*., 2015). Altogether, these studies, among several others, provide solid evidence that mammalian viruses have evolved to suppress different step of RNAi, as initially described for plant and insect RNA viruses. However, the physiological relevance of such VSR activity during viral infection, and in response to authentic human pathogenic RNA viruses, has just been recently reported. More specifically, and as mentioned above, it was shown that VSRs from *human enterovirus 71* (HEV71) and *Influenza A virus* (IAV) are essential to promote viral replication in both human cells as well as in mice model systems (Li *et al.*, 2016; Qiu *et al.*, 2017).

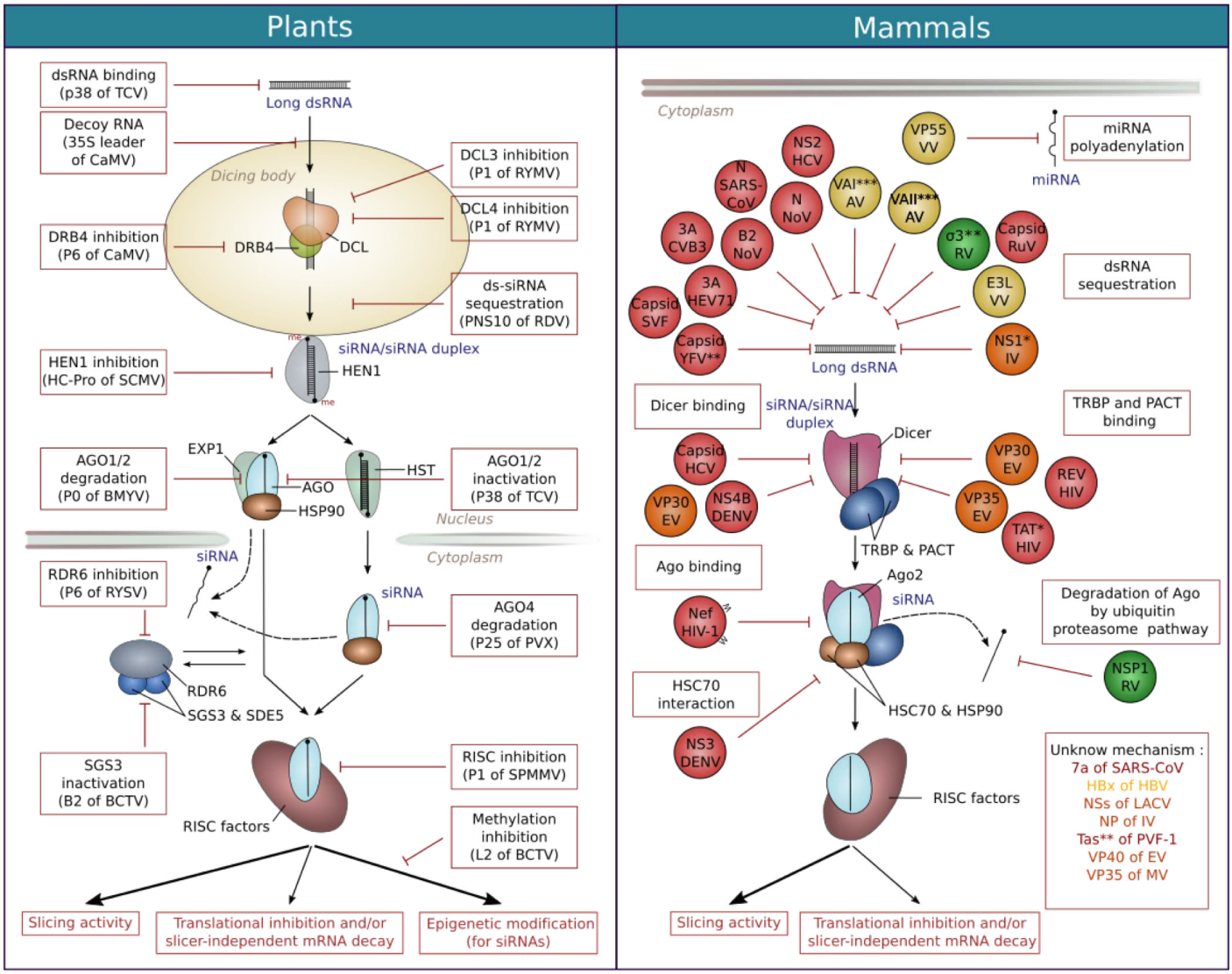

Figure 1.12. Modes of action of virus-encoded proteins that suppress siRNA- and/or miRNA- mediated gene silencing activity from plant and mammal pathogenic viruses.

On the left panel, plant viral suppressors of RNA silencing (VSRs) can disrupt RNA interference (RNAi) pathway, thereby preventing the assembly of functional complex or inhibiting the function of RNAi components. An example is given for each category. On the right panel, in mammals, proteins with VSR activity have been characterized from positive- (red), or negative sense single-stranded RNA virus (orange), double-stranded RNA virus (green) and double-stranded DNA virus (yellow). Some main classes of VSR activity can be distinguished, and some have not been fully characterized to date. * VSR activity is questioned. For instance, the Tat protein of HIV-1 was shown to act at the level of Dicer processing (Bennasser *et al.*, 2005; Ponia *et al.*, 2013), while in two other studies, suppressor activity was not recovered, which may be dependent on the cell type used (Lin and Cullen, 2007). ** In some cases, the activity was determined in non-mammalian cells, such as the capsid of YFV in *Aedes Aegypti* mostiquoes (Samuel *et al.*, 2016). *** The RNA silencing suppression activity is not exerted by a viral protein but, it is the adenovirus-associated RNAs that function as a competitive substrate for Exportin 5 and Dicer (Lu and Cullen, 2004; Andersson *et al.*, 2005). W represents the conserved tryptophan-containing motif allowing an interaction with Ago proteins. The binding of Nef to Ago2 was shown to alter the sorting of GW182 into exosomes. It is noteworthy that the vast majority of VSRs from mammalian viral pathogens that have been characterized so far, interfere with the biogenesis of siRNAs rather than on the RISC activity. AV, *Adenovirus*; CoV, *Coronavirus* (Cui *et al.*, 2015); CVB3, *Coxsackievirus B3* (Mu *et al.*, 2020); DENV, *Dengue virus* (Kakumani *et al.*, 2013, Kakumani *et al.* 2015); EV, *Ebolavirus* (Haasnoot *et al.*, 2007; Fabozzi *et al.*, 2011); HBV, *Hepatitis B virus* (Chinnappan *et al.*, 2014); HCV, *Hepatitis C virus* (Chen *et al.*, 2008; Zhou *et al.* 2020); HEV71, *Human enterovirus 71* (Qiu *et al.*, 2018); HIV-1, *Human immunodeficiency virus-1* (Aqil et al., 2013; Bennasser *et al.*, 2005; Ponia *et al.*, 2013) ; IV, *Influenza virus* (Li *et al.*, 2004; Kennedy *et al.*, 2015); LACV, *La Crosse encephalitis virus* (Soldan *et al.*, 2005); MV, *Marburgvirus* (Li *et al.*, 2016); NoV, *Nodamura virus* (Sullivan and Ganem, 2005); PVF-1, *Foamy virus type 1* (Lecellier *et al.*, 2005); RuV, *Rubella virus* (Xu *et al.*, 2021), RV, *Reovirus* (Lichner *et al.*, 2003, Mukhopadhyay *et al.*, 2019); YFV, *Yellow fever virus* (Samuel *et al.*, 2016); SARS-CoV, *Severe acute respiratory syndrome coronavirus* (Karjee *et al.*, 2010; Cui *et al.*, 2015); SVF, *Semliki Forest virus* (Qian *et al.*, 2020); VV, *Vaccinia virus* (Li *et al.*, 2004; Backes *et al.*, 2012).

VI.II. BACTERIAL SUPPRESSORS OF RNAI (BSRS)

The central role of individual miRNAs, and of the RNAi machinery, in Arabidopsis antibacterial defense, suggested that phytopathogenic bacteria must have evolved strategies to interfere with the functions of RNAi factors. Consistent with this hypothesis, *Pto* DC3000 was shown to produce bacterial suppressors of RNA silencing (BSRs) that suppress different steps of the Arabidopsis miRNA pathway, including miRNA biogenesis and/or stability, or miRNA activity (Navarro *et al.*, 2008). Among these type III-secreted effector proteins, AvrPto was found to reduce the accumulation of some mature miRNAs, potentially by inhibiting the processing of cognate pre-miRNAs. HopH1 and HopN1 inhibit mature miRNA accumulation, possibly by interfering with their biogenesis and/or stability, while HopT1-1 was found to suppress miRNA and siRNA activities, potentially at the level of AGO1 (Navarro *et al.*, 2008). The detailed mode of action of HopT1-1 has been more recently characterized. HopT1-1 was found to physically interact with Arabidopsis AGO1 through two conserved W-motifs (Figure 1.13) (Thiébeauld *et al.*, 2021). Importantly, this protein-protein interaction was determined necessary for the ability of HopT1-1 to suppress both the immunity and gene silencing functions of Arabidopsis AGO1. These findings indicate that the BSR activity of HopT1-1 is tightly coupled with its virulence function, and provide the first example of a bacterial virulence protein able to directly suppress miRISC function. Although the role of mammalian miRNAs in host-bacteria interactions is now well-established (see above), there is currently no evidence indicating that mammalian pathogenic bacteria can interfere with the RNAi machinery.

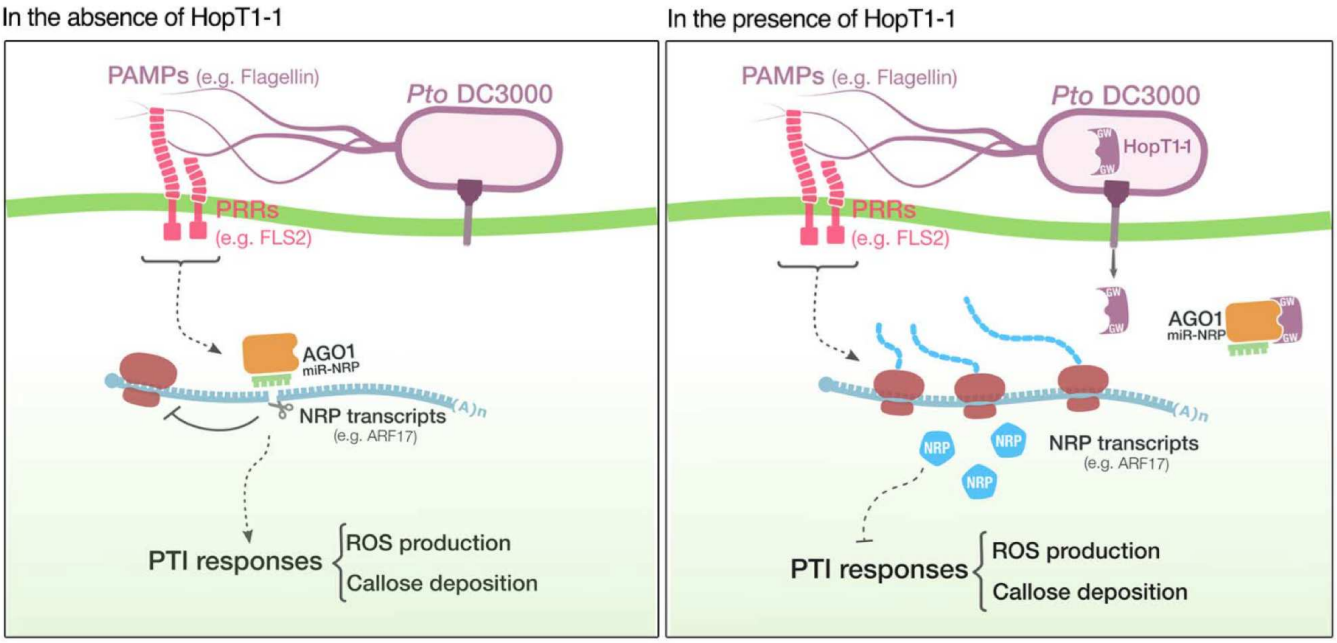

Figure 1.13. HopT1-1 interacts with, and suppresses the activity of *Arabidopsis thaliana* AGO1
On the left panel, in the absence of HopT1-1, Pathogen-Associated Molecular Patterns (PAMPs) from *Pseudomonas syringae* pv. *tomato* DC3000 (*Pto* DC3000) are perceived by Pattern Recognition Receptors (PRRs). This recognition triggers induction of a subset of miRNAs corresponding to PAMP-responsive miRNAs, which are loaded into AGO1. These miRNAs act as positive regulators of defense by targeting Negative Regulators of PTI (NRPs), thereby ensuring an activation of PAMP-triggered immunity (PTI). PTI includes reactive oxygen species (ROS) production and callose deposition. On the right panel, in the presence of HopT1-1, the effector interacts with Arabidopsis AGO1 through two conserved glycine-tryptophan (GW) motifs. This phenomenon alleviates miRNA-directed silencing of NRPs. The accumulation of NRP proteins culminates in the dampening PTI response, including ROS production and callose deposition. FLS2; Flagellin Sensing 2. Scheme derived from Thiébeauld *et al*., 2021.

VII. How host cells can sense pathogen-triggered RNAi suppression activities?

VII.I. Effector-triggered immunity in plants

The first layer of the plant immune system relies on the perception of PAMPs by PRR surface receptors. Upon PAMP perception, PRRs activate a whole cascade of signaling events culminating in PTI. As a counter-defense response, pathogens have evolved effector proteins that suppress different steps of PTI. As an example, the *Pto* DC3000 effector HopT1-1 suppresses AGO1 activity, a major component of PTI, which notably regulates early steps of PTI signaling, including reactive oxygen species (ROS) production and gene transcriptional activation (Li *et al*., 2010b; Liu *et al.*, 2018; Thiébeauld *et al.*, 2021). As part of the evolutionary arms race, plants have evolved a counter-counter-defense mechanism that relies on the perception of effector proteins and/or their activity in host cells. This second layer of the plant immune response is achieved by intracellular plant NLRs (see section below), which share structural homologies with mammalian NLRs, and mount Effector-Triggered Immunity (ETI). It has notably been shown that HopT1-1 can be sensed by host plant cells, thereby resulting in a potent ETI response that is dependent on ETI signaling factors (Thiébeauld *et al.*, *in preparation*). Importantly, such ETI activation is entirely dependent on the ability of HopT1-1 to suppress RNAi, providing evidence that plants have evolved a yet-unknown mechanism to perceive BSR activity. This phenomenon has also been formerly observed in response to VSRs. For example, the tomato *aspermy cucumovirus* 2b protein (Tav2b), when expressed from tobacco *mosaic tobamovirus* (TMV) RNA genome, triggers a potent ETI-like response in tobacco (Li *et al.*, 1999). Importantly, the N-terminal part of Tav2b, as well as specific residues required for VSR activity, were found necessary for ETI activation, suggesting that the VSR and ETI activities of this viral protein are coupled. Identifying the NLRs that recognize these BSR and VSR activities will be important to decipher the mechanisms by which host cells can sense pathogen-triggered RNAi suppression.

VII.II. Overview of the mechanisms by which plant NLRs sense pathogen effectors

ETI activation is known to be triggered by a large polymorphic family of intracellular NLR immune sensors, also referred to as disease resistance proteins in plants (Lolle *et al.*, 2020). They are involved in the detection of evolutionarily divergent pathogen effectors from bacteria, viruses, fungi, oomycetes, nematodes and insects (Lolle *et al.*, 2020; Nguyen *et al.*, 2021; Sun *et al.*, 2020). *NLR* genes are represented by hundred members in different plant species, and are among the most rapidly evolving genes from plant genomes (Guo *et al.*, 2011; Jacob *et al.*, 2013; Lolle *et al.*, 2020; Yue *et al.*, 2012). NLRs fall into two major subclasses, depending on their N-terminal domain. One sub-class possesses Toll–interleukin 1 receptor (TIR) domain, that are called TNLs, while the other one is composed of a coiled-coil (CC) domain, and are thus named CNLs. Plant NLRs share sequence and structural homologies with mammalian NLRs, which notably function in inflammatory response and PAMP perception (Inohara *et al*., 2005; Jones *et al.*, 2016). NLRs are less numerous in mammalian genomes and differ in their N-terminal domains compared to plant NLRs (Ting *et al.*, 2010). Plant and mammalian NLRs share similar modular domains, including the core nucleotide-binding domain (NBD) and leucine-rich repeat (LRR) domain (Figure 1.14). Despite diversity in sequence and functions of plant and mammalian NLRs, they have initially been proposed to operate through similar mechanisms as switch-like activation, between a closed, ADP-bound "off " state and an open, ATP-bound "on" state (Griebel *et al*., 2014). Although the detailed mechanisms of mammalian NLR activation have been extensively studied during the last two decades, only a few recent studies have shown that these intracellular sensors can sense pathogen effectors –rather than PAMPs– (see below) (Kufer *et al.*, 2019; Lopes Fischer *et al.*, 2020; Ngwaga *et al.*, 2021). On the contrary, plant NLRs have been almost exclusively characterized in pathogen effector recognition, and an overview of the established pathogen effector recognition models is presented hereafter.

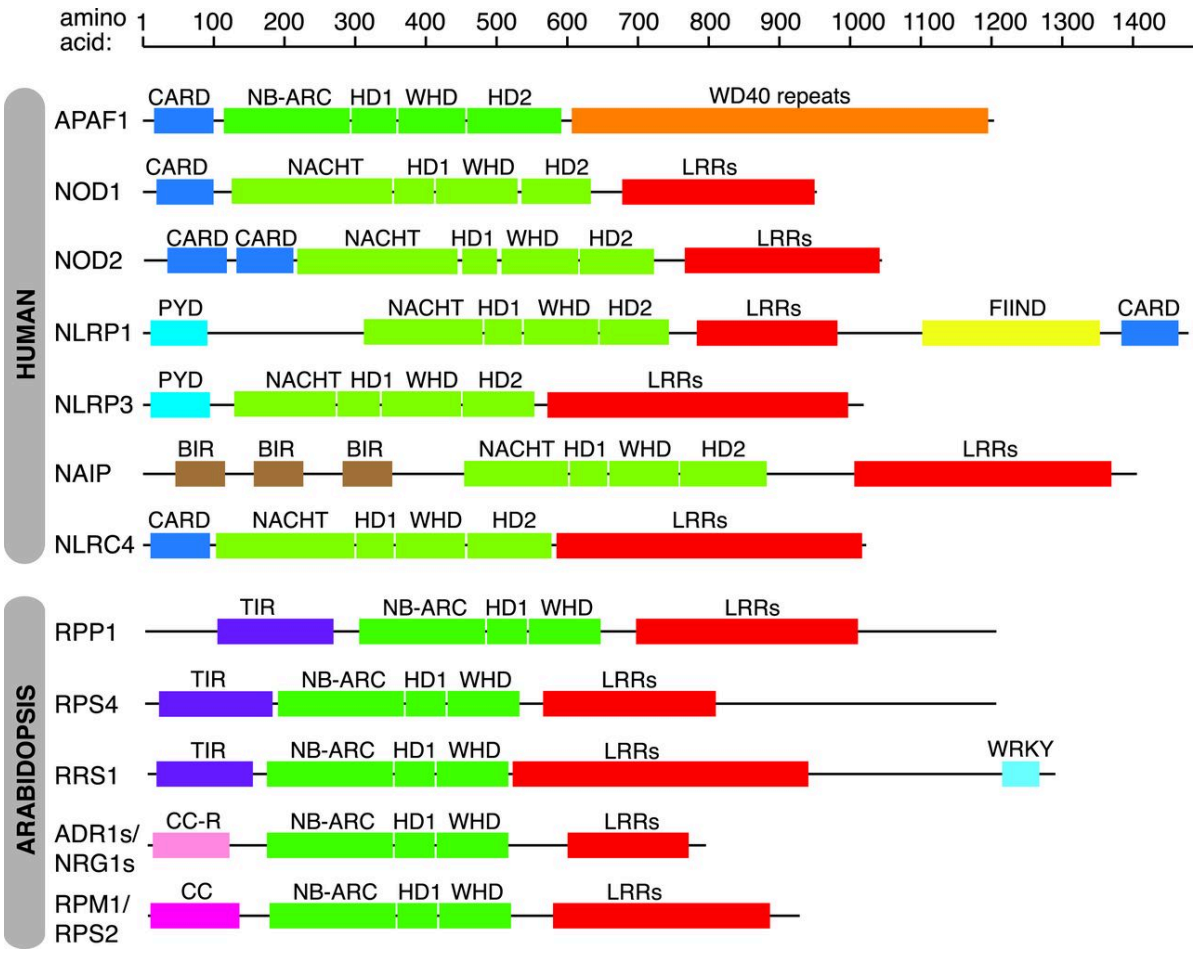

Figure 1.14. Diversity of NLR and NLR-like architectures in human and Arabidopsis.
Domain structures of representative NOD-like receptor (NLR) proteins from human and Arabidopsis are shown. NLRs share a similar modular domain architecture, including the core NBD and LRR domain, although in both clades there is diversity in N- and C-terminal accessory domains. Humans possess additional NLRs not known to be directly involved in pathogen sensing. CARD; caspase activating and recruitment domain, CC; coiled coil, NACHT; domain present in NAIP, NB; nucleotide binding, NB-ARC; nucleotide-binding adaptor shared by APAF-1 and R proteins, TIR; Toll/Interleukin-1 receptor, WRKY; WRKY-containing DNA-binding domain. Schematical representation derived from Jones *et al*., 2016.

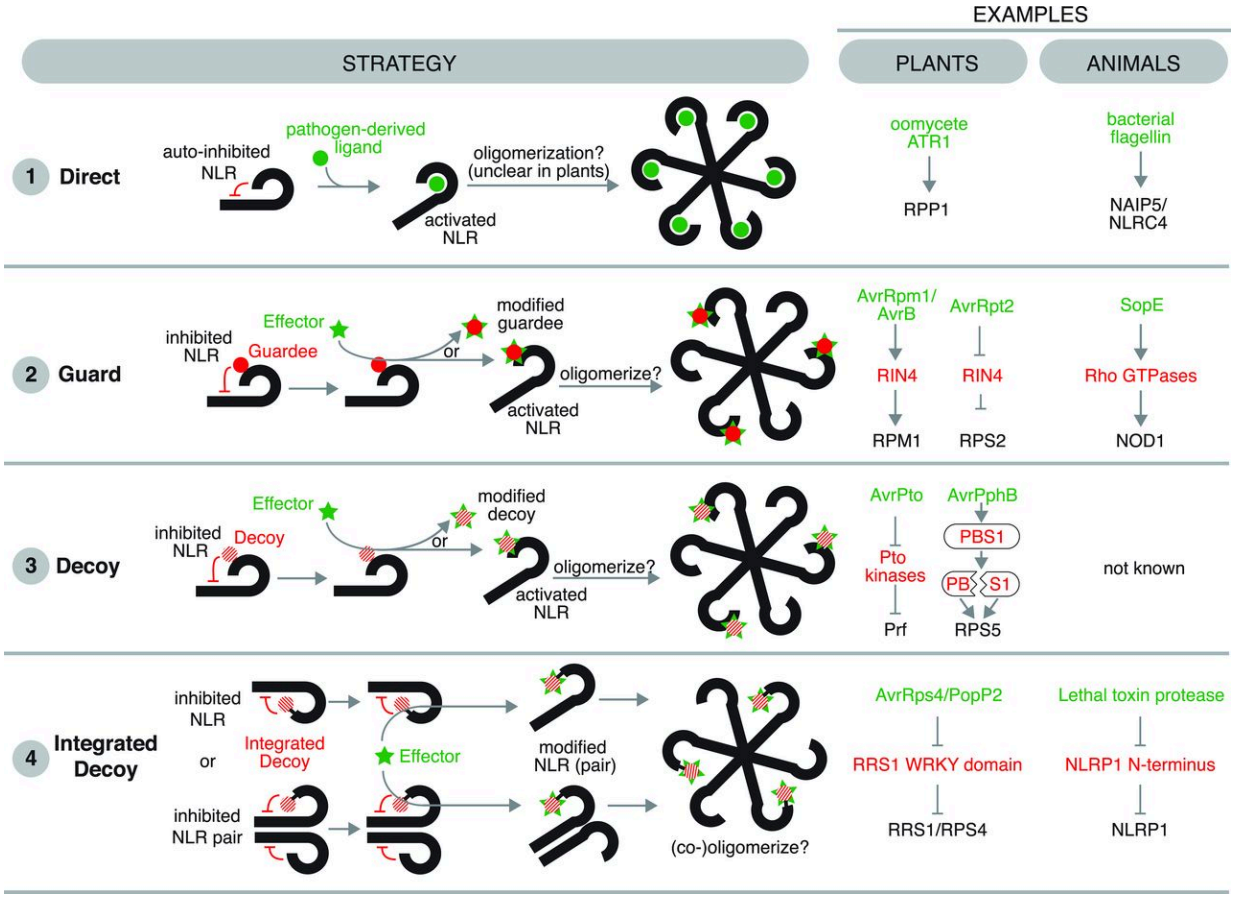

Figure 1.15. Proposed mechanisms of pathogen recognition in plants and animals. Four mechanisms of pathogens detection are proposed and are illustrated with one specific NLR example. The first strategy corresponds to a direct recognition of pathogen-derived ligands. The guard and decoy strategies are analogous, since the inhibition state is relieved upon effector-mediated modification of the guardee or decoy proteins. Guardees are distinguished from decoys by having an additional and separate function in host defense, whereas decoys are merely mimics of host defense proteins. The last strategy relies on NLR with integrated decoy domain, which functions in NLR pair. Scheme derived from Jones *et al*., 2016.

In plants, the recognition of pathogen effectors by NLRs can occur directly or indirectly, with four proposed mechanisms (Figure 1.15) (Cui *et al.,* 2015a; Jones *et al.*, 2016; Sun *et al.*, 2020). The first molecular mechanism relies on a direct interaction between the NLR and its cognate effector. A few direct interactions between NLRs and pathogen effectors have been experimentally validated (Ellis *et al.*, 2007; Jia *et al.*, 2000). However, in most cases, it is thought that plant NLRs perceive pathogen effectors indirectly, by sensing the effector-triggered perturbation activity of cellular targets, named "guardees". This second recognition model postulates that NLRs monitor the integrity of "guardees", which play a central role in PTI, and trigger ETI upon pathogen-induced modifications of such guardees. This model has been initially illustrated with the two Arabidopsis NLRs, RPM1 and RPS2, which are associated with the plasma membrane to guard the integrity of the host RPM1-interacting protein 4 (RIN4) (Axtell and Staskawicz, 2003; Mackey *et al.*, 2002; Ray *et al.*, 2019). RIN4 is modified by *P. syringae* type III-secreted effectors AvrB, AvrRpm1, and AvrRpt2. For instance, AvrB and AvrRpm1 were shown to induce phosphorylation coupled with conformational changes of RIN4, which are sensed by RPM1 and activates ETI (Chung *et al.*, 2011, 2014; Li *et al.*, 2014; Liu *et al.*, 2011; Mackey *et al.*, 2002). The cysteine protease AvrRpt2 effector was also shown to trigger the RIN4 elimination, which subsequently activates RPS2-mediated ETI signaling (Mackey *et al.*, 2002; Axtell and Staskawicz, 2003; Kim *et al.*, 2005). The guard hypothesis has been validated in the context of other NLR-effector interactions (Hoorn and Kamoun, 2008). The third recognition model is the "decoy" strategy, which is also based on indirect recognition of the effector as for the guard model. Decoys are not essential for PTI but mimic critical host defense proteins, which are normally targeted by pathogen effectors. In this model, the decoy serves as a bait to trap pathogen effectors, and in turn activates ETI with attenuated suppression effect on PTI (Hoorn and Kamoun, 2008). For example, the kinase AvrPphB susceptible 1 (PBS1) is probably functioning like a decoy, and has no defined basal resistance function. PBS1 is cleaved by pathogen-secreted protease AvrPphB, which is recognized by NLR resistance to *Pseudomonas syringae* 5 (RPS5) (Ade *et al.*, 2007; Kim *et al.*, 2016). Another proposed effector recognition mechanism relies on the "integrated decoy". This model is based on an "integrated" domain carrying by the NLR, and which is normally targeted by the pathogen effectors. One of the most studied examples of the integrated decoy model is provided by the Resistance to *Pseudomonas syringae 4* (*RPS4*) - *Resistance to Ralstonia Solanacearum 1* (RRS1) pair of NLRs. More specifically, the NLR RRS1 protein carries at its C terminus a WRKY domain, which is normally present in WRKYs, a family of transcription factors that are essential for plant immune transcriptional reprogramming (Buscaill and Rivas, 2014; Phukan

et al., 2016). Some studies have shown that RRS1 interacts with RPS4 to prevent RPS4 autoactivation, and the activation of this heterocomplex requires binding with AvrRps4 bacterial effector (Noutoshi *et al.*, 2005; Sohn *et al.*, 2014). Because RRS1 has no clear basal resistance function, it might serve as a host integrated decoy, whose targeting by pathogen effector activates transcriptional immune reprogramming.

VII.III. ETI IN MAMMALS AND UNDERLYING MECHANISMS

The pattern recognition theory proposed by Charles Janeway Jr. provided important insights into the recognition mechanisms of pathogens by mammals (Janeway, 1989). However, an additional layer of pathogen detection is necessary to discriminate commensal from pathogenic bacteria, which both share PAMPs. Thus, pioneering theoretical model also proposed that the host organism could react to damage-associated molecular patterns (DAMPs), which are host-derived patterns that are released into the extracellular milieu as a result of microbial infection, to induce inflammatory and adaptive immune responses (Matzinger, 1994). It is noteworthy, that such DAMPs have been now characterized in both animal and plant organisms. The discontinuity theory of immunity has been further proposed. This model suggests that the immune system might be activated by changes in the cellular environment through pathogen-triggered perturbations in intracellular signaling pathways, rather than by detection of pathogen-derived molecules (Pradeu *et al.*, 2013). Such cellular perturbations include disruption of vesicular trafficking, altered actin cytoskeleton, pathogen replication in the host cytosol and interference with host immune signaling, which are defined as "patterns of pathogenesis" (Vance *et al.*, 2009). These patterns of pathogenesis employed by pathogenic bacteria may be detected by host factors, and allow to discriminate the effects triggered by pathogenic bacteria versus commensals. Pathogen detection may also occur through sensing of homeostasis-altering molecular processes (HAMPs), which includes manipulation of the actin cytoskeleton or inappropriate ROS production (Liston and Masters, 2017).

In addition, recent advances suggest that pathogen recognition in mammals also involves detection of pathogen-derived virulence activities and/or pathogen-induced disruption of cellular homeostasis (Kufer *et al.*, 2019; Lopes Fischer *et al.*, 2020; Ngwaga *et al.*, 2021). As discussed above, plant NLRs serve as sentinels of virulence activities. In mammals, some NLRs form inflammasome complexes that mediate the release of interleukin-1 family cytokines

and lead to a cell death phenomenon referred to as pyroptosis (Cookson and Brennan, 2001). Inflammatory-related cell death is a common outcome of ETI activation through NLRs, which releases inflammatory mediators that amplify antimicrobial responses, akin to the plant hypersensitive response (HR). Three type of inflammasomes have been now described to mount ETI in response to pathogen virulence activity, including NLR family pyrin domain containing 1 B (NLRP1B), NOD-, LRR- and pyrin domain-containing protein 3 (NLRP3) and pyrin. Some examples of ETI are described below, others are shown in Figure 1.16. The first example is the detection of proteolytic activity at NLRP1B. Anthrax lethal factor of *Bacillus anthracis* is a protease, which cleaves the N-terminal fragment of certain rodent NLRP1B (Levinsohn *et al.*, 2012; Chavarría-Smith and Vance, 2013; Hellmich *et al.*, 2012). Interestingly, another pathogen effector is able to activate NLRP1B (Sandstrom *et al.*, 2019). The *S. flexneri* type III-secreted effector IpaH7.8 was also shown to specifically ubiquitinylate NLRP1B (Sandstrom *et al*., 2019). These protease or ligase activities direct degradation of the NLRP1B auto-inhibitory domain, thereby inducing inflammation. The second example is provided by the sensing of the pore-forming toxin activities by NLRP3 (Craven *et al*., 2009; Muñoz-Planillo *et al.*, 2013). For instance, the α-hemolysin from *Staphylococcus aureus* is a bacterial pore-forming toxin that permeabilizes the host plasma membrane. This activity causes potassium efflux that triggers the NLRP3 inflammasome, and subsequently pyroptotic cell death (Craven *et al*., 2009; Muñoz-Planillo *et al.*, 2013). Consequently, NLRP3 can sense cytosolic potassium levels, corresponding to a HAMP for NLRP3. Other virulence factors activate the NLRP3-dependent inflammasome through disruption of intracellular membranes, such as the *Yersinia* type III-secreted effectors YopB and YopD (Zwack *et al*., 2015). These two effectors also activate the non-canonical caspase-11 inflammasome that is known to sense bacterial LPS in the cytosol (Zwack *et al*., 2017). The third mechanism of ETI activation is occurring through a subversion of host immune signaling (Figure 1.17). For instance, the *Yersinia* type III-secreted effector YopJ inhibits innate immune signaling by interfering with specific MAPK kinase kinases (MKKs) (Orth *et al*., 2000), which in return activates receptor-interacting protein kinase 1 (RIPK1)- and caspase-8-dependent apoptosis (Lopes Fischer *et al*., 2020). Some toxins are also able to inactivate host Rho GTPases, which orchestrate several cellular functions, such as actin cytoskeletal dynamics, epithelial barrier integrity, production of ROS or antimicrobial peptides (Dufies and Boyer, 2021; Popoff, 2014). For examples, *Clostridium botulinum* C3, *Clostridium difficile* TcdB, *Vibrio parahaemolyticus* VopS and *Histophilus somni* IbpA are toxins inactivating host RhoA, and subsequently activate the pyrin inflammasome (Xu *et al.*, 2014).

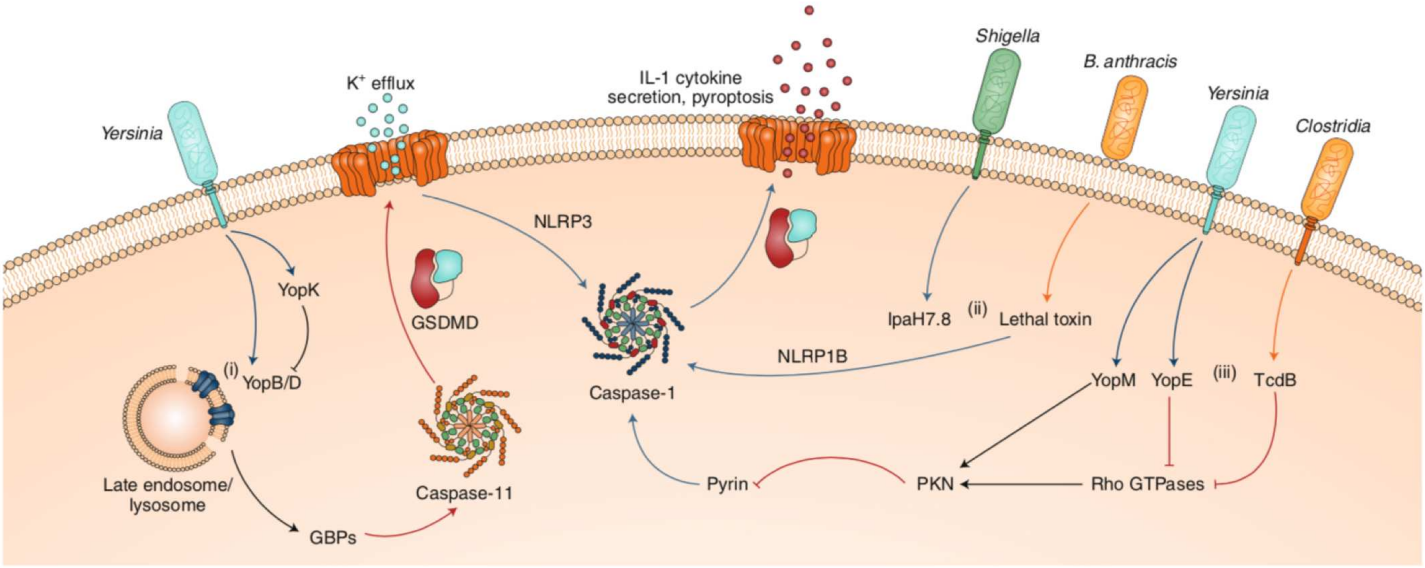

Figure 1.16. Effector-triggered immunity engages inflammasomes by sensing pathogen-derived virulence activities.
(i) *Yersinia* effectors YopB and YopD damage intracellular endosomal membranes, leading to recruitment of guanylate binding proteins (GBPs) and downstream activation of the caspase-11 inflammasome. The caspase-11-induced gasdermin D (GSDMD) pores also trigger K^+ efflux, thereby subsequently activating the NOD-, LRR- and pyrin domain-containing protein 3 (NLRP3) inflammasome. *Yersinia* suppresses this defense mechanism by preventing hyper-translocation of YopB and YopD through the activity of another effector, YopK. **(ii)** *Bacillus anthracis* lethal toxin (LeTx) or *Shigella* IpaH7.8 effector activate NLRP1B inflammasome, by cleaving or degrading its N terminus, respectively. **(iii)** *Yersinia* YopE and *Clostridium difficile* TcdB modulate the actin cytoskeleton by suppressing Rho GTPases. This suppression triggers inactivation of protein kinase C-related kinases (PKNs), which are sensitive to GTPase activity, and consequently, induces the pyrin inflammasome. *Yersinia* effector YopM directly activates PKNs, thereby maintaining pyrin suppression. Scheme derived from Lopes Fischer *et al*., 2020.

These toxins modify switch-I residue in Rho-subfamily by glucosylation, adenylylation, ADP-ribosylation and deamidation activities. Moreover, only the catalytic activity of these bacterial toxins triggers this inflammasome response, suggesting that the disruption of Rho GTPase function by these effectors is sensed by pyrin. In contrast to the inactivation of Rho GTPases, the *Salmonella* effectors SopB, SopE and SopE2 activate them. For example, Nucleotide binding oligomerization domain containing 1 (NOD1) and NOD2 NLRs have been shown to monitor bacterial peptidoglycan fragments, corresponding to the direct ligand-receptor model (Mukherjee *et al.*, 2019). Nonetheless, NOD1 was also determined to sense the activation of host cytoskeletal regulators Rac family small GTPase 1 (RAC1) and Cdc42 by the secreted *Salmonella* effector SopE (Keestra *et al*., 2013; Sun *et al.*, 2018). This activation triggers NOD1 signaling, which results in NF-κB-dependent inflammatory responses. Like with *Samonella* effectors, the disruption of the tight junctions of the intestinal epithelium by *Shigella* effectors activities is sensed by NOD1 and Guanine exchange factor H1 (GEF-H1), which activates the NF-κB pathway (Fukazawa *et al*., 2008). Collectively, these data suggest that NOD1 and NOD2 exhibit a guard-type activation of actin cytoskeleton dynamics mediated by the central regulators RhoGTPases in response to pathogen detection. Other cellular perturbations are sensed by host cells such as endoplasmic reticulum stress or pathogen-induced amino acid starvation (detailed in the Figure 1.17) (Keestra-Gounder *et al.*, 2016).

Finally, an ETI-like response has also been observed as a consequence of a disruption of protein synthesis upon *L. pneumophila* infection. This response requires five translocated bacterial effectors, Lgt1, Lgt2, Lgt3, SidI, SidL, that inhibit host protein synthesis (Fontana *et al.*, 2011). Macrophages infected with *L. pneumophila* exhibit sustained activation of NF-κB, since these five effectors prevent the resynthesis of inhibitor of nuclear factor kappa B (IκB). By contrast, infection with a *L. pneumophila* mutant lacking the five effectors still activates TLRs and NF-κB signaling, but NF-κB activation was more transient and was not sufficient to fully induce an ETI-like response. This response is presumably caused by a normal IκB synthesis in response to this *L. pneumophila* mutant. This model resembles to the indirect "guard" model that has been described in plants, whereby host cells guard the integrity of host translation. However, it is currently unknown whether such response would require some NLRs for ETI activation.

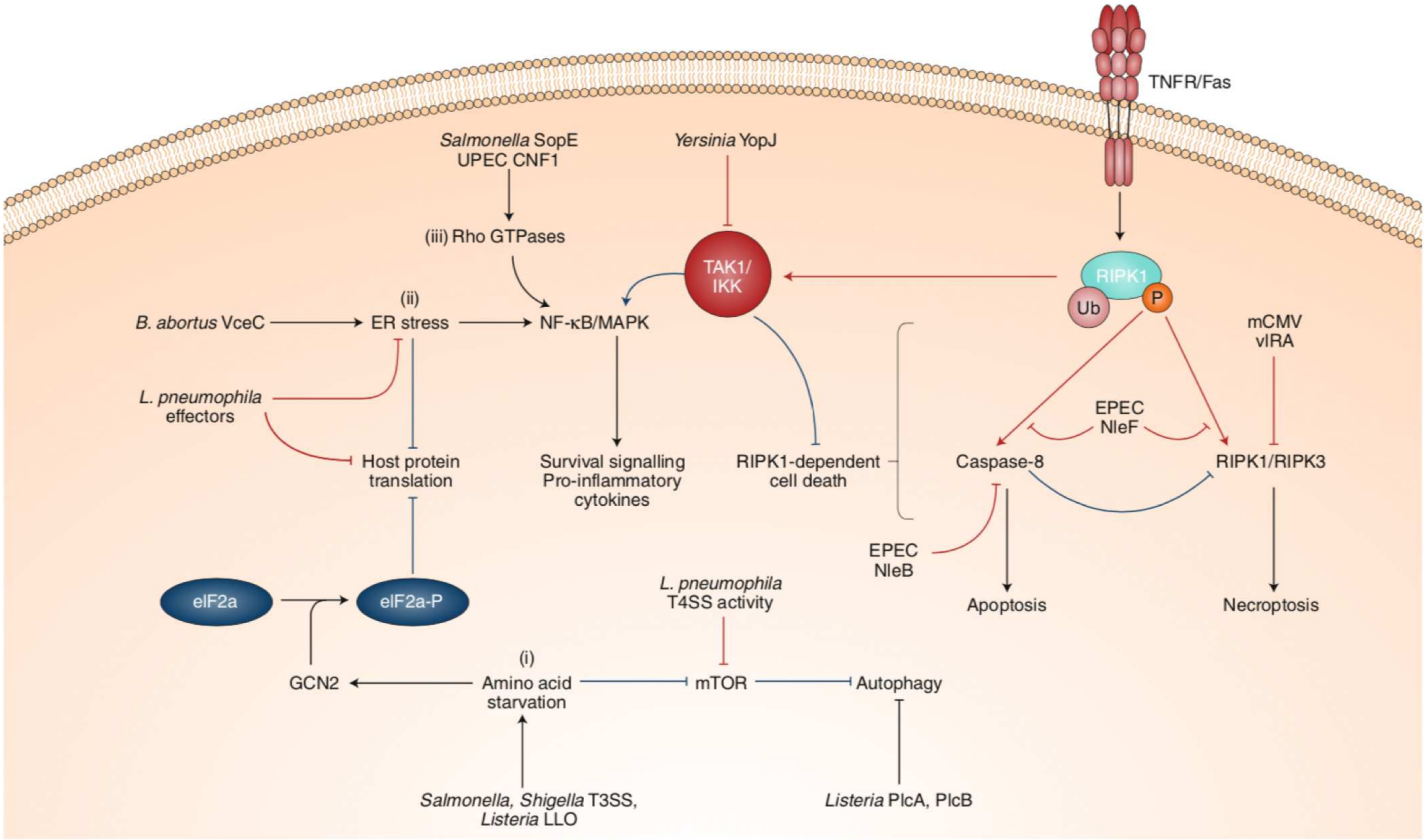

Figure 1.17. Pathogen manipulation of fundamental cellular processes and signaling pathways induces effector-triggered immunity.
In addition to inflammasomes, host cells possess several other defense mechanisms activated in response to different virulent activities. Many of these pathways trigger signaling cascades that upregulate a subset of innate immune-responsive genes. These pathways promote host cell defense or serve to eliminate invading pathogens through different mechanisms including autophagy and cell death. Here are presented some examples of effector-triggered immunity (ETI) and pathogen adaptations to evade these host immune responses. **(i)** Pathogen-induced amino acid starvation can either suppress target of rapamycin (mTOR) and activate autophagy or activate the cytosolic kinase general control nonderepressible 2 (GCN2), which lead to a blockage in host protein synthesis. Some pathogen effectors, such as *Listeria* PlcA and PlcB, inhibit mTOR signaling and autophagy, respectively, in order to evade detection. **(ii)** *Legionella* and *Brucella* trigger endoplasmic reticulum (ER) stress and consequently suppress protein translation. This activity induces nuclear factor-kappa B (NF-κB) and mitogen-activated protein kinase (MAPK) signaling and triggers expression of subset of proinflammatory cytokines. To counteract this immune defense, *Legionella* also possesses effectors that suppress ER stress and host protein translation, thereby partially masking itself from ETI. **(iii)** Rho GTPases are activated by SopE effector from *Salmonella* and the toxin cytotoxic necrotizing factor 1 (CNF1) from uropathogenic *Escherichia coli* (UPEC), which triggers NF-κB pathway to induce inflammatory cytokines and promote cell survival. Other effectors, such as *Yersinia* YopJ, that suppresses NF-κB and MAPK pathways, induce RIPK1-dependent apoptosis. When pathogens inhibit apoptosis, they can concomitantly activate a cell death mechanism, namely the RIPK1-dependent necroptosis. Some pathogens have evolved to suppress both of these responses, for example through the effectors NleB, NleF and EspL from enteropathogenic *Escherichia coli* (EPEC) or the viral inhibitor of RIP activation (vIRA) from *cytomegalovirus* (CMV), which suppress necroptosis. Scheme derived from Lopes Fischer *et al*., 2020.

VIII. *LEGIONELLA PNEUMOPHILA*: CAUSATIVE AGENT OF LEGIONNAIRES' DISEASE AND PONTIAC FEVER

VIII.I. THE HISTORY OF LEGIONELLA PNEUMOPHILA

The identification of *Legionella pneumophila* has been made in 1977, following the 58th annual convention of the American Legion in Philadelphia (Pennsylvania, USA) in July 1976. An outbreak of pneumonia caused by a previously unknown bacterium occured, affecting 221 attendees and causing 34 fatal cases (Fraser *et al.*, 1977). The presence of a Gram-negative bacillus in the lungs and tracheobronchial tree of infected patients was identified by Joseph E. McDade and Charles C. Shepard, as the cause of the disease (McDade *et al.*, 1977). They subsequently named this bacterium *Legionella pneumophila* and the genus was called *Legionella,* which at that time was composed only of a single known species. After this discovery, further studies revealed that *Legionella* had already been isolated in 1947, but had not been further characterized at this time (McDade *et al.*, 1979). Nowadays, the genus *Legionella* is known to include more than 65 different species, and at least 27 of those have been documented as human pathogens. Since 1976, numerous outbreaks of Legionnaires' disease have been described in North America and Europe.

VIII.II. EPIDEMIOLOGY AND ECOLOGY OF AN OPPORTUNISTIC WATERBORNE PATHOGEN

The great majority of Legionnaires' disease is caused by *L. pneumophila*, mainly by *L. pneumophila* serogroup 1 despite the description of 15 serogroups (Sg), with approximately 84% worldwide and 95% in Europe of *Legionella* infections (Harrison *et al.*, 2007; Muder and Yu, 2002; Yu *et al.*, 2002). Additionally, *L. longbeachae* is responsible for approximatively 1% of cases worldwide. Interestingly, this trend does not appear to apply in Australia and New Zealand, where *L. pneumophila* accounts for only 50% of the cases, while *L. longbeachae* accounts for 30–50% of registered cases (Yu *et al.*, 2002). However, it has been noticed that the prevalence of *L. longbeachae* is increasing in Europe since the last decade (Bacigalupe *et al.*, 2017). Other species and serogroups cause human diseases, such as *L. bozemanae*, *L. micdadei*, *L. pneumophila* Sg3 and Sg6 (Beauté and Network, 2017; Yu *et al.*, 2002). The

annual notification rate of Legionnaire's disease increased continuously, from 1.3 to 2.2 for 100 000 people in 2014 and 2018, respectively (European Centre for Disease Prevention and Control (ECDC), 2020). However, Legionellosis is probably underestimated because of the difficulty in their identification and the absence of simple serodiagnostic reagents for *Legionella* non-*pneumophila* (Vaccaro *et al.*, 2016).

L. pneumophila is a Gram-negative rod-shaped γ-proteobacteria, and was the first bacterium identified to multiply within a large range of protozoan host organisms, mainly aquatic amoebae, which represent its main replicative niche in the environment (Boamah *et al*., 2017; Hoffmann *et al.*, 2014). *L. pneumophila* is the most prevalent *Legionella* species to infect humans, however, this species does not reflect the environmental distribution in the genus (Doleans *et al*., 2004). They are ubiquitously found in freshwater environments (rivers, ponds, streams, lakes, and thermal pools), as well as in moist soil, mud and composted material (Figure 1.18) (Newton *et al.*, 2010). The multiplication of *Legionellae* is facilitated in water systems in the presence of nutrients, appropriated temperature, and thus is in contact with humans in both natural and urban environments. *L. pneumophila* can also be recovered as free-living biofilm-associated bacteria, where it intercalates into existing biofilms (Abdel-Nour *et al*., 2013; Taylor *et al*., 2009). The ability of *L. pneumophila* to replicate in amoebae allows them to survive in harsh environmental conditions for long periods, tolerating high temperature (from 0 to 68°C) and various pH range (from 5.0 to 8.5). Furthermore, they are protected from water disinfection procedures (Berjeaud *et al.*, 2016).

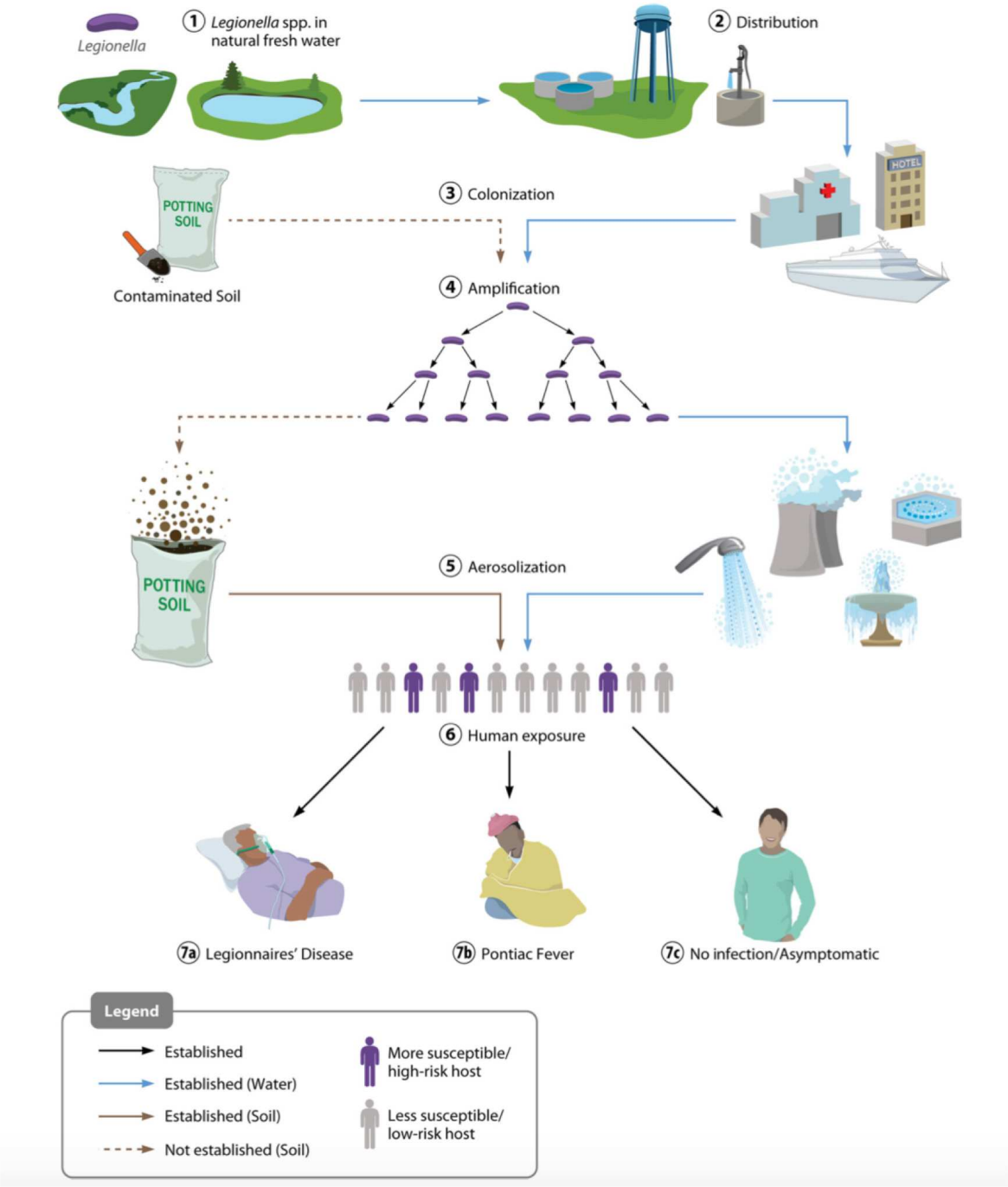

Figure 1.18. Transmission route of *Legionella* from natural environment towards human infections.
(1) *Legionella* is found in freshwater sources, **(2)** where they are distributed at low concentrations from points of water purification **(3)** to colonize downstream local plumbing networks and cooling systems (among other sites). **(4)** *Legionella* amplifies under permissive environmental conditions. **(5)** Aerozilation can then expose a human population, **(6)** which includes individuals with increased susceptibility. **(7a)** After exposition, susceptible individuals (due to age or underlying medical conditions) have at high risk of Legionnaires' disease, **(7b)** the whole population is at risk for Pontiac fever, **(7c)** while some individuals will have asymptomatic form or are not infected. Contaminated soil appears to involve aerosol exposure, but the route is less well understood. Scheme derived from Mercante and Winchell, 2015.

Legionellosis is a relevant cause of community- (2-15%) and hospital-acquired pneumonia (Principe *et al*., 2017). Although most cases of Legionnaires' disease occur sporadically, epidemic form can arise. Inhaling *Legionella*-containing aerosols is the commonly cause of infection in humans from contaminated man-made water sources, such as showers, hot tubs, plumbing networks, and air-conditioning systems (Fields, 1996). Human-to-human transmission is rare, although one case has been reported (Borges *et al.*, 2016; Correia *et al.*, 2016). *L. pneumophila* can infect healthy individuals, however the majority of infection occurred in immunosuppressed or predisposed patients (Cunha and Cunha, 2017; Muder and Yu, 2002). Susceptibility to disease is associated with advanced age (predisposition for people over 50 years-old), predominantly in men, smoking, organ transplants, heavy consumption of alcoholic beverages, weakened immune system (immunosuppressive therapies) and underlying medical problem (Farnham *et al*., 2014). It is also noteworthy that a genetically-determined susceptibility of humans to Legionellosis has been reported (Hawn *et al*., 2003). The average case-fatality rate is 8% in Europe and 7% in the USA (Centers for Disease Control and Prevention (CDC), 2020; European Centre for Disease Prevention and Control (ECDC), 2020). *L. pneumophila* infections show a seasonal pattern, and occur especially in late summer to autumn.

VIII.III. DETECTION, SYMPTOMS AND TREATMENTS

The time required for the detection of the pathogen remains critical for the final disease outcome. Originally, the serological-based assay was the predominant method for diagnosing *Legionella* infections, but the use of new and more rapid techniques, such as urinary antigen test and polymerase chain reaction (PCR)–based detection methods, is increasing (Mercante and Winchell, 2015). Nevertheless, the urinary antigen test is widely used as a first-line diagnostic, and it allows only the detection of *L. pneumophila* Sg1. Today, the PCR-based methods are more used in reference centers and allow the detection of *Legionella* non-*pneumophila* species (Cross *et al.*, 2016). Nevertheless, the standard reference method remains culture on defined growth medium, since it allows the identification of different *Legionella* species and serogroups (Dunne *et al.*, 2017).

After exposition to *L. pneumophila*, people can develop two different illness, referred to as Legionnaires' disease or Pontiac fever, collectively known as Legionellosis. Legionnaires' disease is very similar to other types of pneumonia, with symptoms such as cough, shortness of breath, fever, muscle aches and headaches. Gastrointestinal stomach symptoms are common with diarrhea being the most distinctive symptom. The symptoms usually appear 2 to 10 days after being exposed to the bacteria. Fatal courses of the disease occur when the bacterium disseminates deeper into the lung. Pontiac fever is a mild and non-fatal illness, with primarily fever and muscle aches, and does not cause pneumonia. Symptoms begin between a few hours to three days after being exposed to bacteria and is more common in younger people. Pontiac fever is usually identified only when cases occur as part of a cluster or outbreak.

Legionella infection can be effectively treated with antibiotics, although one ciprofloxacin (fluoroquinolone)-resistant *L. pneumophila* strain has been isolated and reported from a patient in the Netherlands (Bruin *et al.*, 2014). Given the rare antibiotic resistance events, the recommended antibiotic therapy against *Legionella* is fluoroquinolones or macrolides, especially azithromycin or levofloxacin (Pedro-Botet and Yu, 2006). A full recovery is most of the time observed if appropriate antibiotics are given sufficiently early during disease development.

VIII.IV. THE INTRACELLULAR LIFESTYLE OF L. PNEUMOPHILA IN PROTISTS AND MAMMALIAN MACROPHAGES

L. pneumophila presents a biphasic life cycle, comprising a replicative (avirulent) and a transmissive (virulent) forms (Molofsky and Swanson, 2004). The differentiation between these two phases occurs during the transition between intracellular and extracellular environments, which triggers a gene expression program leading to metabolic and morphogenetic changes (Oliva *et al.*, 2018). In favorable environment, *L. pneumophila* multiplies intracellularly through the repression of genes involved in the motility, osmotic-, acid-resistance and cytotoxicity, and through the enhanced expression of genes necessary for bacterial replication (Chauhan and Shames, 2021; Oliva *et al.*, 2018). Conversely, when nutrients become limited, *L. pneumophila* arrests its replication and triggers another gene expression program (Brüggemann *et al.*, 2006).

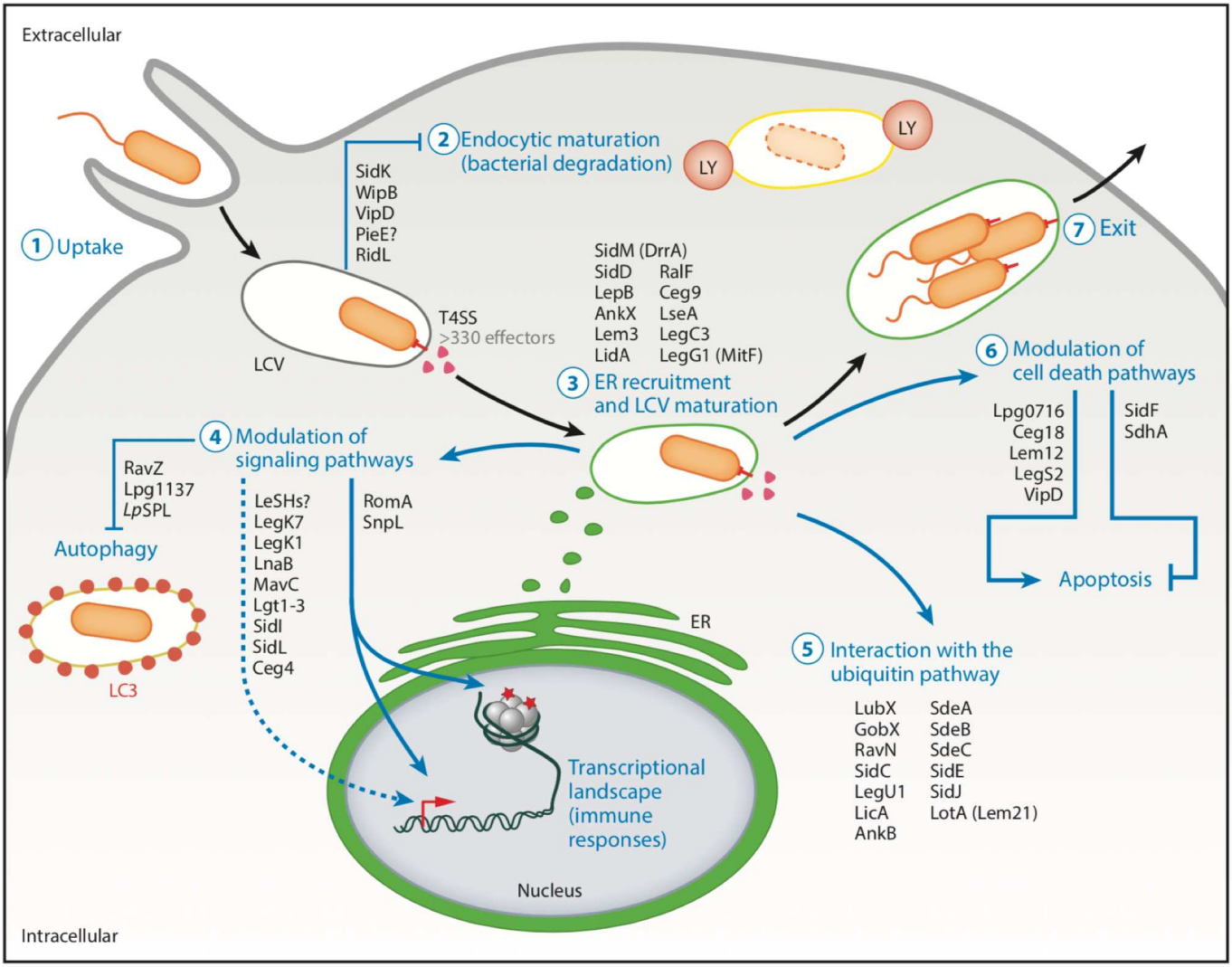

Figure 1.19. Effectors interfere with various steps of the *Legionella pneumophila* life cycle.
The intracellular cycle of *L. pneumophila* and the effectors secreted by the type-IV secretion system that control cellular processes at each step of the bacterial cycle are represented. **(1)** *L. pneumophila* is uptaken by the host cell, **(2)** then it avoids endocytic maturation and **(3)** it recruits endoplasmic reticulum (ER)-derived vesicles to the *Legionella*-containing vacuole (LCV). This allows the formation of its replicative niche, **(4-6)** where bacteria replicate and modulate host cell signaling. **(7)** Once the replication is achieved, *L. pneumophila* exits from the cell and infects a new host cell. LY; lysosome. Scheme derived from Mondino *et al*. 2020.

The ability of *Legionella* to replicate in protozoa in its natural environment has equipped this bacterium with an arsenal of virulence mechanisms necessary to invade and replicate in human alveolar macrophages. *L. pneumophila* infections have been studied in a wide variety of mammalian host cells, such as macrophage-like tissue culture cells and mouse bone marrow-derived macrophages or even HeLa, A549, and CHO-K1 epithelial cell derivatives. Among all these model systems, the primary mechanism of infection is based on invasion of the host cell, and subsequently followed by a rapid establishment and maturation of a membrane-bound replicative niche known as the *Legionella*-containing vacuole (LCV) (Figure 1.19) (Derré and Isberg, 2004; Isberg *et al.*, 2009; Tilney *et al.*, 2001). During the formation of LCV, *L. pneumophila* evades phagolysosomal degradation (Horwitz, 1983a). Bacterial cells are then protected from intracellular defenses and can uptake nutrients to promote their replication. The intracellular life cycle of *L. pneumophila* in human cells is very similar to the one observed in amoebae cells, despite some differences at the cellular level (Escoll *et al.*, 2014).

L. pneumophila is usually taken-up by the host cell through a unique uptake process called ‘‘coiling phagocytosis’, by binding the complement receptor 1 (CR1) and complement receptor 3 (CR3) on human phagocytic cells (Horwitz, 1984; Payne and Horwitz, 1987). Attachment on its natural protist host is released on the galactose/N-acetylgalactosamine-inhibitable lectin (Gal/GalNAc) of *Vermamoeba vermiformis* or the mannose binding lection (MBL) of *Acanthamoeba castellanii* (Declerck *et al.*, 2007; Venkataraman *et al.*, 1997). Coiling phagocytosis in macrophages, in contrast to the common zipper-like uptake of pathogens, consists in the asymmetrical engulfment of the bacteria by unilateral pseudopods encircling extracellular bacterial prior to entry (Rittig *et al.*, 1998). Similarly, the uptake of *L. pneumophila* by *A. castellanii* is mediated by the same coiling pseudopods mechanism as in human macrophages (Bozue and Johnson, 1996). However, conventional phagocytosis by macrophages have been observed by other *Legionella* strains and species or macropinocytosis in bone marrow-derived macrophages, and seems to differ according to the bacterial strain as well as the mammalian phagocyte (Elliott and Winn, 1986; Molmeret *et al.*, 2005; Rechnitzer and Blom, 1989; Watarai *et al.*, 2001). In addition to coiling phagocytosis by protists, engulfment of *L. pneumophila* by *Hartmannella vermiformis* occurs mainly by zipper-like conventional phagocytosis and uptake by *Dictyostelium discoideum* seems to happen by macropinocytosis, a receptor-independent mechanism of endocytosis (Abu Kwaik, 1996; Peracino *et al.*, 2010). It is also thought that Pili are involved in the attachment of bacterial cells to human macrophages and *Acanthamoeba polyphaga*, and likely to other host cells (Stone and

Abu Kwaik, 1998). Importantly, even if uptake of *L. pneumophila* occurs mainly by host-driven phagocytosis, the Dot/Icm type IV system, corresponding to the type four secretion system (T4SS), enhances endocytic events in macrophage-like cells as well as in *A. castellanii* (Hilbi *et al.*, 2001; Khelef *et al.*, 2001). Shortly after internalization, *L. pneumophila* manipulates host cellular trafficking and establishes its intracellular niche, in which bacteria differentiate into a replicative form for efficient multiplication (Isberg *et al.*, 2009). The formation of the nascent phagosome after *L. pneumophila* phagocytosis by mammalian cells is actin-dependent and is governed by the type IV secretion system, which injects more than 330 effectors in host cells (Charpentier *et al.*, 2009; Elliott and Winn, 1986; Ensminger, 2016; Hayashi *et al.*, 2008; King *et al.*, 1991; Schroeder, 2018; Welsh *et al.*, 2004). Several host cell pathways are activated in response to *L. pneumophila* invasion, such as Mitogen-activated protein kinase (MAPK) cascades in human macrophages and in *D. discoideum* (Li *et al.*, 2009; Welsh *et al.*, 2004). *L. pneumophila* also exploits phosphoinositide (PI) lipids during the establishment of the replicative vacuole (Thi and Reiner, 2012). One feature of *L. pneumophila* infection is its ability to evade the endocytic pathway, thereby preventing phagosome-lysosome fusion (Derré and Isberg, 2004; Horwitz, 1984, 1983b).

The nascent phagosome containing *L. pneumophila* rapidly intercepts early secretory vesicles that cycle between the endoplasmic recticulum (ER) and Golgi apparatus, ER and mitochondria, for the establishment of its replication vacuole (Horwitz, 1983a; Kagan and Roy, 2002; Tilney *et al.*, 2001). At four hours post-infection, these components start to disappear from the LCV, and concurrently, the LCV becomes studded with ribosomes, turning the LCV into a rough ER-like vacuole (Tilney *et al.*, 2001). The remodeling of LCV creates an ER-like organelle that supports replication of *L. pneumophila* (Derré and Isberg, 2004; Horwitz, 1983b; Kagan and Roy, 2002; Tilney *et al.*, 2001). *L. pneumophila* also hijacks secretory vesicles, ER and mitochondria when infecting amoebal hosts like *Hartmannella vermiformis* and *D. discoideum* (Abu Kwaik, 1996; Fajardo *et al.*, 2004; Francione *et al.*, 2009; Lu and Clarke, 2005). In addition to these protein recruitments, *L. pneumophila* also exploits polyubiquitinated (polyUb) proteins that accumulate at the vacuole (Dorer *et al.*, 2006; Lomma *et al.*, 2010). With the help of several translocated proteins, *L. pneumophila* negatively regulates vacuolar acidification by blocking the host vacuolar ATPase, a proton pump presents throughout the membranes of the endocytic pathway (Xu *et al.*, 2010). Regarding the LCV maturation, secreted effectors were shown to interact with host small GTPases of the Rab family, representing an important group of regulatory proteins orchestrating microtubule stabilization, LCV motility as

well as intracellular replication of *L. pneumophila* (Rothmeier *et al*., 2013; Urwyler *et al.*, 2009). Some type IV-dependent effectors bind phosphoinositide lipids to decorate the LCV, which are crucial factors involved in host cell membrane dynamics (Weber *et al*., 2014).

The replication of *L. pneumophila* starts between 4 and 10h after phagocytosis, with a generation time of about an 1h (Escoll *et al.*, 2014). Moreover, bacterial replication is directed by *Legionella*-induced mitochondrial fragmentation, which leads to a Warburg-like phenotype in macrophages, seen in cancer cells, in order to create a replication permissive niche in host cells (Escoll *et al.*, 2017). The Warburg-like phenotype corresponds to the dependency on a high glycolytic rate and high glucose uptake by the preferential conversion of the majority of their absorbed glucose to lactate, even under oxygen-rich conditions (Warburg, 1956). Once replication has ceased, *L. pneumophila* escapes from its LCV through pore formation and membrane lysis (Alli *et al*., 2000; Kirby *et al*., 1998). Bacterial cells continue a few more round of replication in the cytosol (Molmeret *et al.*, 2004). When nutrient levels are low, *L. pneumophila* undergoes phenotypic changes and becomes flagellated, converting into a virulent transmissive form (Byrne and Swanson, 1998). Then, *L. pneumophila* can initiate another intracellular cycle in neighboring cells or start an extracellular growth cycle. In protozoan hosts, non-lytic release occurs, liberating vesicles of respirable size that contain numerous bacteria (Berk *et al*., 1998). At this point, the infection of humans can occur by aerosolization of infectious particles of free bacteria, bacteria within released vesicles (from amoebae), or even bacterium-filled protists (Muder *et al*., 1986). Inhaled bacteria can enter in the lungs and are taken-up by resident alveolar macrophages to repeat the cycle within a new host cell. *L. pneumophila* that have escaped the protist host are more infectious and can cause a more robust disease in humans (Cirillo *et al.*, 1999), explaining why amoebae have been referred to as the "Trojan horses of the microbial world" or the "training grounds" for *L. pneumophila* (Brown and Barker, 1999; Fonseca and Swanson, 2014; Molmeret *et al.*, 2005).

During bacterial replication, *L. pneumophila* secretes a series of effectors to promote bacterial pathogenesis. Different types of secretion systems have been characterized. One of which is the Dot/Icm apparatus (type 4B secretion system; equivalent to the Tra/Trb bacterial conjugation systems), able to translocate more than 330 proteins into the target host cells (Ensminger, 2016; Schroeder, 2018). This secretion system was detected in all *Legionella* strains with the type-II secretion system (T2SS), and the type-I secretion systems (T1SS) was restricted to *L. pneumophila* species. *L. pneumophila* encodes also a 4A Lvh secretion system (T4ASS; equivalent to the *Agrobacterium tumefaciens* Vir system) (Qin *et al.*, 2017).

The T1SS allows secretion of substrates into the extracellular space, and it is required for entry into the host cell, but seems dispensable to the intracellular cycle (Fuche *et al.*, 2015). The T2SS system is required for intracellular replication in amoebae and also for pathogenesis in humans, including biofilm establishment, sliding motility, intracellular infection of macrophages, dampening the host innate immune response and bacterial persistence in the lungs (Cianciotto, 2013). This system can translocate more than 25 effectors in host cells. For the T4ASS, it is assumed that it contributes to interspecies horizontal gene transfer (Glöckner *et al.*, 2008), and is also involved in virulence-related phenotypes under conditions mimicking the spread of Legionnaires' disease from environmental niches (Bandyopadhyay *et al.*, 2007). The T4BSS plays a critical role for LCV biogenesis, especially organelle recruitment and inhibition of phagosome-lysosome fusion, and intracellular replication inside mammalian macrophages (Berger and Isberg, 1993; Marra *et al.*, 1992). These effector proteins target cellular process conserved in protozoa and mammals (Mondino et al., 2020a; Schroeder, 2018). Interestingly, a large variety of eukaryotic-like effector proteins are encoded by *L. pneumophila,* proposed to be acquired from all domains of life (plant, animal, fungal, archaea) (Cazalet *et al.*, 2004; Gomez-Valero *et al.*, 2019). This observation suggests that these effector proteins were horizontally transferred from its eukaryotic hosts (amoebae) (de Felipe *et al.*, 2005a), and now uses them to interfere with signal transduction in mammalian cells and to subvert host functions. For instance, some studies have conducted an in-depth characterization of type IV-dependent eukaryotic-like kinase effectors in the course of human infection (Ge *et al.*, 2009; Hervet *et al.*, 2011; Lee *et al.*, 2020; Michard *et al.*, 2015; Moss *et al.*, 2019). Among

these effectors, LegK7 was shown to hijack the conserved Hippo signaling pathway by molecularly mimicking host Hippo kinase (Lee and Machner, 2018). Another host signaling pathway modulated by *L. pneumophila* is the NF-κB pathway, due to its central role in host innate immune responses. Several *Legionella* effectors interfere with this host response at different stages of infection. In particular, LegK1 encodes a serine/threonine kinase that strongly activates NF-κB signaling (Ge *et al*., 2009). More specifically, LegK1 was shown to phosphorylate two serine 32 of IκBα, which is typically phosphorylated by the mammalian kinases IKKα or IKKβ, to activate the NF-κB-dependent signaling pathway. Another example includes LegK2. This type IV-secreted effector contributes to bacterial intracellular replication, and this phenotype is dependent on its kinase activity (Hervet *et al*., 2011; Michard *et al.*, 2015). LegK2 was found to interact with host Actin Related Protein 2/3 (ARP2/3), thereby inhibiting actin polymerization on the phagosome and preventing late endosomes from fusing with the phagosome (Hervet *et al.*, 2011; Michard *et al.*, 2015). The last example illustrating the role of eukaryotic-like kinase is LegK4. LegK4 phosphorylates 70-kDa heat shock proteins (Hsp70) and disrupts its ATPase activity, which in turn inhibits its protein folding capacity and results in global translation inhibition (Moss *et al.*, 2019).

Thanks to this myriad of effectors, *L. pneumophila* interferes with several host signaling pathways. This includes MAPK pathway, which is essential for the activation of immune responses, the host transcriptional machinery by modifying histone marks, or mRNA processing and elongation (Rolando *et al.*, 2013; Schuelein *et al.*, 2018). In addition, several reports found that *L. pneumophila* interacts with the ubiquitin and apoptotic pathways. Indeed, some type IV-secreted effectors act as ubiquitin ligases or interact with components of the host ubiquitination machinery (Qiu and Luo, 2017). Others possess the ability either to prevent or promote cell death, probably to maintain the integrity of its replication niche or to favour its release from host cells (Speir *et al.*, 2014). Moreover, an emerging class of metaeffectors have been shown to function as "effectors of effectors" through targeting and regulating the function of other effectors (Joseph and Shames, 2021). This term was coined since the discovering that the effector LubX spatiotemporally regulates the effector SidH (Kubori *et al*., 2010).

Considering the large repertoire of *L. pneumophila* effectors, it is noteworthy that deletion in a single effector gene is often associated with a lack of phenotype. This is likely due to functional redundancy between those effectors, with compensatory roles between many of

them. Indeed, some effectors possess the same biological activity or different activities that interfere on the same cellular process. For instance, the Lgt family of effectors affects eukaryotic protein synthesis and are differentially regulated during bacterial growth (Belyi *et al.*, 2014). This large effector repertoire is also found in all *Legionella* species, as the genus harbors more than 18,000 effectors (Gomez-Valero *et al*., 2019). However, the effector repertoire differs among species. Interestingly, many of them are conserved only in *L. pneumophila* strains and rarely in other *Legionella* species (Mondino *et al.*, 2020a).

IX. INNATE IMMUNITY TRIGGERED DURING *LEGIONELLA PNEUMOPHILA* INFECTION

Control of *L. pneumophila* infection in macrophages is mediated by several immune responses, including inflammasome-, TNFα- and IFN-dependent resistance mechanisms. In mammalian cells infected with *L. pneumophila*, NF-κB signaling is activated in two waves. The first one is dependent on TLRs, and thus relies on the perception of *L. pneumophila* PAMPs when bacteria cells contact host cells and during the early phase of infection. The second one is mediated by effectors and occurs after several hours of infection (Asrat *et al.*, 2014; Losick and Isberg, 2006). *L. pneumophila* is sensed by multiple PRRs, such as TLRs, NLRs and cytosolic nucleic acid sensors (Figure 1.20), which results in PAMP-triggered NF-κB signaling. Several reports have shown that the LPS of *L. pneumophila* is recognized by TLR2, although it was thought that LPS are generally recognized by TLR4 (Braedel-Ruoff *et al.*, 2005; Fuse *et al.*, 2007; Girard *et al.*, 2003). In addition to LPS, it was shown that lipopeptides and lipoproteins trigger TLR2 activation (Akamine *et al.*, 2005; Archer and Roy, 2006; Hawn *et al.*, 2006; Shim *et al.*, 2009). TLR2 recognition contributes to the production of NF-κB-dependent proinflammatory mediators such as TNFα and various chemokines (Massis and Zamboni, 2011). As *L. pneumophila* is a flagellated bacterium, flagellin is also recognized by TLR5, and this receptor plays a critical role in human cells (Hawn *et al.*, 2003). Finally, TLR9 also contributes to anti-*Legionella* innate immunity, and is activated by unmethylated CpG present at high frequencies in bacterial DNA (Bhan *et al.*, 2008). Moreover, reports in mice have shown that the deficiency for a single TLR does not result in a significant enhanced susceptibility to *L. pneumophila* (Massis and Zamboni, 2011). However, the deletion of MyD88, the common TLR-adaptor protein, renders mice highly susceptible to infection (Archer and Roy, 2006; Archer *et al.*, 2010; Hawn *et al.*, 2006; Neild *et al.*, 2005; Spörri *et al.*, 2006). These results suggest that several MyD88-dependent TLRs are required for optimal lung immunity in *Legionella* pneumonia.

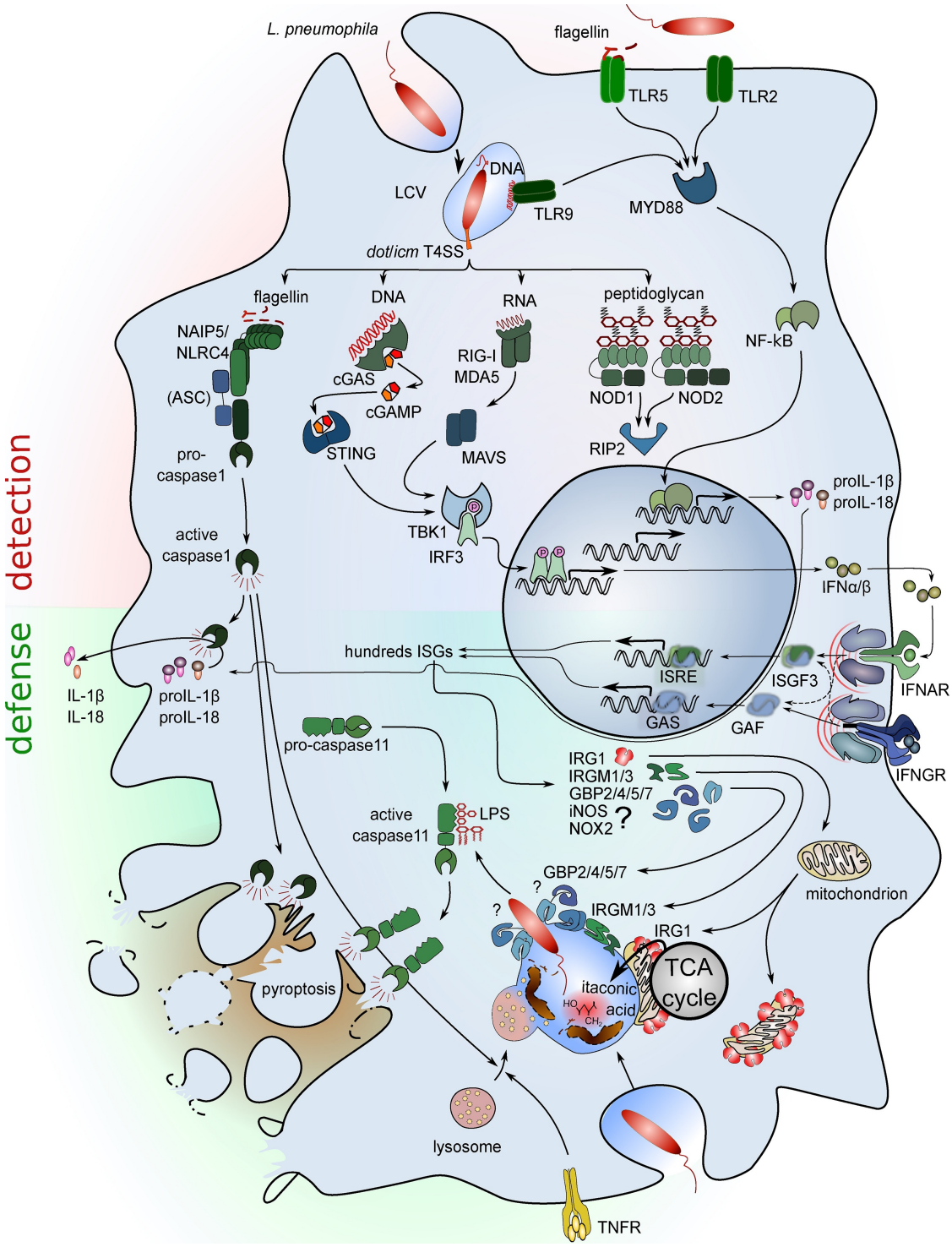

Figure 1.20. Overview of innate immune sensing and antibacterial defense mechanisms in macrophages infected by *L. pneumophila*.
L. pneumophila is sensed by the Toll-like receptors 2 (TLR2) and TLR5 on the cell surface and by TLR9 in phagosomes. The sensing primarily activate signaling via Myeloid differentiation factor 88 (MyD88) and nuclear factor-kappa B (NF-κB) to induce production of proinflammatory mediators such as precursor, prointerleukin-1β (proIL-1β) and Tumor Necrosis Factor α (TNF-α). In addition, NLR family apoptosis inhibitory protein 5(NAIP5)/NLR family CARD domain containing 4 (NLRC4), caspase-11, Nucleotide-binding oligomerization domain-containing protein 1 (NOD1)/NOD2, cyclic GMP-AMP synthase (cGAS), and probably retinoic acid-inducible gene I (RIG-I) as well as melanoma-differentiation-associated gene 5 (MDA5) detect diverse bacterial components, such as bacterial flagellin, lipopolysaccharide (LPS), peptidoglycan, DNA, and RNA, respectively, which access the host cytosol in a partially type-IV secretion system-dependent manner. NAIP5 and NLRC4 together with caspase-1 and apoptosis-associated speck-like protein (ASC) form a canonical inflammasome to regulate IL-1β and IL-18 production, and to activate pyroptosis. Furthermore, both NAIP5/NLRC4 inflammasome activation as well as the binding of TNFα to its receptor Transcription factor-like nuclear regulator (TFNR) have been shown to enhance fusion of *Legionella*-containing vacuoles (LCVs) with lysosomes. Caspase-11 binds to LPS and forms a non-canonical inflammasome that activate pyroptosis. NOD1 and NOD2 signal through Receptor Interacting Protein 2 (RIP2) to stimulate expression of NFκB-dependent proinflammatory genes. The DNA sensor cGAS signals through Stimulator of interferon genes (STING), TANK-binding kinase 1 (TBK1) and Interferon regulatory factor 3 (IRF3) to induce expression of type I interferon (IFN) α/β. In addition, the RNA sensors RIG-I and MDA5 as well as their adapter molecule Mitochondrial antiviral-signaling protein (MAVS) can also contribute to the production of type I IFNs. Autocrine type I IFNs and IFNγ (which is produced by lymphoid cells, not depicted here) are recognized by their receptors Interferon alpha/beta receptor (IFNAR) and Interferon gamma receptor 1 (IFNGR), respectively. This triggers the activation of the transcription factor complexes Interferon-stimulated gene factor 3 (ISGF3) and Gamma interferon activation factor (GAF), which bind to IFN-stimulated response element (ISRE) and gamma-activated sites (GAS) binding sites, respectively, and induce transcription of hundreds of IFN-stimulated genes (ISGs). These ISGs encode for several antimicrobial molecules of which for example Immunoresponsive gene 1 (IRG1), Immunity-related GTPase family M protein 1/3 (IRGM1/3) and Guanylate-binding proteins (GBPs) are localized around LCVs to control intracellular infection. Scheme derived from Naujoks *et al*., 2018.

NLRs are also involved in immunity against *L. pneumophila*, since both NOD1 and NOD2 effectively participate in the mice pulmonary detection of bacterial cell wall molecules, such as peptidoglycan, which induces chemokine production (Berrington *et al.*, 2010; Frutuoso *et al.*, 2010). Other members of NLR proteins family contribute to antibacterial defense. For example, murine NLR family apoptosis inhibitory protein 5 (Naip5) and Naip6 or hNAIP sense flagellin and recruit another NLR protein called NLR Family CARD Domain Containing 4 (NLRC4) to activate caspase-1, with Naip5 being more effective in mice (Vinzing *et al.*, 2008; Zamboni *et al.*, 2006). Naip5/NLRC4 are required for the detection of the N-terminus and conserved carboxy-terminal domain of flagellin (Lightfield *et al*., 2008, 2011). The recognition leads to the cleavage of caspase-1, the pyroptosis and the production of IL-1β (Derré and Isberg, 2004; Fink and Cookson, 2006). Although Naip5/NLRC4 activation induces predominantly caspase-1 activation, caspase-1-independent responses have also been reported (Pereira *et al*., 2011). It was also shown in mice that LPS binds caspase-11, which triggers pore formation and partially accounts for the IL-1α secretion. It also facilitates the efflux of potassium and the non-canonical activation of NLRP3 (Mascarenhas and Zamboni, 2017). The DNA-sensing Absent In Melanoma 2 (AIM2) inflammasome is activated by sensing dsDNA from *L. pneumophila* (Ge *et al.*, 2012). AIM2 binds apoptosis-associated speck-like protein (ASC) to activate caspase-1, and leads to pyroptosis of mouse and human cells and IL-1β secretion (Bürckstümmer *et al.*, 2009; Fernandes-Alnemri *et al.*, 2009; Hornung *et al.*, 2009; Roberts *et al.*, 2009).

Finally, several reports have reported the production of type I IFN (IFNα/β) in response to *L. pneumophila*, activated by bacterial nucleic acids in the cytosol (Massis and Zamboni, 2011; Naujoks *et al.*, 2018). Indeed, sensing of *Legionella* DNA or RNA in the cytosol requires the DNA sensor cyclic GMP-AMP synthase (cGAS) or cytosolic RNA sensors RIG-I and MDA5, respectively (Monroe *et al.*, 2009; Naujoks *et al.*, 2018). Such sensing mechanism contributes to type I IFN response, which in turn, with IFNγ, strongly activates macrophage-intrinsic defense, thereby restricting intracellular bacterial growth (Naujoks *et al.*, 2016).

X. CONTEXT AND THESIS OBJECTIVES

It is now well-established that plant and mammalian pathogenic bacteria can reprogram miRNA genes expression during infections. The relevance of some of these bacterially-responsive miRNAs in controlling bacterial infections has also been well-characterized. Some of these miRNAs control bacterial infection, while others are used by bacteria to promote pathogenesis. There is also emerging evidence indicating that the Arabidopsis miRNA machinery is required for antibacterial resistance, and as a corollary, that some bacterial effectors have evolved to suppress this small RNA pathway to enable disease. By contrast, there is currently no evidence indicating that miRNA factors, such as Argonaute proteins, could contribute to antibacterial defense in mammals. It is also unknown whether mammalian pathogenic bacteria could have evolved strategies to directly interfere with the miRNA machinery to promote pathogenesis.

This thesis work aimed to address these questions, by making use of recent findings obtained with a phytopathogenic bacterial effector, namely the HopT1-1 type III-secreted effector from *Pseudomonas syringae* pv. *tomato* strain DC3000 (*Pto* DC3000). More specifically, this effector was found to directly interact with Arabidopsis AGO1 through two conserved W-motifs, which represent AGO-binding platforms previously found in some AGO co-factors as well as in some VSRs encoded by plant and human RNA viruses (Aqil *et al*., 2013; Azevedo *et al*., 2010; El-Shami *et al*., 2007; Thiébeauld *et al*., 2021; Till *et al*., 2007). Importantly, these W-motifs were not only required for HopT1-1-triggered suppression of miRNA activity but also for the dampening of plant immunity. This indicates that the RNAi suppression activity of HopT1-1 is tightly linked to its virulence function. Here, we wanted to determine whether bacterial effectors from human pathogenic bacteria could use a similar strategy to promote pathogenicity. Our first objective was to predict and screen a series of candidate W-motifs containing effectors from human pathogenic bacteria for their ability to interfere with RNAi. We found that the type IV-secreted effector LegK1 from *L. pneumophila* was the sole candidate bacterial effector triggering a potent suppression of both miRNA and siRNA activities in human cells. We further aimed to combine molecular biology, biochemical and physiological approaches to conduct an in-depth characterization of this *Legionella* effector in both RNAi suppression and bacterial pathogenesis.

CHAPTER II: RESULTS

I. AUTHOR CONTRIBUTIONS

Didier Filopon in collaboration with Lionel Schiavolin, two former post-doctoral scientists from the laboratory, performed the Wsearch prediction on secreted virulence factors from a large set of human pathogens. Subsequently, they selected candidates and generated the plasmids expressing each bacterial effector, which were designed by Gateway cloning method. Didier Filopon optimized the use of CXCR4-2p reporter in HeLa cells. CRISPR/Cas9 HeLa cell lines targeting *ago1*, *ago2*, *ago1/2* and *dicer* were generated by the group of Sarah Gallois-Montbrun (Institut Cochin, Paris, France). Chi Hai Vu, former post-doctoral scientist from the laboratory, created the construct used for the purification of the truncated recombinant wild-type 6His-LegK1$^{2-386}$ protein. I then realized the constructions for the different mutants and control protein, and carried out the expression and purification of each recombinant protein. Isabelle Barbosa, from Hervé Le Hir (IBENS, Paris, France), provided helpful advices on the purification of recombinant proteins and *in vitro* pull-down assays. Magali Charvin, engineer in the laboratory, performed most of the RT-qPCR experiments. I previously generated the transfections in human cells, the cell lysis and RNA extraction of samples. Khadeeja Adam Sy, engineer in the laboratory, performed the transfections, the cell lysis and the luminescence assay in Figure S2.2 and the Western blot in Figure S2.3 and Figure 2.9B. Bérengère Lombard carried out the mass spectrometry (MS) experimental work and Damarys Loew supervised MS and data analysis (Institut Curie, Paris, France). On my side, I performed the transient transfections and the immunoprecipitations of Ago2. The infection assays of amoeba and human macrophages were performed in collaboration with Monica Rolando, from Carmen Buchrieser Lab (Institut Pasteur, Paris, France). Finally, the homology-based modeling of LegK1 was carried out by Pierre Barraud (IBPC, Paris, France). I along with Lionel Navarro designed the experiments, analyzed the data, and interpreted the results of all the experiments performed on this project.

II. ABSTRACT

RNA interference (RNAi) is an ancestral post-transcriptional gene regulatory mechanism orchestrated by short-interfering RNAs (siRNAs) and microRNAs (miRNAs). In both plants and mammals, miRNAs act as central regulators of host-bacteria interactions by controlling multiple steps of the infection. As a counter-defense mechanism, type III-secreted effectors from a *Pseudomonas syringae* strain were found to suppress the plant miRNA pathway to enable disease. However, it remains unknown whether human pathogenic bacteria could have evolved similar strategies to promote pathogenesis in host cells. Here, we report that the *Legionella pneumophila* type IV-secreted effector LegK1 efficiently suppresses siRNA- and miRNA- activities in human cells, through both its serine/threonine kinase activity and an identified tryptophan (W)-based Argonaute (Ago)-binding platform. In addition, we found that LegK1 uses its Ago-binding platform to interact with human Ago1, Ago2, Ago4 but also PABPC1 and DDX6, which are part of active and assembled RNA-Induced Silencing Complexes (RISCs). We further show that LegK1 can directly interact with the PIWI domain of human Ago2 *in vitro*, and that this protein-protein interaction in human cells appears to involve the W-binding pockets of Ago2. We also demonstrate that two conserved W-motifs embedded in the kinase domain of LegK1 are responsible for the ability of this bacterial effector to bind human Ago proteins. Importantly, a *L. pneumophila* strain deleted of *legK1* exhibits an altered ability to replicate in both amoeba and human macrophages at an early stage of the infection, supporting a critical role of LegK1 in pathogenesis. Finally, we found that the growth defect of this bacterial mutant can be fully rescued in macrophages lacking Ago4, unravelling both physical and genetic interaction between LegK1 and human Ago4. Overall, these findings provide the first evidence that a human pathogenic bacterium can directly suppress RNAi to promote pathogenicity. They also uncover a common virulence strategy employed by both plant and human pathogenic bacteria.

III. INTRODUCTION

Legionella pneumophila is the causative agent of Pontiac fever and of the more severe Legionnaires' disease, which is manifested by a lung inflammation leading to a severe form of pneumonia (Mondino *et al*., 2020a). *L. pneumophila* is a rod-shaped Gram-negative bacterium, which is found as free-living biofilm-embedded bacteria in the environment or in protozoan aquatic amoeba, in which they can replicate (Mondino *et al*., 2020a). This bacterium can also accidently infects human lungs through the inhalation of *Legionella*-containing aerosols (Cunha *et al*., 2016). More specifically, when *L. pneumophila* reaches human lung tissues, it invades alveolar lung macrophages and multiply in a membrane-bound replicative niche referred to as the *Legionella*-containing vacuole (LCV) (Horwitz, 1984, 1983b; Mondino et al., 2020a; Newton *et al.*, 2010). Immediately after phagocytosis, LCV escapes the endocytic pathway and recruits many host proteins and vesicles, including ribosomes and rough endoplasmic reticulum (rER), to form a rough ER-like compartment and initiates replication (Derré and Isberg, 2004; Horwitz, 1983a; Kagan and Roy, 2002; Kagan *et al.*, 2004; Tilney *et al*., 2001). The *L. pneumophila* Dot/Icm type IV secretion system (T4SS) plays a central role in LCV formation and in multiple aspects of pathogenesis (Segal and Shuman, 1998; Vogel *et al*., 1998). It ensures the secretion of more than 330 effector proteins in host cells, which subvert a large array of cellular functions, including host vesicular trafficking, ubiquitination, autophagy, translation, and innate immune pathways (Ensminger, 2016; Hubber and Roy, 2010; Joshi and Swanson, 2011; Kubori *et al.*, 2010; Mondino *et al*., 2020a; Schroeder, 2018). Interestingly, a significant proportion of *L. pneumophila* type IV secreted-effectors resembles eukaryotic-like proteins, and have likely co-opted eukaryotic domains for their virulence functions (Cazalet *et al*., 2004, Gomez-Valero *et al*., 2019). Among them, the family of LegK proteins is composed of eukaryotic-like kinase domains targeting specific host proteins *(Ge et al., 2009; Lee et al., 2020; Michard et al*., 2015; Moss *et al*., 2019). For example, LegK1 is a type IV-dependent translocated serine/threonine protein kinase that directly phosphorylates the NF-κB inhibitor IκBα, as well as other IκB family and NF-κB family members, resulting in a potent activation of NF-κB signaling (Ge *et al*., 2009). *Legionella* NF-κB activator B (LnaB) is another *L. pneumophila* type IV-secreted effector that strongly activates NF-κB signaling through an unknown mechanism (Losick *et al*., 2010). These bacterial effectors likely contribute for the sustained type IV-dependent NF-κB signaling detected during *L. pneumophila* infection, which occurs independently and downstream of the NF-κB signaling triggered by *L. pneumophila* Pathogen-Associated Molecular Patterns (PAMPs) (Abu-Zant *et al*., 2007; Bartfeld *et al*., 2009;

Losick and Isberg, 2006). Furthermore, this response is relevant for *L. pneumophila* intracellular replication because it promotes the up-regulation of anti-apoptotic genes as well as host cell survival (Abu-Zant *et al*., 2007; Bartfeld *et al.*, 2009; Losick and Isberg, 2006). Nevertheless, because NF-κB-signaling components are absent in amoeba cells (Hempstead and Isberg, 2013; Sebé-Pedrós *et al.*, 2011), it remains unknown whether activation of NF-κB signaling is the primary virulence function of LegK1 and LnaB, or alternatively, the manifestation of a counter-counter defense triggered upon perception of these effectors by human cells (Ngwaga *et al*., 2021).

MicroRNAs (miRNAs) are small non-coding RNAs that post-transcriptionally regulate genes in multiple eukaryotic organisms through the targeting of sequence complementary mRNA targets. In mammals, the miRNA biogenesis pathway involves the processing of miRNA precursors by the RNAse III enzyme Dicer, leading to the production of ~20-22 bp miRNA duplexes (Bartel, 2018). These miRNA duplexes subsequently bind to an Argonaute (Ago) protein, and one strand, the guide, remains associated to this silencing effector to form a miRNA-Induced Silencing Complex (miRISC) (Bartel, 2018). The miRISC further directs silencing of mRNA targets through endonucleolytic cleavage (so-called "slicing"), translation repression and/or mRNA degradation (Bartel, 2018; Jonas and Izaurralde, 2015). Four Ago proteins (Ago1-4) are encoded by the human genome. Ago2 is catalytically active and is the central component of miRISC (Bartel, 2018; Cheloufi *et al*., 2010; O'Carroll *et al*., 2007; Yang *et al*., 2010). Ago1, Ago3 and Ago4 can also contribute to miRNA-directed silencing in specific conditions (Bartel, 2018; Bridge *et al*., 2017; Hauptmann *et al*., 2013, 2014; Ruda *et al*., 2014; Schürmann *et al*., 2013). Mechanistically, the phosphorylation of human Ago2 at serine 387 by Akt enzymes promotes the binding of Ago2 to TNRC6 proteins, which are central Ago co-factors containing Ago-binding tryptophan (W)-motifs (Bridge *et al*., 2017; Horman *et al.*, 2013; Till *et al.*, 2007). These events are critical for miRISC assembly as they ensure the recruitment of downstream factors required for miRNA-directed translational inhibition and mRNA degradation (Bridge *et al*., 2017; Horman *et al.*, 2013; La Rocca *et al.*, 2015). By contrast, the lack of phosphorylation at this serine directs the activity of Ago2 towards miRNA-directed slicing of cellular targets (Horman *et al*., 2013).

Although mammalian miRNAs were initially characterized in cell proliferation, apoptosis and various pathologies, including cancer and cardiovascular diseases, they have also been extensively studied in the context of host-pathogen interactions (Adams *et al*., 2014; Aguilar *et al*., 2019; Bueno *et al*., 2008; Jovanovic and Hengartner, 2006; Quiat and Olson, 2013). In particular, a large set of mammalian miRNAs control bacterial infections. There is also emerging evidence indicating that some human pathogenic bacteria exploit individual miRNAs to promote pathogenesis in host cells. These miRNAs regulate various cellular processes during bacterial infection, including innate immune responses, host cell cycle, cell death and survival pathways, autophagy, and cytoskeleton organization (Aguilar *et al*., 2019). For example, *L. pneumophila* triggers the differential regulation of 85 human miRNAs during infection of human macrophages (Herkt *et al.*, 2020). Among them, the PAMP-responsive NF-κB-dependent microRNA miR146a, which acts as an anti-inflammatory miRNA, is up-regulated during *L. pneumophila* infection and controls the replication of this bacterium in human macrophages (Herkt *et al*., 2020; Jung *et al.*, 2016; Li *et al*., 2010a; Taganov *et al.*, 2006). Furthermore, the trio miR-125b, miR221 and miR579, which targets host repressors of *L. pneumophila* intracellular growth, are co-repressed during infection of human macrophages (Herkt *et al*., 2020). Intriguingly, emerging evidence indicate that host miRNAs not only post-transcriptionally regulate endogenous mRNAs during infection, but can additionally reprogram gene expression in bacterial cells. This is notably the case of let-7b-5p, which was recently shown to be transferred from human epithelial alveolar cells towards *Pseudomonas aeruginosa* cells, in which it represses factors required for biofilm formation (Koeppen *et al*., 2021). Altogether, these studies, among many others, indicate that human miRNAs are fundamental components of host-bacteria interactions. They also suggest that human pathogenic bacteria might have evolved strategies to interfere with the host miRNA machinery as part of their virulence functions.

Antiviral RNA interference (RNAi) has been extensively characterized in plants, fungi, insects and worms (Ding, 2010; Hamilton and Baulcombe, 1999; Jin *et al*., 2021; Lu *et al*., 2005; Wang *et al.*, 2006b). The core mechanism of antiviral RNAi involves the recognition and processing of dsRNA replication intermediates by the RNAse III enzyme Dicer, leading to the production of ~20-22 nt long virus-derived small interfering RNA (vsiRNA) duplexes (Berkhout, 2018b; Ding *et al.*, 2018; Maillard *et al*., 2019; Schuster *et al*., 2019). These vsiRNA duplexes subsequently bind to an Ago protein, and the guide strand further triggers the

degradation of complementary viral transcripts and/or inhibit their translation. The occurrence and relevance of antiviral RNAi in mammals has been, until recently, controversial. However, emerging evidence indicate that antiviral RNAi is effective in mammalian embryonic stem cells, adult stem cells and progenitor cells, in which the classical antiviral interferon (IFN) response –known to repress RNAi– is ineffective (Maillard *et al.*, 2013a, 2016; van der Veen *et al.*, 2018; Xu *et al.*, 2019). Besides being hypo-responsive to IFN, these pluripotent or multipotent cells are equipped with a functional antiviral Dicer. More specifically, a Dicer isoform, which lacks a part of the N-terminal helicase segment –known to inhibit Dicer-mediated dsRNA processing– is preferentially expressed in mouse and human stem cells (Poirier *et al*., 2021). This truncated Dicer, named antiviral Dicer (aviD), exhibits an enhanced dsRNA processing activity compared to the full-length Dicer, and is required for RNAi against *Zika virus* (ZIKV) and *severe acute respiratory syndrome coronavirus 2* (SARS-CoV-2) in brain organoids (Poirier *et al*., 2021).

As a counter-defence strategy, mammalian viruses have evolved Viral Suppressors of RNA silencing (VSRs), a phenomenon which has been initially characterized in plant-viral and insect-viral interactions (Ding *et al*., 2018). Most of the characterized VSRs from mammalian viruses bind dsRNAs, thereby preventing Dicer-mediated dsRNA processing and vsiRNAs biogenesis (Ding *et al.*, 2018; Li *et al*., 2004; Maillard *et al.*, 2019; Sullivan and Ganem, 2005). This is one of the reason why deep-sequencing of small RNAs during infections of somatic cells with RNA viruses have failed to detect vsiRNAs (Backes *et al*., 2014; Bogerd *et al.*, 2014; Girardi *et al.*, 2013; Parameswaran *et al*., 2010). By contrast, vsiRNAs are readily detectable during infection of VSR-defective viruses. This has been initially reported during infection of rodent somatic cells and suckling mice with a *Nodamura virus* mutant that does not express the VSR B2 (Li *et al*., 2013). It has also been shown during infection of human somatic cells with VSR-defective *human enterovirus 71* (HEV71) and *Influenza A virus* (IAV), which are responsible for hand-foot-and-mouth disease (HFMD) and influenza, respectively (Li *et al.*, 2016; Qiu *et al.*, 2017). In those conditions, vsiRNAs are loaded in Ago2, and orchestrate slicing of viral RNAs in an IFN-independent manner (Li *et al.*, 2016; Qiu *et al.*, 2017). Besides their role in suppressing vsiRNAs biogenesis, VSRs can additionally act downstream of small RNA biogenesis. For examples, the *Influenza virus* Non-Structural 1 (NS1) and the *vaccinia virus* E3L sequester siRNAs, thereby inhibiting their loading in Ago2, while the *human immunodeficiency virus-1* (HIV-1) Negative Regulatory Factor (Nef) protein interacts with Ago2 through two conserved W-motifs to dampen its miRNA-directed slicing activity in human

cells (Aqil *et al*., 2013; Bucher *et al*., 2004; Li *et al.*, 2004).

Although the role of mammalian miRNAs in host-bacterial interactions is now well-established, there is currently no evidence indicating that mammalian pathogenic bacteria can interfere with the RNAi machinery. This phenomenon has, however, previously been reported in the context of plant-bacteria interactions. More specifically, it was shown that a subset of type III-secreted proteins from the phytopathogenic *Pseudomonas syringae* pv. *tomato* strain DC3000 (*Pto* DC3000) can suppress different steps of the Arabidopsis miRNA pathway to promote pathogenicity (Navarro *et al*., 2008). Among those bacterial effectors, the Hrp outer protein T1-1 (HopT1-1) was recently shown to directly interact with Arabidopsis AGO1 through two conserved W-motifs (Thiébeauld *et al*., 2021). Importantly, this process is required for the suppression of both AGO1-directed miRNA activity and PAMP-triggered immunity, indicating that the silencing suppression activity of HopT1-1 is coupled with its virulence function (Thiébeauld *et al*., 2021). Here, we investigated whether such virulence strategy could also be employed by bacterial effectors from human pathogenic bacteria. We found that the *L. pneumophila* LegK1 effector efficiently suppresses siRNA and miRNA activities in human cells, through both its predicted Ago-binding platform as well as its kinase activity. The predicted Ago-hook platform was also found required for the interaction with Ago1, Ago2 and Ago4 in human cells. We further show that LegK1 directly interacts with human Ago2 through two W-motifs, embedded in its kinase domain, and that the Ago2 W-binding pockets appear to be necessary for such protein-protein interaction. Importantly, we found that LegK1 promotes bacterial growth in both amoeba and human macrophages at early stage of infection, highlighting the relevance of this effector in *L. pneumophila* pathogenesis. Finally, we show that the targeting of human Ago4 by LegK1 is likely essential to promote *L. pneumophila* growth in human macrophages, unveiling an unanticipated role of Ago4 in antibacterial defense. Overall, these findings provide the first evidence indicating that an effector from a human pathogenic bacterium can directly target the RISC machinery to promote pathogenicity. They also indicate that the use of an Ago-binding platform is a shared virulence strategy employed by both plant and mammalian pathogenic bacteria.

IV. RESULTS

IV.I. THE LEGIONELLA PNEUMOPHILA TYPE IV-SECRETED EFFECTOR LEGK1 SUPPRESSES SIRNA-GUIDED GENE SILENCING MEDIATED BY HUMAN AGO2

To determine whether effectors from human pathogenic bacteria could have evolved functional Ago-binding domains, we retrieved the protein sequences from 25 genomes of pathogenic bacteria and subjected them to the Wsearch prediction algorithm (Figure 2.1A) (Zielezinski and Karlowski, 2015, 2017). The score of each W-motif was determined using the animal Bidirectional Position-Specific Scoring matrix (BPSSM) generated from experimentally-verified Ago-binding proteins and their orthologous sequences (Zielezinski and Karlowski, 2015). For the first pre-selection, we applied an arbitrary cutoff of greater than six on the average W-scores of all motifs present in the candidate protein sequence. This cutoff was chosen based on the average W-scores motif of the experimentally validated HopT1-1 effector from the phytopathogenic *Pto* DC3000 (Thiébeauld *et al*., 2021). Among the bacterial candidate proteins exhibiting the highest W-score, we further selected known secreted virulence factors or putative virulence factors predicted to be secreted (Table S2.1). To monitor the possible effect of a subset of these candidate effectors on RNAi activity, we made use of a previously described siRNA-based *CXCR4* reporter system (Doench *et al*., 2003). This reporter relies on the co-transfection of two plasmids along with exogenous siRNAs bearing perfect match with the 3'UTR of *CXCR4* (Figure 2.1B) (Doench *et al*., 2003). More specifically, one plasmid expresses the *firefly luciferase* coding sequence fused to the 3'UTR of *CXCR4*, while the other one expresses the coding sequence of the *renilla luciferase* (non-targeted by siRNA), used as a transfection control (Figure 2.1B). By using *ago1*$^{-/-}$, *ago2*$^{-/-}$, *ago1*$^{-/-}$/*ago2*$^{-/-}$ or *dicer*$^{-/-}$ CRISPR/Cas9-based mutants in HeLa cells (Figure 2.1C-D), we demonstrated that the silencing of the *CXCR4* reporter was compromised in the *ago2*$^{-/-}$ and *ago1*$^{-/-}$/*ago2*$^{-/-}$ cell lines compared to the control line (CTL), as revealed by a higher luminescence activity in the corresponding conditions (Figure 2.1D). By contrast, the luminescence levels remained low in the *ago1*$^{-/-}$ and *dicer*$^{-/-}$ lines, and were comparable to the level observed in CTL (Figure 2.1D). The latter result indicates that the silencing of the *firefly luciferase* remained unchanged in human cells depleted of Ago1 or Dicer. Collectively, these data revealed that the silencing of the *CXCR4* reporter is dependent on Ago2 but not on Ago1. They also provide evidence that

Dicer is not required for this process, which is consistent with the exogenous delivery of a mature form of anti-*CXCR4* siRNAs.

We next cloned our candidate bacterial effectors in an expression vector driven by the human *cytomegalovirus* (CMV) immediate-early enhancer and promoter, and validated their expression by RT-qPCR analysis upon transient transfection of each plasmid in HeLa cells (Figure S2.1). We further co-transfected in HeLa cells individual effector with the *CXCR4* reporter, along with exogenous anti-*CXCR4* siRNAs, and monitored the luminescence intensity in each condition. Using this approach, we found that the LegK1 effector from *Legionella pneumophila* (strain Paris) triggered a higher luminescence intensity compared to control cells expressing *eGFP* (Figure 2.1E). This effect was comparable to the ones detected in HeLa cells lacking Ago2 (Figure 2.1D), or in HeLa cells expressing the VSR *Hepatitis B virus* HBx (Figure S2.2) (Chinnappan *et al.*, 2014). Altogether, these data indicate that LegK1 efficiently suppresses siRNA-guided gene silencing mediated by human Ago2.

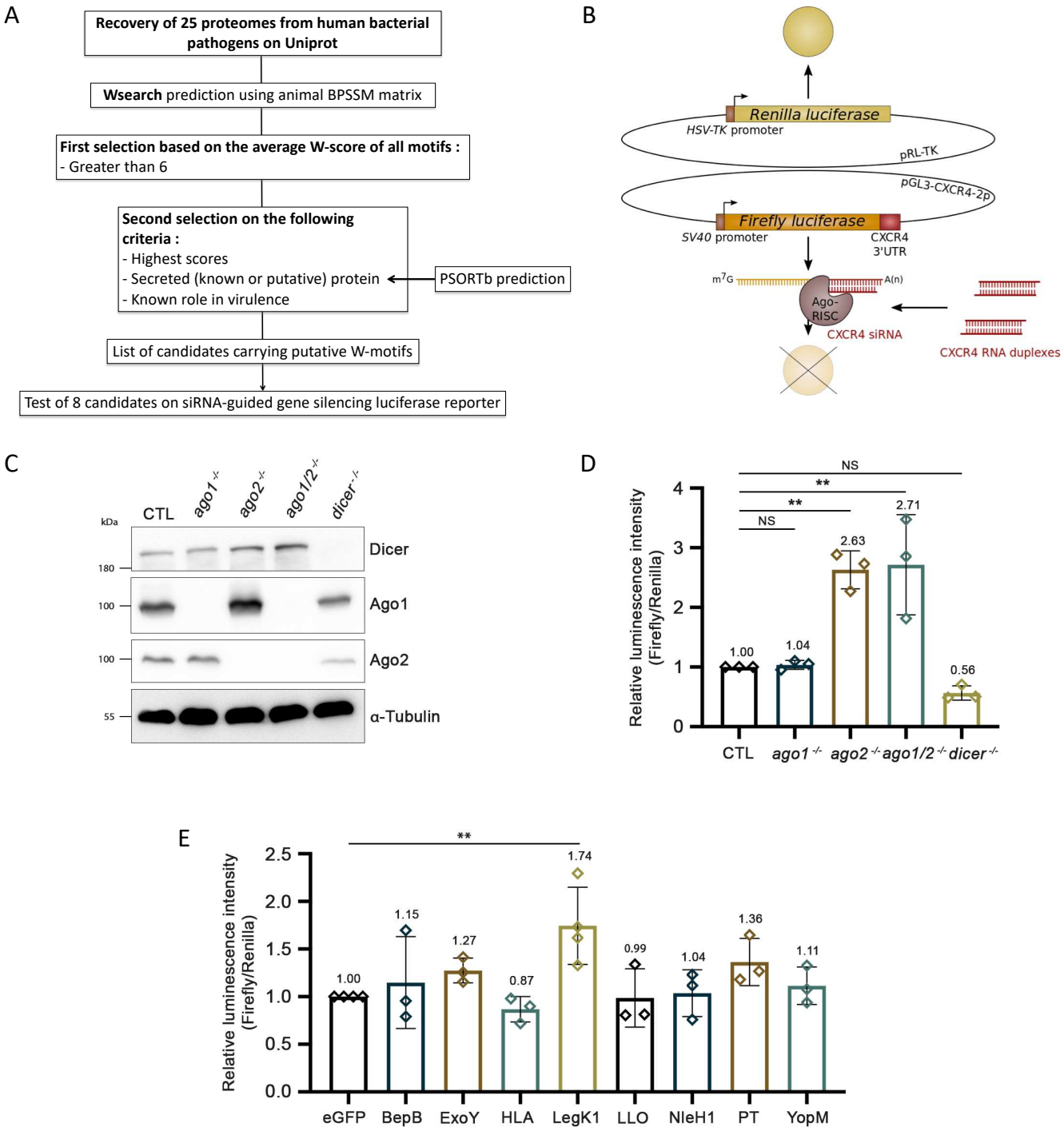

Figure 2.1. Screening of candidate bacterial proteins carrying W-motifs revealed that LegK1 is the sole protein triggering RNAi suppression activity in human cells.

(A) *In silico* approach used to identify bacterial proteins possessing W-motifs. Wsearch algorithm is based on a Bidirectional Position-Specific Scoring Matrix (BPSSM). PSORTb is a bacterial localization prediction program that was used to identify predicted secreted proteins (https://www.psort.org/psortb/). **(B)** Schematic representation of the luciferase-based siRNA reporter assay. The RNAi reporter assay consists on the co-transfection of (i) the pGL3-CXCR4-2p vector containing the *firefly luciferase* transgene with *CXCR4* siRNA binding sites in the 3'UTR, (ii) the vector expressing the non-targeted *renilla luciferase* as an internal control for normalization, and (iii) exogenous *CXCR4* siRNA duplexes. Of note, the siRNAs are perfectly complementarity to the *CXCR4* 3'UTR sequence. CMV; *Cytomegalovirus*, HSV-TK; *Herpes simplex virus* (HSV) thymidine kinase promoter, SV40; *Simian virus 40;* RISC; RNA-induced Silencing complex. **(C)** Immunoblotting of Argonaute and Dicer proteins in *ago1*$^{-/-}$, *ago2*$^{-/-}$, *ago1/2*$^{-/-}$, and *dicer*$^{-/-}$ HeLa cell lines. The expression levels of Ago1, Ago2 and Dicer proteins in control (CTL) or knock-out HeLa cells were determined by Western Blot analysis using indicated antibodies. α-Tubulin was used as a loading control. **(D)** Luciferase-based siRNA silencing assay in *ago1*$^{-/-}$, *ago2*$^{-/-}$, *ago1/2*$^{-/-}$, and *dicer*$^{-/-}$ HeLa cell lines. Control and knock-out HeLa cells were co-transfected with expression vectors for *firefly luciferase*, *renilla luciferase* and *CXCR4* siRNA duplexes. Luciferase expression was measured at 48h post-transfection. The luminescence intensity of Firefly luciferase relative to the one of Renilla was calculated and further normalized to the siCTL condition. Error bars indicate the standard deviations (SD) from three independent experiments. P-values were calculated using ordinary one-way ANOVA (Dunnett's multiple comparisons test). **, $P < 0.01$; NS, not significant. **(E)** Luciferase-based siRNA silencing assay in the presence of candidate bacterial proteins in HeLa cells. HeLa cells were co-transfected with expression vectors for *firefly luciferase*, *renilla luciferase*, *CXCR4* siRNA duplexes and vector expressing bacterial proteins individually. The luciferase activity was measured at 48h post-transfection. The luminescence intensity of Firefly luciferase relative to the one of Renilla was calculated and further normalized to the eGFP condition. Error bars indicate the SD from at least three independent experiments. P-values were calculated using ordinary one-way ANOVA (Dunnett's multiple comparisons test). **, $P < 0.01$; NS, not significant. HLA; α-hemolysin, LLO; Listeriolysin O, PT; Pertussis toxin S1.

IV.II. LegK1 suppresses siRNA- and miRNA-guided gene silencing and this phenomenon requires both its kinase activity and its putative Ago-binding platform

LegK1 is an experimentally validated Dot/Icm type IV-secreted effector possessing an eukaryotic-like serine/threonine kinase activity (Ge *et al.*, 2009). Here, we additionally found that this bacterial effector contains a putative Ago-binding platform composed of four predicted W-motifs (Table S2.2). The tryptophan residues located at positions 41, 283 and 293 of the LegK1 protein sequence, namely W41, W283 and W293, exhibit the highest W-score, and were thus selected for further analyses (Figure 2.2A, Table S2.2). To characterize these motifs, we next generated tryptophan to phenylalanine substitutions (W>F) in the three selected tryptophan residues. In parallel, we generated a K121A substitution in the LegK1 ATP-binding site, which was previously shown to abolish the catalytic activity of this bacterial effector (Ge *et al.*, 2009). The resulting W>F triple and K121A mutants, referred to here as LegK1-3W and LegK1-KA, respectively, were as stable as the WT LegK1 when expressed in HEK293T cells (Figure 2.2B). We further analyzed the ability of LegK1, and of the mutant versions, to suppress RNAi activity. To this end, we used a RNAi reporter system, which is based on the co-transfection of one plasmid expressing the *enhanced GFP* (*eGFP*) along with *GFP* RNA duplexes perfectly targeting a single site located at the 5' part of the *eGFP* coding sequence (Figure 2.2C). This siRNA-based reporter system has been previously used to characterize VSRs from human pathogenic viruses (Fabozzi *et al.*, 2011; Li *et al.*, 2004; Mu *et al.*, 2020a), and was found here to be robustly silenced by anti-*GFP* siRNAs, as revealed by low abundant or undetectable eGFP mRNAs and proteins when expressed in HeLa and HEK293T cell lines (Figure 2.2D-F). By contrast, the eGFP protein accumulation in HeLa cells was moderately increased in the *ago2*$^{-/-}$ HeLa cell line expressing the anti-*eGFP* siRNA duplexes, a molecular effect which was further enhanced in the *ago1*$^{-/-}$/*ago2*$^{-/-}$ HeLa cell line (Figure 2.2D). These results indicate that both Ago1 and Ago2 direct the silencing of this *GFP*-based reporter system. Of note, the fact that the accumulation of the GFP protein was not restored to the control level in *ago1*$^{-/-}$/*ago2*$^{-/-}$ HeLa cells suggests that Ago3 and/or Ago4 must additionally contribute to this process. Interestingly, when the same analysis was conducted in HEK293T cells expressing LegK1, we found that the eGFP protein accumulation remained elevated compared to the levels found in cells expressing the empty vector or the type III-secreted effector *Yersinia pestis* (YopM), which is deprived of BSR activity and thus served as a negative control (Figures 2.2E, S2.3). This result indicates

that LegK1 counteracts the silencing of the *eGFP* reporter directed by anti-*eGFP* siRNAs. It is noteworthy that the silencing suppression effect mediated by LegK1 over the *eGFP* reporter was even more pronounced than the one triggered by T6B (Figure 2.2E), a TNRC6B-derived peptide containing multiple W-motifs, which competes with endogenous TNRC6/GW182 proteins for Ago-binding, and was shown to disrupt the function of multiple Ago proteins (Hauptmann *et al.*, 2015). This effect was also more pronounced than in HeLa cells depleted of Ago2 or Ago1/Ago2 proteins (Figure 2.2D-E). Collectively, these results suggest that LegK1 suppresses siRNA-guided gene silencing mediated by multiple Ago proteins. In addition, we noticed that LegK1 triggered an enhanced *eGFP* mRNA accumulation, suggesting that this effector likely interferes with siRNA-directed slicing and/or mRNA degradation (Figure S2.4). Importantly, the RNAi suppression effects detected in response to LegK1 no longer occurred in the presence of the LegK1-3W and LegK1-KA mutants (Figures 2.2E, S2.4). These data therefore indicate that both the putative Ago-binding platform and the kinase activity of LegK1 are required for siRNA-guided gene silencing.

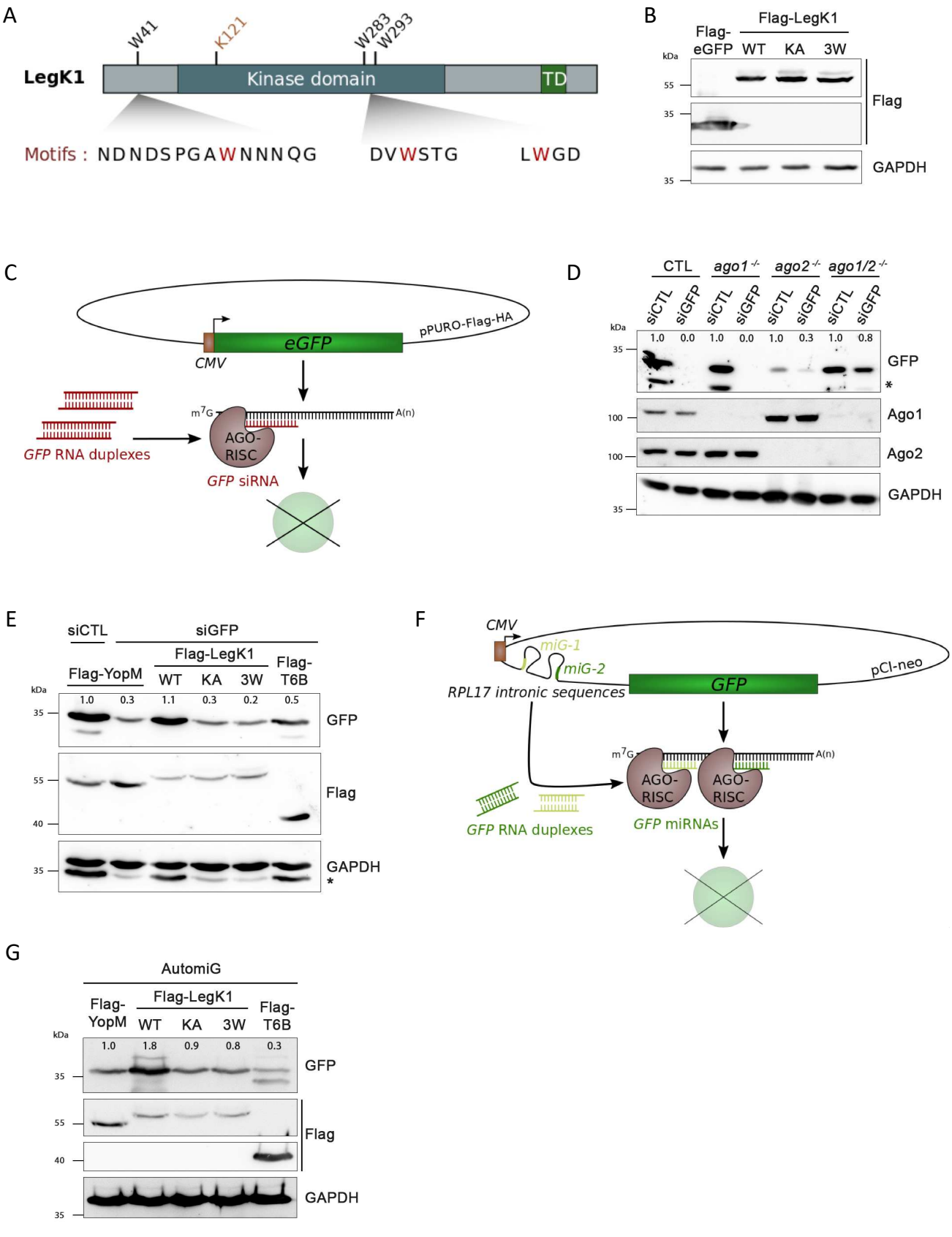

Figure 2.2. LegK1 suppresses siRNA- and miRNA- guided gene silencing through both its kinase activity and its predicted Ago-binding platform.

(A) Schematic representation of the LegK1 protein sequence. The position and amino acid sequence of three out of the four W-motifs predicted by Wsearch (Zielezinski and Karlowski, 2015) are depicted. The lysin 121 is an essential residue located inside the ATP-binding pocket for eukaryotic-like serine/threonine kinase activity. TD; transmembrane domain. **(B)** Immunoblot of the different LegK1 WT and mutant versions. HEK293T cells were transfected with vectors expressing either Flag-HA-eGFP, 2xFlag-HA-LegK1 (WT), 2xFlag-HA-LegK1-KA (kinase-dead mutant) or 2xFlag-HA-LegK1-3W (three putative W-motifs mutant) proteins. Protein levels in transfected cell lysates were detected by Western blot analysis using anti-Flag antibody. GAPDH was used as a loading control. **(C)** Schematic representation of the siRNA-guided *GFP* reporter. The RNAi reporter assay consists on the co-transfection of a pFlag-HA-eGFP constructs, allowing the expression of the *eGFP* under the control of the *CMV* immediate early promoter, along with *GFP* RNA duplexes or AllStars negative control siRNAs. The anti-GFP siRNAs exhibit perfect complementarity to the *GFP* RNA transcripts. CMV; *cytomegalovirus*, RISC; RNA-induced Silencing complex.

(legend continued on next page)

(D) *eGFP*-based silencing reporter assay in *ago1*$^{-/-}$, *ago2*$^{-/-}$, *ago1/2*$^{-/-}$, and *dicer*$^{-/-}$ HeLa cell lines. Control (CTL) and knock-out HeLa cell lines were co-transfected with expression vectors expressing eGFP and *GFP* siRNA duplexes (siGFP) or AllStars negative control siRNAs (siCTL). At 48h post-transfection, cell lysates were subjected to Western Blot analysis with indicated antibodies. GAPDH was used as a loading control. The eGFP protein levels are relative to the ones of GAPDH and further normalized to the siCTL condition. The corresponding relative values are indicated above the GFP blot. This quantification was carried out using the ImageJ software. * represents aspecific band. The results shown are representative of three independent experiments. **(E)** *eGFP*-based siRNA silencing reporter assay in the presence of LegK1 WT, kinase-dead or triple W-binding mutants. HEK293T cells were co-transfected with expression vectors for *eGFP*, *GFP* RNA duplexes or AllStars negative control siRNAs and vector expressing Flag-HA-YopM, 2xFlag-HA-LegK1-WT, 2xFlag-HA-LegK1-KA (kinase-dead mutant), 2xFlag-HA-LegK1-3W (three putative W-motifs mutant) or Flag-HA-T6B (TNRC6B-derived peptide) recombinant proteins. At 48h post-transfection, cell lysates were subjected to Western Blot analysis with indicated antibodies. GAPDH was used as a loading control. The eGFP protein levels are relative to the ones of GAPDH and further normalized to the YopM control condition (with siCTL). The corresponding relative values are depicted at the top of the GFP immunoblot. This quantification was carried out using the ImageJ software. * represents aspecific band. The results shown are representative of three independent experiments. **(F)** Schematic representation of the AutomiG reporter (adapted from Carré *et al*., 2013). A region encompassing the first coding nucleotides of exon-2, the second intron, and the first nucleotide of exon-3 from the *Drosophila RpL17* gene (CG3203) was fused to the coding sequence of the *GFP* and cloned under the control of *CMV* promoter. Within the *RpL17* intron, a fragment of a miRNA cluster including the pre-miR-5 and pre-miR-6-1 sequences was inserted and the miR-5 and miR-6-1 pre-miRNA sequences were replaced by the synthetic miG-1 and miG-2 pre-miRNA sequences, respectively. Mature *miG-1* and *miG-2* miRNAs match two distinct targets with perfect complementarity to the *GFP* coding sequence. CMV; *cytomegalovirus*, RISC; RNA-induced Silencing complex. **(G)** AutomiG silencing assay in the presence of LegK1 WT, kinase-dead or triple W-binding mutants. HEK293T cells were co-transfected with vector expressing AutomiG and Flag-HA-YopM, 2xFlag-HA-LegK1-WT, 2xFlag-HA-LegK1-KA (kinase dead), 2xFlag-HA-LegK1-3W (three W-motifs mutant) or Flag-HA-T6B recombinant proteins. At 48h post-transfection, cell lysates were subjected to Western Blot analysis with indicated antibodies. GAPDH was used as a loading control. The GFP protein levels are relative to the ones of GAPDH and further normalized to the YopM control condition. The corresponding relative values are depicted at the top of the GFP immunoblot. This quantification was carried out using the ImageJ software. The results shown are representative of three independent experiments.

Next, we investigated whether LegK1 could additionally suppress miRNA function. To this end, we used a previously characterized *GFP*-based construct that contains two artificial miRNA precursors embedded in an intronic sequence located upstream of the *GFP* coding sequence (Figure 2.2F) (Carré *et al.*, 2013). This construct is designed to produce two anti-*GFP* mature artificial miRNAs, namely miG-1 and miG-2, which are perfectly complementary to the *GFP* mRNA sequence (Figure 2.2F). Upon transfection in HeLa cells, this construct was shown to trigger the self-silencing of the *GFP* reporter, a phenomenon which was found to be dependent on the miRNA biogenesis factors Drosha and DGCR8 (Carré *et al.*, 2013). Interestingly, when this construct was transiently co-expressed with the WT version of LegK1 in HEK293T cells, we found an enhanced GFP protein level compared to cells co-expressing the reporter construct and the control effector YopM (Figures 2.2G, S2.3). This was, however, not the case upon co-transfection of the reporter construct with the T6B peptide (Figure 2.2G, see discussion section). Therefore, unlike T6B, LegK1 can suppress miG-1 and miG-2-dependent silencing of the *GFP* reporter. By contrast, the GFP protein levels remained low in HEK293T cells co-expressing the reporter construct with the LegK1-KA and LegK1-3W versions (Figure 2.2G), supporting a role for both the kinase activity and the putative Ago-binding platform in this silencing suppression phenomenon. Altogether, these data provide evidence that LegK1 can efficiently suppress both siRNA and miRNA functions through its kinase and putative Ago-dependent binding platform.

IV.III. TNFα- AND IL1β-TRIGGERED ACTIVATION OF NF-κB-DEPENDENT IMMUNE SIGNALING DOES NOT ALTER SIRNA-GUIDED GENE SILENCING

Besides its RNAi suppression activity, the catalytic activity of LegK1 has previously been shown to activate the NF-κB-dependent immune signaling pathway (Ge *et al*., 2009). To determine whether the observed LegK1-triggered RNAi suppression activity could occur as a consequence of an activation of the NF-κB pathway, we examined the effects of well-characterized elicitors of NF-κB signaling on siRNA-directed gene silencing activity. For this purpose, we transiently co-transfected the eGFP reporter along with GFP RNA duplex and empty vector in HEK293T cells, and then challenged these cells with TNFα or IL1β (Zhang *et al*., 2017). As a control for RNAi suppression and NF-κB activation, we co-transfected the eGFP reporter along with GFP RNA duplex and the plasmid expressing LegK1. TNFα or IL1β triggered the phosphorylation of the serine 32 of IκBα in HEK293T cells, to the same extent as LegK1 (Figure S2.5), validating that both molecules can activate NF-κB-dependent immune signaling in our experimental settings. However, they did not interfere with siRNA-guided gene silencing, as revealed by low eGFP protein levels, as observed in the control condition treated with anti-GFP siRNA duplexes (Figure S2.5). By contrast, and as shown above, LegK1 triggered the derepression of the eGFP, which was manifested by an enhanced accumulation of the eGFP protein compared to the same control condition (Figure S2.5). Collectively, these data indicate that the induction of the NF-κB-dependent immune signaling pathway by TNFα or IL1β is not sufficient to suppress siRNA-guided gene silencing. Although these data suggest that LegK1-triggered activation of the NF-κB-dependent immune signaling pathway is unlikely responsible for the detected RNAi suppression effect, additional experiments will be needed to further test this possibility (see discussion section).

IV.IV. LegK1 uses its putative Ago-binding platform to interact with protein complexes containing the human RISC factors Ago1, Ago2, Ago4, PABPC1 and DDX6

The presence of predicted W-motifs in the protein sequence of LegK1, and their relevance in RNAi suppression activity (Figure 2.2, Table S2.2), suggested that this bacterial effector could interact with human Ago proteins. To test this possibility, we first assessed the ability of LegK1-WT, LegK1-KA and LegK1-3W to interact with human Ago1 and Ago2 by co-immunoprecipitation experiments. For this purpose, we expressed the Flag-tagged LegK1-WT, LegK1-KA and LegK1-3W versions in HEK293T cells and further used Flag antibodies on the different lysates to immunoprecipitate the cellular partners. Using this assay, we found that both human Ago1 and Ago2 were detected in the Flag-LegK1 immunoprecipitates, a phenomenon which was not observed on lysate of control cells expressing the Flag-eGFP fusion protein (Figure 2.3A). It is noteworthy that we also specifically detected human Ago4 in the Flag-LegK1 immunoprecipitates (Figure S2.6). These data indicate that LegK1 can interact with protein complexes containing, at least in part, Ago1, Ago2 and/or Ago4 proteins. Interestingly, we also recovered in these Flag-LegK1 immunoprecipitates the PABPC1 and DDX6 proteins, which are well-characterized Ago2-RISC factors required for miRNA-directed translational repression and/or RNA decay (Fabian *et al.*, 2009; Rouya *et al*., 2014). The latter results suggest that LegK1 might interact with mature Ago-RISCs engaged in miRNA repression. Importantly, the above interactions were maintained with the catalytic mutant LegK1-KA, while they were significantly reduced with the LegK1-3W mutant version (Figure 2.3A). The latter data indicate that the predicted Ago-binding platform of LegK1 is required for the interaction of this effector with Ago-RISCs, while its kinase activity is dispensable for this process.

We further investigated whether LegK1 could bind human Ago2 via a protein-protein interaction or through RNAs. For this purpose, we co-transfected the Flag-LegK1 and GFP-Ago2 plasmids in HEK293T cells and further conducted an anti-Flag immunoprecipitation in the presence or absence of RNAse A. We found that the RNAse A treatment, which was used at a concentration that efficiently degrades total RNAs (data not shown), did not alter the ability of Flag-LegK1 to interact with GFP-Ago2 (Figure 2.3B). Therefore, LegK1 binds to Ago2 in

an RNA-independent manner and likely through a protein-protein interaction possibly involving its predicted Ago-binding platform.

IV.V. LEGK1 DIRECTLY INTERACTS WITH HUMAN AGO2 AS WELL AS WITH ITS PIWI DOMAIN

We next investigated whether LegK1 could directly bind human Ago2. For this purpose, we conducted an *in vitro* interaction assay using GST-Ago2 and His6-LegK1$^{2:386}$ recombinant proteins expressed and purified from *E. coli* (Figure 2.3C-D). It is noteworthy that the LegK1$^{2:386}$ truncated version is deprived of its predicted transmembrane domain and maintain its kinase activity, as previously reported (Ge *et al*., 2009). Importantly, we found that the GST-tagged Ago2 protein efficiently bound to His6-LegK1$^{2:386}$, while it did not interact with TAP, which served as a negative control (Figure 2.3D).

Because the PIWI domain of human Ago2 is known to interact with W-motifs rich proteins such as TNRC6/GW182 proteins (El-Shami *et al.*, 2007; Lian *et al*., 2009; Pfaff *et al*., 2013; Takimoto *et al.*, 2009; Till *et al*., 2007), we additionally expressed and purified a CBP-tagged PIWI domain of human Ago2 from *E. coli* (Figure 2.3C), and further used the recombinant proteins for *in vitro* pull-down experiments through calmodulin affinity resin. Using this assay, we found that the CBP-PIWI recombinant protein interacted with His6-LegK1$^{2:386}$, a phenomenon which was not further improved in the presence of total RNAs extracted from HEK293T cells (Figure 2.3E). Altogether, these data indicate that LegK1 can directly interact with Ago2, at least in part, through interaction surfaces embedded in its PIWI domain.

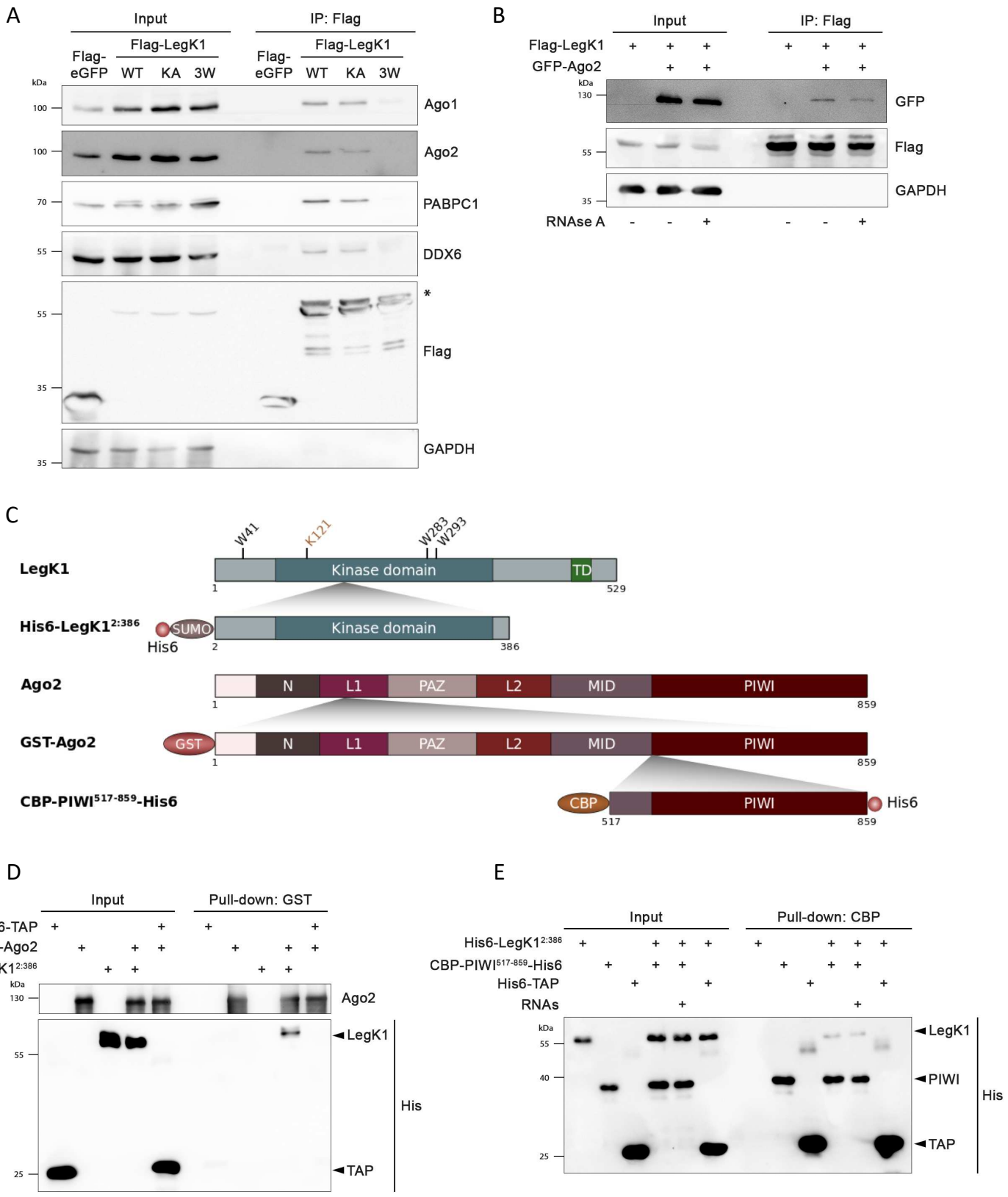

Figure 2.3. LegK1 interacts with components of the miRISC in human cells, and can also directly interacts with the PIWI domain of Ago2 *in vitro*

(A) Co-immunoprecipitation of LegK1 WT, kinase-dead or triple W-motif mutants in human cells. HEK293T cells were transfected with vector expressing Flag-eGFP, 2xFlag-HA-LegK1 (WT), 2xFlag-HA-LegK1-KA (kinase-dead mutant) or 2xFlag-HA-LegK1-3W (three putative W-motifs mutant) recombinant proteins. At 48h post-transfection, cells were lysed and proteins were immunoprecipitated using an anti-Flag antibody. Total cell lysates (input) and the immunoprecipitates were analyzed by Western blot analyses using indicated antibodies. GAPDH was used as a loading control. * represents aspecific band. The results shown are representative of three independent experiments. **(B)** Co-immunoprecipitation of LegK1 in the presence of RNAse A. HEK293T cells were transfected with a vector expressing 2xFlag-HA-LegK1 or co-transfected with vectors expressing 2xFlag-HA-LegK1 and GFP-Ago2 recombinant proteins. At 48h post-transfection, cells were lysed, incubated with or without RNase A, and proteins were further immunoprecipitated using an anti-Flag antibody. Total cell lysates (input) and the immunoprecipitates were analyzed by Western blot using indicated antibodies. GAPDH was used as a loading control. The results shown are representative of three independent experiments. **(C)** Schematic representation of the purified recombinant proteins used for *in vitro* pull-down assays. The position of the three tryptophan from predicted W-motifs and the lysin from the ATP-binding pocket are shown above the LegK1 sequence. CBP; calmodulin binding protein, GST; glutathione S-transferase, SUMO; Small Ubiquitin-like Modifier, TD; transmembrane domain.

(legend continued on next page)

(D) Pull-down assay between human Ago2 and LegK1 recombinant proteins. GST-Ago2 was incubated with His6-LegK1 (a.a. 2:386) or His6-TAP and subjected to a GST pull-down assay using glutathione-sepharose beads. Protein complexes were eluted with 10 mM reduced glutathione followed by Western blot analysis with indicated antibodies. TAP was used as a negative control. The results shown are representative of three independent experiments. **(E)** Pull-down assay between PIWI domain of human Ago2 and LegK1 recombinant proteins in presence of RNAs. CBP-PIWI-His6 (a.a. 517-817) or His6-TAP, which consists in a calmodulin binding peptide (CBP) used as negative control, were incubated with His6-LegK1 (a.a. 2:386), with or without RNAs extracted from human cells, and subjected to a CBP pull-down assay using calmodulin affinity resin. Protein complexes were eluted and subjected to Western blot analysis with anti-His antibodies. The results shown are representative of three independent experiments.

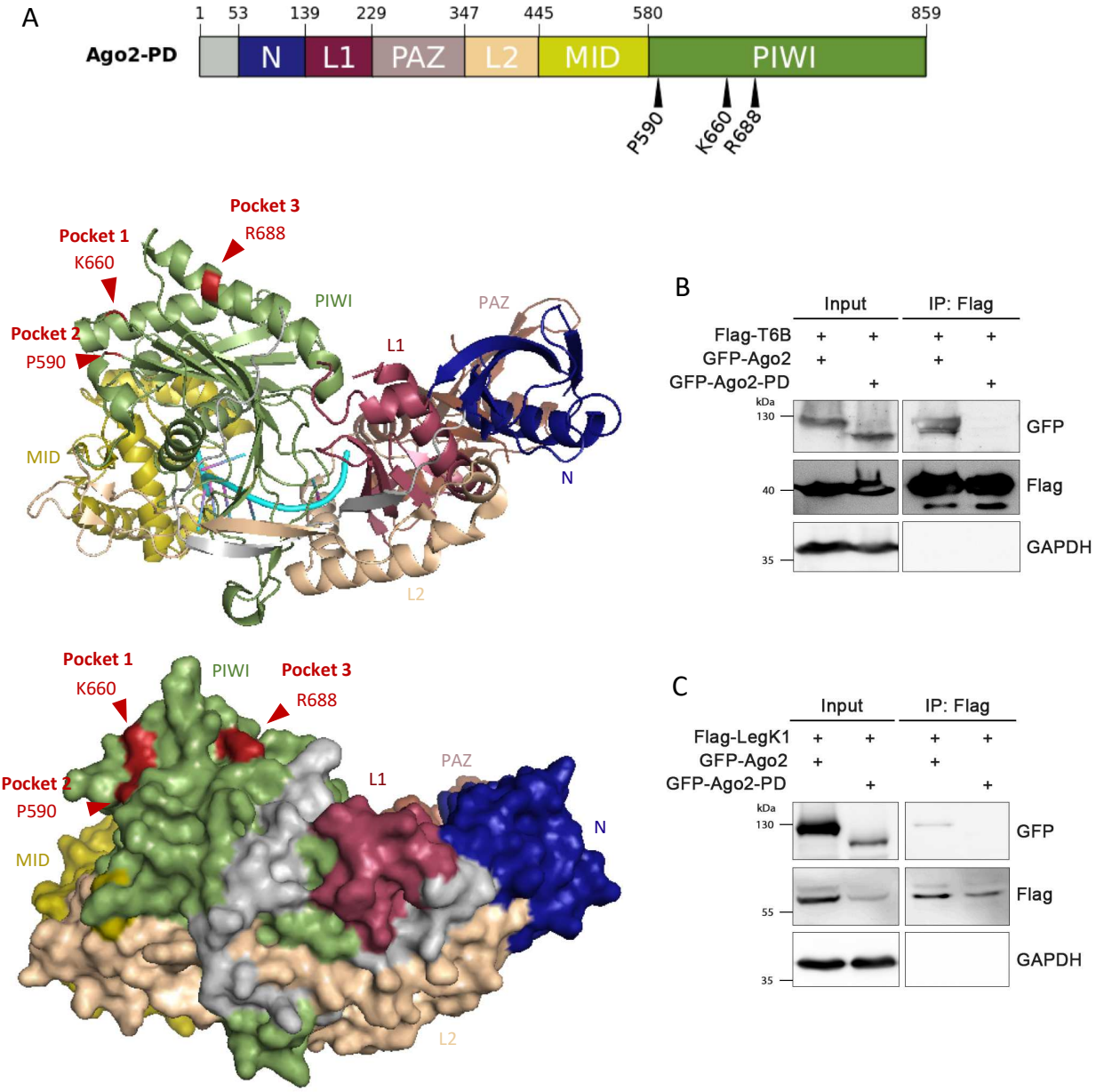

Figure 2.4. The three W-binding pockets of human Ago2 are critical for interaction of Ago2 with T6B, and potentially with LegK1.
(A) Schematic representation of the W-binding regions in the PIWI domain of Ago2. On top, schematic representation of the Ago2 primary sequence with the N (navy), PAZ (brown), MID (yellow), PIWI (green) domains and linkers L1 (purple) and L2 (pink). In the center, cartoon representation of Ago2 (PDB ID: 4OLA) indicating the position of the hydrophobic W-binding regions in the PIWI domain of Ago2 composed of three W-bound residues (P590, K660, R688). A generic guide RNA (teal) can be traced for nucleotides 1–8 and 21. At the bottom, surface presentation of Ago2 and its three W-binding pockets. **(B)** Co-immunoprecipitation of T6B in presence of Ago2 WT or pocket-dead mutant. HEK293T cells were co-transfected with vectors expressing Flag-HA-T6B and GFP-Ago2 WT or mutated on the three W-binding pockets (Ago2-3W) recombinant proteins. At 48h post-transfection, cells were lysed and proteins were immunoprecipitated using an anti-Flag antibody. Total cell lysates (input) and the immunoprecipitates were analyzed by Western blot using indicated antibodies. GAPDH was used as loading control. The results shown are representative of three independent experiments. **(C)** Co-immunoprecipitation of LegK1 in presence of Ago2 WT or pocket-dead mutant. HEK293T cells were co-transfected with vectors expressing 2xFlag-HA-LegK1 and GFP-Ago2 WT or mutated on the three W-binding pockets (Ago2-PD) recombinant proteins. At 48h post-transfection, cells were lysed and proteins were immunoprecipitated using an anti-Flag antibody. Total cell lysates (input) and the immunoprecipitates were analyzed by Western blot using indicated antibodies. GAPDH was used as loading control. The results shown are from one independent experiment and should thus be considered as preliminary.

IV.VI. THE TRYPTOPHAN-BINDING POCKETS OF HUMAN AGO2 LIKELY BIND THE TNRC6B-DERIVED PEPTIDE T6B, AND MIGHT ALSO BE REQUIRED FOR AGO2-LEGK1 INTERACTION

Three evenly spaced tryptophan-binding pockets in the human Ago2 PIWI domain were previously shown to play a central role in the interaction with the W-motifs rich proteins TNRC6/GW182 proteins (Pfaff *et al*., 2013; Schirle and MacRae, 2012; Sheu-Gruttadauria and MacRae, 2018; Till *et al*., 2007). These pockets, composed of K660 (pocket 1), P590 (pocket 2) and R688 (pocket 3), are known to cluster together in a small region near the bottom of the human Ago2 PIWI domain, and are organized in an equilateral triangle at the surface of such domain (Figure S2.7A-C) (Sheu-Gruttadauria and MacRae, 2018). To determine whether LegK1 could make use of these tryptophan-binding pockets for Ago2-binding, we decided to generate a triple $Ago2_{K660S\text{-}P590G\text{-}R688S}$ mutant, referred to here as the Ago2-PD (Ago2-pocket dead) mutant, which theoretically disables the three pockets (Figure 2.4A). It is noteworthy that, so far, only single and combinatorial double tryptophan-binding pocket mutants of Ago2 have been generated and characterized in previous studies (Sheu-Gruttadauria and MacRae, 2018; Till *et al.*, 2007). It was thus important to verify that the Ago2-PD mutant version is stable and altered in its ability to bind known Ago-binding W-motifs proteins in human cells prior protein-protein interaction assays with LegK1. To test this, we co-transfected the Flag-T6B construct with either the GFP-Ago2 or GFP-Ago2-PD fusion constructs in HEK293T cells, and further immunoprecipitated T6B with a Flag antibody. It is noteworthy that in these experiments, we observed a reduced molecular weight of the GFP-Ago2-PD proteins compared to the GFP-Ago2 proteins by SDS-PAGE (Figure 2.4B, input data), which might be, at least in part, due to altered post-translational modifications of the Ago2-PD mutant (see discussion section). Importantly, we solely recovered the GFP-Ago2, but not the GFP-Ago2-PD mutant version, in the T6B immunoprecipitates (Figure 2.4B), supporting the disrupted function of the tryptophan-binding pockets in the Ago2-PD mutant. We next repeated the same co-transfection and co-immunoprecipitation assays but this time with the Flag-LegK1 construct (Figure 2.4C). Our first preliminary result indicates that the GFP-Ago2-PD fusion was not recovered in the Flag-LegK1 immunoprecipitates (Figure 2.4C), indicating that LegK1 was unable to interact with the Ago2 pocket-dead mutant. However, additional biological replicates will be needed to confirm this observation. Altogether, our data suggest that LegK1 can bind to human Ago2 through its W-binding pockets. They also suggest that one or several predicted Ago-binding

motifs of LegK1 must orchestrate the interaction between this bacterial effector and human Ago proteins.

IV.VII. THE TWO W-MOTIFS THAT ARE EMBEDDED IN THE LEGK1 KINASE DOMAIN EXHIBIT BINDING CAPACITY TO THE FOUR HUMAN AGO PROTEINS

To further examine whether the three selected W-motifs of LegK1 could bind human Ago proteins, we first attempted to express and purify from *E. coli* the LegK1$^{2:386}$ truncated version carrying the three W>F substitutions. However, the resulting LegK1 mutant protein formed insoluble inclusion bodies, preventing further *in vitro* pull-down experiments (Figure S2.8). To circumvent this problem, and to determine which of the three selected W-motifs could contribute to Ago-binding, we next chemically synthesized biotinylated peptides containing each candidate W-motifs (W41, W283 and W293), surrounded by native amino acid residues, referred to here as W1, W2 and W3 peptides (Figure 2.5A). In parallel, we synthetized identical peptides with a substitution of the candidate tryptophan into phenylalanine, named F1, F2 and F3 mutant peptides, predicted to alter putative interaction with Ago proteins (Figure 2.5A). Equimolar amount of wild-type and mutant peptides were bound to streptavidin magnetic beads, and were incubated with HEK293T cell lysate. After washing, eluted bound proteins were analyzed by Western blot using specific anti-Ago antibodies. Using this approach, we found that the W1 peptides did not bind to any of the human Ago protein, indicating that the W41 motif is not a functional Ago-binding platform (Figure 2.5B). By contrast, the W2 and W3 peptides exhibited a clear binding to human Ago1, Ago2, Ago3 and Ago4, but not to the negative control GAPDH (Figure 2.5B). Therefore, the W2 and W3 peptides can selectively interact with the four human Ago proteins. By contrast, the binding to these Ago proteins was lost in the presence of the F2 peptides, providing evidence that the W283 residue is a functional Ago-binding motif. The F3 mutant peptides remained, however, competent in interacting with the four Ago proteins (Figure 2.5B). The latter data suggested either that the W293F substitution was not sufficient to alter the W3 peptide-Ago interaction or that the W293 was not required for Ago-binding. To test these possibilities, we further synthesized a peptide carrying a substitution of the tryptophan residue into alanine, named the A3 peptide, a substitution regularly used on W-rich proteins to impair interaction with Ago proteins (Figure 2.5A) (El-Shami *et al.*, 2007; Till *et al.*, 2007). We further monitored the Ago-binding capacity of the A3 peptide and found that this peptide no longer interacted with human Ago proteins (Figure 2.5C), supporting a key role for the W293 motif in the interaction with human Ago proteins. Collectively, these data indicate that both the W283 and W293 motifs, which are embedded in the kinase domain of LegK1, behave as canonical Ago-binding motifs. This

conclusion is further supported by the fact that these two W-motifs are interspaced by 9 amino acid residues, which is a common feature of W-motifs from Ago-binding proteins that are typically separated by a flexible linker length of ~10-15 amino acid residues (Schirle and MacRae, 2012; Sheu-Gruttadauria and MacRae, 2018, see discussion section).

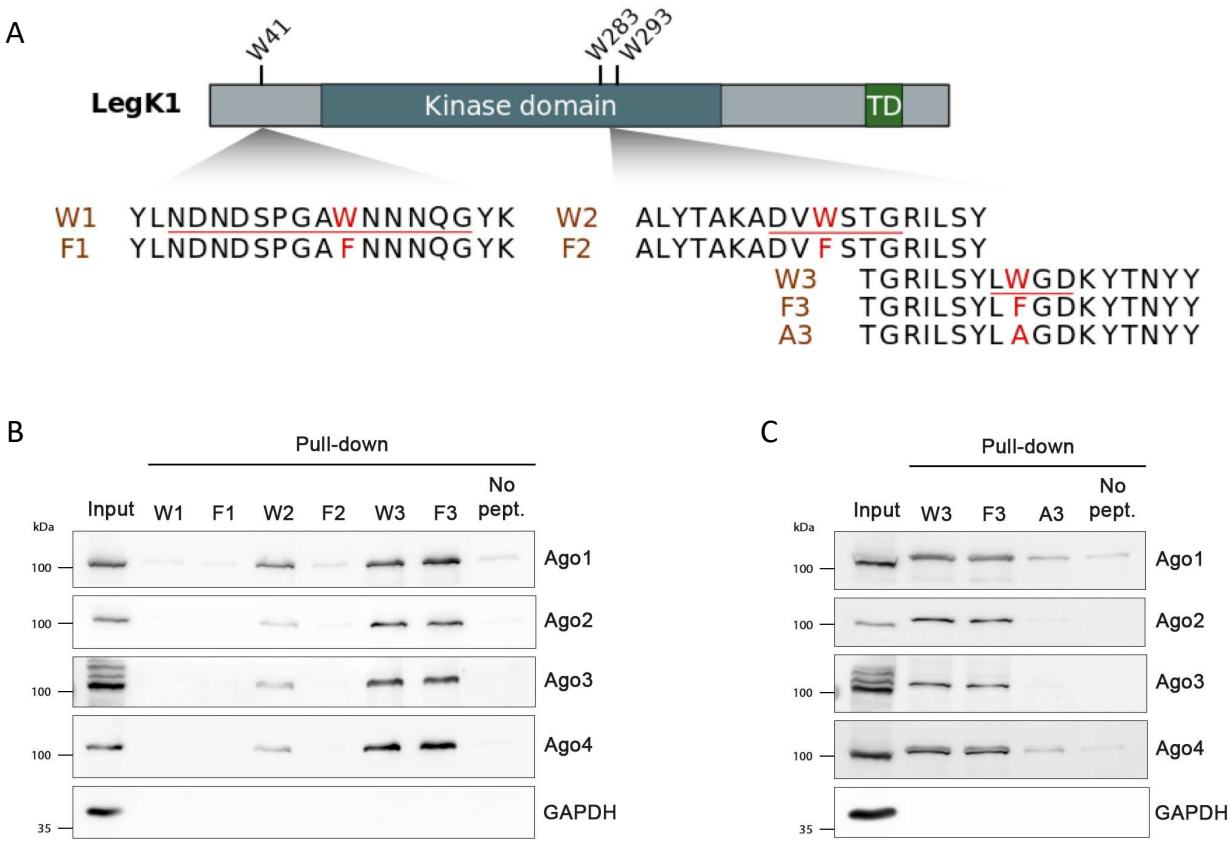

Figure 2.5. Peptides containing each W-motif from the kinase domain of LegK1 efficiently bind the four human Argonaute proteins.
(A) Schematic representation of synthetic biotinylated LegK1-derived peptides containing individual W-motifs. The amino acid sequence of the predicted W-motifs is underlined in red and the position of the tryptophan is written in red. Each biotinylated peptide sequence is depicted and its name is written in brown. TD; transmembrane domain. **(B, C)** Pull-down assays between W-motif-containing peptides and human Argonautes. Synthetic biotinylated peptides containing the WT (W) or the mutated version (F or A) of each predicted W-motif of LegK1 were mobilized on streptavidin magnetic beads. Incubation of beads without peptides was used as negative control. Specific peptide-loaded beads or only beads (no pept.) were further incubated with HEK293T cell lysates. The presence of four human Argonautes in cell lysate (input) and bound to the beads was assessed by Western blot analysis using the indicated antibodies. GAPDH was used as loading control. The results shown are representative of three independent experiments for B and two independent experiments for C.

IV.VIII. The W283 motif of the L. pneumophila (strain Paris) LegK1 protein sequence exhibits natural amino acid sequence variation across Legionella species, while the W293 motif, and its surrounding residues, display extensive conservation

To analyze the sequence conservation of the two functional W-motifs from the *L. pneumophila* (strain Paris) LegK1 protein, we retrieved the LegK1 protein sequences from the available *Legionella* genomes and aligned them between each other. LegK1 was found present in all the *L. pneumophila* strains, but also in other *Legionella* species (Figure 2.6B) (Gomez-Valero *et al.*, 2019; Mondino *et al*., 2020a). Importantly, the tryptophan residues corresponding to the W283 motif of the LegK1 protein sequence from the *L. pneumophila* (strain Paris), were found conserved across all the *L. pneumophila* analyzed but also in two other *Legionella* species, namely *L. norrlandica* and *L. waltersii* (Figure 2.6A-B). With the exception of a few variable residues surrounding this tryptophan residue in the *L. waltersii* LegK1 protein sequence, the amino acids around the other tryptophan motifs of the *L. pneumophila* strains and of *L. norrlandica* were also found conserved (Figure 6A-B). These observations suggest that the corresponding LegK1 protein domains from *L. pneumophila* strains and from *L. norrlandica* must maintain their Ago-binding capacity. By contrast, the LegK1 protein sequences from the remaining *Legionella* species, which are notably mostly composed of non-pathogenic *Legionella* species –with the exception of some human pathogenic *L. longbeachae* strains– exhibited not only substitutions from tryptophan to tyrosine residues, but also sequence variability in the surrounding amino acids (Figure 2.6A-B). These observations suggest that the corresponding LegK1 protein domains are potentially not competent for Ago-binding, although experimental data are needed to support this assumption. By conducting a similar analysis at the residues corresponding to the W293 motif of the *L. pneumophila* (strain Paris), we noticed that these tryptophan residues, and their surrounding amino acids, exhibit an extensive sequence conservation across all the LegK1 protein sequences analyzed (Figure 2.6A-B). This result suggests that the corresponding conserved LegK1 protein domains likely preserved their capacity to interact with human Ago proteins. Altogether, these data provide evidence that the W283 motif of the *L. pneumophila* (strain Paris) LegK1 protein sequence exhibits natural amino acid sequence variation across *Legionella* species other than *L. pneumophila*, *L. norrlandica* and *L. waltersii*. They also unveiled an extensive conservation of the W293 motif of the *L. pneumophila* (strain Paris) LegK1 protein sequence, and its surrounding residues, across all the *Legionella* species possessing LegK1 in their genomes.

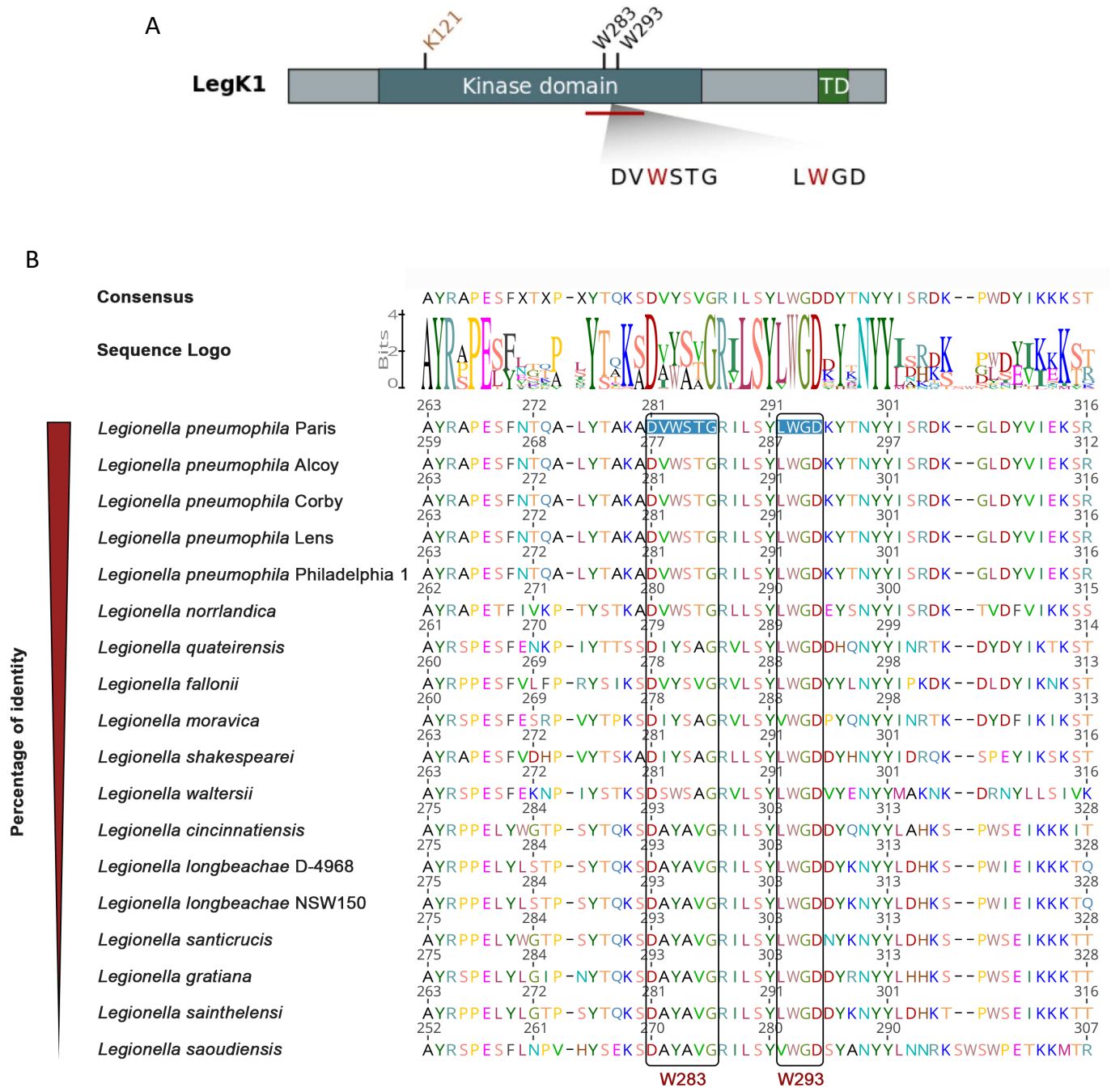

Figure 2.6. **Alignment of LegK1 orthologs from *Legionella* species, including *Legionella pneumophila* and *Legionella longbeachae* strains.**
(A) Schematic representation of LegK1 protein sequence depicting the positions and sequences of the two functional W-motifs. The area underlined in red corresponds to the alignment shown in B. **(B)** Alignment of LegK1 orthologs around the two functional W-motifs. The protein sequence of LegK1 (*lpp1439* gene) from *Legionella pneumophila* Paris was used as a reference sequence to determine the presence of orthologs in *Legionellales* order (taxid: 445). A protein-BLAST (Basic Local Alignment Search Tool) was performed on NCBI (National center for biotechnology information) website. An identity cutoff of 40%, an Expect (*E*)-value cutoff of 10^{-5} and a minimum percentage match length of subject and query of 65% were used. The set of ortholog protein sequences was aligned using ClustalW2, and partial sequences around the two functional W-motifs are shown.

IV.IX. Ongoing characterization of the relationship between Ago-binding and catalytic activities of LegK1

The fact that the two functional W-motifs of LegK1 are embedded in its kinase domain (Figure 2.6) prompted us to investigate the relationship between the W-motifs and the catalytic activity of LegK1. For this purpose, we first made use of the available LegK1-3W constructs and determine whether this mutant version would be altered in its ability to phosphorylate IκBα. Given that the purified His6-LegK1$^{2:386}$-3W was found insoluble (Figure S2.8), we examined the phosphorylation of the serine 32 of the purified His6-IκBα recombinant protein upon incubation with immunoprecipitate of LegK1-WT, LegK1-KA or LegK1-3W from HEK293T cell lysates (Figure S2.9A). By using this approach, we found that the serine 32 of IκBα was not phosphorylated in the presence of both LegK1-KA and LegK1-3W mutant versions, of LegK1, while this post-translational modification was readily detected in the presence of LegK1-WT (Figure S2.9A). These data indicate that the W>F mutations in the three W-motifs of LegK1 abolish its kinase activity. Although we cannot rule out that the triple mutations in the W-motifs alter the folding of LegK1, these data suggest that the Ago-binding and kinase activities might be tightly interconnected. Next, we expressed and purified from *E. coli* the LegK1$^{2:386}$ truncated version carrying individual W->F substitutions, and further performed *in vitro* interaction by incubating LegK1$^{2:386}$-WT, LegK1$^{2:386}$-KA, LegK1$^{2:386}$-W41F, LegK1$^{2:386}$-W283F or LegK1$^{2:386}$-W293F with IκBα recombinant proteins. We found that the three individual mutants of LegK1 on each W-motif were still capable of phosphorylating the serine 32 of IκBα, to the same extent as the LegK1$^{2:386}$-WT version (Figure S2.9B). These experiments therefore indicate that mutating individual W-motifs does not alter the kinase activity of LegK1, arguing for a possible uncoupling of the two activities. Nevertheless, it is at the moment impossible to reach solid conclusions with our current results. Therefore, additional mutant versions, including the single LegK1$^{2:386}$-W293A and double LegK1$^{2:386}$-W283FW293A, will need to be further tested to obtain a complete picture of the functional relevance of the W-motifs in the kinase and Ago-binding activities of LegK1 (see discussion section).

IV.X. LEGK1 DOES NOT PHOSPHORYLATE HUMAN AGO2

Since LegK1 can physically interact with human Ago2 and possesses an eukaryotic-like serine/threonine kinase activity (Figure 2.3) (Ge *et al.*, 2009), we reasoned that it could directly phosphorylate Ago2 residues to inhibit its functions. To test this hypothesis, we first decided to analyze specific phosphorylation sites on Ago2 through a mass spectrometry approach. More specifically, we transfected the eGFP, LegK1-WT or LegK1-KA constructs in HEK293T cells and further subjected the corresponding cell lysates to Ago2 immunoprecipitation and Parallel-Reaction Monitoring (PRM) (Figures 2.7A-D, S2.10). The latter approach relies on a liquid chromatography-mass spectrometry (LC-MS)-based targeted peptide quantification method. In more details, Ago2 immunoprecipitates were separated by SDS-PAGE, gel slices were excised for each purification, and subsequently in-gel digested by trypsin. Digested peptides were then analyzed by LC-MS/MS on a Q Exactive HF-X mass spectrometer. Results from this analysis allowed us to retrieve four phosphopeptides and to quantify the phosphates on the serine residues at positions 387, 824 and 828 (*pS*) of Ago2. Nevertheless, we did not observe a differential phosphorylation status of these targeted serine residues in the presence of LegK1 or LegK1-KA compared to the control eGFP condition (Figure 2.7A-D). These data indicate that LegK1 does not interfere with the phosphorylation status of those serine residues of Ago2. However, this approach was limited to the phosphorylation of the serine residues from the recovered phosphopeptides in the samples and did not provide information on the phosphorylation status of all the remaining serine and threonine residues of Ago2. As a complementary approach, we decided to perform an *in vitro* kinase assay in the presence of the truncated LegK1$^{2:386}$ or LegK1$^{2:386}$-KA versions. Because IκBα has previously been shown to be phosphorylated by LegK1 on the serine residues 32 and 36 (Ge *et al*., 2009), we used this host target as an internal control for LegK1 phosphorylation. By incubating purified IκBα with LegK1$^{2:386}$ proteins, we found a clear incorporation of ^{32}P radioactivity (Figure 2.7E), confirming previous findings (Ge *et al.*, 2009). By contrast, we did not find any incorporation of ^{32}P radioactivity upon incubation of purified Ago2 with LegK1$^{2:386}$ proteins, as observed upon incubation of purified TAP control proteins with LegK1$^{2:386}$ (Figure 2.7E). Collectively, these data indicate that LegK1 does not phosphorylate human Ago2 *in vitro*. Given that the LegK1 kinase-dead mutant did not suppress siRNA and miRNA activities (Figures 2.2), they also suggest that LegK1 must suppress RNAi by phosphorylating either other components of Ago-RISCs, and/or other host factor(s) that indirectly regulate the activity of Ago-RISCs.

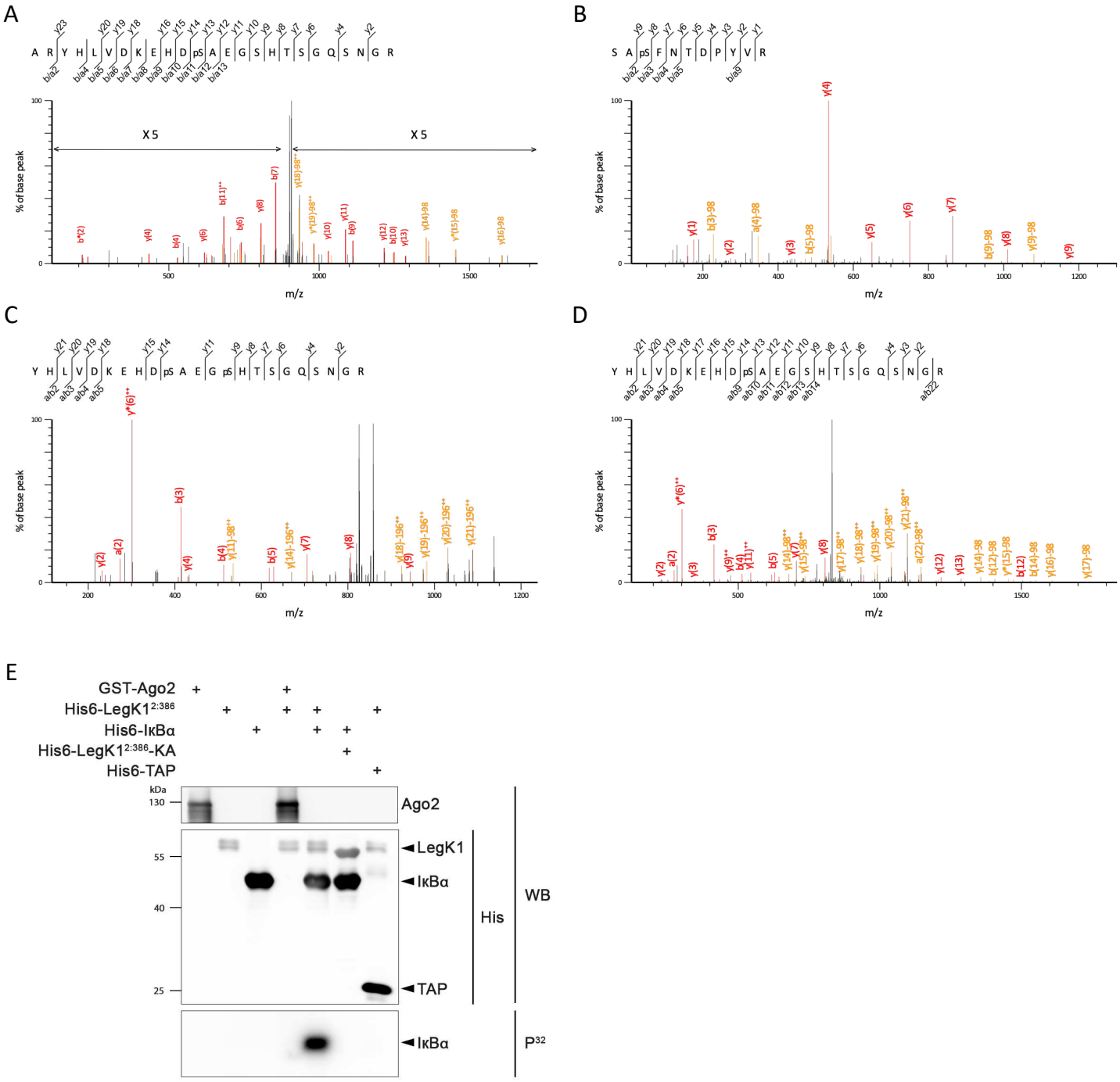

Figure 2.7. LegK1 does not phosphorylate Ago2 in human cells.
(A,B,C,D) Quantification of Ago2 phosphorylation on selected serine residues by Parallel-Reaction Monitoring (PRM) approach obtained by Liquid Chromatography with tandem mass spectrometry (LC-MS/MS). HEK293T cells were transfected with vectors expressing Flag-HA-eGFP, 2xFlag-HA-LegK1 or 2xFlag-HA-LegK1-KA (Kinase-dead mutant). At 24h post-transfection, endogenous Ago2 proteins were immunoprecipitated using anti-ago2 antibody. Representative HCD fragmentation spectra of human Ago2 phosphorylated-peptides obtained on a Q Exactive HF-X mass spectrometer are shown. The spectrum represents the peptide sequence and the observed ions of the phospho-peptide. **(A)** MS/MS of the tryptic (2 missed cleavages) ARYHLVDKEHD*p*SAEGSHTSGQSNGR (m/z 940.083+) peptide with the position of the phosphate group at S284 (mascot score 75.2) and labeled to show singly and doubly charged b and y ions, as well as ion corresponding to neutral losses of NH3 (*) and H3PO4 group (98Da). **(B)** MS/MS of the tryptic SA*p*SFNTDPYVR (m/z 668.782+) peptide with the position of the phosphate group at S387 (mascot score 57.2) and labeled to show singly charged a, b and y ions, as well as ion corresponding to neutral losses of H3PO4 group (98Da). **(C)** MS/MS of the tryptic (1 missed cleavage) YHLVDKEHD*p*SAEGpSHTSGQSNGR (m/z 891.023+) peptide with the position of the phosphate group at S824 and S828 (mascot score 24.9) and labeled to show singly and doubly charged a, b and y ions, as well as ion corresponding to neutral losses of NH3 (*) and H3PO4 group (98Da). **(D)** MS/MS of the tryptic (1 missed cleavage) YHLVDKEHD*p*SAEGpSHTSGQSNGR (m/z 864.373+) peptide with the position of the phosphate group at S824 (mascot score 82.5) and labeled to show singly and doubly charged a,b and y ions, as well as ion corresponding to neutral losses of NH3 (*) and H3PO4 group (98Da). **(E)** *In vitro* kinase assay of LegK1 in presence Ago2. Purified His6-LegK1$^{2:386}$ or His6-LegK1-KA$^{2:386}$ recombinant proteins were incubated with [γ-P^{32}] ATP in presence of GST-Ago2, His6-IκBα or His6-TAP, as negative control, into the reaction. Incorporation of phosphate into the protein was examined by autoradiography of the reaction mixtures resolved on the SDS-PAGE gel, as shown. Loading amount of different recombinant proteins was assessed by Western blot analysis using indicated antibodies. Blots are representative of triplicate experiments.

IV.XI. LEGK1 PROMOTES INTRACELLULAR REPLICATION OF L. PNEUMOPHILA IN BOTH ACANTHAMOEBA CASTELLANII AND HUMAN MACROPHAGES

To determine whether LegK1 could contribute to *L. pneumophila* pathogenesis, we first generated an isogenic *legk1* deletion mutant, referred to here as the *Lpp* Δ*legK1* strain. A whole-genome sequencing of the *Lpp* Δ*legK1* strain validated a unique deletion in the *legK1* gene, which did not affect the fitness of *L. pneumophila* as monitored by *in vitro* bacterial growth (data not shown). Next, we inoculated the wild-type (WT) or the *Lpp* Δ*legK1* strains onto *Acanthamoeba castellanii*, a natural protozoan host of *L. pneumophila,* and further monitored bacterial titer over a timecourse of infection. Interestingly, we found that the ability of the *Lpp* Δ*legK1* strain to replicate in *A. castellanii* was significantly reduced at 24 hours post-infection, which was not the case at later timepoints (Figure 2.8A). These data therefore indicate that the depletion of *legK1* from *L. pneumophila* leads to a delayed intracellular replication in *A. castellanii* at an early stage of infection. Because *L. pneumophila* can additionally infect human macrophages, we further conducted the same assay in human THP-1 macrophages. Similarly, we found that the intracellular growth of the *Lpp* Δ*legK1* strain was significantly reduced at 24 hours post-infection compared to the one of the WT strain (Figure 2.8B), further supporting a positive role of LegK1 on *L. pneumophila* replication. Therefore, LegK1 contributes to *L. pneumophila* replication at an early stage of infection, in both natural and accidental host cells.

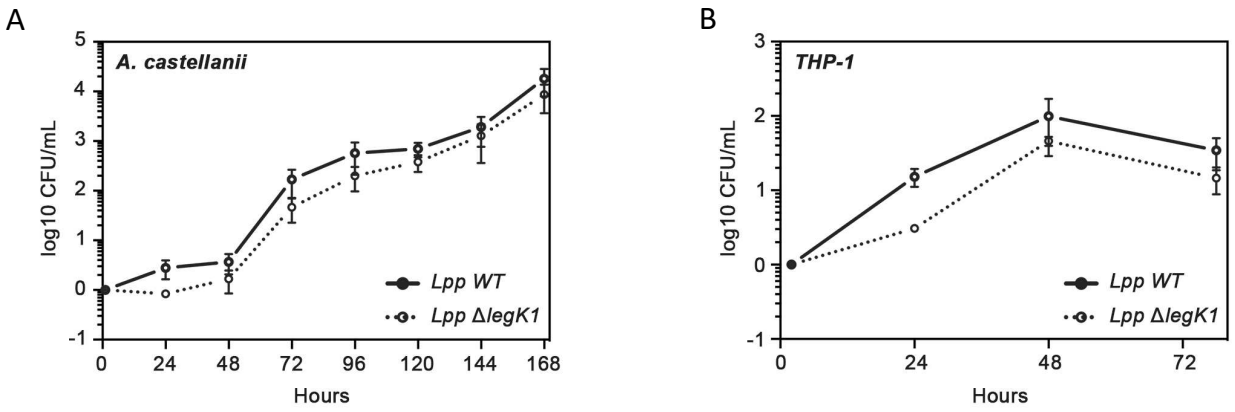

Figure 2.8. LegK1 promotes *L. pneumophila* replication in *Acanthamoeba castellanii* and human macrophages at an early stage of infection.
(A) Intracellular replication of the WT or *legK1*-deleted strains of *L. pneumophila* in *A. castellanii. A. castellanii* were infected with WT (Paris) or Δ*legK1* (*lpp1439*) mutant *L. pneumophila* strain at a multiplicity of infection (MOI) of 0.1. Intracellular growth was determined by recording the number of colony-forming units (CFU) through plating on buffered charcoal yeast extract (BCYE) agar at the indicated time points after infection. Results shown are log10 ratio CFU/mL, where CFU were normalized to the associated condition at 2h post-infection, corresponding to the entry of bacteria in the host cell. Error bars indicate the mean and standard error of mean (± SEM) from three independent experiments. **(B)** Intracellular replication of the WT or *legK1*-deleted strains of *L. pneumophila* in human macrophages. THP-1 macrophages were infected with WT (Paris) or Δ*legK1* mutant *L. pneumophila* strain at a MOI of 10. Intracellular growth was determined by recording the number of CFU through plating on BCYE agar at the indicated time points after infection. Results shown are log10 ratio CFU/mL, where CFU were normalized with the associated condition at 2h post-infection, corresponding to the entry of bacteria in the host cell. Error bars indicate the ± SEM from two independent experiments.

IV.XII. HUMAN AGO4 IS A MAJOR GENETIC TARGET OF LEGK1 IN INFECTED MACROPHAGES

We next wondered whether the ability of LegK1 to suppress Ago functions is required for *L. pneumophila* pathogenesis. To address this question, we first made use of available RNA-sequencing (RNA-seq) datasets and analyzed the expression levels of human *Ago1-Ago4* in different cell lines (Figures 2.9A, S2.11). We found that the level of *Ago4* mRNAs was more elevated in THP-1 monocytes compared to HEK293T and A549 epithelial cells, a phenomenon which was also detected at the protein levels, as revealed by western blot analysis (Figure 2.9A-B). Such expression pattern is consistent with a recent report showing that the antiviral *Ago4* transcript is highly expressed in innate immune cells such as monocytes, macrophages, dendritic cells and granulocytes (Figure S2.11) (Adiliaghdam *et al*., 2020). Conversely, Ago2 mRNAs and proteins accumulated to significant and comparable levels in THP-1 monocytes, HEK293T and A549 cells, while *Ago1* and *Ago3* mRNAs exhibit a low abundance in these cell lines (Figure 2.9A-B). Since Ago2 and Ago4 are the most abundant Ago proteins in THP-1 cells, and because LegK1 can interact with both factors (Figure 2.9A-B and S2.11), we decided to knock them out in THP-1 cells, which is a relevant genetic background for *L. pneumophila* infection assays. More specifically, a single synthetic guide RNA approach was employed to generate CRISPR/Cas9-based deletions at the second exon of *Ago2* or at the third exon of *Ago4* (Figure S2.12A-B). Independent cell lines were selected and further characterized molecularly. Using Sanger sequencing, we demonstrated that the selected lines carry deletions at the regions targeted by the guide RNAs (Figure S2.12C-D). In addition, a lack of Ago2 and Ago4 proteins was observed by immunoblotting in the *ago2*$^{-/-}$ and *ago4*$^{-/-}$ THP-1 reference lines, respectively (Figure 2.9C), confirming that they are true individual knock-out of these silencing factors. The characterized *ago2*$^{-/-}$ and *ago4*$^{-/-}$ THP-1 lines, and the THP-1 reference cell line, were further differentiated in macrophages, inoculated with either the *L. pneumophila* WT or the *Lpp* Δ*dotA* mutant strain, and the bacterial titers of these strains were subsequently monitored over the timecourse of infections. Results from these assays revealed a similar replication of the *L. pneumophila* WT strain in the THP-1 reference line compared to the *ago2*$^{-/-}$ and *ago4*$^{-/-}$ cell lines (Figure S2.13). This first observation indicates that Ago2 and Ago4 unlikely control the growth of the *L. pneumophila* WT strain in human macrophages. We next infected *ago2*$^{-/-}$ and *ago4*$^{-/-}$ macrophages with the *Lpp* Δ*legK1* strain. Importantly, while the growth defect of the *Lpp* Δ*legK1* strain remained unaltered in the *ago2*$^{-/-}$ line at 24 hours post-infection, we found

that it was fully rescued in the *ago4*$^{-/-}$ line (Figure 2.9D-E). These data indicate that in the absence of human Ago4 protein, the *L. pneumophila* strain deleted of *legK1* is able to successfully replicate at an early stage of infection. We conclude that human Ago4 –but not Ago2– is a major, and biologically relevant, genetic target of LegK1 in infected macrophages.

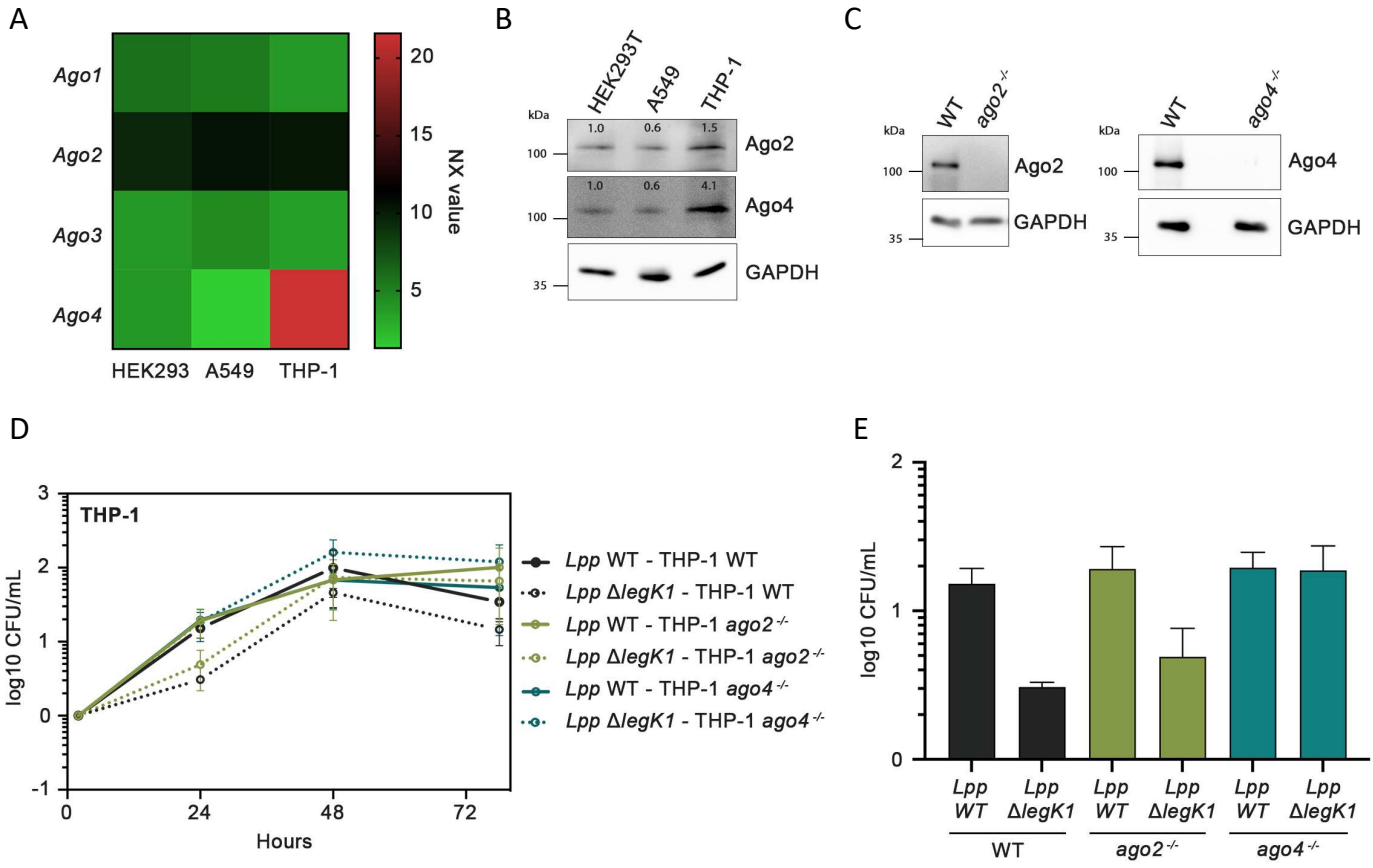

Figure 2.9. A depletion of Ago4 in human THP-1 macrophages rescues the growth-defect of a *L. pneumophila* strain deleted of *legK1*.
(A) Heatmap of the four human Ago transcript levels in HEK293T, A549 and THP-1 cell lines. The RNA-sequencing data were recovered from the Human Protein Atlas (HPA) and are reported as Normalized eXpression (NX) values (www.proteinatlas.org). The consensus NX value for each gene represents the maximum NX value in the three data sources: HPA, GTEx and FANTOM5. In brief, all Transcript Per Million (TPM) values per sample were scaled to a sum of 1 million TPM (denoted pTPM) to compensate for the non-coding transcripts that had been previously removed. Next, all TPM values of all the samples within each data source were TMM normalized, followed by Pareto scaling of each gene within each data source. The resulting transcript expression values, denoted Normalized eXpression (NX), were calculated for each gene in every sample to estimate the mRNA levels. **(B)** Immunoblotting of Ago2 and Ago4 in HEK293T, A549 and THP-1 cell lines. The protein levels of Ago2 and Ago4 in the indicated cell lines were determined by Western Blot analysis using indicated antibodies. GAPDH was used as a loading control. The results shown are representative of two independent experiments. **(C)** Immunoblotting of Ago2 and Ago4 in *ago2*$^{-/-}$ and *ago4*$^{-/-}$ THP-1 cell lines isolated from CRISPR-Cas9 knockout THP-1 cell lines. The protein levels of Ago2 and Ago4 proteins were determined by Western Blot analysis using indicated antibodies. GAPDH was used as a loading control. The results are from one independent experiment. **(D)** Intracellular replication of the WT or *legK1*-deleted strains of *L. pneumophila* in human macrophages depleted of Ago2 or Ago4. *WT, ago2*$^{-/-}$ and *ago4*$^{-/-}$ THP-1 cells were infected with WT (Paris) or the Δ*legK1* mutant *L. pneumophila* strain at a multiplicity of infection (MOI) of 10. Intracellular growth was determined by recording the number of colony-forming units (CFU) through plating on buffered charcoal yeast extract (BCYE) agar at the indicated time points after infection. Results shown are log10 ratio CFU/mL, where CFU were normalized with the associated condition at 2h post-infection, corresponding to the entry of bacteria in the host cell. The data presented for THP-1 WT infections are the same as the ones shown in Figure 8B of this thesis chapter. Error bars indicate ± SEM from two independent experiments. **(E)** Intracellular replication of the WT or *legK1*-deleted strains of *L. pneumophila* in human macrophages depleted of Ago2 or Ago4 at 24 hours post-infection (hpi). The plotted data are the same as the data shown in D at 24 hpi. Error bars indicate ± SEM from two independent experiments.

CHAPTER III: DISCUSSION

I. LEGK1 SUPPRESSES SIRNA AND MIRNA ACTIVITIES THROUGH BOTH ITS CATALYTIC ACTIVITY AND ITS PREDICTED AGO-BINDING PLATFORM

In the present study, we have demonstrated that the type IV-secreted effector LegK1 from *L. pneumophila* suppresses both siRNA- and miRNA-guided silencing when expressed in human cells. This phenomenon was demonstrated by making us of different silencing reporter systems (Figures 2.1, 2.2). First, we used the previously described siRNA-based CXCR4-2p sensor and characterized the genetic requirement for its silencing in *ago1*$^{-/-}$, *ago2*$^{-/-}$, *ago1/2*$^{-/-}$ and *dicer*$^{-/-}$ HeLa cell lines. We showed that the silencing of the CXCR4-2p reporter was dependent on human Ago2, but not on Ago1 nor on Dicer (Figure 2.1). We then used this system to screen for candidate effectors or toxins from human pathogenic bacteria that could potentially interfere with the silencing of this reporter. Out of 8 candidates tested, we found that LegK1 was the sole bacterial protein capable of triggering a derepression of the CXCR4-2p reporter, a phenomenon which was also observed with the VSR *Hepatitis B virus* HBx, which served as a positive control (Chinnappan *et al.*, 2014). Collectively, these data indicate that LegK1 can suppress siRNA-guided gene silencing mediated by human Ago2. In addition, because the CXCR4-2p reporter does not rely on Dicer (Figure 2.1), our results suggest that LegK1 can act downstream of this small RNA biogenesis factor, possibly by interfering with Ago2-miRISC functions.

Next, we used a siRNA-based *eGFP* reporter and characterized the genetic requirement for its silencing in the above HeLa mutant cell lines. We found that this reporter was partially derepressed in the *ago2*$^{-/-}$ cell line, while it remained fully silenced in the *ago1*$^{-/-}$ cell line. Interestingly, an additive derepression effect was observed in the double *ago1*$^{-/-}$/*ago2*$^{-/-}$ HeLa cell line, suggesting that human Ago1 and Ago2 act in concert to silence this reporter system (Figure 2.2). Nevertheless, the derepression observed in the double *ago1*$^{-/-}$/*ago2*$^{-/-}$ HeLa cell line did not reach the level detected in the presence of control siRNAs, indicating that Ago3 and/or Ago4 must additionally contribute to the silencing of this reporter system. When we analyzed the effect of LegK1 on this reporter in HEK293T cells, in which LegK1 proteins are detectable, we found that LegK1 fully suppresses siRNA-directed silencing of this reporter

(Figure 2.2). Collectively, these results suggest that LegK1 likely alters the functions of human Ago1 and Ago2, but also possibly of Ago3 and/or Ago4.

To determine whether LegK1 could additionally suppress miRNA activity, we used a third miRNA-based *GFP* reporter system, whose silencing was previously shown to be dependent on the human miRNA biogenesis factors Drosha and DGCR8 (Carré *et al.*, 2013). We found that LegK1 was also capable of derepressing this reporter system (Figure 2.2), supporting a role for this effector in suppressing miRNA function. Finally, we monitored the effects of a catalytically inactive and a triple W-motifs mutants of LegK1 on the last two reporter systems. We found that the derepression of these reporters, found in the presence of LegK1, no longer occurred with the two mutants (Figure 2.2). Altogether, these data provide evidence that LegK1 acts as a *bona fine* bacterial suppressor of RNA silencing (BSR) by altering both siRNA- and miRNA-guided gene silencing. They also indicate that the BSR activity of LegK1 is dependent on both its catalytic activity and predicted Ago-binding platform.

II. THE TNRC6B-DERIVED PEPTIDE T6B DEREPRESSES THE SIRNA-BASED EGFP REPORTER BUT NOT THE MIRNA-BASED GFP REPORTER

T6B is a short TNRC6B-derived peptide containing multiple W-motifs (Hauptmann *et al.*, 2015), which was used here as positive control for silencing suppression. This peptide is known to precipitate all four endogenous Ago proteins from human cells (Hauptmann *et al.*, 2015), and was additionally shown to trigger the derepression of a miRNA-based luciferase reporter (Hauptmann *et al.*, 2015). Results from our analyses revealed that T6B can derepress the siRNA-based *eGFP* reporter, indicating that this peptide suppresses siRNA-guided gene silencing (Figure 2.2). Nevertheless, the RNAi suppression effect induced by T6B was less pronounced than the one triggered by LegK1, suggesting that this peptide might be less competent than LegK1 in suppressing Ago functions in human cells. Surprisingly, we also found that the miRNA-based *GFP* reporter remained fully silenced in the presence of T6B, despite a high accumulation of this peptide in our experimental settings (Figure 2.2). Given that T6B was found to physically interact with all human Ago proteins (Hauptmann *et al.*, 2015), the binding of this peptide to each Ago protein might have a differential inhibitory effect

towards the activity of each Ago proteins. Further analyses involving an in-depth characterization of the impact of T6B on the activity of each Ago proteins, coupled with a characterization of the Ago protein(s) required for the silencing of the miRNA-based *GFP* system, would be necessary to address these issues.

III. LEGK1 INTERACTS WITH AGO PROTEINS BUT ALSO WITH PABPC1 AND DDX6, SUGGESTING THAT IT MIGHT INTERFERE WITH THE FUNCTIONS OF ASSEMBLED MIRISCS

MicroRNAs use different mechanisms to inhibit the expression of their targets through a combination of translational repression, slicing and/or mRNA degradation (Fabian and Sonenberg, 2012; Huntzinger and Izaurralde, 2011; Iwakawa and Tomari, 2015; Jonas and Izaurralde, 2015). In resting or quiescent cells, Ago2-bound mature miRNAs are found in low molecular weight complexes, which are devoid of factors required for miRNA-mediated gene silencing such as GW182/TNRC6 proteins (Olejniczak *et al.*, 2013). This process appears to be important to protect and store miRNAs in resting conditions, and thus to prepare cells for upcoming miRNA post-transcriptional gene regulation (Olejniczak *et al.*, 2013). Upon mitogenic stimulation, Ago2-bound miRNAs are present in high molecular weight RISC (HMW-RISC) containing GW182/TNRC6 proteins, which are central Ago co-factors containing Ago-binding tryptophan (W)-motifs (El-Shami *et al*., 2007; Lian *et al.*, 2009; Olejniczak *et al*., 2013; Pfaff *et al.*, 2013; Takimoto *et al*., 2009; Till *et al.*, 2007). Mechanistically, the assembly of high molecular weight (HMW)-RISC is initiated by the phosphorylation of human Ago2 at serine 387 by Akt enzymes, which in turn promote the binding of the adapter protein LIMD1 with Ago2 and ensures a tight association between miRISC and GW182/TNRC6 proteins (Bridge *et al*., 2017). These series of molecular events orchestrate the recruitment of downstream accessory factors that are critical for miRISC functions (Behm-Ansmant *et al*., 2006; Bridge *et al*., 2017; Chekulaeva *et al*., 2011; Horman *et al*., 2013; La Rocca *et al.*, 2015; Lian *et al.*, 2009; Liu *et al.*, 2005). More specifically, GW182/TNRC6 proteins ensure the recruitment of the cytoplasmic PABP, as well as PAN3 and NOT1, which are subunits of the PAN2–PAN3 and CCR4–NOT deadenylase complexes (Fabian *et al*., 2009; Huntzinger *et al*., 2010). Deadenylation is first catalyzed by the PAN2-PAN3 complex, by removing long poly(A) tails, and subsequently by CCR4-NOT complex, which shortens poly(A) tails and completes deadenylation (Yamashita *et al.*, 2005). PABPC1

bound to the 3′ poly(A) tail of eukaryotic mRNAs, and plays critical roles in mRNA translation and stability (Kahvejian *et al.*, 2005). Importantly, it has been proposed that the recruitment of GW182/TNRC6 proteins to the Ago2-miRISC promotes the dissociation of PABP from mRNA target (Huntzinger *et al*., 2013; Moretti *et al*., 2012; Yi *et al*., 2018; Zekri *et al*., 2013). Such dissociation leads to the removal of the protection effect exerted by PABP over mRNA poly(A) tails and of the break of the loop structure formed by the interaction between PABP and eIF4G, which results in a repression of translation initiation of mRNA targets, an triggers their destabilization (Huntzinger *et al*., 2013; Moretti *et al*., 2012; Yi *et al*., 2018; Zekri *et al*., 2013). In addition, GW182/TNRC6 proteins recruit mRNA decapping proteins, such as DCP1/2 or proteins required for RNA unwinding, such as DDX6 (Chen *et al.*, 2014; Chu and Rana, 2006; Rouya *et al*., 2014). The decapping is achieved by the recruitment of the decapping activator DDX6 by NOT1 subunit from CCR4-NOT complex, which promotes the removal of the 5' cap structure via the DCP1/DCP2 complex (Chen *et al.*, 2014). Collectively, these studies indicate that miRNA-mediated inhibition of translation initiation, mRNA deadenylation and mRNA decay are interconnected mechanisms, which depend on the interaction between GW182/TNRC6, PABP and deadenylase complexes.

Based on the above knowledges on miRNA-directed regulation of mRNA targets, and on strong suppression effects triggered by the predicted Ago-binding platform of LegK1 on siRNA- and miRNA-mediated gene regulation (Figure 2.2), we tested whether this bacterial effector could interact with some of these miRISC factors. Using a co-immunoprecipitation approach, we found that LegK1 can not only interact with Ago proteins (*i.e.* Ago1, Ago2, Ago4) but also with PABPC1 and DDX6 in HEK293T cells (Figure 2.3). Because PABPC1 and DDX6 are downstream accessory factors recruited to miRISC through GW182/TNRC6 proteins (Chen *et al*., 2014; Chu and Rana, 2006; Fabian *et al*., 2009; Huntzinger *et al*., 2010; Rouya *et al*., 2014), these data suggest that LegK1 might bind HMW-RISC, and in turn alter the above-mentioned miRNA-mediated repression mechanisms. This would result in a LegK1-triggered rapid and effective RNAi suppression effects, as observed on the three silencing reporters tested (Figures 2.1, 2.2). Intriguingly, the *Sweet potato mild mottle virus* (SPMMV) VSR P1, which also possesses conserved and functional W-motifs in its N-terminal region, was found to co-fractionate with HMW-RISC loaded with small RNAs, thereby repressing effectively RISC activity (Giner *et al*., 2010). Another study revealed that the hook domain of TNRC6A exhibits an increased affinity for RNA-loaded Ago1 and Ago2 proteins compared to RNA-free Ago1 and Ago2 proteins, suggesting that proteins carrying functional W-motifs are more likely to

associate with assembled miRISCs (Elkayam *et al*., 2017). It will thus be interesting to investigate whether LegK1 could also preferentially interact with HMW-RISC in human cells, and in turn alter translational initiation repression, deadenylation and/or decapping of artificial miRNA/siRNA reporters, but also of endogenous miRNA targets. Furthermore, because the SPMMV P1 viral protein was found to inhibit the loading of RISC in a W-dependent manner (Giner *et al*., 2010), it will also be important to assess whether LegK1 could also reduce the loading of small RNAs in human Ago2-RISC. Finally, because LegK1 was found to i) efficiently suppress the siRNA-directed gene silencing of the *CXCR4-2p* reporter (Figure 2.2), which has previously been shown to be regulated at the level of slicing and/or mRNA degradation (Doench *et al.*, 2003), ii) trigger an increased accumulation of *eGFP* mRNAs from the siRNA-based *eGFP* reporter system (Figure S2.4), iii) directly interact with the PIWI domain of Ago2 (Figure 2.3), which is known to direct endonucleolytic cleavage of small RNA target transcripts (Bartel, 2018), we will investigate whether this bacterial effector could additionally interfere with the slicing activity of human Ago2.

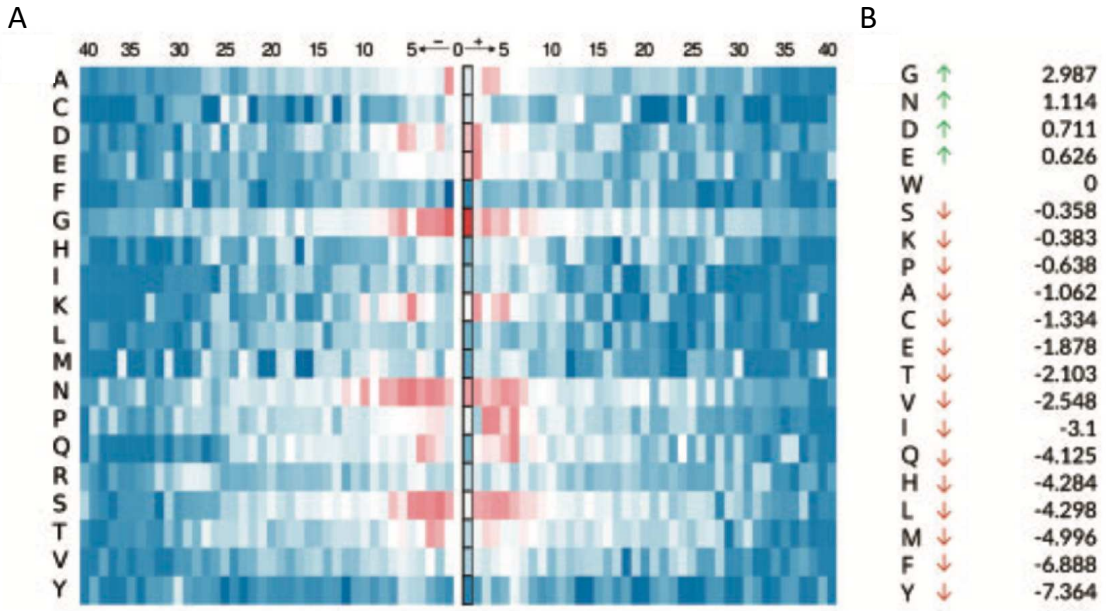

Figure 3.1. Positional analysis of the amino acid composition of W-motifs from experimentally validated Ago-binding proteins in eukaryotes. **(A)** Heat map representation of the position-specific scoring matrix (PSSM) used by the Wsearch algorithm. The color code represent amino acid preferences that are present (red) or absent (blue) on a given motif position around the tryptophan. **(B)** Preference of amino acid at the position 1 around the tryptophan. Scheme derived from Zielezinski *et al*., 2015.

IV. LegK1 is composed of two tandemly organized tryptophan residues that can efficiently bind the four human Ago proteins

LegK1 was predicted to possess four putative W-motifs, with Wsearch scores ranging from -6.48 to 11.56 (Table S2.2). These motifs were identified using a previously established Wsearch program designed to retrieve canonical W-motifs exhibiting a preferential amino-acid composition around the tryptophan residues. More specifically, the program searches for the presence of small, polar and non-hydrophobic amino acids surrounding the hydrophobic tryptophan, such as G, N, D, E and S (Figure 3.1) (Zielezinski and Karlowski, 2015). Because only a few W-motifs, out of the 36 tryptophan residues from the Ago-binding domain (ABD) of TNRC6B are required for interaction with Ago and exhibit some redundancy between each other (Sheu-Gruttadauria and MacRae, 2018), we first decided to generate combinatorial mutations in the three most promising W-motifs of LegK1 for functional assays. Although this triple mutant was stable when expressed in human cells, it was compromised in its ability to suppress RNAi and to interact with Ago1, Ago2, Ago4, PABPC1 and DDX6 in human cells (Figures 2.2, 2.3). By contrast, the catalytically inactive version of LegK1 was fully competent in binding these miRISC factors, despite its compromised RNAi suppression activity (Figures 2.2, 2.3). These results indicate that these protein-protein interactions are all dependent on the predicted Ago-binding platform of LegK1, while they do not rely on the ability of this effector to phosphorylate its host cellular targets. To further dissect the functional relevance of each of the three W-motifs in Ago-binding, we next decided to synthesize biotinylated LegK1-derived peptides carrying individual W-motifs, and to test them in pull-down experiments using lysates from human cells. As a result of these assays, we found that the two predicted W-motifs embedded in the kinase domain of LegK1, namely W283 and W293 residues, were able to bind the four human Argonaute proteins, while the W41 residue was not competent to do so (Figure 2.5). To further assess the contribution of the W283 and W293 residues for Ago-binding, we used tryptophan to phenylalanine and tryptophan to alanine substitutions, which are point mutations previously shown to interfere with the association between W-rich proteins and Ago proteins (El-Shami *et al.*, 2007; Eulalio *et al.*, 2008; Takimoto *et al.*, 2009; Till *et al.*, 2007). Interestingly, we found that the phenylalanine substitution at the W283 residue was sufficient to abolish the interaction between the peptide and human Ago proteins, supporting a major role of this tryptophan in Ago-binding. By contrast, we found that the phenylalanine substitution at the W293 residue was not sufficient to alter the interaction of the peptide with human Ago

proteins (Figure 2.5). This result might be explained by the fact that the substitution of tryptophan to phenylalanine has been previously shown to reduce, albeit not abolish, the interaction with Ago proteins (El-Shami *et al*., 2007). This might also be due to other residue(s) surrounding the W293 residue, which might contribute to the interaction with Ago proteins, thereby maintaining the Ago-binding despite the presence of the phenylalanine substitution (Till *et al*., 2007). On the contrary, we found that the substitution of W293 to alanine, which is the most frequently used substitution in GW182/TNRC6-related studies (El-Shami *et al.*, 2007; Pfaff *et al*., 2013; Takimoto *et al*., 2009; Till *et al*., 2007), fully abrogated the interaction of the peptide with human Ago proteins (Figure 2.5). Collectively, these data indicate that the W283 and W293 residues, which are embedded in the kinase domain of LegK1, are both competent for Ago-binding. This conclusion is supported by the observation that these tryptophan residues are interspaced by 9 amino acids, which is a typical feature of functional W-motifs embedded in the ABD of GW182/TNRC6 proteins or in other functional W-rich proteins. In fact, several studies have shown that the tryptophan repeats are in most cases separated by 8 to 14 amino acid residues, reaching in some cases 100 residues (Figure 3.2) (Eulalio *et al.*, 2009b; Schirle and MacRae, 2012; Sheu-Gruttadauria and MacRae, 2018; Till *et al.*, 2007; Zielezinski and Karlowski, 2015). The presence of a few amino acids between the tryptophan molecules organized in tandemly repeated motifs is thought to form a flexible linker (Schirle and MacRae, 2012; Sheu-Gruttadauria and MacRae, 2018). This presumably facilitates the interaction of the W-motifs with the different W-binding pockets exposed at the surface of the human Ago2, which are separated from a distance of 25 Å from each other (Schirle and MacRae, 2012; Sheu-Gruttadauria and MacRae, 2018). Importantly, the tandemly W-motifs can cooperatively contribute to the interaction with Ago proteins. This has notably been studied in the context of TNRC6B-Ago2 interaction, which is abolished when the 36 tryptophan residues of the ABD of TNRC6B are substituted to alanine (Sheu-Gruttadauria and MacRae, 2018). Importantly, adding back two W residues found in the motif I of the ABD was sufficient to restore binding, while neither W residue alone was competent for this process (Sheu-Gruttadauria and MacRae, 2018). Based on these findings and on the results obtained with LegK1, we propose that the W283 and W293 residues are likely both important to ensure a tight association between LegK1 and human Ago proteins. However, additional experiments, involving single and double mutations in the W283 and W293 on the native LegK1 protein will be necessary to further test this hypothesis. For this purpose, we plan to use a Bio-Layer Interferometry (BLI) approach, which will be instrumental to precisely measure the affinity of these mutant versions to Ago proteins. In addition, we will make use of the silencing reporter systems described in this study

to determine whether these single or double mutant versions could alter LegK1-triggered RNAi suppression activity.

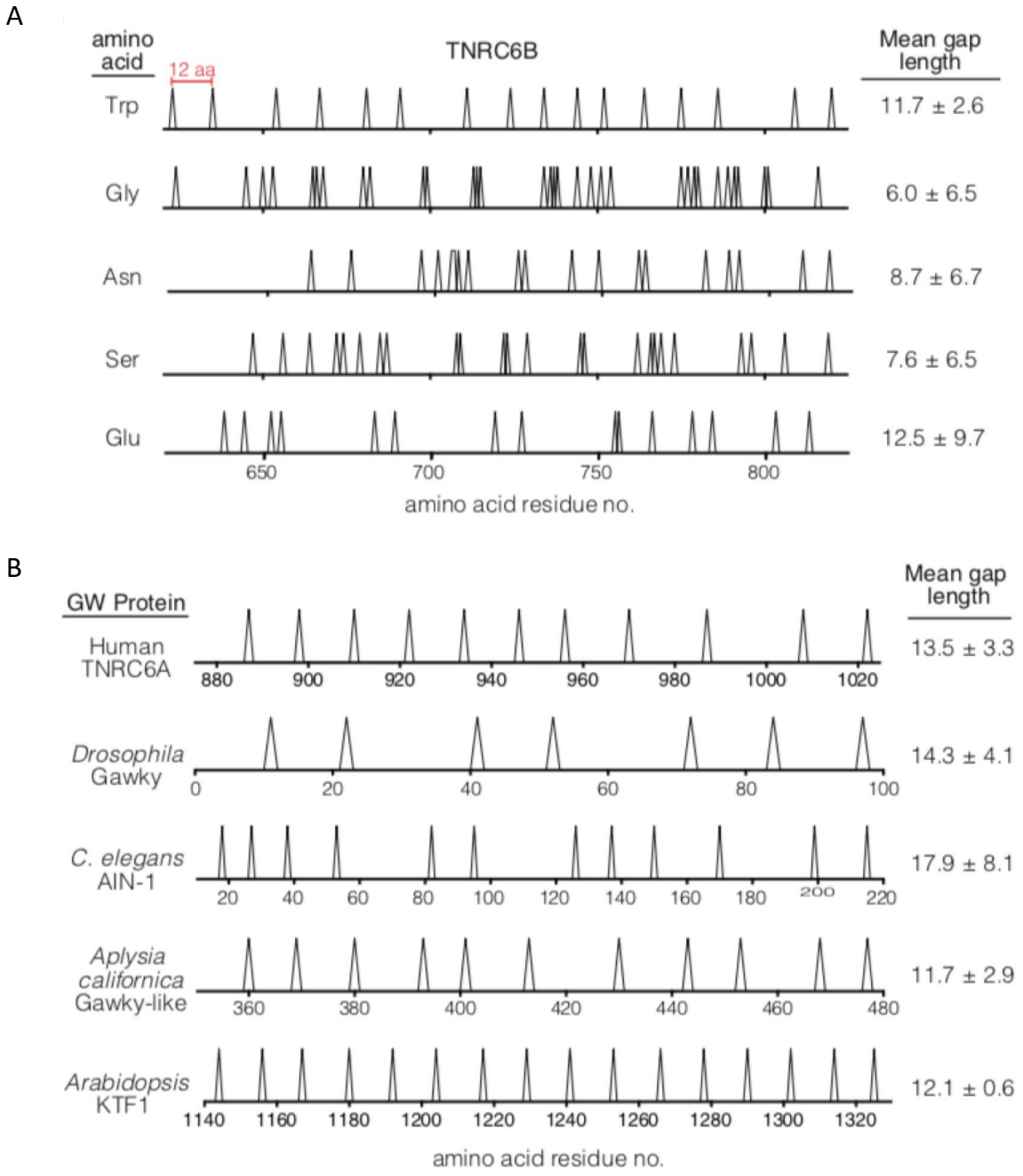

Figure 3.2. Tryptophan spacing in Ago-binding domains
(A) Schematic representation of regularly spaced tryptophan residues within a W-rich region of TNRC6B. Positions of tryptophan residues in the primary sequence are indicated as peaks. The mean gap length is presented in number of amino acid between tryptophan residues (± standard deviation) and are indicated on the right. Positions of other residues, such as glycine (Gly), asparagine (Asn), serine (Ser) and glutamic acid (Glu) with a similar representation in the same region are shown below for comparison. **(B)** Schematic representation of regularly spaced tryptophan residues within a W-rich region of diverse Ago-binding proteins. Scheme derived from Sheu-Gruttadauria and MacRae, 2018.

V. Relevance of the tryptophan-binding pockets of human Ago2 in the interaction with the T6B peptide and LegK1

Previous reports discovered three W-binding pockets clustered together in a small region near the bottom of the Ago2 PIWI domain (Figure S2.7) (Schirle and MacRae, 2012; Sheu-Gruttadauria and MacRae, 2018). These studies revealed that disabling individual or two W-binding pocket(s) was not sufficient to abolish the ability of the ABD of TNRC6B to bind Ago2 (Sheu-Gruttadauria and MacRae, 2018). Considering that any single pocket is sufficient to maintain the interaction, we decided to generate an Ago2 pocket dead mutant (Ago2-PD), which is disabled for the three W-binding pockets. Importantly, we found that the Ago2-PD mutant, which has never been generated and characterized so far, was no longer able to interact with the T6B peptide (Figure 2.4). The disrupted ability of Ago2-PD to bind to T6B supports previous observations (Schirle and MacRae, 2012; Sheu-Gruttadauria and MacRae, 2018), and provides evidence that the three W-binding pockets are critical for the interaction of Ago2 with an experimentally validated W-containing peptide. In addition, preliminary data revealed that the Ago2-PD mutant was similarly compromised in its ability to bind LegK1 (Figure 2.4). This suggests that LegK1 uses these W-binding pockets to interact with human Ago2, although additional independent experiments will be needed to confirm this finding. We have noticed, however, that the three combinatorial mutations in the PIWI domain of Ago2 resulted in a reduced molecular weight of the mutant compared to the wild-type protein by Western blot analyses (Figure 2.4). This phenomenon might be caused by altered post-translational modifications of the Ago2-PD mutant compared to the wild-type Ago2 protein. Accordingly, several ubiquitylation sites have been identified by mass spectrometry around the mutated residues, such as lysine residues 550, 566 downstream and 720, 726 upstream (Figure 3.3) (Akimov *et al.*, 2018; Udeshi *et al.*, 2013). Many phosphorylation sites have also been identified on the Ago2 protein (Figure 3.3) (Lopez-Orozco *et al.*, 2015; Quévillon Huberdeau *et al.*, 2017; Rüdel *et al.*, 2011), and therefore the three point mutations may also prevent interactions with kinases and thus alter the phosphorylation status of Ago2. In addition, we cannot exclude that the three point mutations alter the folding of human Ago2, thereby subjecting the protein to hydrolysis. Additional experiments, including the analysis of Ago2-PD post-translational modifications by mass spectrometry will thus be needed to better characterize this Ago2 mutant version.

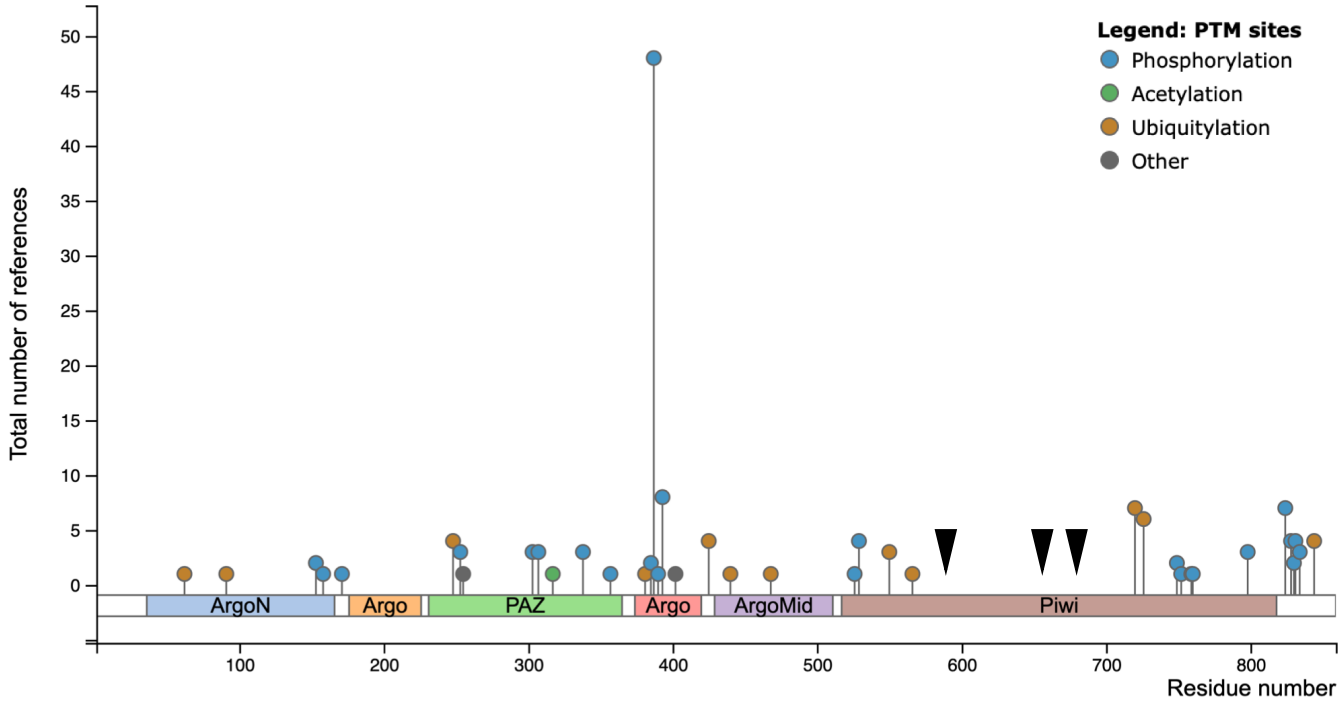

Figure 3.3. Schematic representation of post-translational modification sites at human Ago2 protein.
Positions of the different post-translational modification (PTM) sites previously described in the literature are indicated. The three point mutations performed to construct the Ago2-PD mutant are indicated by the black arrows. Scheme derived from https://www.phosphosite.org.

The molecular characterization of the three W-binding pockets has revealed a pocket preference for the tryptophan residues in TNRC6B (Sheu-Gruttadauria and MacRae, 2018). This suggests that the three W-binding pockets are not fully redundant with each other, even if each pocket is able to interact with multiple different tryptophan residues (Sheu-Gruttadauria and MacRae, 2018). Since LegK1 possesses two functional W-motifs in its kinase domain, it will be interesting to investigate which W-binding pockets can be used by each W-motifs. In addition, it will be important to investigate whether LegK1 could outcompete GW182/TNRC6 proteins for Ago2 binding, thereby preventing the recruitment of downstream accessory proteins required for miRNA-mediated gene silencing. To test these hypotheses, we intend to use a BLI approach to quantify the interaction i) between LegK1 and the different W-binding disabled pockets, namely the Ago2-P590G, -K660S or -R688S mutant versions, and ii) between the T6B peptide and Ago2 in the presence of the wild-type version of LegK1 or the single or double mutant versions in W283 and/or W293 residues. Finally, we intend to co-crystalize LegK1 and human Ago2, notably to better appreciate the interaction interfaces between the W283 and W293 residues of LegK1 and the three W-binding pockets of Ago2.

VI. COULD LEGK1 ADDITIONALLY USE ITS FUNCTIONAL W-MOTIFS TO PHYSICALLY INTERACT WITH DEADENYLASE CCR4-NOT AND PAN2-PAN3 COMPLEXES?

Besides their ability to bind Ago proteins, GW182/TNRC6 proteins can interact with deadenylase complexes through W-motifs, which are mainly located in their C-terminal silencing domains (contrary to the above mentioned W-motifs found in the N-terminal ABD domain of GW182/TNRC6 proteins) (Figure 3.4A) (Braun *et al*., 2011; Chekulaeva *et al*., 2011; Christie *et al.*, 2013; Fabian *et al*., 2011; Huntzinger *et al*., 2013). It has also been reported that GW182/TNRC6 proteins directly bind PAN3 and NOT1/NOT9 proteins, which are part of PAN2-PAN3 and CCR4-NOT deadenylase complexes, respectively, and are both critical for miRNA-mediated gene silencing (Figure 3.4B-C) (Braun *et al.*, 2011; Chen *et al.*, 2014). Characterization of these interactions indicates that glycine/serine/threonine-tryptophan (G/S/TW) or tryptophan-glycine/serine/threonine (WG/S/T) motifs function by recruiting components of the two deadenylation complexes (Chekulaeva *et al*., 2011; Huntzinger *et al*., 2013). As observed at the W-motifs required for Ago-binding, the tryptophan to alanine substitutions in the M2 region of the TNRC6C silencing domain were found to abolish the binding of TNRC6C to PAN3, indicating that this region is essential for TNRC6C-PAN3 interaction (Christie *et al*., 2013). In addition, the authors reported the presence of a hydrophobic W-binding pocket inside PAN3 pseudokinase, which ensures the binding of PAN3 to TNRC6C (Christie *et al.*, 2013). Regarding the second complex, it was shown that both the N-terminal and C-terminal domains of GW182/TNCR6 proteins recruit CCR4-NOT complex (Chekulaeva *et al.*, 2011). In a more detailed analysis, the authors showed that both domains also contribute to the recruitment of CCR4–NOT complex through W-motifs (Chekulaeva *et al.*, 2011). In particular, two distinct sequences allow the interactions of TNRC6A silencing domain (C-terminal) with NOT1, corresponding to CCR4-interacting motifs (CIMs) 1 and CIM-2 (Fabian *et al.*, 2011; Huntzinger *et al.*, 2013). Interestingly, the LWG triplet repeats in the CIM-2 (C-terminal domain) of GW182 was found essential for the interaction with NOT1 and for the deadenylation of target RNAs (Fabian *et al.*, 2011). By using a crystal structure analysis, two W-binding pockets in NOT9, another component of CCR4–NOT complex, were also reported to be important for the interaction with human TNRC6A and TNRC6C (Chen *et al.*, 2014). In addition, the distances between the two bound tryptophan residues was found similar to what has been previously described in the Ago2 W-binding pockets (Schirle and

MacRae, 2012; Sheu-Gruttadauria and MacRae, 2018). Therefore, this spatial arrangement is a shared feature between W-binding pockets in Ago2 and NOT9, which is essential to bind adjacent tryptophan residues. Collectively, these findings indicate that W-motifs are important for the binding to both Ago proteins and deadenylation factors. Therefore, they represent critical residues for recruiting diverse machineries required for RNAi. Importantly, the two W-motifs mentioned above, *i.e.* S/T(G)W and LWG, correspond to the two W-motifs identified in LegK1 (Figure 2.2, Table S2.2). Indeed, both the first motif, W283; DVWSTG and the second, W293; LWGD are suitable for the above-mentioned criteria. These findings suggest that LegK1 may additionally interact via these two W-motifs with deadenylation complexes. If the suggested mechanism holds true, LegK1 would be able to act at the RISC level by both interacting with Ago proteins, but also with PAN2-PAN3 and CCR4-NOT complexes. This would be consistent with the fact that LegK1 can interact with DDX6, a direct partner of NOT1 (Chen *et al.*, 2014). This yet-speculative scenario would be particularly relevant to achieve a robust suppression of RNAi activity as observed on the three silencing reporter systems used in this study.

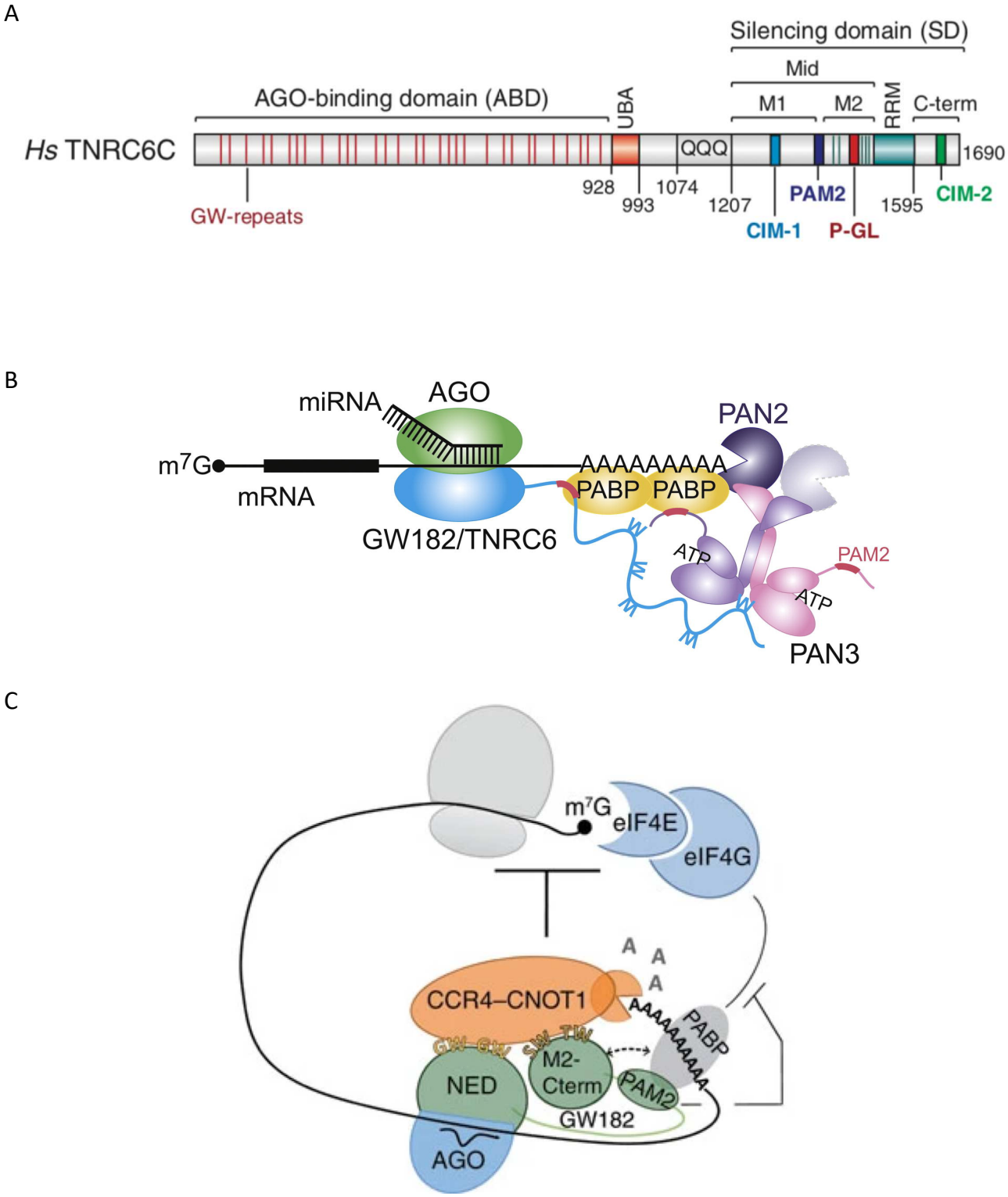

Figure 3.4. Molecular interactions between GW182/TNRC6 proteins and deadenylase complexes.
(A) Domain organization of human TNRC6C. ABD; Ago-binding domain, UBA; ubiquitin associated-like domain, QQQ; region rich in glutamine, Mid; middle region containing the PAM2 motif (dark blue), which divides the Mid region into the M1 and M2 regions, RRM; RNA recognition motif, C-term; C-terminal region, SD; silencing domain. Amino acid positions at domain boundaries are indicated below the protein outlines. The position of the conserved CIM-1, CIM-2 and P-GL motifs are indicated. Vertical red lines indicate the positions of GW repeats (referred to as W-repeats). Vertical green lines indicate the positions of tryptophan residues in the M2 region that are involved in NOT1-binding. Scheme derived from Huntzinger *et al*., 2013. **(B)** Schematic representation describing the interactions between GW182/TNRC6 and the PAN2-PAN3 deadenylation complex. Scheme derived from Christie *et al*., 2013. **(C)** Schematic representation of the interactions between GW182/TNRC6 and the CCR4–NOT deadenylation complex. Scheme derived from Chekulaeva *et al*., 2011.

VII. THE CATALYTIC ACTIVITY OF LEGK1 IS ESSENTIAL FOR RNAI SUPPRESSION, BUT IS NOT REQUIRED FOR AGO2 PHOSPHORYLATION

Using two different silencing reporter systems, we found that the catalytically inactive LegK1 mutant version was fully impaired in its ability to trigger RNAi suppression (Figure 2.2). However, this mutant was unaltered in its capacity to bind Ago1, Ago2, Ago4, PABPC1 and DDX6 in human cells (Figure 2.3). Given that LegK1 directly binds human Ago2, we wondered whether this bacterial effector could directly phosphorylate Ago2 to alter its functions. Nevertheless, we did not observe any change in the phosphorylation status of human Ago2 in the presence of LegK1 (Figure 2.7), indicating that Ago2 is not a substrate of LegK1. In addition, we provided evidence that the triple W-motifs mutant of LegK1 was not only impaired in its ability to bind RISC factors, but also to phosphorylate its known IκBα substrate (Figures 2.3, S2.9). These results indicate that disabling the three W-motifs of LegK1 compromises its catalytic activity. Therefore, it is currently difficult to pinpoint which of the two activities –Ago-binding *vs.* kinase activity– are responsible for RNAi suppression (see the following section for more details). Thus, at the time being, it is still possible that LegK1 suppresses RNAi only through its kinase activity or additionally through its Ago-binding platform. Regardless of the scenario involved, our results suggest that LegK1 must phosphorylate other RNAi component(s) than Ago2 and/or proteins that can indirectly regulate RNAi to achieve efficient suppression of miRNA- and siRNA-guided gene silencing. It will thus be important to further conduct a phospho-proteomic analysis to identify the whole set of host cellular substrates of LegK1, and subsequently assess whether any of these targets could contribute, directly or indirectly, to miRISC functions.

VIII. Relationship between the Ago-binding platform and the kinase activity of LegK1

The two W-motifs of LegK1, allowing the binding to human Ago proteins, are located in the kinase domain of this bacterial effector. Importantly, we found that point mutations in the three tryptophan residues resulted in a complete loss of the kinase activity of LegK1 (Figure S9). Therefore, we cannot uncouple the catalytic activity from the Ago-binding functions of this bacterial effector using this triple mutant version. Nevertheless, we observed that individual mutations in the W-motifs (LegK1-W283F and -W293F) exhibit functional kinase activity *in vitro* (Figure S2.9). These observations suggest that these two tryptophan residues unlikely alter the folding of LegK1, and thus its catalytic activity. We next performed a homology-based modelling analysis of LegK1 by selecting the most related kinases, whose crystal structures have been resolved (Figure 3.5). Using this approach, we noticed that the W283 residue and its surrounding amino acids are rather conserved across these kinases (Figure 3.5A). By contrast, the region corresponding to the W293 residue exhibits sequence variation at the position of the tryptophan and its surrounding residues (Figure 3.5A), indicating that this region is less conserved across kinases. Furthermore, we found that the W283 residue is located on a helix in a buried region of the protein, while the W293 residue is more exposed at the protein surface, even if it remains partially hidden (Figure 3.5). These preliminary observations suggest that the W283 residue of LegK1 is less likely to bind the W-binding pockets of Ago proteins compared to W293 residue in native conditions. However, the co-crystallization of LegK1 with Ago2 will be necessary to raise more accurate conclusions on the spatial arrangement of the W-motifs of LegK1 relative to Ago2 interaction interfaces.

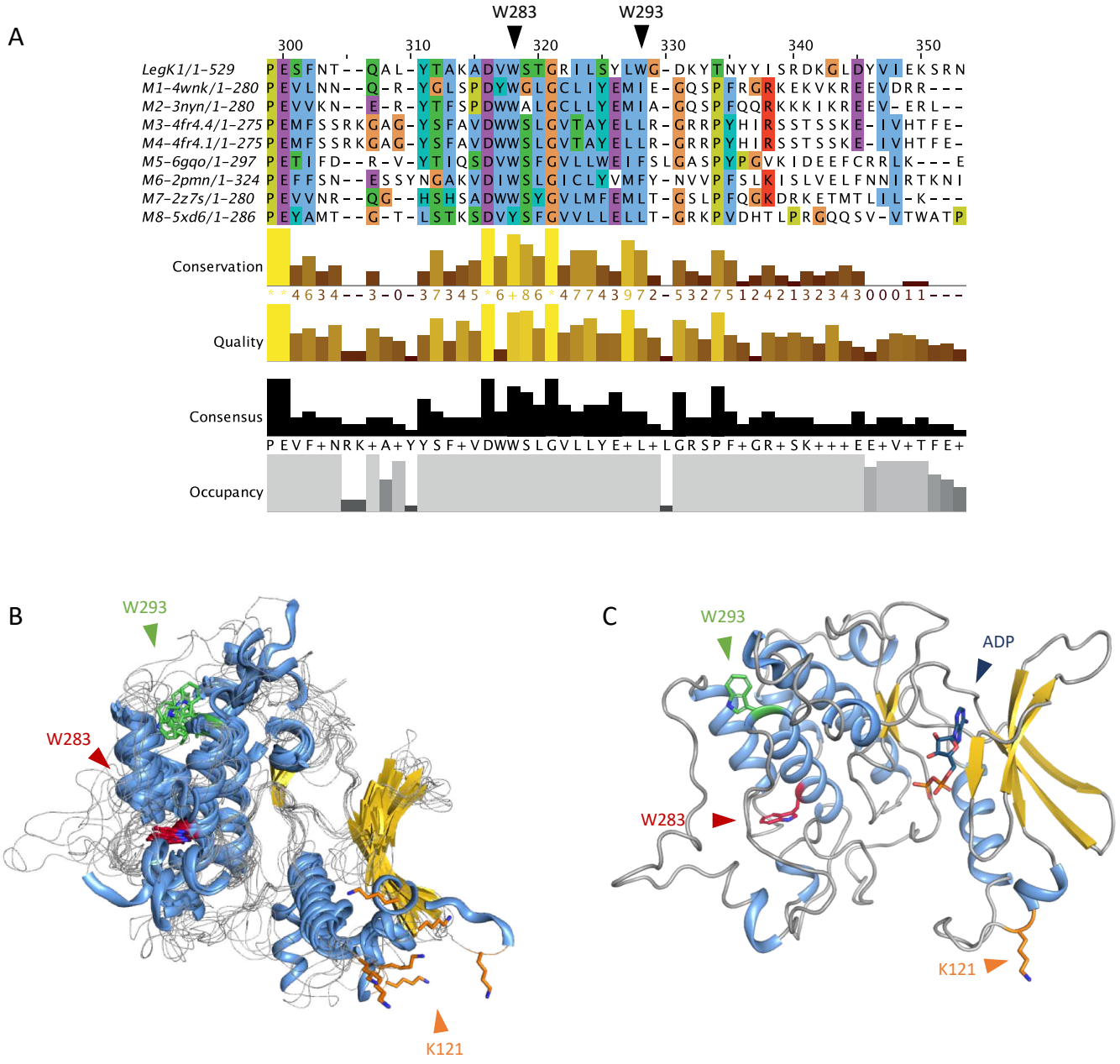

Figure 3.5. Homology-based modelling of the LegK1 structure.
(A) Alignment of homolog kinase protein sequences to LegK1 around the two functional W-motifs. A selection of 8 templates defined as monomers in their oligomeric state was performed from SWISS-MODEL server (Biozentrum, Basel). A cut-off on the GMQE score (Global Model Quality Estimate) greater than 0.28 has been applied. The two tryptophan W283 and W293 residues are depicted by a black arrow above the LegK1 protein sequence. **(B)** Superposition of cartoon representation of a multiple LegK1 homology-models based on the structure of 8 homolog kinases. The superposition has been carried out with the PyMOL software (PDB ID: 4WNK, 3NYN, 4FR4 chain D, 4FR4 chain A, 6GQO, 2PMN, 2Z7S, 5XD6). The position of residues corresponding to the W283 (red), W293 (green) and K121 (orange) residues on each model have been indicated by an arrow. **(C)** Cartoon representation of a LegK1 homology-model based on the structure of the human serine/threonine-protein kinase 32A PDB (ID: 4FR4). The residues corresponding to the W283 (red), W293 (green), K121 (orange) of LegK1 and the ADP molecule are depicted by an arrow.

To further study in more depth the relationship between the Ago-binding domain and the kinase, several resources will be generated and characterized molecularly. First, because single W283F and W293F mutants maintain a functional kinase activity (Figure S2.9), we will investigate whether these mutants could be impaired in Ago-binding as well as in RNAi suppression. This analysis will not only include the W293F mutation, but also the W293A mutation, which was found to abolish the interaction with the four human Ago proteins in our peptide pull-down experiments (Figure 2.5). Second, since mutation in a single functional tryptophan residue from tandemly organized W-repeats is often not sufficient to abolish the interaction between W-rich proteins and Ago proteins –as previously discussed–, we will generate a W283F/W293A double mutant of LegK1 and perform similar assays as with the single W283F and W293A mutants. The latter strategy should therefore maximize our chance to abolish the interaction between LegK1 and Ago proteins, while possibly maintaining an unaltered kinase activity of the bacterial effector. If this is the case, this would allow us to uncouple the two functions and therefore directly assess the impact of the Ago-binding platform of LegK1 on its RNAi suppression activity. By contrast, if the kinase activity of this double mutant is abolished, as observed with the triple W-motif mutants of LegK1, our results will suggest either that the two activities are tightly interconnected or that the combined W283F and W293A mutations possibly alter the protein folding of LegK1.

IX. THE TWO FUNCTIONAL W-MOTIFS OF LEGK1 ARE EMBEDDED IN A STRUCTURED KINASE DOMAIN, A FEATURE THAT IS NOT FOUND IN CHARACTERIZED W-RICH PROTEINS

Unexpectedly, the two functional W-motifs of LegK1 are not positioned in a disordered region, such as the ones found in the unstructured N-terminal domain of GW182/TNRC6 proteins (El-Shami *et al.*, 2007; Pfaff *et al.*, 2013; Takimoto *et al.*, 2009; Till *et al.*, 2007; Zielezinski and Karlowski, 2015). Instead, they were found embedded in the kinase domain of LegK1. Furthermore, by using the above predicted model structure of the kinase domain of LegK1 obtained using related kinase structures available in databases (Figure 3.5 and prediction from I-TASSER, https://zhanglab.dcmb.med.umich.edu/I-TASSER/), we found that the two functional tryptophan residues appear to be part of a single helix. Collectively, these observations suggest that functional W-motifs are not only present in unstructured domains, as

previously thought, but could also be part of structured protein segment. Our data imply to revisit the possible functions of proteins exhibiting predicted Ago-binding platforms in structured domains, such as kinase domains, which were previously retrieved through *in silico* analyses, with high Wsearch score, but not characterized molecularly (Zielezinski and Karlowski, 2015, 2017).

X. THE W283 MOTIF OF *L. PNEUMOPHILA* EXHIBITS NATURAL VARIATION ACROSS *LEGIONELLA* SPECIES, WHILE THE W293 MOTIF OF *L. PNEUMOPHILA* IS CONSERVED ACROSS THESE BACTERIA

The determine whether the two functional W-motifs and their surrounding residues could be conserved across *Legionella* species, we retrieved the whole set of LegK1 ortholog protein sequences and aligned them between each other. By doing so, we noticed that the W283 motif is conserved across *L. pneumophila* strains, *L. norrlandica* and *L. waltersii*, whereas it exhibits natural variation across the remaining *Legionella* species (Figure 2.6). Interestingly, these sequence polymorphisms are notably found at the residues corresponding to the *L. pneumophila* W283, which display a substitution from tryptophan to tyrosine (Figure 2.6). According to the comparative analysis from Wsearch algorithm (Zielezinski and Karlowski, 2015), a tyrosine residue lacks the properties required for Ago-binding, being even determined as one of the least likely residue to compose Ago-binding platforms (Figure 3.1). This observation suggests that a tryptophan to tyrosine substitution is potentially not competent for Ago-binding. To further test this assumption, we have synthesized a biotinylated peptide carrying the tyrosine residue along with surrounding residues from the *L. quateirensis* strain, which corresponds to the homologous sequence from the *L. pneumophila* W2 peptide carrying the W283 residue (Figure 2.5). We will further test, using the same pull-down peptide experiment, whether this *L. quateirensis*-derived peptide could be altered in Ago-binding. In contrary to the W283 motif, we found that the region corresponding to the *L. pneumophila* W293 motif was extremely conserved across all the ortholog LegK1 protein sequences analyzed, which was also the case of surrounding amino acids (Figure 2.6). We therefore propose that this conserved W-motif likely act as a functional Ago-binding platform across all the *Legionella* species/strains analyzed. However, as discussed above, the presence of the tandemly repeated W-motifs is likely necessary to ensure a tight association with Ago proteins,

while individual W-motif are unlikely sufficient to ensure robust LegK1-Ago interactions. Based on these observations, we speculate that *Legionella* species/strains that have preserved both W-motifs are likely the most competent for RNAi suppression. It would therefore be interesting to clone representative LegK1 orthologous sequences, encoding effector proteins with the two intact W-motifs or a single W motif corresponding to the W293 of *L. pneumophila*, and assess their ability to suppress RNAi in human cells using our silencing reporter systems. It would also be informative to collect clinical data of these overall *Legionella* strains and determine whether the bacteria carrying the two intact W-motifs could be more associated with clinical infections compared to the other strains, which have maintained solely one intact W-motif. Furthermore, given that the *L. pneumophila* (Paris) *legK1* deleted strain was found impaired in its ability to replicate in human macrophages at an early stage of infection (Figure 2.8), it would also be interesting to assess whether the *Legionella* strains/species expressing LegK1 proteins carrying a single intact W-motif could also exhibit a delay in intracellular replication compared to the *Legionella* strains/species expressing LegK1 proteins with the two intact W-motifs.

XI. DOES LEGK1 ACT AS A MOLECULAR MIMICRY OF HOST KINASES TO SUPPRESS RNAI?

Bacteria can express eukaryotic-like proteins to subvert diverse signaling networks. This phenomenon is particularly widespread in the case of *Legionella* species, which were found to encode more than 200 eukaryotic-like proteins from their genome sequences (Gomez-Valero *et al*., 2019). This process is likely essential for bacterial virulence, as it allows the subversion of specific host cellular functions, a concept that has been referred to as "molecular mimicry" (Mondino *et al*., 2020b). For example, the sequencing of the *L. pneumophila* strain Paris genome unveiled the presence of proteins carrying eukaryotic-like kinase domains, which were generally absent from prokaryote genomes. These *L. pneumophila* genes encode serine/threonine protein kinases, termed LegK1-4, one tyrosine kinase, LegK5, two structural homolog to kinases, LegK7 and SidJ and atypical protein kinase, Lpg2603 (Cazalet *et al.*, 2004). Some of these eukaryotic-like proteins have been well-characterized. LegK7 was found to functionally mimic the host Hippo kinase MST1/2 by phosphorylating MOB1A, thereby hijacking the conserved Hippo signaling pathway (Lee and Machner, 2018). The crystal

structure of LegK7-MOB1A complex revealed that the N-terminal half of LegK7 is structurally similar to eukaryotic protein kinases (Lee *et al*., 2020). Indeed, the authors provide evidence that LegK7 forms a complex with MOB1A in order to use the N-terminal extension of MOB1A as a binding platform for the recruitment of downstream substrates, to exploit host Hippo signaling. Lpg2603 was shown to require eukaryote-specific host signaling molecule inositol hexakisphosphate for its activation, indicating a host adaptation. Finally, LegK1 was determined to activate the NF-κB pathway by mimicking host inhibitor of IKKs (Ge *et al*., 2009). In an unstimulated cell condition, NF-κB hetero- and homodimers are inhibited by interaction with IκB family proteins. NF-κB signaling is induced when IKKs are activated, leading to the phosphorylation of IκB, which results in its ubiquitination and subsequent proteasomal degradation (Mulero *et al*., 2019). NF-κB is then translocated into the nucleus to mediate transcription of a large number of genes. LegK1 was found to phosphorylate serine residues of the IκB, thereby mimicking IKKs to activate NF-κB signaling. The binding of LegK1 to Ago proteins may outcompete essential endogenous W-rich components of the miRISC, such as GW182/TNRC6 proteins. In addition, under the assumption that LegK1 can also interact with deadenylation complexes, we can imagine that LegK1 could also mimic host HIPK family kinases, that are known to bind and inhibit the function of the CCR4-NOT complex (Rodriguez-Gil *et al*., 2016). Alternatively, LegK1 could mimic as yet-unknown endogenous amoeba and human kinases, which are essential to negatively regulate miRISC functions. We are thus anticipating that the use of LegK1 as a molecular probe of host cellular functions, will be instrumental to better understand the endogenous mechanisms of miRISC regulation.

XII. LEGK1 PROMOTES INTRACELLULAR REPLICATION OF *L. PNEUMOPHILA* IN BOTH AMOEBA AND HUMAN MACROPHAGES

The long-lasting coevolution of *Legionella* in a wide range of host cells, including numerous amoeba species and ciliate protozoa, has shaped *Legionella* genomes (Burstein *et al*., 2016; Gomez-Valero *et al*., 2019). It has notably recently been shown that the combined selective pressures of different amoebal hosts drive the evolution of *Legionella* species (Park *et al*., 2020a). The presence of a whole repertoire of eukaryotic-like proteins indicate that these proteins were acquired through horizontal gene transfer from protist organisms (Cazalet *et al*., 2004; de Felipe *et al.*, 2005b; Gomez-Valero *et al.*, 2014, 2019; Lurie-Weinberger *et al*., 2010). These findings lead to the suggestion that LegK1 originates from an amoebal host acquisition. The sophisticated strategies that have evolved *Legionella* species to survive within protozoan are also required for some of these bacteria to replicate within human phagocytic cells. Hence, we can assume that the mechanisms used by LegK1 to promote pathogenicity are effective in both amoeba and human macrophages. Consistent with this idea, we found that the *L. pneumophila* Δ*legK1* strain was compromised in its ability to replicate in both amoebal and human macrophage cells at an early stage of infection (Figure 2.8). These data indicate that LegK1 contributes to the intracellular growth of *L. pneumophila* in these host cells. To further confirm these results, and to assess the possible role of the kinase activity and the Ago-binding platform of LegK1 in this process, we are planning to express *in trans* either a wild-type copy of LegK1 under its native promoter or different point mutants of LegK1 in the Δ*legK1* strain for complementation assays. More specifically, we intend to express the kinase dead LegK1-KA mutant, but also a W-motif mutant of LegK1 that will ideally be found impaired in its ability to bind Ago proteins but that will still be active in phosphorylating its substrates –discussed above but not yet identified–. The proposed functional assays will be essential to verify a role for LegK1 in promoting *L. pneumophila* intracellular replication in host cells, but also to assess the biological relevance of the kinase and Ago-binding activities of LegK1 in its virulence function.

XIII. THE ABILITY OF LEGK1 TO SUPPRESS RNAI IS LIKELY THE PRIMARY VIRULENCE FUNCTION OF THIS BACTERIAL EFFECTOR

Although it is generally thought that amoeba lack innate immunity, they may still have a primitive immune system to discriminate between pathogenic and non-pathogenic bacteria, which is thought to be mediated by a MAPK pathway (Escoll *et al*., 2014). This signaling pathway appears to be directly involved in the modulation of immune-responsive genes such as TirA, which encodes a protein with similarities to mammalian Toll-like receptors (TLRs) (Chen *et al.*, 2007; Li *et al*., 2009). Interestingly, it has also been reported that some amoebal genes encode proteins with homology to known PRRs (Cosson and Soldati, 2008). Nevertheless, the caspase-mediated apoptosis and the NF-κB-dependent pathways, two immune pathways that have a well-established importance in *L. pneumophila*-infection in mammalian macrophages, seem not conserved in amoeba. This is supported by an *in silico* analysis aiming to retrieve conserved protein domains involved in mammalian immune processes in the genomes of *L. pneumophila* unicellular host organisms, including *Dictyostelium discoideum*, *Acanthamoeba castellanii*, *Naegleria gruberi* and the ciliated protozoa *Tetrahymena thermophila* (Table 3.1) (Escoll *et al.*, 2014). Interestingly, none of the canonical NF-κB-related domains, including IPT NFKB, Uban and RHD-n_c-Rel, were found in these genome sequences (Table 3.1). Despite the apparent lack of NF-κB-related pathway in these *L. pneumophila* natural host organisms, this bacterium was shown to activate the NF-κB pathway as well as some NF-κB-controlled anti-apoptotic genes, rendering infected macrophages hypo-responsive to apoptotic stimuli (Abu-Zant *et al.*, 2007; Bartfeld *et al.*, 2009; Losick and Isberg, 2006). Among the type IV-secreted effectors involved in this process, LegK1 and LnaB were shown to activate an anti-apoptotic and protective NF-κB-immune response, which appears to be required for intracellular replication (Ge *et al.*, 2009; Losick *et al*., 2010). The strong ability of LegK1 to suppress RNAi activity in human cells, along with the lack of NF-κB-related pathway in natural host organisms of *L. pneumophila*, suggest that LegK1 has more likely been acquired from amoeba to suppress RNAi in the first place. This assumption is supported by the fact that many RNAi components are present in the *Entamoeba histolytica* genome (Zhang *et al.*, 2008, 2011). Even if *E. histolytica* lacks a canonical Dicer, which contains two RNase III domains, it contains a gene encoding a single RNase III domain (Zhang *et al*., 2008). The RNAi components found in the *E. histolytica* genome additionally

include three *Ago* genes, which encode proteins composed of both PAZ and PIWI domains (Zhang *et al*., 2008). Moreover, one of these proteins was shown to associate with 27nt small RNAs, suggesting that this factor could act as a canonical silencing effector. The genome of *E. histolytica* also encodes one RNA-dependent RNA polymerase (RdRP) and a protein with a partial RdRP domain (Zhang *et al*., 2011). Such genome analysis was also performed with the Drosha and its partner DGCR8 sequences, but no homologs have been identified in the *E. histolytica* genome. The authors also characterized the endogenous small RNA repertoire and found multiple small RNA species (16nt, 22nt and 27nt) (Zhang *et al*., 2008). Furthermore, high-throughput sequencing revealed the presence of miRNAs in the social amoeba *Dictyostelium discoideum*, which were produced by one of the two Dicer-like proteins, namely DrnB (Avesson *et al*., 2012; Hinas *et al*., 2007; Liao *et al*., 2018; Meier *et al.*, 2016). In association with the dsRNA binding protein RbdB, it has been proposed that the DrnB-RbdB complex constitutes the microprocessor complex in *D. discoideum* (Avesson *et al.*, 2012; Liao *et al.*, 2018; Meier *et al.*, 2016). Interestingly, the genome of *D. discoideum* is composed of five genes encoding Ago-like proteins of the PIWI clade, *agnA* to *agnE* (Meier *et al.*, 2016). Previous experiments have shown that AgnA is required for the production of siRNAs (Boesler *et al*., 2014). Overall, these studies further support our hypothesis that the primary function of LegK1 is to suppress RNAi, rather than activate the NF-κB pathway. This hypothesis is further supported by the fact that the human Ago4 protein was found here as a major genetic target of LegK1 during infection (Figure 2.9). Given that we also observed a delay in the replication of the *Lpp* Δ*legK1* strain in *A. castellanii*, which is deprived of NF-κB-related component, we propose that this phenotype is also caused by the ability of LegK1 to suppress RNAi. To further test this hypothesis, we have acquired different *D. discoideum* Ago mutants (collaboration with Fredrik Söderbom Lab, Uppsala, Sweden). We will first test whether the intracellular growth of the *Lpp* Δ*legK1* could also be altered in a wild-type *D. discoideum*, as observed in *A. castellanii*, and further assess whether such growth defect could be potentially rescued in any of the Ago-defective mutants.

Protein domain	Dictyostelium discoideum	Acanthamoeba castellanii	Tetrahymena thermophila	Naegleria gruberi	Examples of proteins in higher eukaryotes containing the corresponding described domain	Role in immunity of example proteins
WRKY	DDB_G0275267	ACA1_216030 ACA1_291040	–	-	WRKY transcription factor protein 1	Pathogen defense (plants) (Eulgem et al. 1999)
TIR	DDB_G0289237	-	-	-	TLRs	PRR (Takeda et al. 2003)
CD36	DDB_G0267406 DDB_G0267440 DDB_G0287035	ACA1_126030	TTHERM_00371120 TTHERM_00238900 TTHERM_00046450	-	Scavenger receptor class B member 1 (SCARB1, CD36L1)	PRR (Baranova et al. 2008)
Caspase	DDB_G0277689 DDB_G0293196	ACA1_087710	-	-	Caspase-1	IL-1β maturation (Thornberry et al. 1992)
MATH-TRAF	DDB_G0272340 DDB_G0274899 DDB_G0280369 DDB_G0285149	-	TTHERM_00476630	NAEGRDRAFT_72663	TNF receptor-associated factor-6 (TRAF6)	TLR/IL-1 signaling (Takeda et al. 2003)
Death Domain	-	-	-	-	MyD88	TLR/IL-1 signaling (Takeda et al. 2003)
IPT_NFKB	-	-	-	-	p65 subunit of transcription factor NF-κB	Transcription of immune response genes (Gilmore and Wolenski 2012)
Uban	-	-	-	-	NF-κB modulator NEMO	NF-κB signaling (Gilmore and Wolenski 2012)
RHD-n_c-Rel	-	-	-	-	NF-κB c-Rel	NF-κB signaling (Gilmore and Wolenski 2012)
LBP_BPI_CETP	DDB_G0271242 DDB_G0288097	ACA1_143930 ACA1_252520 ACA1_208310 ACA1_382630 ACA1_281820 ACA1_234080 ACA1_368250 ACA1_382580	TTHERM_00823420 TTHERM_01287960 TTHERM_00137710 TTHERM_00190810 TTHERM_00433940 TTHERM_00433910	NAEGRDRAFT_78340 NAEGRDRAFT_47514 NAEGRDRAFT_82253 NAEGRDRAFT_76153	Lipopolysaccharide-binding protein (LBP)	PRR (Jack et al. 1997)
PG_binding_1	DDB_G0280311 DDB_G0286137	ACA1_152930	TTHERM_00220760	-	Matrix metalloproteinase-3 (Stromelysin 1, MMP3)	Immunity to intestinal bacteria (Li et al. 2004) Degradation of IL-1β (Ito et al. 1996)
Gal_Lectin	-	ACA1_126170 ACA1_184380 ACA1_030220 ACA1_201210 ACA1_318670 ACA1_029840 ACA1_047640 ACA1_047640 ACA1_033480 ACA1_059570	-	NAEGRDRAFT_72022	D-galactoside/L- rhamnose binding SUEL lectin protein	PRR (invertebrates) (Watanabe et al. 2009)
GILT	-	ACA1_184120 ACA1_116130	-	-	Gamma-interferon-inducible lysosomal thiol reductase (GILT)	MHC Class II-restricted antigen presentation (Hastings and Cresswell 2011)
NRAMP	DDB_G0275815 DDB_G0276973	ACA1_225890	TTHERM_00680650 TTHERM_00691720 TTHERM_00697030	-	Natural resistance-associated macrophage protein 1 (Nramp1)	Resistance against intraphagosomal pathogens (Alter-Koltunoff et al. 2008)

Only species whose genome has been completely sequenced have been analyzed: *Dictyostelium discoideum*, *Acanthamoeba castellanii*, *Naegleria gruberi* and the ciliated protozoa *Tetrahymena thermophila*

Table 3.1. Proteins containing domains related to the human immune system from unicellular *Legionella* host organisms.
Analysis of conserved domains of proteins involved in mammalian immune responses in genome of *Dictyostelium discoideum*, *Acanthamoeba castellanii*, *Naegleria gruberi* and *Tetrahymena thermophila*. Table derived from Escoll *et al.,* 2014.

XIV. Occurrence and relevance of LegK1-triggered suppression of Argonaute activities during *L. pneumophila* infection of human macrophages

Throughout this study, we showed that the LegK1 effector is able to suppress the silencing of different RNAi reporter systems in human cells. We subsequently found that LegK1 directly interacts with human Ago2 *in vitro*, but also with Ago1, Ago2 and Ago4 in human cells (Figures 2.2, 2.3). Importantly, we also demonstrated that the growth defect of the *Lpp* Δ*legK1* strain was fully rescued in human macrophages depleted of Ago4 (Figure 2.9), uncovering both a physical and genetic interactions between LegK1 and human Ago4. These data also unveil a novel function of human Ago4 in antibacterial defense. However, it is currently unknown whether the ability of LegK1 to suppress RNAi is also achieved in the context of infection, and whether such phenomenon would be dependent on the targeting of human Ago4. To get a first insight into the possible role of LegK1 in suppressing RNAi during infection, we plan to use a HEK293 cell line expressing the FcγRII protein (gift from Craig Roy, New Haven, USA), as these cells efficiently internalize immunoglobulin G (IgG)-opsonized *L. pneumophila* (Arasaki and Roy, 2010). We will make use of this system, and of the silencing reporters that we have already used in this study, to investigate whether the *L. pneumophila* wild-type, Δ*legK1*, and a strain overexpressing LegK1 could interfere with the silencing of these RNAi reporters. It is noteworthy that this approach would be more complicated in THP-1 cells, which are more refractory to plasmid transfection. In addition, we plan to conduct proteome and transcriptome analyses in THP-1 macrophages infected with these *L. pneumophila* strains, coupled with a deep-sequencing of Ago4-loaded small RNAs. These unbiased approaches, will determine to which extend Ago4-dependent miRNA targets could be regulated by LegK1 during infection. These genomics analyses will also be informative to determine whether LegK1 could module pathways involved in key steps of infection, such as the evasion from the endocytic pathway and avoidance of vacuole acidification, remodeling of the *Legionella*-containing vacuole, recruitment of secretory vesicles, endoplasmic reticulum, polyubiquitinated proteins, mitochondria or ribosomes, or the modulation of host immune processes. Moreover, to further evaluate the relevance of Ago4 in antibacterial defense, we plan to overexpress Ago4 in HEK293 cell line expressing FcγRII before infecting with the wild-type *L. pneumophila* strain, and determine whether Ago4 overexpression could reduce the replication of this bacterium, as recently demonstrated in a

context of viral infection (Adiliaghdam *et al.*, 2020). However, because human Ago4 does not possess an endonuclease activity, we will not evaluate the impact of mutations in the predicted catalytic tetrad but, instead of mutations that are predicted to be important for the binding of Ago4 to small RNAs. Overall, the proposed experiments should allow us to better understand the impact of LegK1-directed RNAi suppression during pathogenesis and will be essential to better characterized Ago4 in antibacterial defense towards *L. pneumophila*.

XV. CROSSTALK BETWEEN RNAI AND CLASSICAL INNATE IMMUNE PATHWAYS

A mutual regulation of RNAi and interferon (IFN) response has been recently reported (Berkhout, 2018b; Ding *et al*., 2018; Maillard *et al.*, 2019; Takahashi and Ui-Tei, 2020). The IFN signaling was shown to inhibit RNAi through an interaction of a RIG-I-like receptors (RLRs) family protein, namely LPG2, with Dicer and its two modulators TRBP and PACT (Takahashi *et al*., 2018; David *et al.*, 2019; Miyamoto and Komuro, 2017; van der Veen *et al*., 2018). These molecular interactions inhibit the processing of dsRNAs, thereby reducing the production of siRNAs (David *et al.*, 2019; Miyamoto and Komuro, 2017; Takahashi *et al*., 2018; van der Veen *et al.*, 2018). Moreover, RNAi was found to be repressed shortly after viral infection through a poly-ADP-ribosylation of Ago2 and its associated proteins, which in turn promotes the expression of interferon-stimulated genes (ISGs) (Seo *et al.*, 2013). This suggests that an inhibition of Ago2-RISC activity could be causal for the stimulation of IFN signaling. Collectively, these studies suggest that a bi-directional crosstalk likely occurs between RNAi and IFN response, which appears to be regulated through protein-protein interactions between RLR and Dicer proteins (Takahashi and Ui-Tei, 2020). Consequently, active antiviral RNAi was observed only under specific cellular or experimental conditions, corresponding to infection of differentiated cells using viruses that are deprived of their VSRs, in pluripotent stem cells or in somatic cells that are deficient in IFN response (Li *et al*., 2013, 2016; Maillard *et al.*, 2013a, 2016; Qiu *et al.*, 2017; Zhang *et al.*, 2020). One reason to explain these observations is that the embryonic stem cells (ESCs) are known to be hypo-responsive to IFN (Takahashi and Ui-Tei, 2020), presumably to protect them from the cytotoxic effect of IFN. Although embryonic stem cells are hypo-responsive to IFN, they are highly resistant to viral infection, implying other defense mechanisms in place, including antiviral RNAi. Recently, an isoform of Dicer has been identified in mammalian stem cells, which encodes a Dicer protein

deprived of a segment within its N-terminal helicase domain (Poirier *et al*., 2021). This isoform, referred to as aviD, was found more effective in processing dsRNAs compared to the full-length Dicer protein (Poirier *et al*., 2021). This study therefore provides evidence that mammalian stem cells are equipped with a machinery adapted for antiviral RNAi.

While the ability of type II IFN (IFN-γ) to activate macrophages is known to be associated with antibacterial activity, studies have also ascribed antibacterial activity to type I IFNs (IFN-α/β) (Decker *et al*., 2005; Snyder *et al*., 2017). The production of type I IFN has notably been shown to be required for antibacterial immunity against *L. pneumophila* in mice (Lippmann *et al*., 2008, 2011; Opitz *et al*., 2006; Plumlee *et al*., 2009). By extrapolation, we can therefore assume that bacterial-triggered IFN-I activation could also negatively regulate RNAi activity during infection of macrophages with *L. pneumophila.* Although LegK1 was shown to activate NF-κB immune response, it seems not to interfere with the host MAPK (Erk1/2, JNK, and p38) and IFN signaling (Ge *et al*., 2009), suggesting that this effector unlikely suppresses RNAi by enhancing the latter pathway. Nevertheless, it will still be important to determine whether inactivation of the IFN-dependent immune pathway in THP-1 macrophages, for instance through inactivation of the IFN subunit receptor IFNAR1, could potentiate RNAi suppression eventually triggered by the *L. pneumophila* WT strain or a strain overexpressing LegK1. Furthermore, because the mouse Ago4 has recently been shown to promote IFN response during antiviral defense (Adiliaghdam *et al*., 2020), it will be important to assess whether the Ago4-dependent phenotypes observed in the context of *L. pneumophila* infection could be related to a misregulation of IFN signaling, either in the *ago4*$^{-/-}$ THP-1 line or upon overexpression of human Ago4 in the HEK293 cell line expressing FcγRII.

Although a mutual negative crosstalk between the IFN immune pathway and RNAi is now emerging, nothing is known about the relationship between the NF-κB immune pathway and RNAi. Because LegK1 has previously been reported to trigger a potent activation of NF-κB signaling (Ge *et al*., 2009), and because we found here that this effector concomitantly represses RNAi activity, these observations suggested that activation of the NF-κB signaling could be causal for the dampening of RNAi. To get some insights into this possibility, we used the siRNA-dependent *eGFP*-based reporter system in HEK293T cell line and further challenged these cells with TNFα or IL1β, which are known elicitors of NF-κB signaling. Although a marked phosphorylation of the serine 32 of IκBα was found in those conditions, which is consistent with an activation of NF-κB signaling by TNFα or IL1β, the reporter system

remained silenced (Figure S2.5). These results suggest that an activation of NF-κB signaling is not sufficient to suppress RNAi. To reinforce these results, and trigger NF-κB pathway in conditions that are comparable to the transfection of the LegK1 expressing vector, we are planning to repeat these assays upon transfection of a vector overexpressing Nod1, which has previously been shown to strongly activate NF-κB signaling (Bartfeld *et al.*, 2009). If the *eGFP*-based reporter system remains silenced in the latter condition, we will be able to safely conclude that activation of NF-κB signaling is not required for RNAi suppression. In addition, this result will suggest that LegK1-triggered activation of NF-κB signaling, in condition that are comparable to Nod1 overexpression, is unlikely causal for RNAi suppression. We also propose to repeat the LegK1-triggered RNAi suppression assays in the presence of well-characterized inhibitors of NF-κB signaling. The latter assay will be essential to precisely assess the role –if any– of LegK1-triggered activation of NF-κB signaling in RNAi suppression activity. To further investigate the possible crosstalk between NF-κB signaling and RNAi, we additionally propose to monitor the transcriptional regulation of RNAi factors upon activation of NF-κB signaling. This study will be particularly relevant at the level of Ago4 regulation, because this factor was found more expressed in immune-related cells (Figure S2.11) (Adiliaghdam *et al.*, 2020), which are hyper-responsive to NF-κB signaling. For example, it would be interesting to determine whether human Ago4 could possess NF-κB binding sites in its promoter region, as previously reported in the promoter regions of RNAi factors from different mosquito species (Campbell *et al.*, 2008).

XVI. COULD HUMAN CELLS MOUNT EFFECTOR-TRIGGERED IMMUNITY UPON PERCEPTION OF LEGK1?

L. pneumophila induces a sustained activation of NF-κB signaling in infected human macrophages (Abu-Zant *et al.*, 2007; Asrat *et al.*, 2014; Bartfeld *et al.*, 2009; Losick and Isberg, 2006; Shin *et al.*, 2008). Accordingly, the nuclear translocation of the subunit of the canonical form of NF-κB is detected in human cells at 3h post-infection with *L. pneumophila* (Abu-Zant *et al.*, 2007; Losick and Isberg, 2006). However, the activation of NF-κB signaling is reduced and remained just transient in response to the *L. pneumophila* Icm/Dot type IV secretion system (T4SS)-defective strain, indicating that type IV-secreted effectors from this bacterium are likely responsible for the sustained activation of NF-κB signaling in host cells (Abu-Zant *et al.*, 2007; Bartfeld *et al.*, 2009; Losick and Isberg, 2006). A biphasic immune response has therefore been proposed during *L. pneumophila* infection, which first relies on an early type IV-independent immune response, triggered by bacterial PAMPs detection, and subsequently on a type IV-dependent response, which is mediated by effectors at a later phase of the infection (Bartfeld *et al.*, 2009). It has also been proposed that the second NF-κB-dependent immune response could be potentiated by PAMP-triggered immune pathways (Shin *et al.*, 2008). Such dynamics of immune responses is reminiscent of the responses orchestrated by the plant immune system, composed of PAMP-triggered immunity (PTI), activated through the sensing of PAMPs by cell-surface PRRs, and effector-triggered immunity (ETI), activated upon perception of evolutionarily divergent pathogen effectors by intracellular NLRs (Yuan *et al.*, 2021a). Importantly, both PRRs and NLRs have recently been shown to exhibit a mutual potentiation of plant immunity, which was found necessary to mount effective resistance against a virulent *Pseudomonas syringae* strain (Ngou *et al.*, 2021; Yuan *et al.*, 2021b).

Several studies have attempted to identify *L. pneumophila* type IV-secreted effectors that are responsible for the activation of the second phase of NF-κB signaling during infection. Among which, the two effectors LnaB and LegK1 were found to trigger a potent activation of NF-κB signaling when expressed individually from human cells (Ge *et al.*, 2009; Losick *et al.*, 2010). This response is analogous to ETI triggered through the recognition of bacterial effectors by plant NLRs (Fontana *et al.*, 2011; Kufer *et al.*, 2019; Lopes Fischer *et al.*, 2020; Ngwaga *et al.*, 2021). Intriguingly, the type III-secreted effector HopT1-1 from the phytopathogenic *Pto* DC3000 strain, which directly binds Arabidopsis AGO1 and suppresses its RNA silencing and

immune-related functions through conserved W-motifs (Thiébeauld *et al.*, 2021), is also sensed by plant cells. This effector-detection process results in a potent ETI response that was found dependent on canonical NLR-mediated immune-signaling factors. Furthermore, the AGO1-binding platform of HopT1-1 was fully required for ETI activation, indicating that the RNAi suppression activity of this effector is directly coupled with ETI activation and sensed by host cells (Thiébeauld *et al.*, 2021, unpublished data). Similarly, it would be possible that the potent NF-κB signaling triggered by LegK1 in human cells, would simply results from the manifestation of an ETI response that would be triggered as a result of RNAi suppression. In this scenario, mammalian cells would have evolved a mechanism to sense LegK1-triggered suppression of Ago activities, and in turn activate a host counter-counter defense, akin to ETI. This mechanism would be reminiscent of the guard hypothesis, whereby human Ago proteins would be guarded by NLRs, which would mount ETI upon effector-mediated perturbation of Ago activities. To test this intriguing hypothesis, it will be interesting to investigate whether NLRs could be recovered from mammalian Ago complexes and further determine if any of these NLRs could be required for LegK1-induced ETI activation.

XVII. Role and regulation of human Argonaute proteins during bacterial infections

It is now well-established that mammalian miRNAs act as crucial regulators of cellular host-bacteria interactions by interfering with various conserved cellular processes (Figure 3.6) (Aguilar *et al*., 2019; Das *et al*., 2016; Maudet *et al*., 2014a; Zhou *et al.*, 2018). However, little is known about the role and regulation of the human miRNA machinery during host-bacteria interactions. To address this issue, a recent study has investigated the dynamics of subcellular localization of human Ago2 and its biological relevance at an early stage of *Shigella* infection (Filopon, Schiavolin, Bonnet *et al*., *in preparation*). *Shigella* is known to induce its host cell internalization in a macropinocytic-like process, and rapidly escapes from its phagocytic vacuole to reach the cytosol, which represents its main replicative niche. Importantly, the authors found that *Shigella* triggers a rapid and transient recruitment of human Ago2 at bacterial invasion sites prior vacuolar rupture. More specifically, the recruitment of Ago2 was found at the level of macropinosomes, whose physical contact with the *Shigella*-containing vacuole is required for efficient and rapid vacuolar rupture (Chang *et al.*, 2020; Weiner *et al.,* 2016). Furthermore, it was found that human Ago2, as well as the miRNA factors TNRC6A and Drosha, positively regulate *Shigella*-induced vacuolar rupture. This phenotype additionally required the phosphorylation at serine 387 of Ago2, but also the W-binding pockets of Ago2, supporting a role for an assembled Ago2-miRISC in this process. Importantly, a pre-loaded Ago2-miRISC was further shown to directly target *RhoGDIα* mRNAs, which encodes a well-characterized negative regulator of RhoGTPases (Dovas and Couchman, 2005). This miRNA-dependent targeting was required for *Shigella*-induced vacuolar rupture, because inactivation of RhoGDIα in a *drosha* knock-down background, which normally exhibits a delayed vacuolar rupture, fully rescued this phenotype. Based on these findings, it has been proposed a model whereby *Shigella* subverts the activity of Ago2-miRISC at the level of macropinosomes to repress RhoGDIα and promote a rapid vacuolar rupture (Figure 1.11). This phenomenon likely occurs through the release of RhoGDIα-directed inhibition of Cdc42, a RhoGTPase that has previously been shown to orchestrate an efficient and rapid vacuolar rupture during *Shigella* infection (Mellouk *et al*., 2014).

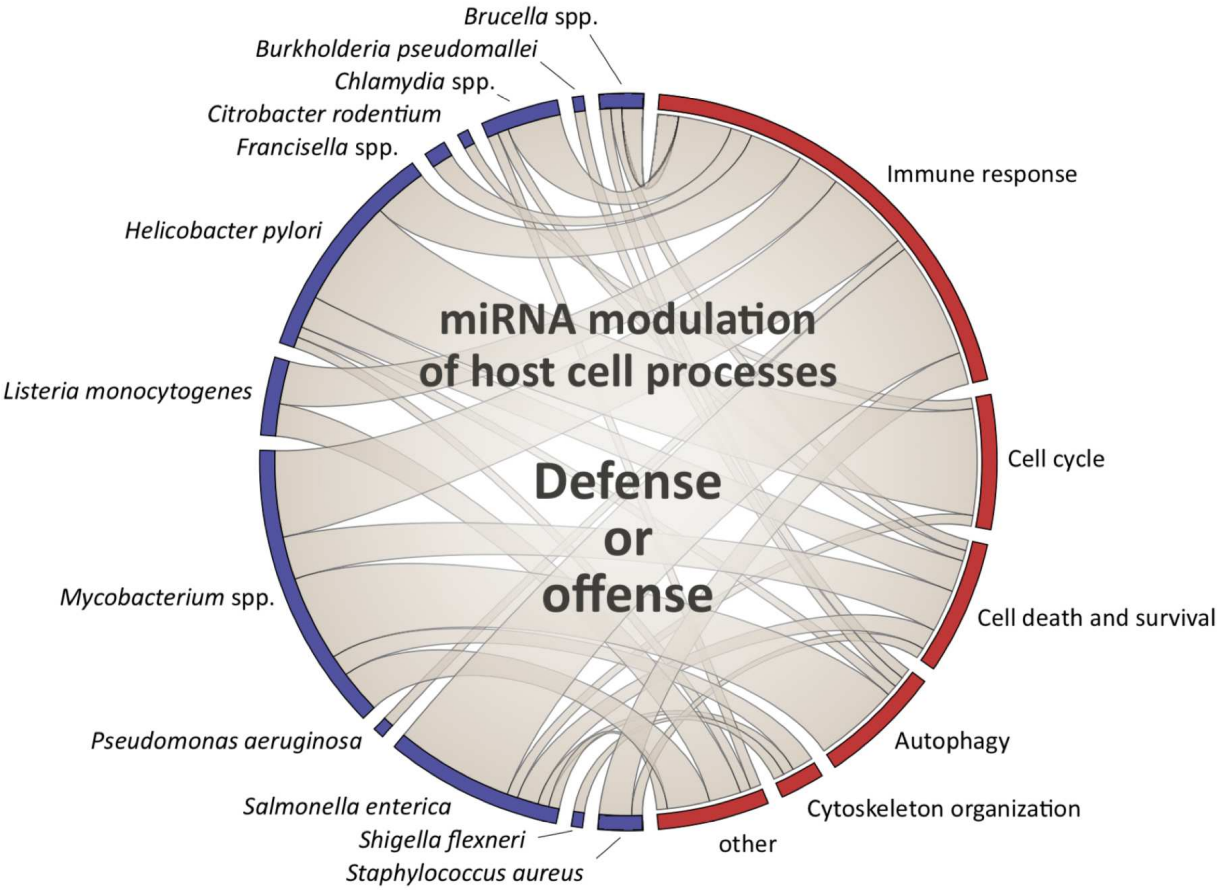

Figure 3.6. miRNAs modulate multiple host cell functions during intracellular bacterial infections.
Changes of miRNA profile can reflect host responses to clear bacterial infection or can be a strategy employed by bacterial pathogens to subvert host cell processes. Ribbon width represents roughly the number of miRNAs described for each relationship in the litterature. Scheme derived from Aguilar *et al*., 2019.

Although our study showed that human Ago4 is both a physical and genetic target of LegK1 (Figures 9 and S6), we do not know the detailed dynamics and biological relevance of Ago4 during *L. pneumophila* infection. By analogy with what has been described during *Shigella* infection, we made use of available proteomic data to determine whether the LCV could be enriched in Ago1-4 proteins. However, we did not retrieve these RNAi factors at the LCV, suggesting that these factors are either not associated with the LCV or that the timepoints used in these studies were not optimal for recovering any of these factors at the LCV. Nevertheless, Rho GTPases have been shown to regulate the actin dynamics necessary for *L. pneumophila* invasion of human cells (Prashar *et al.*, 2018). The Rho GTPases-dependent activation of cellular proteins mediates the formation of primordial membrane wraps that entrap the filamentous bacteria at the cell surface (Aktories, 2011; Prashar *et al*., 2018). It will thus be interesting to investigate whether *L. pneumophila* could manipulate Ago-miRISCs to regulate Rho/Rac/Cdc42 GTPases, thereby promoting bacterial uptake. Furthermore, because *L. pneumophila* replicates in the LCV, it must have evolved mechanisms to favour its biogenesis, while preserving its integrity. This is a major distinction from the lifestyle of *Shigella*, which instead needs to rapidly rupture its vacuole to replicate in host cells. It would therefore be interesting to assess whether human Ago4 could be retrieved at the LCV at an early stage of infection, but also at the newly formed bacterial-induced rough ER (rER), which is a known site for miRNA-mediated translational inhibition (Barman and Bhattacharyya, 2015; Bose *et al*., 2017, 2020; Stalder *et al.*, 2013). By contrast with the above *Shigella*-induced vacuolar rupture mechanism, *L. pneumophila* might have evolved to suppress human Ago activities at the rER to inhibit miRNA-directed translational inhibition of RhoGDIα, thereby ensuring a proper LCV formation. Before testing these intriguing but yet-speculative scenario, it will first be important to test if the formation of phagosome and/or the LCV could be altered in the *ago4*$^{-/-}$ THP-1 macrophages compared to wild-type THP-1 macrophages.

CHAPTER IV: CONCLUSIONS AND PROPOSED MODEL

Over the course of this thesis work, we ascribed a previously unidentified RNAi suppression activity of the type IV-secreted effector LegK1 from *L. pneumophila.* We discovered that this bacterial effector efficiently suppresses miRNA- and siRNA-guided gene silencing in human cells. Importantly, this phenomenon was found to be dependent on both its Ago-binding and kinase activities. In addition, we showed that LegK1 can directly bind human Ago2, at least in part through interaction interfaces with the Ago2 PIWI domain. Finally, we demonstrated that LegK1 positively regulates the growth of *L. pneumophila* in human macrophages, at an early stage of infection, and that this process presumably requires the targeting of human Ago4. Based on these findings, we propose a model whereby LegK1 directly interacts with human Ago proteins through two conserved W-motifs, which form an Ago-binding platform (Figure 4.1). It is possible that LegK1 would associate with a low molecular weight Ago2-miRISC (LMW-miRISC) to suppress Ago2-directed slicer activity and/or reduce the binding of Ago proteins with small RNAs (1). Alternatively, or additionally, LegK1 might outcompete with TNRC6 proteins and/or other W-rich RNA factors, for the interaction with Ago proteins (2). This yet-speculative dominant negative effect of LegK1 over Ago-cofactors would disrupt the assembly of high molecular weight RISCs (HMW-RISCs), which are orchestrated by TNRC6 proteins, thereby reducing small RNA-directed translational repression and mRNA decay. Although not shown in this hypothetical model, LegK1 could additionally interact and interfere with the functions of HMW-RISCs, without altering their assembly. Because i) W-motifs are important for the interaction of TNRC6 proteins with deadenylation complexes, ii) the two W-motifs of LegK1 are embedded in amino acid sequence contexts that are favorable for interactions with deadenylation factors, we propose that LegK1 might additionally bind deadenylation complexes to reinforce RNAi suppression effects (3). Although the catalytic activity of LegK1 was found required for RNAi suppression, this bacterial effector does not directly phosphorylate human Ago2. This suggests that LegK1 could phosphorylate other yet-unknown RNAi components or proteins that indirectly control miRISC activity (4). Overall, this work reports on the first bacterial effector from a human pathogenic bacterium that can directly suppress RNAi in human cells. It also provides a sound baseline not

only for elucidating the detailed mode of action of LegK1 in the future, but also for unraveling the role and regulation of human Ago4 in the context of host-bacteria interactions.

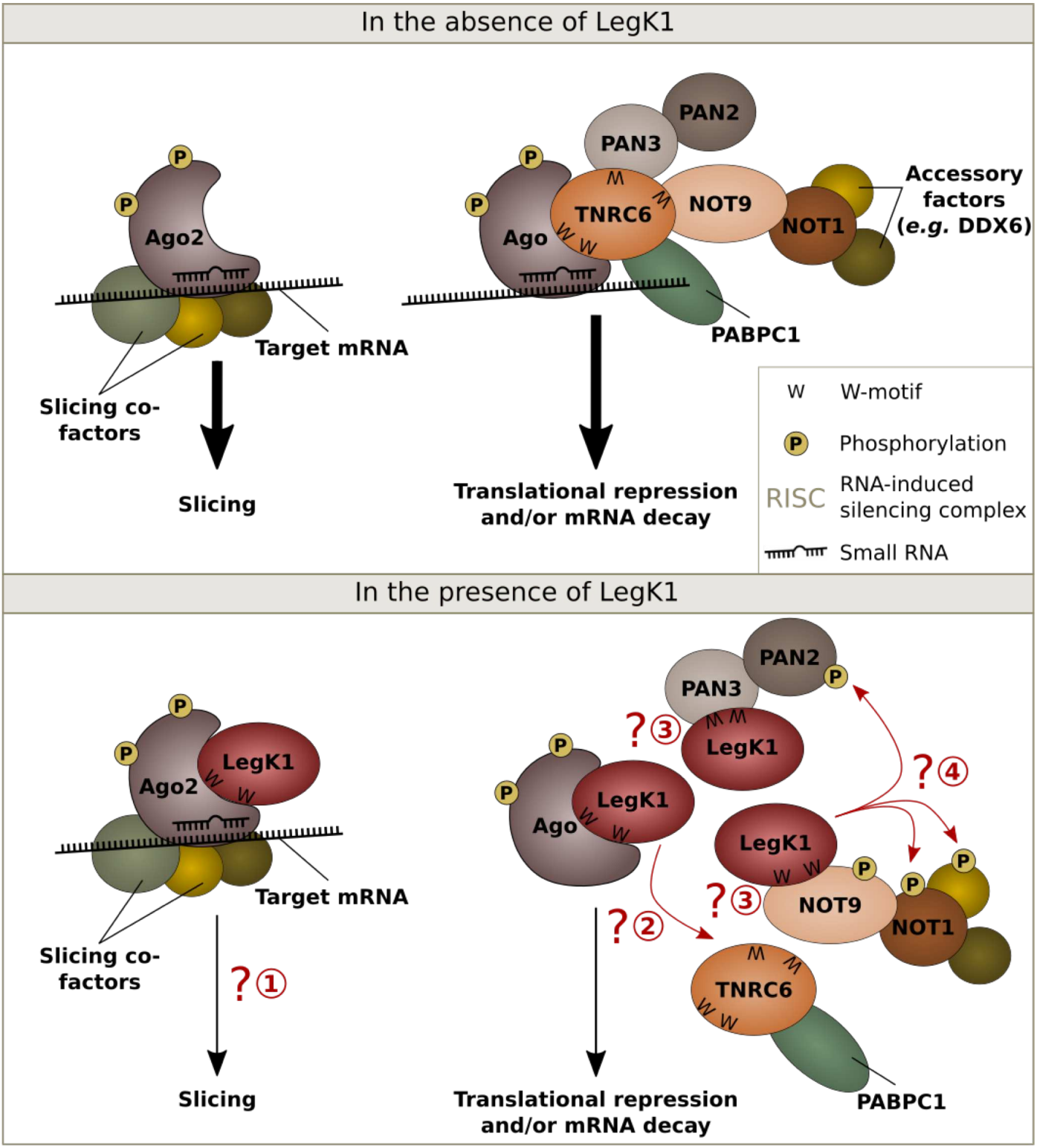

Figure 4.1. Proposed model illustrating the hypothetical mechanisms by which LegK1 could suppress RNAi.
In the absence of LegK1, low (on the left) and high (on the right) molecular weight RNA-induced silencing complexes (RISCs) direct slicing or translational repression and target mRNA decay, respectively. In the presence of LegK1, the effector directly binds to Ago through two conserved tryptophan (W)-motifs, which act as an Ago-binding platform. This interaction could either **(1)** inhibit slicing activity of Ago2 and/or **(2)** outcompete with endogenous TNRC6 proteins and/or other W-rich RNA factors for the interaction with Ago proteins, thereby reducing RISC assembly. Although not shown here, LegK1 could also interact and interfere with high molecular weigh RISCs, without altering their assembly. **(3)** Given that some W-motifs contribute to the interaction with CCR4-NOT and PAN2/PAN3 deadenylation complexes, which are similar to the two W-motifs from LegK1, we propose that the effector may additionally interact with PAN3 and NOT9, two subunits of these deadenylation complexes to reinforce its RNAi suppression activity. **(4)** Additionally, LegK1 could phosphorylate RNAi machinery components or other proteins that indirectly regulate siRNA- and miRNA- gene silencing activities. Ago; Argonaute, DDX6; DEAD-Box RNA Helicase 6, PAN; poly(A)-nuclease, TNRC6; Trinucleotide repeat-containing gene.

CHAPTER V: MATERIALS AND METHODS

I. PLASMIDS AND CONSTRUCTIONS

All plasmids used in this study are listed in Table 5.1. To identify bacterial effectors that could interefere with RNAi, we generated vectors expressing several bacterial candidates which were selected based on the presence of canonical W-motifs identified through the Wsearch program (Zielezinski and Karlowski, 2015). Briefly, PCR amplification (Table 5.2) of *Lysteriolysin O* (LLO) and *α-Hemolysin* (HLA) coding sequences using pAD-hly-Myc plasmid and *Staphylococcus aureus* SH1000 genomic DNA as templactes, respectively (gift from Dr. Alice Lebreton, IBENS, Paris, France). *BepB* coding sequence was amplified from *Bartonella Henselae* gDNA, *ExoY* and *Hcp1* from *Pseudomonas aeruginosa* PAO1 strain, *NleH1* from *Escherichia coli* O157:H7 gDNA (girft from Dr. Julie Guignot, Institut Cochin, Paris, France), *Pertussis toxin* from *Bordetella pertussis* Tohama gDNA (gift from Dr. Benoit Garin, Institut Pasteur, Paris, France) and *YopM* from *Yersinia pestis* gDNA (gift from Dr. Lauriane Quenee, Institute Biosafety Officer at Caltech, Los Angeles, USA). Finally, the coding sequence of *legK1* (*lpp*1439) was PCR amplified using gDNA of *Legionella pneumophila* Paris strai, (provided by Dr. Carmen Buchrieser, Institut Pasteur, Paris, France). As positive control for this reporter, the coding sequence of VP35 was amplified from pEF5-VP35-V5 plasmid, (gift from Walter de Vries, University of Amsterdam, Amsterdam, Netherlands). All resulting PCR products were introduced into the pENTR/D-TOPO entry vector (Invitrogen, K240020). They were sequenced and then recombined into the GATEWAY binary destination vector pPURO-FLAG-HA using LR clonase (11791020, Invitrogen), allowing an expression under the control of the cytomegalovirus (CMV) immediate early promoter.

The molecular characterization of LegK1 was then done in HEK293T cell line, using a pPURO-2xFlag-HA. This plasmid was constructed from pPURO-FLAG-HA expression vector, by insertion of a second Flag by PCR (Table 5.2). The *LegK1* coding sequence was then inserted from pENTR/D-TOPO-LegK1 into pPURO-2xFlag-HA through the GATEWAY technology, as previously described. Point mutations have been introduced in this plasmid to generate the kinase-dead mutant (LegK1-KA) and the mutant on the three putative W-motifs (LegK1-3W). These point mutations, K121A and the three point mutations W41F, W283F and W293F, were

carried out using site-directed mutagenesis PCR with appropriate primers containing the desired nucleotide changes (Table 5.2), and followed by selection with DpnI digestion. All mutants were subsequently confirmed by Sanger sequencing.

Name	Plasmid used	Comment
AutomiG	From Carré *et al.*, 2013	
pBABE-GFP-IκBα-wt	Addgene, #15263	
pENTR/D-TOPO	Promega	
pET22-6His-SUMO	From Hervé Le Hir lab (IBENS, Paris, France)	
pET22-6His-SUMO-LegK1$^{2-386}$	This study	
pET22-6His-SUMO-LegK1$^{2-386}$-KA	This study	Mutation on K121A
pET28-CBP-6His	From Hervé Le Hir lab (IBENS, Paris, France)	
pET28-CBP-6His-IκBα	This study	
pET28-CBP-6His-PIWI$^{517-859}$	This study	
pET28-TAP	From Hervé Le Hir lab (IBENS, Paris, France)	
pFlag-HA-BepB	This study	
pFlag-HA-eGFP	From Filopon, Schiavolin, Bonnet *et al*., *In preparation*	
pFlag-HA-ExoY	This study	
pFlag-HA-HLA	This study	
pFlag-HA-LegK1	This study	
pFlag-HA-LLO	This study	
pFlag-HA-NleH1	This study	
pFlag-HA-PT	This study	
pFlag-HA-YopM	This study	
pFlag-HA-T6B	From Hauptmann *et al.*, 2015	
p2xFlag-HA-LegK1-K121A	This study	Kinase-dead
p2xFlag-HA-LegK1-W41F	This study	
p2xFlag-HA-LegK1-W283F	This study	
p2xFlag-HA-LegK1-W293F	This study	
p2xFlag-HA-LegK1-3W	This study	Mutations on the three putative W-motifs, W41F, W283F and W293F
p3xFlag-HBx	From Antoine Alam (Sanofi, Marcy l'Etoile, France)	
pGFP-Ago2	Addgene, #11590	
pGFP-Ago2-PD	This study	Mutations on P590G, K660S and R688S
pGL3-CXCR4-2p	From Doench *et al.*, 2003	
pGST-Ago2	Addgene, #24317	
pRL-TK	Promega	
pPURO-FLAG-HA	Promega	
pPURO-2xFlag-HA	This study	

Table 5.1. Plasmids used in the study.

For siRNA-guided *GFP* silencing reporter, the plasmid pPURO-Flag-HA-eGFP was cloned in a previous study (Filopon, Schiavolin, Bonnet *et al., in preparation*), to express enhanced green fluorescent protein (*eGFP*). The miRNA-guided *GFP* silencing reporter, referred to as AutomiG, was kindly provided by Prof. Christophe Antoniewski (Carré *et al*., 2013). Vector expressing TNRC6B-derived peptide (T6B) was used as positive control of the siRNA-guided GFP silencing reporter, and was kindly provided by Prof. Gunter Meister (Hauptmann *et al.*, 2015). For the co-immunoprecipitation assays, a plasmid expressing human Ago2 fused to GFP in the N-terminal region of Ago2 was obtained from Addgene (#11590). The GFP-Ago2 pocket-dead (GFP-Ago2-PD) mutant was generated through three point mutations on P590G, K660S and R688S residues, by PCR-based site-directed mutagenesis using mismatched primers (Table 5.2). For recombinant protein purification, DNA fragment

encoding LegK1 amino acids 2 to 386 version was amplified by PCR, digested with NotI and XhoI enzymes and inserted into pET22-6His-SUMO plasmid, kindly given by Dr. Hervé Le Hir (IBENS, Paris, France). This construct allows the expression of LegK1$^{2–386}$ recombinant protein in fusion with an amino-terminal SUMO and a polyhistidine tags. The pET22-LegK1$^{2-386}$-KA was generated by introducing the K121A point mutation, as previously described (Ge *et al.*, 2009). The full-length GST-Ago2 was purified from the pGST-Ago2 plasmid, obtained from Addgene (#24317). A construct including only the PIWI domain of Ago2 and a fraction of MID domain was generated by PCR amplification of Ago2 amino-acids 517 to 659. PIWI$^{517-859}$ DNA was digested by BamHI and HindIII enzymes and cloned into pET28-CBP-6His allowing a fusion with the Calmodulin binding protein (CBP) and a polyhistidine tag in amino-terminal and in carboxyl-terminal ends, respectively. Finally, the full-length IκBα was purified from pET28-CBP-6His-IκBα plasmid. IκBα DNA were PCR amplified from pBABE-GFP-IκBα-wt (Addgene, #15263) and was digested and cloned into pET28-CBP-6His, as described for pET28-CBP-6His-PIWI$^{517-859}$. The negative control protein TAP, consisting of the CBP tag, was purified from a plasmid pET28 derivative, kindly provided by Dr. Hervé Le Hir. All constructions were confirmed by Sanger sequencing.

II. HUMAN CELL CULTURE

HeLa cells (ATCC® CCL-2™), HeLa CRISPR/Cas9 cell lines and Human embryonic kidney 293T cells (HEK293T) cells (ATCC® CRL-3216™) were cultured in high glucose Dulbecco's modified Eagle's medium (DMEM) (containing 4,5 g/l of glucose) (L0103-500, Dominique Dutscher) supplemented with 10% fetal bovine serum (FBS). A549 cells were cultured in Ham's F-12K Nutrient Mixture (Kaighn's Modification) (10-025-CVR, Corning) supplemented with 10% FBS. THP-1 cells (ATCC® TIB-202™) were cultured in Gibco Roswell Park Memorial Institute (RPMI) 1640 medium (L0498-500, Dominique Dutscher) supplemented with 10% FBS. Cells were maintained at 37°C in a humidified 5% CO_2 atmosphere. All cell lines were tested negative for mycoplasma contamination.

Primer	Sequence (5' to 3')
BepB-RT_F	GCCACACTCCCTTCACATTT
BepB-RT_R	TTTTTCGGCAAGCTCTTGAT
bepB-stp-R	TTAGCTGGCAATAGCAAGCG
Cassette_F	GATGAAGGCACGAACCCAGTTGACA
Cassette_R	CGGCTTGAACGAATTGTTAGGTGGC
CCL20-RT_F	TTTATTGTGGGCTTCACACG
CCL20-RT_R	GATTTGCGCACACAGACAAC
eGFP-RT_F	GACGTAAACGGCCACAAGTT
eGFP-RT_R	GAACTTCAGGGTCAGCTTGC
ExoY-GW_F	CACCATGCGTATCGACGGTCAT
ExoY-RT_F	CGAATACCGTCTTTGGCATT
ExoY-RT_R	AGTTCGAGCTTTTCCCCTTC
ExoY-stp-Rev	TCAGACCTTACGTTGGAA
FinalPCR_F	CGGTCATGCTAAATGATTCAAGAATG
FinalPCR_R	CTTCATTCACTACCCAATTTAATACTGAATTGG
Flag2-pDEST-F2	CATGATATTAAGTACCCTTATGACGTGCCCGATTAC
FLAG2-pdest-R	AGGGTACTTAATATCATGATCCTTGTAGT
GAPDH-RT_F	GAACATCATCCCTGCCTCTACT
GAPDH-RT_R	ATTTGGCAGGTTTTTCTAGACG
hAgo2-K660S_F	CGCTTCAGCCCCACCCGCATCATCTTCTA
hAgo2-K660S_R	GGTGGGGCTGAAGCGCGTGGACTTGTAGA
hAgo2-P590G_F	CAGCAGGGCGTCATCTTTCTGGGAGCAGA
hAgo2-P590G_R	GATGACGCCCTGCTGGAACACCGGCGGCC
hAgo2-R688S_F	GCCATCAGCGAGGCCTGTATCAAGCTAGA
hAgo2-R688S_R	GGCCTCGCTGATGGCCAGCAACTCGTGGT
hcp1-F	CACCATGGCTGTTGATATGTTCATCAA
hcp1-R	TTAGGCCTGCACGTTCTGG
Hcp1-RT_F	GGACCTGTCGTTCACCAAGT
Hcp1-RT_R	GGACACCAGGACTTCCTTCA
Hla_F	CACCATGGCAGATTCTGATATTAACATTAAAACC
Hla_R	TTAATTTGTCATTTCTTCTTTTTCCCA
HLA-RT_F	AACGAAAGGAACCATTGCTG
HLA-RT_R	AAGGCCAGGCTAAACCACTT
IL8-RT_F	GCAGCTCTGTGTGAAGGTGC
IL8-RT_R	CTGTGTTGGCGCAGTGTGG
IRF1-RT_F	CGATACAAAGCAGGGGAAAA
IRF1-RT_R	GTGGAAGCATCCGGTACACT
LegK1-downstream_F	GCCACCTAACAATTCGTTCAAGCCGGTATTGCGGTTGGAAATTAAAAATCT
LegK1-downstream_R	CTTCATTCACTACCCAATTTAATACTGAATTGG
LegK1-K121A-F	TTAGTTGCCATACAAAACCATAGTGAACGC
LegK1-K121A-R	GTTTTGTATGGCAACTAATTTATTCTTTGGTGG
LegK1-RT_F2	CACCGAGATGCCTTATGGTT
LegK1-RT_R2	GCTTTTCATTTCCTCCACCA
LegK1-upstream_F	CGGTCATGCTAAATGATTCAAGAATG
LegK1-upstream_R	TGTCAACTGGGTTCGTGCCTTCATCCGAGGCATGATATTGACTTCAATTT
LegK1-W283F_F	GATGTTTTCTCAACAGGCAGGATATTAAG
LegK1-W283F_R	TGTTGAGAAAACATCAGCTTTTGCTGTGT
LegK1-W293F_F	TATTTGTTCGGTGATAAATATACTAATTATT
LegK1-W293F_R	ATCACCGAACAAATAACTTAATATCCTGC
LegK1-W41F-F	GTGCCTTCAATAATAATCAAGGATACAAAT
LegK1-W41F-R	ATTATTGAAGGCACCTGGTGAATCATTATC
LLO_F	CACCATGAAAAAAATAATGCTAGTGTTTATTACAC
LLO_R	TTATTCGATTGGATTATCTACTTTATTA
LLO-RT_F	CGTCCATCTATTTGCCAGGT
LLO-RT_R	ATTTCGGATAAAGCGTGGTG
Lpp1439-promoteur_F	GGGCGAGCTCGAGTGTTTTCATCTCTTTCAATTG
Lpp1439-promoteur_R	GGCTGGTACCTTAATTTCCAACCGCAATACCCA
NleH1-GWF	CACCATGCTATCACCATCTTCT
NleH1-RT_F	GATTATGCACCGCCAGAGTT
NleH1-RT_R	CTTTTGTTGCATCCTCAGCA
NleH1-stp-Rev	CTAAATTTTACTTAATACCACACT
PIWI-hAgo2-BamHI_F	GAGCGGATCCATGCTGGTGGTGGTCATCCTGC
PIWI-hAgo2-HindIII_R	GGTAAAGCTTCAGGTGGTACCTGGCCC
PT_F	CACCATGCGTTGCACTCGGGCAA
PT_R	CCAGGTCTAGAACGAATACG
PT-RT_F	CAGAGCGAATATCTGGCACA
PT-RT_R	AATACTCCGTGGTCGTGGTC
RomA-NotI_F	GAATGCGGCCGCATGCCAAGAAGCAAGAATGATAG
RomA-XhoI_R	GCTCCTCGAGTCAAAAAAACTTGCTTTCGAGTGTG
T6B_F	CACCATGGATTGTCAGGCTGTCTTGCAGAC
T6B-nostp_R	GAGCTCCCCCCATCCAGACT
T6B-RT_F	CCTGAGGGGAAATCTGACAA
T6B-RT_R	CCCCATCCAGACTTCATTTG
YopM-GWF	CACCATGTTCATAAATCCAAGAAAT
YopM-RT_F	AGCGTTACCTCCACGCTTAG
YopM-RT_R	GGAGCTGTTTCAGGTTTTGC
YopM-stp-Rev	CTACTCAAATACATCATCTTC

Table 5.2. Primers used in the study.

III. CRISPR/CAS9-BASED KNOCK-OUT CELL LINES

Control (CTL), *ago1*$^{-/-}$, *ago2*$^{-/-}$, *ago1*$^{-/-}$/*ago2*$^{-/-}$ and *dicer*$^{-/-}$ HeLa cell lines were kindly provided by Dr. Sarah Gallois Montbrun (Institut Cochin, Paris, France) (unpublished, Eckenfelder *et al.*, 2017). *ago2*$^{-/-}$ and *ago4*$^{-/-}$ THP-1 cell lines were generated from pools (Synthego®). Briefly, single cells were isolated by dilution, and then clonal populations were expanded. Whole cell extracts were screened for Ago2 or Ago4 depletion by Western Blot. One knock-out cell line was selected and confirmed by DNA sequencing.

IV. HUMAN CELL TRANSFECTIONS

For the characterization of siRNA-based luciferase reporter, control (CTL), *ago1*$^{-/-}$, *ago2*$^{-/-}$, *ago1*$^{-/-}$/*ago2*$^{-/-}$ and *dicer*$^{-/-}$ HeLa cell lines were first transfected with Lipofectamine 2000 (11668019, Invitrogen). One day before transfection, HeLa cell lines were trypsinized, resuspended in DMEM, and seeded in 48-well plates at a density of $7x10^4$ cells per well. Cells were transiently co-transfected with 100 ng pGL3-CXCR4-2p, 50 ng of pRL-TK as transfection control, and 250 pM of AllStars Negative Control siRNA (Qiagen, 1027280) or CXCR4 siRNA (Eurofins Genomics) (Table 5.3). For the initial screening of bacterial effectors, WT HeLa cells were seeded at the same density that previously described. Cells were transiently co-transfected with 100 ng pGL3-CXCR4-2p, 50 ng of pGL3, 400 ng of vector expressing bacterial candidate or HBx as positive control, and 250 pM of AllStars Negative Control siRNA or CXCR4 siRNA. Firefly and Renilla luciferase expressions were determined as described in Dual-luciferase silencing reporter section.

Small RNAs	Target sequences (5' to 3')	References
siCTL	-	AllStars Negative Control siRNA – Qiagen - 1027280
siCXCR4	GUUUUCACUCCAGCUAACACA	Eurofins Genomics
siGFP	GCAAGCUGACCCUGAAGUUC	GFP Duplex I – Thermo Fisher Scientific - P-002048-01-20
miG1	GAAGUUCACCUUGAUGCCGUUC	From Carré *et al* ., 2013
miG2	UCCUUGAAGUCGAUGCCCUUCA	From Carré *et al* ., 2013

Table 5.3. Small RNAs used in the study.

For the detection of recombinant wild-type or mutant LegK1 proteins by Western blot analysis, HEK293T cells were seeded in 24-well plates at a density of $1.4x10^5$ cells, and were transiently transfected during 48h with either 500 ng of p2xFlag-HA-LegK1-WT, -KA or -3W plasmid using JetPrime (Polyplus, 114-15), according to manufacturer's instruction.

For the characterization of siRNA-based *GFP* sensor, CTL, *ago1*$^{-/-}$, *ago2*$^{-/-}$, *ago1*$^{-/-}$/*ago2*$^{-/-}$ and *dicer*$^{-/-}$ HeLa cell lines were transiently co-transfected with Lipofectamine 2000 during 48h and analyzed by Western blot analysis. One day before transfection, HEK293T cells were trypsinized, resuspended in DMEM, and seeded in 24-well plates at the same density as mentioned above. Cells were co-transfected with 200 ng of pPURO-Flag-HA-eGFP and 30 pmol of GFP RNA duplex (RNA GFP duplex I, P-002048-01-20, Thermoscientific) or AllStars Negative Control siRNA. For the quantification of GFP RNA transcripts from this reporter by RT-qPCR, HEK293T cells were seeded in 12-well plates at a density of $2.8x10^6$ cells per well. Cells were transiently co-transfected with 400 ng of pPURO-Flag-HA-eGFP and 60 pmol of GFP RNA duplex or AllStars Negative Control siRNA. To determine the siRNA suppression activity of the different versions of LegK1 on the siRNA-based GFP sensor, HEK293T cells were transiently co-transfected with Lipofectamine 2000 during 48h and analyzed by Western blot analysis. One day before transfection, HEK293T cells were seeded in 24-well plates at the same density that previously described. Cells were transiently co-transfected with 200 ng of pPURO-Flag-HA-eGFP, 30 pmol of GFP RNA duplex or AllStars Negative Control siRNA, and 1 µg of p2xFlag-HA-LegK1-WT, -KA, -3W, pFlag-HA-YopM as negative control or pFlag-HA-T6B as positive control. For the quantification of *GFP* RNA transcripts from this reporter by RT-qPCR, the experiment was carried out in a 12-well plate with doubled concentrations.

To determine the miRNA suppression activity of the different versions of LegK1 on the miRNA-based GFP sensor, HEK293T cells were transfected with Lipofectamine 2000 and the samples were collected 48h after transfection. GPF protein levels were further analyzed by Western blot analyses. One day before transfection, HEK293T cells were seeded in 24-well plate and cells were co-transfected with 200 ng of AutomiG and 1µg of plasmid expressing either wild type or LegK1 mutant, YopM or T6B.

For the co-immunoprecipitation assays, HEK293T cells were trypsinized, resuspended in DMEM, and seeded in 10 cm^2 dishes at a density of $6.2x10^6$ cells per well. One day after, cells were transiently transfected during 48h with 10 µg of pFlag-eGFP or p2xFlag-HA-LegK1-WT, -KA, -3W using JetPrime. For the co-immunoprecipitation assay followed by RNAse A treatment or using Ago2 Pocket-dead (Ago2-PD) mutant, HEK293T cells were seeded in the same manner. One day after, cells were co-transfected for 48h with 10 µg of pGFP-Ago2-WT or -PD and 10 µg of pFlag-HA-T6B or 14 µg of p2xFlag-HA-LegK1 using Lipofectamine 2000. To determine the catalytic activity of LegK1-3W in the kinase assay, HEK293T cells were seeded in 6 cm^2 dishes at a density of $8.4x10^5$ cells per well and were transiently transfected for 48h with 4 µg of pFlag-eGFP or p2xFlag-HA-LegK1-WT, -KA, -3W using JetPrime. Finally, for the mass spectrometry analysis, HeLa cells were seeded in 15 cm^2 dishes at a density of $1.4x10^7$ cells per well and were transfected for 24h with 20 µg of pFlag-eGFP, p2xFlag-HA-LegK1-WT or -KA using JetPrime.

V. BACTERIAL STRAINS AND MUTANT CONSTRUCTIONS

Legionella pneumophila strain Paris and its derivatives were cultured in N-(2-acetamido)-2-aminoethanesulfonic acid (ACES)-buffered yeast extract broth or on ACES-buffered charcoal-yeast (BCYE) extract agar (Feeley *et al.*, 1979). The *ΔlegK1* mutant (*Δlpp1439*) was constructed using the three-step PCR technique (Table 5.2) (Beloin *et al.*, 2004). In brief, the gene of interest was inactivated by introduction of a gentamycin resistance cassette into the chromosome. Therefore, three overlapping fragments, corresponding to upstream region, antibiotic cassette and downstream region of the gene of interest were amplified independently and purified on agarose gels. The three resulting PCR products were mixed at the same molar concentration (15 nM) and a second PCR with flanking primer pairs was performed. For chromosomal recombination, the construct was introduced into *L. pneumophila* by natural competence. Antibiotics were added at the concentration of 12.5 µg/ml for gentamycin. All strains were grown at 37°C. The specific deletion of the *legK1* gene in the *Δlpp1439* was validated by whole genome sequencing.

VI. *ACANTHAMOEBA CASTELLANII* CULTURE

Acanthamoeba castellanii (ATCC50739) was cultured in PYG 712 medium (2% proteose peptone, 0.1% yeast extract, 0.1 M glucose, 4 mM $MgSO_4$, 0.4 M $CaCl_2$, 0.1% sodium citrate dihydrate, 0.05 mM Fe $(NH_4)_2(SO_4)_2$ x $6H_2O$, 2.5 mM NaH_2PO_3, 2.5 mM K_2HPO_3) at 20°C for 72 h prior to harvesting for *L. pneumophila* infection.

VII. *ACANTHAMOEBA CASTELLANII* AND THP-1 INFECTION ASSAYS

A. castellanii were washed once with Infection Buffer (PYG 712 medium without proteose peptone, glucose and yeast extract) and seeded in 25 cm^2 flasks (TPP) at a concentration of $4x10^6$ cells per flask. *L. pneumophila* wild-type and mutant strains were grown on BCYE agar to stationary phase, diluted in Infection Buffer and mixed with *A. castellanii* at a Multiplicity of infection (MOI) of 0.1. After a 1h invasion period, the *A. castellanii* layer was washed three times with Infection Buffer. Intracellular multiplication was monitored using 300 µl of sample, centrifuged (14,500 rpm) and vortexed to break up *amoeba* and plated on BCYE plates to monitor the number of intracellular bacteria. For THP-1 infection, cells were seeded into 12-well tissue culture trays (Falcon, BD lab ware) at a density of $2x10^5$ cells/well and pretreated with 10^{-8} M phorbol 12-myristate 13-acetate (PMA) for 72 h, in 5% CO_2 at 37°C, to induce differentiation into macrophage-like adherent cells. Stationary phase *Legionella* were resuspended in RPMI 1640 serum free medium and added to THP-1 cells monolayer at a MOI of 10. After 2h incubation, cells were treated with 100 µg/ml gentamycin for 1h to kill extracellular bacteria. Infected cells were then washed with PBS before incubation with serum-free medium. At 24h, 48h and 72h post-infection, THP-1 were lysed with 0.1% Triton X-100. The amount of *Legionella* was monitored counting the number of colony-forming units (CFU) determined by plating on BCYE agar.

VIII. DUAL-LUCIFERASE SILENCING REPORTER ANALYSES

The initial screening in HeLa cells was carried out using a siRNA-guided luciferase silencing reporter, consisting on the expression of pGL3-CXCR4-2p vector (Doench *et al.*, 2003), along with CXCR4 RNA duplexes. In parallel, a Renilla luciferase control reporter vector was used, corresponding to the pRL-TK. WT or CRISPR/Cas9 HeLa cell lines were transiently co-transfected in 48-well plates, harvested 48h post-transfection, washed with PBS 1X and then lysed in 65 µL of 1X Passive Lysis Buffer (Dual-Luciferase® Reporter Assay System, Promega, E1910) by shaking for 15 min at room temperature. Firefly and Renilla activities were measured in 10 µL of cell lysate with the Luciferase reporter assay system, according to the supplier's protocol. Briefly, bioluminescence was initiated by automatic injection of 30 µL Luciferase Assay Reagent II. After 1-second shaking and an additional 1-second delay, Firefly luciferase emission signals were recorded on TriStar LB 941 Multimode Microplate Reader luminometer (Berthold Technologies), using a 10-second measurement period for each condition. The Renilla luciferase emission signals were then measured after injection of 30 µL of Stop & Glo® Reagent, in the same manner as used for Firefly luminescence detection. All measurements were carried out in three technical replicates. Firefly luminescence expression was corrected with the Renilla control, and further normalized by the negative control condition, corresponding to the CTL HeLa cell line or eGFP transfected WT HeLa cells.

IX. *EGFP/GFP*-BASED SILENCING REPORTER SYSTEM ANALYSES

The suppression activity on siRNA- and miRNA-guided *GFP* silencing reporters were both determined by Western blot analyses. Cells were co-transfected in 24-well plates, harvested at 48h post-transfection, washed with PBS 1X and lysed in 100 µL Laemmli 1X Loading Buffer. For each condition, 40 µL of samples were loaded on SDS-PAGE and subjected to Western Blot. The suppression activity on siRNA-guided *eGFP* silencing reporter was also assessed by RT-qPCR analysis. To do so, cells were transiently co-transfected in 12-well plates, harvested at 48h post-transfection, washed with PBS 1X and resuspended into 500

µL of TRIzol Reagent (Thermo Fisher Scientific, 15-596-018). Cell samples were then subjected to RNA extraction and RT-qPCR, according to the manufacturer instructions.

In some experiments, cells were transiently co-transfected with siRNA-guided silencing reporters and p2xFlag-HA-LegK1 or pFlag-HA empty control plasmid, to ensure that each transfection received the same amount of total DNA. Cells were then treated for 1h with 10 ng/ml of TNFα (H8916-10UG, Sigma-Aldrich), for 4h with 20 ng/µl of IL1-β (InvivoGen, rcyec-hil1b) or DMSO. Cell extracts were subjected to Western Blot analysis, as described previously. Quantification of eGFP protein from Western blot analysis was performed by densitometric analysis, using the ImageJ software, and was then normalized to the YopM-siCTL or Empty vector-siCTL conditions.

X. WESTERN BLOT ANALYSES

Cells were transiently co-transfected in 24-well plates, harvested at 48h post-transfection. Cells were further washed with PBS1X and lysed either in Laemmli 1X Loading Buffer or in Radio-Immunoprecipitation Assay (RIPA) buffer, for which the concentration was determined using the Bradford reagent (Bio-Rad, 5000006EDU). Approximately 100 µg of proteins were denatured 5 min at 95°C and then subjected to SDS-PAGE and Western blot analyses, according to standard procedures. The detection of proteins of interest was performed using primary and secondary antibodies (Table 5.4). Proteins were detected with Agrisera ECL SuperBright (Agrisera, AS16 ECL-S-100) using a LAS 4000 mini (GE Healthcare).

Antibody name	Clone/ Catalog#	Supplier	Species	Size (kDa)	Dilution
Ago3 antibody	39787	Active Motif	Mouse	110	1 :1,1000
Anti-Flag® M2 Antibody	F1804	Sigma-Aldrich	Mouse	-	1 :1,1000
Anti-PABPC1 Antibody	HPA045423	Atlas Antibodies	Rabbit	70	1 :1,1000
Argonaute 1 (D84G10) XP® Rabbit mAb	5053	Cell Signaling Technology	Rabbit	97	1 :1,1000
Argonaute 2 (C34C6) Rabbit mAb	2897	Cell Signaling Technology	Rabbit	97	1 :1,1000
Argonaute 4 (D10F10) Rabbit mAb	6913	Cell Signaling Technology	Rabbit	97	1 :1,1000
α-Tubulin (DM1A) Mouse mAb	3873	Cell Signaling Technology	Mouse	52	1 :1,1000
Dicer Antibody	3363	Cell Signaling Technology	Rabbit	220	1 :1,1000
Drosha (D28B1) Rabbit mAb	3364	Cell Signaling Technology	Rabbit	160	1 :1,1000
DDX6 antibody	A300-460A	Bethyl Laboratories	Rabbit	54	1 :1,1000
GAPDH (14C10) Rabbit mAb	2118	Cell Signaling Technology	Rabbit	37	1 :1,1000
GFP (D5.1) Rabbit mAb	2956	Cell Signaling Technology	Rabbit	-	1 :1,1000
Phospho-IκBα (Ser32) (14D4) Rabbit mAb	2859	Cell Signaling Technology	Rabbit	40	1 :1,1000

Table 5.4. Antibodies used in the study.

XI. CO-IMMUNOPRECIPITATION ANALYSES

Cells were transiently co-transfected in 10 cm^2 dishes, harvested at 48h post-transfection, washed twice with ice cold PBS1X and lysed with Lysis Buffer (20 mM, Tris–HCl (pH 7.4), 150 mM NaCl, 2 mM EDTA, 0,5% NP-40, 1 mM DTT, 1X protease inhibitor (EDTA-free complete Protease Inhibitor Cocktail, 11873580001, Roche) and 1:100 phosphatase inhibitor (P5726, Sigma-Aldrich). In some experiments, cell lysates were treated with 100 ng/µL RNase A (R1253, ThermoFisher) for 1h at 37°C. The RNAse A treatment was checked on agarose gel by loading 20 µL of input. For each condition, 30 µL of input was collected and its concentration was measured using the Bradford reagent in order to load 100 µg of input proteins for the following analysis. Thirty µl of Dynabeads Protein G (Invitrogen, 10003D) were incubated with 7 µg of anti-FLAG M2 antibody (Sigma-Aldrich, F1804) or anti-Ago2 (Sigma-Aldrich, SAB4200085) for 1h30 at 4°C in PBS containing 0,1% of Tween20. Dynabeads Protein G linked to the antibodies were then incubated overnight with cell lysates at 4°C under agitation. The immunoprecipitates were washed three times with IP Buffer (50 mM Tris–HCl (pH 7.4), from 150 mM to 250 mM NaCl, 0,05% NP-40, 1X protease inhibitor and phosphatase inhibitor) and eluted in Laemmli 4X Loading Buffer. Protein samples were denatured 5 min at 95°C and resolved on SDS-PAGE gel and analyzed by Western blot.

XII. EXPRESSION AND PURIFICATION OF RECOMBINANT PROTEINS

All recombinant proteins were expressed from the *E. coli* strain BL21(DE3) codon plus (ThermoFisher, EC0114) in 1L of Terrific broth (TB). Cultures were grown at 37°C until an OD600 of 2 and protein production was induced with 1 mM Isopropyl-β-D-thiogalactopyranoside (IPTG), followed by overnight growth at 18°C. Bacterial cells expressing 6His-SUMO-LegK1$^{2–386}$, 6His-SUMO-LegK1-KA$^{2–386}$, 6His-CBP-PIWI$^{517-859}$, 6His-CBP-IκBα and 6His-TAP were collected by centrifugation, resuspended in Lysis Buffer (1.5X PBS, 1 mM $MgAc_2$, 0,1 % NP-40, 20mM imidazole, 10 % glycerol), and lysed by sonication during 4 min on ice. Lysate was clarified by high-speed centrifugation (18000 rpm) and then purified on 250 µL Ni-NTA resin (Thermo Fisher Scientific, 88221). Resin was pre-equilibrated in Lysis Buffer, and supernatant was incubated with resin for 2h at 4°C. His fusion

proteins linked to the resin was washed once with Lysis Buffer, then once with Wash Buffer B1.5 (1.5X PBS, 250 mM NaCl, 1 mM $MgAc_2$, 0,1 % NP-40, 50 mM imidazole, 10 % glycerol), and finally with Lysis Buffer. Proteins were eluted in Elution Buffer B1.5 (1.5X PBS, 1 mM $MgAc_2$, 0,1 % NP-40, 150 mM imidazole, 10 % glycerol). Excess imidazole was removed by overnight dialysis using Spectrum™ Labs Spectra/Por™ 2 12-14 kD MWCO (FisherScientific, 15310762) into Dialysis Buffer (1.5X PBS, 1 mM $MgAc_2$, 10 % glycerol, 2 mM DTT) before storage at -80°C.

Bacterial cells expressing GST-Ago2 recombinant protein were collected by centrifugation, resuspended in Lysis Buffer (1.5X PBS, 1 mM $MgAc_2$, 1mM DTT, 0,1% NP-40, 10% glycerol), and lysed by sonication during 4 min on ice. Lysate was clarified by high-speed centrifugation and then purified on 500 µL of Glutathione Sepharose 4B Resin (Merck, GE-17-0756-01). Beads were pre-equilibrated in Lysis Buffer and supernatant was incubated with resin for 2h at 4°C. GST fusion proteins linked to the beads were washed once with Lysis Buffer, then once with Wash Buffer (1.5X PBS, 250 mM KCl, 1 mM $MgAc_2$, 1 mM DTT, 0,1 % NP-40, 10 % glycerol), and finally with Lysis Buffer. Proteins were eluted in Elution Buffer B1.5 (50 mM Tris pH8.0, 250 mM KCl, 1 mM $MgAc_2$, 1 mM DTT, 0,1 % NP-40, 10 % glycerol, 10 mM reduced gluthatione). Proteins were subjected to overnight dialysis using the same dialysis tubing as mentioned above into Dialysis Buffer (10 mM HEPES pH7.5, 250 mM KCl, 1 mM $MgAc_2$, 10 % glycerol, 2 mM DTT) before storage at -80°C. All recombinant protein concentrations were determined using the Bradford reagent. Proteins were analyzed by Coomassie Blue staining after SDS-PAGE.

XIII. *IN VITRO* INTERACTION ASSAYS

Glutathione Sepharose 4B Resin and calmodulin resin (Agilent Technologies, 214303) were washed twice with Blocking Buffer (20 mM Hepes pH 7.5, 150 mM NaCl, 0,1 % NP-40) and then blocked into Blocking Buffer supplemented with NaCl, 2 mg/mL glycogen carrier, 10 mg/mL tRNA and 10 mg/mL BSA during 2h at 4°C. Subsequently, beads were washed twice with Blocking Buffer and resuspended into Storage Buffer (10 mM HEPES pH 7.5, 250 mM NaCl, 1 mM EDTA). For *in vitro* interaction assays using GST pull-down, 5 µg of each purified proteins was incubated in B1.5 Buffer (1.5X PBS, 1 mM $MgAc_2$, 2 mM DTT, 10% glycerol).

The same volume of 2X BB Buffer (40 mM Hepes pH=7.5, 83 mM NaCl, 1 mM $MgAc_2$, 0,2% NP-40, 11,7% glycerol, 2 mM DTT) were added. After 20 min of interaction at 30 °C under rotation, 12 µL of Glutathione Sepharose 4B were added. Beads were washed three times with 500 µL of 1X BB 250/10 Buffer (20 mM HEPES pH=7.5, 250 mM NaCl, 1 mM $MgAc_2$, 0,2 % NP-40, 10 % glycerol, 1 mM DTT), and then proteins were eluted by incubation with 20 µL of Elution Buffer (50 mM Tris·HCl (pH 7.5), 250 mM KCl,1 mM $MgAc_2$, 1 mM DTT, 0.1 % NP-40, 10 % glycerol, 10 mM reduced Glutathione) for 5 min at 30 °C, shaking at 1,400 rpm. Finally, proteins bound to GST beads were eluted with Laemmli 4X Loading Buffer and were separated onto SDS-PAGE gel and analyzed by Western blot.

For binding assay using CBP pull-down, proteins were prepared according to the same protocol as mentioned above. In some experiments, from 5 to 15 µg of human cell extract RNAs were incubated with protein samples. After 20 min of interaction at 30 °C under rotation, 12 µL of Calmodulin Affinity Resin were added. Beads were washed three times with 500 µL of 1X BB 250/10 Buffer (20 mM Hepes pH=7.5, 250 mM NaCl, 2 mM $MgAc_2$, 2 mM imidazole, 2 mM $CaCl_2$, 0,1 % NP-40, 10 % glycerol, 1 mM DTT). Proteins were eluted by incubation with 20 µL of Elution Buffer (10 mM Tris·HCl (pH 7.5), 250 mM KCl,1 mM $MgAc_2$, 1 mM DTT, 0.1 % NP-40, 10 % glycerol, 20 mM EGTA) for 5 min at 30 °C, shaking at 1,400 rpm. Laemmli 4X Loading Buffer was added and proteins were separated onto SDS/PAGE gel and analyzed by Western blot analyses.

XIV. *IN VITRO* KINASE ASSAYS

In vitro phosphorylation of 1 µg of purified GST-Ago2 or 6His-CBP-IκBα recombinant proteins was performed in the presence of 1 µg of 6His-LegK1$^{2–386}$ or 6His-LegK1$^{2–386}$-KA in 20 µl of phosphorylation buffer containing 25 mM Tris HCl (pH 7.5), 200 mM NaCl, 10 mM MgCl2, 50 µM unlabeled ATP. Reactions were split in two, where in one part 10 µCi [γ-32P] ATP was added. The phosphorylation reaction was performed for 1h at 30°C and stopped by adding 4X Laemmli Loading Buffer. A Western blot analysis was carried out on unlabeled samples. Labeled samples were analyzed by SDS-PAGE, which was exposed to a phosphor screen and visualized by Typhoon FLA 9500 biomolecular imager.

The kinase activity of wild-type and mutant LegK1 versions was determined using IκBα recombinant protein, a known substrate of LegK1 (Ge *et al.*, 2009). For this, HEK293T cells were seeded in 6 cm^2 dishes and transfected with either pFlag-HA-eGFP, p2xFlag-HA-LegK1-WT, -KA or -3W. Cells were lysed and subjected to a Flag immunoprecipitation. The resulting immunoprecipitates were incubated with Phosphorylation Buffer (250 mM Tris-HCl pH 7.5, 50 mM $MnCl_2$, 50 mM DTT) and 1 µg of purified 6His-CBP-IκBα recombinant proteins for 30 min at 30°C. Proteins were mixed with Laemmli 4X Loading Buffer and then analyzed by Western blot analyses using the phospho-IκBα (Ser32) (14D4) antibody (Table 5.4).

XV. PEPTIDE PULL-DOWN ASSAYS

Biotinylated peptides (synthetized by Genscript, sequences shown in Table 5.5 were resuspended in DMSO, and heated at 40°C for 5 min. For binding assays, 10 µg of peptides were diluted into 200 µL of PBS containing 0.1% of Tween 20 and were incubated for 30 min at room temperature in the presence of 30 µL of Dynabeads® MyOne™ Streptavidin T1 (Thermo Fisher Scientific, 65601). The beads were then washed once in 0.1% PBS Tween and twice in IP Buffer (50 mM Tris-HCl pH 7.4, 150 mM NaCl, 5 mM MgCl2, 0.0,5% NP-40, 1/100 Phosphatase inhibitor and 1X protease inhibitor). HEK293T cells were washed twice with ice cold PBS1X and scraped with Lysis Buffer (see co-immunoprecipitation assays). Cells were incubated at 4°C under rotation for 30 min and the supernatant was harvested by centrifugation at 16,000 g for 10 min at 4 °C. Beads-coupled peptides were incubated in the presence of cell lysates for 1 hour at 4°C. After three washing of the beads with IP Buffer, the proteins were eluted in Laemmli 4X Loading Buffer and resolved on SDS-PAGE. The presence of Ago proteins were detected by Western blot analyses.

XVI. RNA EXTRACTIONS AND QUANTITATIVE REAL TIME PCR ANALYSES

For gene expression analyses, total RNAs were isolated by phenol-chloroform extraction using TRIzol Reagent (Thermo Fisher Scientific, 15-596-018), according to the manufacturer instructions. Approximately 0.5 µg of RNAs were then digested by DNAse I (Promega, M6101) at 37°C for 50 min to remove the genomic DNA, followed by 10 min at 65°C to inactivate DNAse. DNAse-digested RNAs were reverse-transcribed into coding DNA

using qScript cDNA Supermix (Quanta Biosciences, 733-1178). The cDNAs were quantified through SYBR Green qPCR mix (Takyon, Eurogentec, UF-NSMT-B0701) and gene-specific primers (Table 5.2) in 384-well plates, following heating at 95 °C for 10 min, 45 cycles of denaturation at 95 °C for 10 sec and annealing at 60 °C for 40 sec. A melting curve was performed at the end of the amplification and transcript levels were then normalized to the abundance of *GAPDH* transcripts.

Name	Sequences
W1	YLNDNDSPGAWNNNQGYK
F1	YLNDNDSPGAFNNNQGYK
W2	ALYTAKADVWSTGRILSY
F2	ALYTAKADVFSTGRILSY
W3	TGRILSYLWGDKYTNYYI
F3	TGRILSYLFGDKYTNYYI
A3	TGRILSYLAGDKYTNYYI

Table 5.5. Biotinylated peptides used in the study.

XVII. PARALLEL-REACTION MONITORING (PRM) BY MASS SPECTROMETRY ANALYSES

HeLa cells were seeded in 15 cm^2 dishes and transiently transfected with either pFlag-HA-eGFP p2xFlag-HA-LegK1-WT or -KA. 24h post-transfection, cells were washed twice with ice cold PBS1X and lysed with Lysis Buffer (as referred in Co-immunoprecipitation section) and 1:100 phosphatase inhibitor (Sigma-Aldrich, P5726). For each condition, 30 µL of input was collected and analyzed by Western blot. Sixty µl of Dynabeads Protein G (Invitrogen, 10003D) were incubated for 1h30 at 4°C under agitation with 16 µg of the anti-Ago2 (Sigma-Aldrich, SAB4200085) in PBS containing 0,1% of Tween 20. Dynabeads Protein G linked to Ago2 antibody were then incubated overnight with cell lysates at 4°C under agitation. The immunoprecipitates were washed three times with IP Buffer (as referred in Co-immunoprecipitation section) and eluted in Laemmli 4X Loading Buffer. Five immunoprecipitations of each condition were performed. Protein samples were denatured 5 min at 95°C, then were simultaneously separated on SDS-PAGE and stained with colloidal blue (LabSafe Gel Blue, Gbiosciences, 786-35). One gel slice was excised for each purification and in-gel digested by using trypsin/LysC (Promega, V5072). Peptides extracted from each band

were then loaded onto a homemade C18 StageTips for desalting. Peptides were eluted using 40/60 MeCN/H_2O + 0.1 % formic acid and vacuum concentrated to dryness.

Peptide samples were resuspended in Buffer A (2/98 MeCN/H_2O in 0.1 % formic acid), separated and analyzed by nanoLC-MS/MS using an RSLCnano system (Thermo Scientific, Ultimate 3000) coupled online to a Q Exactive HF-X mass spectrometer (Thermo Scientific). Peptides were first trapped onto a C18 column (75 µm inner diameter × 2 cm; nanoViper Acclaim PepMapTM 100, Thermo Scientific) with Buffer A at a flow rate of 2.5 µL/min over 4 min. Separation was performed on a 50 cm x 75 µm C18 column (nanoViper C18, 3 µm, 100Å, Acclaim PepMapTM RSLC, Thermo Scientific) regulated to 50°C and with a linear gradient from 2% to 30% buffer B (100% MeCN in 0.1% formic acid) at a flow rate of 300 nL/min over 91 min. The mass spectrometer was operated in Parallel Reaction Monitoring (PRM) mode (see acquisition list Table 5.6). The acquisition list was generated from the peptides obtained from the mix samples (5 replicates) of each condition based on the data-dependent acquisition (DDA) results (data not shown).

Peptide sequence and modifications position	Protein modification	Precursor Mass MH+	Charge	Extracted fragments
ARYHLVDKEHDS[Phospho]AEGSHTSGQSNGR	Phospho (S824)	940,081146	3	y14-98, y11, y9, y8, y7, y18(2+), y18-98(2+), y16-98(2+), y14-98(2+), b7, b9, b11, b11(2+), b14-98(2+)
SAS[Phospho]FNTDPYVR	Phospho (S387)	668,782099	2	y9-98, y8, y7, y6, y5, y4, y9-98(2+), b2, b3-98, b4-98, b5-98, b7-98
YHLVDKEHDS[Phospho (STY)]AEGS[Phospho (STY)]HTSGQSNGR	2 phospho	891,023849	3	y7, y6, y21-98(2+), y20-98(2+), y19-98(2+), y18-98(2+), y14-98(2+), y22-98(3+), b2, b3, b4, b5, b9, b21(3+)
YHLVDKEHDS[Phospho]AEGSHTSGQSNGR	Phospho (S824)	864,368405	3	y11, y8, y7, y6, y21(2+), y21-98(2+), y20(2+), y20-98(2+), y19-98(2+), y18-98(2+), y16-98(2+), y22-98(3+), b3
ELLIQFYK		527,302592	2	y7, y6, y5, y4, y3, y6(2+), y5(2+), b3
SGNIPAGTTVDTK		630,825149	2	y10, y9, y8, y7, y6, y5, y4, y3, y10(2+), y9(2+), b3, b4
SIEEQQKPLTDSQR		829,92084	2	y10, y9, y8, y7, y5, y4, y3, y12, y11, b3, b4, b5, b6
VELEVTLPGEGK		635,848092	2	y11, y10, y9, y8, y7, y6, y5, y4, y3, b3, b4
VLQPPSILYGGR		650,374612	2	y11, y10, y9, y8, y7, y6, y5, y4, y3, y9(2+), y8(2+), b3

Table 5.6. Targeted peptides for mass spectrometry analysis.

XVIII. PARALLEL-REACTION MONITORING (PRM) DATA ANALYSES

The PRM data were analyzed using Skyline version (version 4.1, MacCoss Lab Software, Seattle, Washington [https://skyline.ms/project/home/software/Skyline/begin.view], fragment ions for each targeted mass (Table 5.7) were extracted and peak areas were integrated. The peptide areas were log2 transformed and the mean log2- area was normalized by the mean area of five Ago2 peptides (ELLIQFYK, SGNIPAGTTVDTK, SIEEQQKPLTDSQR, VELEVTLPGEGK and VLQPPSILYGGR) using software R version 3.1.0. On each phospho-peptide, a linear model was used to estimate the mean fold change between the conditions, its 95% confidence interval and the p-value of the two-sided associated t-test.

Peptide sequence and modifications position	Protein modification	log2(LegK1-WT/eGFP)	LegK1-WT/eGFP	CI 2,5%	CI 97,5%	Adjusted p-value
ARYHLVDKEHDS[Phospho]AEGSHTSGQSNGR	Phospho (S824)	-0,594	0,662	-0,894	-0,294	0,001
SAS[Phospho]FNTDPYVR	Phospho (S387)	0,112	1,081	-0,026	0,250	0,141
YHLVDKEHDS[Phospho (STY)]AEGS[Phospho (STY)]HTSGQSNGR	2 Phospho	-0,756	0,592	-1,404	-0,107	0,052
YHLVDKEHDS[Phospho]AEGSHTSGQSNGR	Phospho (S824)	-0,302	0,811	-0,525	-0,080	0,025

Peptide sequence and modifications position	Protein modification	log2(LegK1-KA/eGFP)	LegK1-KA/eGFP	CI 2,5%	CI 97,5%	Adjusted p-value
ARYHLVDKEHDS[Phospho]AEGSHTSGQSNGR	Phospho (S824)	-0,957	0,515	-1,124	-0,789	1,231E-17
SAS[Phospho]FNTDPYVR	Phospho (S387)	-0,192	0,875	-0,416	0,031	0,137
YHLVDKEHDS[Phospho (STY)]AEGS[Phospho (STY)]HTSGQSNGR	2 phospho	-0,636	0,643	-1,036	-0,236	0,004
YHLVDKEHDS[Phospho]AEGSHTSGQSNGR	Phospho (S824)	-0,615	0,653	-0,878	-0,352	3,520E-05

Table 5.7. Quantification of modifications for mass spectrometry analysis.

XIX. PREDICTION OF W-MOTIFS

W-motifs were predicted using the Wsearch algorithm (Zielezinski and Karlowski, 2015), where amino acids surrounding a tryptophan are scored according to a Position-Specific Scoring Matrice (PSSM) derived from experimentally validated Ago-binding motifs from animals. Briefly, the protein sequences of all bacterial organisms tested were retrieved from Uniprot (UniProt Consortium, 2018) and subjected to Wsearch. The score of the different motifs were then added together, corresponding to the final score. For the first pre-selection,

we applied an arbitrary cutoff of greater than six on the average W-scores of all motifs present in the candidate protein sequence. Among the bacterial candidate proteins exhibiting the highest W-score, we further selected known secreted virulence factors or putative virulence factors predicted to be secreted using PSORTb (Yu *et al*., 2010).

XX. ALIGNMENT OF ORTHOLOGOUS LEGK1 PROTEIN SEQUENCES

The protein sequence of LegK1 (from *lpp1439* gene) from *Legionella pneumophila* Paris was used as reference to retrieve orthologous LegK1 protein sequences from *Legionella* species/strains (taxid: 445). To this end, a BLASTP (Basic Local Alignment Search Tool) was performed on the NCBI (National Center for Biotechnology Information) website. An identity cutoff of 40%, an Expect (E)-value cutoff of 10^{-5} and a minimum percentage match length of subject and query of 65% were used. The set of orthologous protein sequences were then aligned using ClustalW2.

XXI. HEATMAP OF *AGO* TRANSCRIPTS

The RNA-sequencing results were generated in the Human Protein Atlas (HPA) and are reported as Normalized eXpression (NX) values, retrieved from www.proteinatlas.org. The consensus NX value for each gene represents the maximum NX value obtained in the three data sources: HPA, GTEx and FANTOM5. In brief, the average Transcripts Per Million (TPM) value of all individual samples for each human cell type was used to estimate the gene expression level. All TPM values per sample were scaled to a sum of 1 million TPM (denoted pTPM) to compensate for the non-coding transcripts that had been previously removed. Next, all TPM values of all the samples within each data source were TMM normalized, followed by Pareto scaling of each gene within each data source. The resulting transcript expression values, denoted NX, were calculated for each gene in every sample.

XXII. QUANTIFICATION AND STATISTICAL ANALYSES

Experimental results were shown as the standard deviation (SD) for all experiments, except for the infection assays showing as the mean and standard error of mean (± SEM). Statistical analysis was carried out using the Prism Software (GraphPad version 8). For statistical comparison between several conditions or two groups, one-way analysis of variance (ANOVA) or an unpaired t test of biological replicates were used, respectively. A value of $P < 0.05$ was considered statistically significant. All statistical tests are specified in the respective figure legends.

BIBLIOGRAPHY

Abdel-Nour, M., Duncan, C., Low, D.E., and Guyard, C. (2013). Biofilms: the stronghold of *Legionella pneumophila*. *Int J Mol Sci 14*, 21660–21675.

Abu Kwaik, Y. (1996). The phagosome containing *Legionella pneumophila* within the protozoan *Hartmannella vermiformis* is surrounded by the rough endoplasmic reticulum. *Appl Environ Microbiol 62*, 2022–2028.

Abu-Zant, A., Jones, S., Asare, R., Suttles, J., Price, C., Graham, J., and Kwaik, Y.A. (2007). Anti-apoptotic signalling by the Dot/Icm secretion system of *L. pneumophila. Cell Microbiol 9*, 246–264.

Adams, B.D., Kasinski, A.L., and Slack, F.J. (2014). Aberrant Regulation and Function of MicroRNAs in Cancer. *Current Biology 24*, R762–R776.

Ade, J., DeYoung, B.J., Golstein, C., and Innes, R.W. (2007). Indirect activation of a plant nucleotide binding site–leucine-rich repeat protein by a bacterial protease. *PNAS 104*, 2531–2536.

Adiliaghdam, F., Basavappa, M., Saunders, T.L., Harjanto, D., Prior, J.T., Cronkite, D.A., Papavasiliou, N., and Jeffrey, K.L. (2020). A Requirement for Argonaute 4 in Mammalian Antiviral Defense. Cell *Rep 30*, 1690-1701.e4.

Agrawal, N., Dasaradhi, P.V.N., Mohmmed, A., Malhotra, P., Bhatnagar, R.K., and Mukherjee, S.K. (2003). RNA interference: biology, mechanism, and applications. Microbiol. *Mol. Biol. Rev. 67*, 657–685.

Aguilar, C., Mano, M., and Eulalio, A. (2019). MicroRNAs at the Host–Bacteria Interface: Host Defense or Bacterial Offense. *Trends in Microbiology 27*, 206–218.

Aguilar, C., Cruz, A.R., Lopes, I.R., Maudet, C., Sunkavalli, U., Silva, R.J., Sharan, M., Lisowski, C., Zaldívar-López, S., Garrido, J.J., et al. (2020). Functional screenings reveal different requirements for host microRNAs in *Salmonella* and *Shigella* infection. *Nat Microbiol 5*, 192–205.

Akamine, M., Higa, F., Arakaki, N., Kawakami, K., Takeda, K., Akira, S., and Saito, A. (2005). Differential Roles of Toll-Like Receptors 2 and 4 in In Vitro Responses of Macrophages to *Legionella pneumophila. Infect Immun 73*, 352–361.

Akimov, V., Barrio-Hernandez, I., Hansen, S.V.F., Hallenborg, P., Pedersen, A.-K., Bekker-Jensen, D.B., Puglia, M., Christensen, S.D.K., Vanselow, J.T., Nielsen, M.M., et al. (2018). UbiSite approach for comprehensive mapping of lysine and N-terminal ubiquitination sites. *Nat Struct Mol Biol 25*, 631–640.

Aktories, K. (2011). Bacterial protein toxins that modify host regulatory GTPases. *Nat Rev Microbiol 9*, 487–498.

Alli, O.A., Gao, L.Y., Pedersen, L.L., Zink, S., Radulic, M., Doric, M., and Abu Kwaik, Y. (2000). Temporal pore formation-mediated egress from macrophages and alveolar epithelial cells by *Legionella pneumophila. Infect Immun 68*, 6431–6440.

Anderson, P., and Kedersha, N. (2008). Stress granules: the Tao of RNA triage. *Trends Biochem Sci 33*, 141–150.

Andersson, M.G., Haasnoot, P.C.J., Xu, N., Berenjian, S., Berkhout, B., and Akusjärvi, G. (2005). Suppression of RNA Interference by Adenovirus Virus-Associated RNA. *J Virol 79*, 9556–9565.

Androulidaki, A., Iliopoulos, D., Arranz, A., Doxaki, C., Schworer, S., Zacharioudaki, V., Margioris, A.N., Tsichlis, P.N., and Tsatsanis, C. (2009). Akt1 controls macrophage response to LPS by regulating microRNAs. *Immunity 31*, 220–231.

Aqil, M., Naqvi, A.R., Bano, A.S., and Jameel, S. (2013). The HIV-1 Nef Protein Binds Argonaute-2 and Functions as a Viral Suppressor of RNA Interference. *PLoS One 8*.

Arasaki, K., and Roy, C.R. (2010). *Legionella pneumophila* Promotes Functional Interactions between Plasma Membrane Syntaxins and Sec22b. *Traffic 11*, 587–600.

Archer, K.A., and Roy, C.R. (2006). MyD88-dependent responses involving toll-like receptor 2 are important for protection and clearance of *Legionella pneumophila* in a mouse model of Legionnaires' disease. *Infect Immun 74*, 3325–3333.

Archer, K.A., Ader, F., Kobayashi, K.S., Flavell, R.A., and Roy, C.R. (2010). Cooperation between multiple microbial pattern recognition systems is important for host protection against the intracellular pathogen *Legionella pneumophila. Infect Immun 78*, 2477–2487.

Asrat, S., Dugan, A.S., and Isberg, R.R. (2014). The Frustrated Host Response to *Legionella pneumophila* Is Bypassed by MyD88-Dependent Translation of Pro-inflammatory Cytokines. *PLoS Pathog 10.*

Avesson, L., Reimegård, J., Wagner, E.G.H., and Söderbom, F. (2012). MicroRNAs in Amoebozoa: Deep sequencing of the small RNA population in the social amoeba *Dictyostelium discoideum* reveals developmentally regulated microRNAs. *RNA 18*, 1771–1782.

Axtell, M.J., and Staskawicz, B.J. (2003). Initiation of RPS2-Specified Disease Resistance in Arabidopsis Is Coupled to the AvrRpt2-Directed Elimination of RIN4. *Cell 112*, 369–377.

Azevedo, J., Garcia, D., Pontier, D., Ohnesorge, S., Yu, A., Garcia, S., Braun, L., Bergdoll, M., Hakimi, M.A., Lagrange, T., et al. (2010). Argonaute quenching and global changes in Dicer homeostasis caused by a pathogen-encoded GW repeat protein. *Genes Dev 24*, 904–915.

Bacigalupe, R., Lindsay, D., Edwards, G., and Fitzgerald, J.R. (2017). Population Genomics of *Legionella longbeachae* and Hidden Complexities of Infection Source Attribution. *Emerg Infect Dis 23*, 750–757.

Backes, S., Shapiro, J.S., Sabin, L.R., Pham, A.M., Reyes, I., Moss, B., Cherry, S., and tenOever, B.R. (2012). Degradation of Host MicroRNAs by Poxvirus Poly(A) Polymerase Reveals Terminal RNA Methylation as a Protective Antiviral Mechanism. *Cell Host Microbe 12*, 200–210.

Backes, S., Langlois, R.A., Schmid, S., Varble, A., Shim, J.V., Sachs, D., and tenOever, B.R. (2014). The mammalian response to virus infection is independent of small RNA silencing. Cell Rep *8*, 114–125.

Badis, G., Saveanu, C., Fromont-Racine, M., and Jacquier, A. (2004). Targeted mRNA degradation by deadenylation-independent decapping. *Mol. Cell 15*, 5–15.

Bandyopadhyay, P., Liu, S., Gabbai, C.B., Venitelli, Z., and Steinman, H.M. (2007). Environmental mimics and the Lvh type IVA secretion system contribute to virulence-related phenotypes of *Legionella pneumophila. Infect Immun 75*, 723–735.

Bao, H., Kommadath, A., Liang, G., Sun, X., Arantes, A.S., Tuggle, C.K., Bearson, S.M.D., Plastow, G.S., Stothard, P., and Guan, L.L. (2015). Genome-wide whole blood microRNAome and transcriptome analyses reveal miRNA-mRNA regulated host response to foodborne pathogen *Salmonella* infection in swine. *Sci Rep 5*, 12620.

Barman, B., and Bhattacharyya, S.N. (2015). mRNA Targeting to Endoplasmic Reticulum Precedes Ago Protein Interaction and MicroRNA (miRNA)-mediated Translation Repression in Mammalian Cells. *J Biol Chem 290*, 24650–24656.

Bartel, D.P. (2018). Metazoan MicroRNAs. *Cell 173*, 20–51.

Bartfeld, S., Engels, C., Bauer, B., Aurass, P., Flieger, A., Brüggemann, H., and Meyer, T.F. (2009). Temporal resolution of two-tracked NF-κB activation by *Legionella pneumophila. Cellular Microbiology 11*, 1638–1651.

Baumberger, N., Tsai, C.-H., Lie, M., Havecker, E., and Baulcombe, D.C. (2007). The Polerovirus silencing suppressor P0 targets ARGONAUTE proteins for degradation. *Curr Biol 17*, 1609–1614.

Bawankar, P., Loh, B., Wohlbold, L., Schmidt, S., and Izaurralde, E. (2013). NOT10 and C2orf29/NOT11 form a conserved module of the CCR4-NOT complex that docks onto the NOT1 N-terminal domain. *RNA Biol 10*, 228–244.

Beauté, J., and Network, on behalf of the E.L.D.S. (2017). Legionnaires' disease in Europe, 2011 to 2015. *Eurosurveillance 22*, 30566.

Behm-Ansmant, I., Rehwinkel, J., Doerks, T., Stark, A., Bork, P., and Izaurralde, E. (2006). mRNA degradation by miRNAs and GW182 requires both CCR4:NOT deadenylase and DCP1:DCP2 decapping complexes. *Genes Dev 20*, 1885–1898.

Belair, C., Baud, J., Chabas, S., Sharma, C.M., Vogel, J., Staedel, C., and Darfeuille, F. (2011). *Helicobacter pylori* interferes with an embryonic stem cell micro RNA cluster to block cell cycle progression. *Silence 2*, 7.

Beloin, C., Valle, J., Latour-Lambert, P., Faure, P., Kzreminski, M., Balestrino, D., Haagensen, J.A.J., Molin, S., Prensier, G., Arbeille, B., et al. (2004). Global impact of mature biofilm lifestyle on *Escherichia coli* K-12 gene expression. *Mol Microbiol 51*, 659–674.

Belyi, Y., Jank, T., and Aktories, K. (2014). Cytotoxic Glucosyltransferases of *Legionella pneumophila.* In Molecular Mechanisms in Legionella Pathogenesis. *Curr Top Microbiol Immunol 376,* 211-26.

Bennasser, Y., Le, S.-Y., Benkirane, M., and Jeang, K.-T. (2005). Evidence that HIV-1 encodes an siRNA and a suppressor of RNA silencing. *Immunity 22*, 607–619.

Bennasser, Y., Yeung, M.L., and Jeang, K.-T. (2006). HIV-1 TAR RNA subverts RNA interference in transfected cells through sequestration of TAR RNA-binding protein, TRBP. *J Biol Chem 281*, 27674–27678.

Berger, K.H., and Isberg, R.R. (1993). Two distinct defects in intracellular growth complemented by a single genetic locus in *Legionella pneumophila*. *Mol Microbiol 7*, 7–19.

Berjeaud, J.-M., Chevalier, S., Schlusselhuber, M., Portier, E., Loiseau, C., Aucher, W., Lesouhaitier, O., and Verdon, J. (2016). *Legionella pneumophila*: The Paradox of a Highly Sensitive Opportunistic Waterborne Pathogen Able to Persist in the Environment. *Front. Microbiol. 8,* 7-486.

Berk, S.G., Ting, R.S., Turner, G.W., and Ashburn, R.J. (1998). Production of respirable vesicles containing live *Legionella pneumophila* cells by two Acanthamoeba spp. *Appl Environ Microbiol 64*, 279–286.

Berkhout, B. (2018a). RNAi-mediated antiviral immunity in mammals. *Curr Opin Virol 32*, 9–14.

Berkhout, B. (2018b). RNAi-mediated antiviral immunity in mammals. *Current Opinion in Virology 32*, 9–14.

Berrington, W.R., Iyer, R., Wells, R.D., Smith, K.D., Skerrett, S.J., and Hawn, T.R. (2010). NOD1 and NOD2 regulation of pulmonary innate immunity to *Legionella pneumophila. Eur J Immunol 40*, 3519–3527.

Berry, B., Deddouche, S., Kirschner, D., Imler, J.-L., and Antoniewski, C. (2009). Viral suppressors of RNA silencing hinder exogenous and endogenous small RNA pathways in *Drosophila*. *PLoS One 4*, e5866.

Bettencourt, P., Marion, S., Pires, D., Santos, L.F., Lastrucci, C., Carmo, N., Blake, J., Benes, V., Griffiths, G., Neyrolles, O., et al. (2013). Actin-binding protein regulation by microRNAs as a novel microbial strategy to modulate phagocytosis by host cells: the case of N-Wasp and miR-142-3p. *Front Cell Infect Microbiol 3*, 19.

Bhan, U., Trujillo, G., Lyn-Kew, K., Newstead, M.W., Zeng, X., Hogaboam, C.M., Krieg, A.M., and Standiford, T.J. (2008). Toll-Like Receptor 9 Regulates the Lung Macrophage Phenotype and Host Immunity in Murine Pneumonia Caused by *Legionella pneumophila*. *Infect Immun 76*, 2895–2904.

Bhayani, M.K., Calin, G.A., and Lai, S.Y. (2012). Functional relevance of miRNA* sequences in human disease. *Mutation Research/Fundamental and Molecular Mechanisms of Mutagenesis 731*, 14–19.

Billeter, A.T., Hellmann, J., Roberts, H., Druen, D., Gardner, S.A., Sarojini, H., Galandiuk, S., Chien, S., Bhatnagar, A., Spite, M., et al. (2014). MicroRNA-155 potentiates the inflammatory response in hypothermia by suppressing IL-10 production. *FASEB J. 28*, 5322–5336.

Billy, E., Brondani, V., Zhang, H., Müller, U., and Filipowicz, W. (2001). Specific interference with gene expression induced by long, double-stranded RNA in mouse embryonal *teratocarcinoma* cell lines. *Proc. Natl. Acad. Sci. U.S.A. 98*, 14428–14433.

Boamah, D.K., Zhou, G., Ensminger, A.W., and O'Connor, T.J. (2017). From Many Hosts, One Accidental Pathogen: The Diverse Protozoan Hosts of *Legionella*. *Front Cell Infect Microbiol 7*, 477.

Boesler, B., Meier, D., Förstner, K.U., Friedrich, M., Hammann, C., Sharma, C.M., and Nellen, W. (2014). Argonaute proteins affect siRNA levels and accumulation of a novel extrachromosomal DNA from the *Dictyostelium* retrotransposon DIRS-1. *J Biol Chem 289*, 35124–35138.

Bogerd, H.P., Skalsky, R.L., Kennedy, E.M., Furuse, Y., Whisnant, A.W., Flores, O., Schultz, K.L.W., Putnam, N., Barrows, N.J., Sherry, B., et al. (2014). Replication of Many Human Viruses Is Refractory to Inhibition by Endogenous Cellular MicroRNAs. *Journal of Virology 88*, 8065–8076.

BOHNSACK, M.T., CZAPLINSKI, K., and GÖRLICH, D. (2004). Exportin 5 is a RanGTP-dependent dsRNA-binding protein that mediates nuclear export of pre-miRNAs. *RNA 10*, 185–191.

Borchert, G.M., Lanier, W., and Davidson, B.L. (2006). RNA polymerase III transcribes human microRNAs. *Nature Structural & Molecular Biology 13*, 1097–1101.

Borges, F., and Martienssen, R.A. (2015). The expanding world of small RNAs in plants. *Nat Rev Mol Cell Biol 16*, 727–741.

Borges, V., Nunes, A., Sampaio, D.A., Vieira, L., Machado, J., Simões, M.J., Gonçalves, P., and Gomes, J.P. (2016). *Legionella pneumophila* strain associated with the first evidence of person-to-person transmission of Legionnaires' disease: a unique mosaic genetic backbone. *Sci Rep 6*, 26261.

Bortolamiol, D., Pazhouhandeh, M., Marrocco, K., Genschik, P., and Ziegler-Graff, V. (2007). The Polerovirus F Box Protein P0 Targets ARGONAUTE1 to Suppress RNA Silencing. *Current Biology 17*, 1615–1621.

Bose, M., Barman, B., Goswami, A., and Bhattacharyya, S.N. (2017). Spatiotemporal Uncoupling of MicroRNA-Mediated Translational Repression and Target RNA Degradation Controls MicroRNP Recycling in Mammalian Cells. *Mol Cell Biol 37*, e00464-16.

Bose, M., Chatterjee, S., Chakrabarty, Y., Barman, B., and Bhattacharyya, S.N. (2020). Retrograde trafficking of Argonaute 2 acts as a rate-limiting step for de novo miRNP formation on endoplasmic reticulum–attached polysomes in mammalian cells. *Life Sci Alliance 3*, e201800161.

Bozue, J.A., and Johnson, W. (1996). Interaction of *Legionella pneumophila* with *Acanthamoeba castellanii*: uptake by coiling phagocytosis and inhibition of phagosome-lysosome fusion. *Infect Immun 64*, 668–673.

Braedel-Ruoff, S., Faigle, M., Hilf, N., Neumeister, B., and Schild, H. (2005). *Legionella pneumophila* mediated activation of dendritic cells involves CD14 and TLR2. *J Endotoxin Res 11*, 89–96.

Braun, J.E., Huntzinger, E., Fauser, M., and Izaurralde, E. (2011). GW182 proteins directly recruit cytoplasmic deadenylase complexes to miRNA targets. *Mol. Cell 44*, 120–133.

Braun, J.E., Truffault, V., Boland, A., Huntzinger, E., Chang, C.-T., Haas, G., Weichenrieder, O., Coles, M., and Izaurralde, E. (2012). A direct interaction between DCP1 and XRN1 couples mRNA decapping to 5' exonucleolytic degradation. *Nat. Struct. Mol. Biol. 19*, 1324–1331.

Brennecke, J., Aravin, A.A., Stark, A., Dus, M., Kellis, M., Sachidanandam, R., and Hannon, G.J. (2007). Discrete small RNA-generating loci as master regulators of transposon activity in *Drosophila*. *Cell 128*, 1089–1103.

Bridge, K.S., Shah, K.M., Li, Y., Foxler, D.E., Wong, S.C.K., Miller, D.C., Davidson, K.M., Foster, J.G., Rose, R., Hodgkinson, M.R., et al. (2017). Argonaute Utilization for miRNA Silencing Is Determined by Phosphorylation-Dependent Recruitment of LIM-Domain-Containing Proteins. *Cell Reports 20*, 173–187.

Brown, M.R., and Barker, J. (1999). Unexplored reservoirs of pathogenic bacteria: protozoa and biofilms. *Trends Microbiol 7*, 46–50.

Brüggemann, H., Hagman, A., Jules, M., Sismeiro, O., Dillies, M.-A., Gouyette, C., Kunst, F., Steinert, M., Heuner, K., Coppée, J.-Y., et al. (2006). Virulence strategies for infecting phagocytes deduced from the in vivo transcriptional program of *Legionella pneumophila. Cell Microbiol 8*, 1228–1240.

Bruin, J.P., Koshkolda, T., IJzerman, E.P.F., Lück, C., Diederen, B.M.W., Den Boer, J.W., and Mouton, J.W. (2014). Isolation of ciprofloxacin-resistant *Legionella pneumophila* in a patient with severe pneumonia. *J Antimicrob Chemother 69*, 2869–2871.

Bucher, E., Hemmes, H., de Haan, P., Goldbach, R., and Prins, M. (2004). The influenza A virus NS1 protein binds small interfering RNAs and suppresses RNA silencing in plants. *J Gen Virol 85*, 983–991.

Bueno, M.J., Pérez de Castro, I., Gómez de Cedrón, M., Santos, J., Calin, G.A., Cigudosa, J.C., Croce, C.M., Fernández-Piqueras, J., and Malumbres, M. (2008). Genetic and epigenetic silencing of microRNA-203 enhances ABL1 and BCR-ABL1 oncogene expression. *Cancer Cell 13*, 496–506.

Bürckstümmer, T., Baumann, C., Blüml, S., Dixit, E., Dürnberger, G., Jahn, H., Planyavsky, M., Bilban, M., Colinge, J., Bennett, K.L., et al. (2009). An orthogonal proteomic-genomic screen identifies AIM2 as a cytoplasmic DNA sensor for the inflammasome. *Nat Immunol 10*, 266–272.

Burstein, D., Amaro, F., Zusman, T., Lifshitz, Z., Cohen, O., Gilbert, J.A., Pupko, T., Shuman, H.A., and Segal, G. (2016). Genomic analysis of 38 *Legionella* species identifies large and diverse effector repertoires. *Nat Genet 48*, 167–175.

Buscaill, P., and Rivas, S. (2014). Transcriptional control of plant defence responses. *Curr Opin Plant Biol 20*, 35–46.

Byrne, B., and Swanson, M.S. (1998). Expression of *Legionella pneumophila* virulence traits in response to growth conditions. *Infect Immun 66*, 3029–3034.

Cai, Q., Qiao, L., Wang, M., He, B., Lin, F.-M., Palmquist, J., Huang, S.-D., and Jin, H. (2018). Plants send small RNAs in extracellular vesicles to fungal pathogen to silence virulence genes. *Science 360*, 1126–1129.

Cai, X., Hagedorn, C.H., and Cullen, B.R. (2004). Human microRNAs are processed from capped, polyadenylated transcripts that can also function as mRNAs. *RNA 10*, 1957–1966.

Campbell, C.L., Black, W.C., Hess, A.M., and Foy, B.D. (2008). Comparative genomics of small RNA regulatory pathway components in vector mosquitoes. *BMC Genomics 9*, 425.

Caplen, N.J., Fleenor, J., Fire, A., and Morgan, R.A. (2000). dsRNA-mediated gene silencing in cultured *Drosophila* cells: a tissue culture model for the analysis of RNA interference. *Gene 252*, 95–105.

Carré, C., Jacquier, C., Bougé, A.-L., Chaumont, F. de, Besnard-Guerin, C., Thomassin, H., Pidoux, J., Silva, B.D., Chalatsi, E., Zahra, S., et al. (2013). AutomiG, a Biosensor to Detect Alterations in miRNA Biogenesis and in Small RNA Silencing Guided by Perfect Target Complementarity. *PLOS ONE 8*, e74296.

Cazalet, C., Rusniok, C., Brüggemann, H., Zidane, N., Magnier, A., Ma, L., Tichit, M., Jarraud, S., Bouchier, C., Vandenesch, F., et al. (2004). Evidence in the *Legionella pneumophila* genome for exploitation of host cell functions and high genome plasticity. *Nat Genet 36*, 1165–1173.

Centers for Disease Control and Prevention (CDC) (2020). Legionnaires' Disease Surveillance. *Summary Report*, United States, 2016-2017.

Ceppi, M., Pereira, P.M., Dunand-Sauthier, I., Barras, E., Reith, W., Santos, M.A., and Pierre, P. (2009). MicroRNA-155 modulates the interleukin-1 signaling pathway in activated human monocyte-derived dendritic cells. *PNAS 106(8),* 2735-40.

Chandan, K., Gupta, M., and Sarwat, M. (2019). Role of Host and Pathogen-Derived MicroRNAs in Immune Regulation During Infectious and Inflammatory Diseases. *Front Immunol 10*, 3081.

Chang, Y.-Y., Stévenin, V., Duchateau, M., Giai Gianetto, Q., Hourdel, V., Rodrigues, C.D., Matondo, M., Reiling, N., and Enninga, J. (2020). Shigella hijacks the exocyst to cluster macropinosomes for efficient vacuolar escape. *PLoS Pathog 16*, e1008822.

Chao, J.A., Lee, J.H., Chapados, B.R., Debler, E.W., Schneemann, A., and Williamson, J.R. (2005). Dual modes of RNA-silencing suppression by Flock House virus protein B2. *Nat. Struct. Mol. Biol. 12*, 952–957.

Charpentier, X., Gabay, J.E., Reyes, M., Zhu, J.W., Weiss, A., and Shuman, H.A. (2009). Chemical genetics reveals bacterial and host cell functions critical for type IV effector translocation by *Legionella pneumophila. PLoS Pathog 5*, e1000501.

Chauhan, D., and Shames, S.R. (2021). Pathogenicity and Virulence of *Legionella*: Intracellular replication and host response. *Virulence 12*, 1122–1144.

Chavarría-Smith, J., and Vance, R.E. (2013). Direct Proteolytic Cleavage of NLRP1B Is Necessary and Sufficient for Inflammasome Activation by Anthrax Lethal Factor. *PLOS Pathogens 9*, e1003452.

Chekulaeva, M., Parker, R., and Filipowicz, W. (2010). The GW/WG repeats of *Drosophila* GW182 function as effector motifs for miRNA-mediated repression. *Nucleic Acids Res 38*, 6673–6683.

Chekulaeva, M., Mathys, H., Attig, J., Colic, M., Parker, R., and Filipowicz, W. (2011). miRNA repression involves GW182-mediated recruitment of CCR4-NOT through conserved W-containing motifs. *Nat. Struct. Mol. Biol. 18*, 1218–1226.

Cheloufi, S., Dos Santos, C.O., Chong, M.M.W., and Hannon, G.J. (2010). A Dicer-independent miRNA biogenesis pathway that requires Ago catalysis. *Nature 465*, 584–589.

Chen, G., Zhuchenko, O., and Kuspa, A. (2007). Immune-like Phagocyte Activity in the Social Amoeba. *Science 317*, 678–681.

Chen, W., Zhang, Z., Chen, J., Zhang, J., Zhang, J., Wu, Y., Huang, Y., Cai, X., and Huang, A. (2008). HCV core protein interacts with Dicer to antagonize RNA silencing. *Virus Research 133*, 250–258.

Chen, Y., Boland, A., Kuzuoğlu-Öztürk, D., Bawankar, P., Loh, B., Chang, C.-T., Weichenrieder, O., and Izaurralde, E. (2014). A DDX6-CNOT1 complex and W-binding pockets in CNOT9 reveal direct links between miRNA target recognition and silencing. *Mol. Cell 54*, 737–750.

Chendrimada, T.P., Finn, K.J., Ji, X., Baillat, D., Gregory, R.I., Liebhaber, S.A., Pasquinelli, A.E., and Shiekhattar, R. (2007). MicroRNA silencing through RISC recruitment of eIF6. *Nature 447*, 823–828.

Chinnappan, M., Singh, A.K., Kakumani, P.K., Kumar, G., Rooge, S.B., Kumari, A., Varshney, A., Rastogi, A., Singh, A.K., Sarin, S.K., et al. (2014). Key elements of the RNAi pathway are regulated by hepatitis B virus replication and HBx acts as a viral suppressor of RNA silencing. *Biochem J 462*, 347–358.

Christie, M., Boland, A., Huntzinger, E., Weichenrieder, O., and Izaurralde, E. (2013). Structure of the PAN3 pseudokinase reveals the basis for interactions with the PAN2 deadenylase and the GW182 proteins. *Mol Cell 51*, 360–373.

Chu, C., and Rana, T.M. (2006). Translation repression in human cells by microRNA-induced gene silencing requires RCK/p54. *PLoS Biol. 4*, e210.

Chung, E.-H., Cunha, L. da, Wu, A.-J., Gao, Z., Cherkis, K., Afzal, A.J., Mackey, D., and Dangl, J.L. (2011). Specific Threonine Phosphorylation of a Host Target by Two Unrelated Type III Effectors Activates a Host Innate Immune Receptor in Plants. *Cell Host & Microbe 9*, 125–136.

Chung, E.-H., El-Kasmi, F., He, Y., Loehr, A., and Dangl, J.L. (2014). A Plant Phosphoswitch Platform Repeatedly Targeted by Type III Effector Proteins Regulates the Output of Both Tiers of Plant Immune Receptors. *Cell Host & Microbe 16*, 484–494.

Cianciotto, N.P. (2013). Type II secretion and *Legionella* virulence. *Curr Top Microbiol Immunol 376*, 81–102.

Cifuentes, D., Xue, H., Taylor, D.W., Patnode, H., Mishima, Y., Cheloufi, S., Ma, E., Mane, S., Hannon, G.J., Lawson, N.D., et al. (2010). A novel miRNA processing pathway independent of Dicer requires Argonaute2 catalytic activity. *Science 328*, 1694–1698.

Cirillo, J.D., Cirillo, S.L., Yan, L., Bermudez, L.E., Falkow, S., and Tompkins, L.S. (1999). Intracellular growth in *Acanthamoeba castellanii* affects monocyte entry mechanisms and enhances virulence of *Legionella pneumophila*. *Infect Immun 67*, 4427–4434.

Clare, S., John, V., Walker, A.W., Hill, J.L., Abreu-Goodger, C., Hale, C., Goulding, D., Lawley, T.D., Mastroeni, P., Frankel, G., et al. (2013). Enhanced susceptibility to *Citrobacter rodentium* infection in microRNA-155-deficient mice. *Infect.Immun. 81*, 723–732.

Cogoni, C., Irelan, J.T., Schumacher, M., Schmidhauser, T.J., Selker, E.U., and Macino, G. (1996). Transgene silencing of the al-1 gene in vegetative cells of *Neurospora* is mediated by a cytoplasmic effector and does not depend on DNA-DNA interactions or DNA methylation. *EMBO J 15*, 3153–3163.

Cookson, B.T., and Brennan, M.A. (2001). Pro-inflammatory programmed cell death. *Trends Microbiol 9*, 113–114.

Correia, A.M., Ferreira, J.S., Borges, V., Nunes, A., Gomes, B., Capucho, R., Gonçalves, J., Antunes, D.M., Almeida, S., Mendes, A., et al. (2016). Probable Person-to-Person Transmission of Legionnaires' Disease. *N Engl J Med 374*, 497–498.

Cosson, P., and Soldati, T. (2008). Eat, kill or die: when amoeba meets bacteria. *Curr Opin Microbiol 11*, 271–276.

Craven, R.R., Gao, X., Allen, I.C., Gris, D., Bubeck Wardenburg, J., McElvania-Tekippe, E., Ting, J.P., and Duncan, J.A. (2009). Staphylococcus aureus alpha-hemolysin activates the NLRP3-inflammasome in human and mouse monocytic cells. *PLoS One 4,* e7446.

Cross, K.E., Mercante, J.W., Benitez, A.J., Brown, E.W., Diaz, M.H., and Winchell, J.M. (2016). Simultaneous detection of *Legionella* species and *L. anisa*, *L. bozemanii*, *L. longbeachae* and *L. micdadei* using conserved primers and multiple probes in a multiplex real-time PCR assay. *Diagn Microbiol Infect Dis 85*, 295–301.

Crosse, K.M., Monson, E.A., Beard, M.R., and Helbig, K.J. (2018). Interferon-Stimulated Genes as Enhancers of Antiviral Innate Immune Signaling. *J Innate Immun 10*, 85–93.

Cui, C., Griffiths, A., Li, G., Silva, L.M., Kramer, M.F., Gaasterland, T., Wang, X.-J., and Coen, D.M. (2006). Prediction and identification of *herpes simplex virus* 1-encoded microRNAs. *J Virol 80*, 5499–5508.

Cui, H., Tsuda, K., and Parker, J.E. (2015a). Effector-Triggered Immunity: From Pathogen Perception to Robust Defense. *Annual Review of Plant Biology 66*, 487–511.

Cui, L., Wang, H., Ji, Y., Yang, J., Xu, S., Huang, X., Wang, Z., Qin, L., Tien, P., Zhou, X., et al. (2015b). The Nucleocapsid Protein of Coronaviruses Acts as a Viral Suppressor of RNA Silencing in Mammalian Cells. *Journal of Virology 89*, 9029–9043.

Cullen, B.R. (2004). Transcription and processing of human microRNA precursors. *Mol. Cell 16*, 861–865.

Cunha, C.B., and Cunha, B.A. (2017). Legionnaire's Disease Since Philadelphia: Lessons Learned and Continued Progress. *Infect Dis Clin North Am 31*, 1–5.

Cunha, B.A., Burillo, A., and Bouza, E. (2016). Legionnaires' disease. *Lancet 387*, 376–385.

Curtale, G., Mirolo, M., Renzi, T.A., Rossato, M., Bazzoni, F., and Locati, M. (2013). Negative regulation of Toll-like receptor 4 signaling by IL-10–dependent microRNA-146b. *PNAS 110*, 11499–11504.

Dallaire, A., and Simard, M.J. (2016). The implication of microRNAs and endo-siRNAs in animal germline and early development. *Dev Biol 416*, 18–25.

Dalmasso, G., Nguyen, H.T.T., Yan, Y., Laroui, H., Charania, M.A., Ayyadurai, S., Sitaraman, S.V., and Merlin, D. (2011). Microbiota modulate host gene expression via microRNAs. *PLoS ONE 6*, e19293.

D'Angelo, W., Acharya, D., Wang, R., Wang, J., Gurung, C., Chen, B., Bai, F., and Guo, Y.-L. (2016). Development of Antiviral Innate Immunity During In Vitro Differentiation of Mouse Embryonic Stem Cells. *Stem Cells Dev. 25*, 648–659.

Daniels, S.M., Sinck, L., Ward, N.J., Melendez-Peña, C.E., Scarborough, R.J., Azar, I., Rance, E., Daher, A., Pang, K.-M., Rossi, J.J., et al. (2015). HIV-1 RRE RNA acts as an RNA silencing suppressor by competing with TRBP-bound siRNAs. *RNA Biol 12*, 123–135.

Das, A., Ganesh, K., Khanna, S., Sen, C.K., and Roy, S. (2014). Engulfment of apoptotic cells by macrophages: a role of microRNA-21 in the resolution of wound inflammation. *J Immunol 192*, 1120–1129.

Das, K., Garnica, O., and Dhandayuthapani, S. (2016). Modulation of Host miRNAs by Intracellular Bacterial Pathogens. *Front Cell Infect Microbiol 6*, 79.

David, R.Y.S., Combredet, C., Najburg, V., Millot, G.A., Beauclair, G., Schwikowski, B., Léger, T., Camadro, J.-M., Jacob, Y., Bellalou, J. (2019). LGP2 binds to PACT to regulate RIG-I– and MDA5-mediated antiviral responses. *Sci. Signal. 12*.

Decker, C.J., and Parker, R. (2012). P-Bodies and Stress Granules: Possible Roles in the Control of Translation and mRNA Degradation. *Cold Spring Harb Perspect Biol 4*, a012286.

Decker, T., Müller, M., and Stockinger, S. (2005). The yin and yang of type I interferon activity in bacterial infection. *Nat Rev Immunol 5*, 675–687.

Declerck, P., Behets, J., De Keersmaecker, B., and Ollevier, F. (2007). Receptor-mediated uptake of *Legionella pneumophila* by *Acanthamoeba castellanii* and *Naegleria lovaniensis*. *J Appl Microbiol 103*, 2697–2703.

Deleris, A., Gallego-Bartolome, J., Bao, J., Kasschau, K.D., Carrington, J.C., and Voinnet, O. (2006). Hierarchical action and inhibition of plant Dicer-like proteins in antiviral defense. *Science 313*, 68–71.

Derré, I., and Isberg, R.R. (2004). Macrophages from Mice with the Restrictive Lgn1 Allele Exhibit Multifactorial Resistance to *Legionella pneumophila. Infect Immun 72*, 6221–6229.

Detzer, A., Engel, C., Wünsche, W., and Sczakiel, G. (2011). Cell stress is related to re-localization of Argonaute 2 and to decreased RNA interference in human cells. *Nucleic Acids Res 39*, 2727–2741.

Diaz-Pendon, J.A., Li, F., Li, W.-X., and Ding, S.-W. (2007). Suppression of Antiviral Silencing by Cucumber Mosaic Virus 2b Protein in Arabidopsis Is Associated with Drastically Reduced Accumulation of Three Classes of Viral Small Interfering RNAs. *Plant Cell 19*, 2053–2063.

Diederichs, S., and Haber, D.A. (2007). Dual role for argonautes in microRNA processing and posttranscriptional regulation of microRNA expression. *Cell 131*, 1097–1108.

Dikic, I., and Elazar, Z. (2018). Mechanism and medical implications of mammalian autophagy. *Nat Rev Mol Cell Biol 19*, 349–364.

Ding, S.-W. (2010). RNA-based antiviral immunity. *Nat Rev Immunol 10*, 632–644.

Ding, S.-W., Han, Q., Wang, J., and Li, W.-X. (2018). Antiviral RNA interference in mammals. *Current Opinion in Immunology 54*, 109–114.

Doench, J.G., Petersen, C.P., and Sharp, P.A. (2003). siRNAs can function as miRNAs. *Genes Dev 17*, 438–442.

Doleans, A., Aurell, H., Reyrolle, M., Lina, G., Freney, J., Vandenesch, F., Etienne, J., and Jarraud, S. (2004). Clinical and environmental distributions of *Legionella* strains in France are different. J *Clin Microbiol 42*, 458–460.

Dorer, M.S., Kirton, D., Bader, J.S., and Isberg, R.R. (2006). RNA Interference Analysis of *Legionella* in *Drosophila* Cells: Exploitation of Early Secretory Apparatus Dynamics. *PLOS Pathogens 2*, e34.

Dorhoi, A., Iannaccone, M., Farinacci, M., Faé, K.C., Schreiber, J., Moura-Alves, P., Nouailles, G., Mollenkopf, H.-J., Oberbeck-Müller, D., Jörg, S., et al. (2013). MicroRNA-223 controls susceptibility to tuberculosis by regulating lung neutrophil recruitment. *J Clin Invest 123*, 4836–4848.

Dovas, A., and Couchman, J.R. (2005). RhoGDI: multiple functions in the regulation of Rho family GTPase activities. *Biochem J 390*, 1–9.

Doxaki, C., Kampranis, S.C., Eliopoulos, A.G., Spilianakis, C., and Tsatsanis, C. (2015). Coordinated Regulation of miR-155 and miR-146a Genes during Induction of Endotoxin Tolerance in Macrophages. *The Journal of Immunology 195*, 5750–5761.

Duan, X., Zhang, T., Ding, S., Wei, J., Su, C., Liu, H., and Xu, G. (2015). microRNA-17-5p Modulates Bacille Calmette-Guerin Growth in RAW264.7 Cells by Targeting ULK1. *PLOS ONE 10*, e0138011.

Dufies, O., and Boyer, L. (2021). RhoGTPases and inflammasomes: Guardians of effector-triggered immunity. *PLoS Pathog 17*, e1009504.

Dunne, W.M., Picot, N., and van Belkum, A. (2017). Laboratory Tests for Legionnaire's Disease. Infect *Dis Clin North Am 31*, 167–178.

Eckenfelder, A., Ségéral, E., Pinzón, N., Ulveling, D., Amadori, C., Charpentier, M., Nidelet, S., Concordet, J.-P., Zagury, J.-F., Paillart, J.-C., et al. (2017). Argonaute proteins regulate HIV-1 multiply spliced RNA and viral production in a Dicer independent manner. *Nucleic Acids Res 45*, 4158–4173.

Eichhorn, S.W., Guo, H., McGeary, S.E., Rodriguez-Mias, R.A., Shin, C., Baek, D., Hsu, S.-H., Ghoshal, K., Villén, J., and Bartel, D.P. (2014). mRNA destabilization is the dominant effect of mammalian microRNAs by the time substantial repression ensues. *Mol. Cell 56*, 104–115.

Elbashir, S.M., Harborth, J., Lendeckel, W., Yalcin, A., Weber, K., and Tuschl, T. (2001). Duplexes of 21-nucleotide RNAs mediate RNA interference in cultured mammalian cells. *Nature 411*, 494–498.

Elkayam, E., Kuhn, C.-D., Tocilj, A., Haase, A.D., Greene, E.M., Hannon, G.J., and Joshua-Tor, L. (2012). The Structure of Human Argonaute-2 in Complex with miR-20a. *Cell 150*, 100–110.

Elkayam, E., Faehnle, C.R., Morales, M., Sun, J., Li, H., and Joshua-Tor, L. (2017). Multivalent Recruitment of Human Argonaute by GW182. *Molecular Cell 67*, 646-658.e3.

Elliott, J.A., and Winn, W.C. (1986). Treatment of alveolar macrophages with cytochalasin D inhibits uptake and subsequent growth of *Legionella pneumophila. Infect Immun 51*, 31–36.

Ellis, J.G., Dodds, P.N., and Lawrence, G.J. (2007). Flax rust resistance gene specificity is based on direct resistance-avirulence protein interactions. *Annu Rev Phytopathol 45*, 289–306.

El-Shami, M., Pontier, D., Lahmy, S., Braun, L., Picart, C., Vega, D., Hakimi, M.-A., Jacobsen, S.E., Cooke, R., and Lagrange, T. (2007). Reiterated WG/GW motifs form functionally and evolutionarily conserved ARGONAUTE-binding platforms in RNAi-related components. *Genes Dev. 21*, 2539–2544.

Ender, C., Krek, A., Friedländer, M.R., Beitzinger, M., Weinmann, L., Chen, W., Pfeffer, S., Rajewsky, N., and Meister, G. (2008). A human snoRNA with microRNA-like functions. *Mol. Cell 32*, 519–528.

Ensminger, A.W. (2016). *Legionella pneumophila*, armed to the hilt: justifying the largest arsenal of effectors in the bacterial world. *Current Opinion in Microbiology 29*, 74–80.

Ernst, C., Odom, D.T., and Kutter, C. (2017). The emergence of piRNAs against transposon invasion to preserve mammalian genome integrity. *Nat Commun 8*, 1–10.

Escoll, P., Rolando, M., Gomez-Valero, L., and Buchrieser, C. (2014). From Amoeba to Macrophages: Exploring the Molecular Mechanisms of *Legionella pneumophila* Infection in Both Hosts. In Molecular Mechanisms in *Legionella* Pathogenesis. *Curr Top Microbiol Immunol 376*, 1-34.

Escoll, P., Song, O.-R., Viana, F., Steiner, B., Lagache, T., Olivo-Marin, J.-C., Impens, F., Brodin, P., Hilbi, H., and Buchrieser, C. (2017). *Legionella pneumophila* Modulates Mitochondrial Dynamics to Trigger Metabolic Repurposing of Infected Macrophages. *Cell Host Microbe 22*, 302-316.e7.

Eulalio, A., Behm-Ansmant, I., and Izaurralde, E. (2007a). P bodies: at the crossroads of post-transcriptional pathways. *Nat. Rev. Mol. Cell Biol. 8*, 9–22.

Eulalio, A., Behm-Ansmant, I., Schweizer, D., and Izaurralde, E. (2007b). P-body formation is a consequence, not the cause, of RNA-mediated gene silencing. *Mol Cell Biol 27*, 3970–3981.

Eulalio, A., Huntzinger, E., and Izaurralde, E. (2008). GW182 interaction with Argonaute is essential for miRNA-mediated translational repression and mRNA decay. *Nat Struct Mol Biol 15*, 346–353.

Eulalio, A., Helms, S., Fritzsch, C., Fauser, M., and Izaurralde, E. (2009a). A C-terminal silencing domain in GW182 is essential for miRNA function. *RNA 15*, 1067–1077.

Eulalio, A., Tritschler, F., and Izaurralde, E. (2009b). The GW182 protein family in animal cells: New insights into domains required for miRNA-mediated gene silencing. *RNA 15*, 1433–1442.

European Centre for Disease Prevention and Control (ECDC) (2020). Legionnaires' disease in Eurpe, 2018. ECDC. *Annual Epidemiological Report for 2018*.

Fabian, M.R., and Sonenberg, N. (2012). The mechanics of miRNA-mediated gene silencing: a look under the hood of miRISC. *Nat. Struct. Mol. Biol. 19*, 586–593.

Fabian, M.R., Mathonnet, G., Sundermeier, T., Mathys, H., Zipprich, J.T., Svitkin, Y.V., Rivas, F., Jinek, M., Wohlschlegel, J., Doudna, J.A., et al. (2009). Mammalian miRNA RISC recruits CAF1 and PABP to affect PABP-dependent deadenylation. *Mol Cell 35*, 868–880.

Fabian, M.R., Cieplak, M.K., Frank, F., Morita, M., Green, J., Srikumar, T., Nagar, B., Yamamoto, T., Raught, B., Duchaine, T.F., et al. (2011). miRNA-mediated deadenylation is orchestrated by GW182 through two conserved motifs that interact with CCR4-NOT. *Nat. Struct. Mol. Biol. 18*, 1211–1217.

Fabozzi, G., Nabel, C.S., Dolan, M.A., and Sullivan, N.J. (2011). Ebolavirus proteins suppress the effects of small interfering RNA by direct interaction with the mammalian RNA interference pathway. *J. Virol. 85*, 2512–2523.

Fajardo, M., Schleicher, M., Noegel, A., Bozzaro, S., Killinger, S., Heuner, K., Hacker, J., and Steinert, M. (2004). Calnexin, calreticulin and cytoskeleton-associated proteins modulate uptake and growth of *Legionella pneumophila* in *Dictyostelium discoideum*. *Microbiology (Reading) 150*, 2825–2835.

Farnham, A., Alleyne, L., Cimini, D., and Balter, S. (2014). Legionnaires' Disease Incidence and Risk Factors, New York, New York, USA, 2002–2011. *Emerg Infect Dis 20*, 1795–1802.

Feeley, J.C., Gibson, R.J., Gorman, G.W., Langford, N.C., Rasheed, J.K., Mackel, D.C., and Baine, W.B. (1979). Charcoal-yeast extract agar: primary isolation medium for *Legionella pneumophila. J Clin Microbiol 10*, 437–441.

de Felipe, K.S., Pampou, S., Jovanovic, O.S., Pericone, C.D., Ye, S.F., Kalachikov, S., and Shuman, H.A. (2005a). Evidence for acquisition of *Legionella* type IV secretion substrates via interdomain horizontal gene transfer. *J Bacteriol 187*, 7716–7726.

de Felipe, K.S., Pampou, S., Jovanovic, O.S., Pericone, C.D., Ye, S.F., Kalachikov, S., and Shuman, H.A. (2005b). Evidence for Acquisition of *Legionella* Type IV Secretion Substrates via Interdomain Horizontal Gene Transfer. *J Bacteriol 187*, 7716–7726.

Félix, M.-A., Ashe, A., Piffaretti, J., Wu, G., Nuez, I., Bélicard, T., Jiang, Y., Zhao, G., Franz, C.J., Goldstein, L.D., et al. (2011). Natural and experimental infection of *Caenorhabditis nematodes* by novel viruses related to nodaviruses. *PLoS Biol 9*, e1000586.

Fernandes-Alnemri, T., Yu, J.-W., Datta, P., Wu, J., and Alnemri, E.S. (2009). AIM2 activates the inflammasome and cell death in response to cytoplasmic DNA. *Nature 458*, 509–513.

Fields, B.S. (1996). The molecular ecology of *legionellae. Trends Microbiol 4*, 286–290.

Filipowicz, W., Bhattacharyya, S.N., and Sonenberg, N. (2008). Mechanisms of post-transcriptional regulation by microRNAs: are the answers in sight? *Nat. Rev. Genet. 9*, 102–114.

Filopon, D., Schiavolin, L., Bonnet, M., Sansonetti, P., Tran Van Nhieu, G., and Navarro, L. *Shigella* hijacks human Ago2 activity to promote the rupture of its phagocytic vacuole. *In Preparation.*

Fink, S.L., and Cookson, B.T. (2006). Caspase-1-dependent pore formation during pyroptosis leads to osmotic lysis of infected host macrophages. *Cell Microbiol 8*, 1812–1825.

Fire, A., Xu, S., Montgomery, M.K., Kostas, S.A., Driver, S.E., and Mello, C.C. (1998). Potent and specific genetic interference by double-stranded RNA in *Caenorhabditis elegans*. *Nature 391*, 806–811.

Flemr, M., Malik, R., Franke, V., Nejepinska, J., Sedlacek, R., Vlahovicek, K., and Svoboda, P. (2013). A retrotransposon-driven dicer isoform directs endogenous small interfering RNA production in mouse oocytes. *Cell 155*, 807–816.

Flores, O., Nakayama, S., Whisnant, A.W., Javanbakht, H., Cullen, B.R., and Bloom, D.C. (2013). Mutational inactivation of herpes simplex virus 1 microRNAs identifies viral mRNA targets and reveals phenotypic effects in culture. *J Virol 87*, 6589–6603.

Fonseca, M.V., and Swanson, M.S. (2014). Nutrient salvaging and metabolism by the intracellular pathogen *Legionella pneumophila. Front Cell Infect Microbiol 4*.

Fontana, M.F., Banga, S., Barry, K.C., Shen, X., Tan, Y., Luo, Z.-Q., and Vance, R.E. (2011). Secreted bacterial effectors that inhibit host protein synthesis are critical for induction of the innate immune response to virulent *Legionella pneumophila. PLoS Pathog 7*, e1001289.

Forster, S.C., Tate, M.D., and Hertzog, P.J. (2015). MicroRNA as Type I Interferon-Regulated Transcripts and Modulators of the Innate Immune Response. *Front Immunol 6*.

Francione, L., Smith, P.K., Accari, S.L., Taylor, P.E., Bokko, P.B., Bozzaro, S., Beech, P.L., and Fisher, P.R. (2009). *Legionella pneumophila* multiplication is enhanced by chronic AMPK signalling in mitochondrially diseased *Dictyostelium* cells. *Dis Model Mech 2*, 479–489.

Fraser, D.W., Tsai, T.R., Orenstein, W., Parkin, W.E., Beecham, H.J., Sharrar, R.G., Harris, J., Mallison, G.F., Martin, S.M., McDade, J.E., et al. (1977). Legionnaires' disease: description of an epidemic of pneumonia. *N. Engl. J. Med. 297*, 1189–1197.

Frutuoso, M.S., Hori, J.I., Pereira, M.S.F., Junior, D.S.L., Sônego, F., Kobayashi, K.S., Flavell, R.A., Cunha, F.Q., and Zamboni, D.S. (2010). The pattern recognition receptors Nod1 and Nod2 account for neutrophil recruitment to the lungs of mice infected with *Legionella pneumophila. Microbes Infect 12*, 819–827.

Fuche, F., Vianney, A., Andrea, C., Doublet, P., and Gilbert, C. (2015). Functional Type 1 Secretion System Involved in *Legionella pneumophila* Virulence. *J Bacteriol 197*, 563–571.

Fukao, A., Mishima, Y., Takizawa, N., Oka, S., Imataka, H., Pelletier, J., Sonenberg, N., Thoma, C., and Fujiwara, T. (2014). MicroRNAs trigger dissociation of eIF4AI and eIF4AII from target mRNAs in humans. *Mol. Cell 56*, 79–89.

Fukaya, T., and Tomari, Y. (2012). MicroRNAs mediate gene silencing via multiple different pathways in *drosophila*. *Mol. Cell 48*, 825–836.

Fukazawa, A., Alonso, C., Kurachi, K., Gupta, S., Lesser, C.F., McCormick, B.A., and Reinecker, H.-C. (2008). GEF-H1 mediated control of NOD1 dependent NF-kappaB activation by *Shigella* effectors. *PLoS Pathog 4*, e1000228.

Fuse, E.T., Tateda, K., Kikuchi, Y., Matsumoto, T., Gondaira, F., Azuma, A., Kudoh, S., Standiford, T.J., and Yamaguchi, K. (2007). Role of Toll-like receptor 2 in recognition of *Legionella pneumophila* in a murine pneumonia model. *J Med Microbiol 56*, 305–312.

Galiana-Arnoux, D., Dostert, C., Schneemann, A., Hoffmann, J.A., and Imler, J.-L. (2006). Essential function in vivo for Dicer-2 in host defense against RNA viruses in *drosophila*. *Nat. Immunol. 7*, 590–597.

Gantier, M.P., Stunden, H.J., McCoy, C.E., Behlke, M.A., Wang, D., Kaparakis-Liaskos, M., Sarvestani, S.T., Yang, Y.H., Xu, D., Corr, S.C., et al. (2012). A miR-19 regulon that controls NF-κB signaling. *Nucleic Acids Res 40*, 8048–8058.

Ge, J., Xu, H., Li, T., Zhou, Y., Zhang, Z., Li, S., Liu, L., and Shao, F. (2009). A *Legionella* type IV effector activates the NF-κB pathway by phosphorylating the IκB family of inhibitors. *Proc Natl Acad Sci U S A 106*, 13725–13730.

Ge, J., Gong, Y.-N., Xu, Y., and Shao, F. (2012). Preventing bacterial DNA release and absent in melanoma 2 inflammasome activation by a Legionella effector functioning in membrane trafficking. *PNAS 109*, 6193–6198.

Ghildiyal, M., and Zamore, P.D. (2009). Small silencing RNAs: an expanding universe. *Nature Reviews Genetics 10*, 94–108.

Ghosh, S., and Jacobson, A. (2010). RNA decay modulates gene expression and controls its fidelity. *Wiley Interdiscip Rev RNA 1*, 351–361.

Gibbings, D.J., Ciaudo, C., Erhardt, M., and Voinnet, O. (2009). Multivesicular bodies associate with components of miRNA effector complexes and modulate miRNA activity. *Nat. Cell Biol. 11*, 1143–1149.

Giner, A., Lakatos, L., García-Chapa, M., López-Moya, J.J., and Burgyán, J. (2010). Viral Protein Inhibits RISC Activity by Argonaute Binding through Conserved WG/GW Motifs. *PLoS Pathogens 6*, e1000996.

Girard, R., Pedron, T., Uematsu, S., Balloy, V., Chignard, M., Akira, S., and Chaby, R. (2003). Lipopolysaccharides from *Legionella* and *Rhizobium* stimulate mouse bone marrow granulocytes via Toll-like receptor 2. *J Cell Sci 116*, 293–302.

Girardi, E., Chane-Woon-Ming, B., Messmer, M., Kaukinen, P., and Pfeffer, S. (2013). Identification of RNase L-dependent, 3'-end-modified, viral small RNAs in Sindbis virus-infected mammalian cells. *MBio 4*, e00698-00613.

Girardi, E., López, P., and Pfeffer, S. (2018). On the Importance of Host MicroRNAs During Viral Infection. *Front Genet 9*.

Glöckner, G., Albert-Weissenberger, C., Weinmann, E., Jacobi, S., Schunder, E., Steinert, M., Hacker, J., and Heuner, K. (2008). Identification and characterization of a new conjugation/type IVA secretion system (trb/tra) of *Legionella pneumophila Corby* localized on two mobile genomic islands. *International Journal of Medical Microbiology 298*, 411–428.

Gomez-Valero, L., Rusniok, C., Rolando, M., Neou, M., Dervins-Ravault, D., Demirtas, J., Rouy, Z., Moore, R.J., Chen, H., Petty, N.K., et al. (2014). Comparative analyses of *Legionella* species identifies genetic features of strains causing Legionnaires' disease. *Genome Biol 15*, 505.

Gomez-Valero, L., Rusniok, C., Carson, D., Mondino, S., Pérez-Cobas, A.E., Rolando, M., Pasricha, S., Reuter, S., Demirtas, J., Crumbach, J., et al. (2019). More than 18,000 effectors in the *Legionella genus* genome provide multiple, independent combinations for replication in human cells. *Proc Natl Acad Sci U S A 116*, 2265–2273.

Gottwein, E., and Cullen, B.R. (2008). Viral and Cellular MicroRNAs as Determinants of Viral Pathogenesis and Immunity. *Cell Host & Microbe 3*, 375–387.

Griebel, T., Maekawa, T., and Parker, J.E. (2014). NOD-like receptor cooperativity in effector-triggered immunity. *Trends Immunol 35*, 562–570.

Gu, H., Zhao, C., Zhang, T., Liang, H., Wang, X.-M., Pan, Y., Chen, X., Zhao, Q., Li, D., Liu, F., et al. (2017). Salmonella produce microRNA-like RNA fragment Sal-1 in the infected cells to facilitate intracellular survival. *Sci Rep 7*.

Gulati, A., Kaur, D., Krishna Prasad, G.V.R., and Mukhopadhaya, A. (2018). PRR Function of Innate Immune Receptors in Recognition of Bacteria or Bacterial Ligands. *Adv Exp Med Biol 1112*, 255–280.

Guo, H., Ingolia, N.T., Weissman, J.S., and Bartel, D.P. (2010). Mammalian microRNAs predominantly act to decrease target mRNA levels. *Nature 466*, 835–840.

Guo, Y.-L., Fitz, J., Schneeberger, K., Ossowski, S., Cao, J., and Weigel, D. (2011). Genome-Wide Comparison of Nucleotide-Binding Site-Leucine-Rich Repeat-Encoding Genes in *Arabidopsis. Plant Physiology 157*, 757–769.

Haase, A.D., Jaskiewicz, L., Zhang, H., Lainé, S., Sack, R., Gatignol, A., and Filipowicz, W. (2005). TRBP, a regulator of cellular PKR and HIV-1 virus expression, interacts with Dicer and functions in RNA silencing. *EMBO Rep 6*, 961–967.

Haasnoot, J., de Vries, W., Geutjes, E.-J., Prins, M., de Haan, P., and Berkhout, B. (2007). The *Ebola* Virus VP35 Protein Is a Suppressor of RNA Silencing. *PLoS Pathog 3*.

Hackett, E.E., Charles-Messance, H., O'Leary, S.M., Gleeson, L.E., Muñoz-Wolf, N., Case, S., Wedderburn, A., Johnston, D.G.W., Williams, M.A., Smyth, A., et al. (2020). Mycobacterium tuberculosis Limits Host Glycolysis and IL-1β by Restriction of PFK-M via MicroRNA-21. *Cell Rep 30*, 124-136.e4.

Hamilton, A.J., and Baulcombe, D.C. (1999). A Species of Small Antisense RNA in Posttranscriptional Gene Silencing in Plants. *Science 286*, 950–952.

Harrison, T.G., Doshi, N., Fry, N.K., and Joseph, C.A. (2007). Comparison of clinical and environmental isolates of *Legionella pneumophila* obtained in the UK over 19 years. *Clin Microbiol Infect 13*, 78–85.

Harvey, J.J.W., Lewsey, M.G., Patel, K., Westwood, J., Heimstädt, S., Carr, J.P., and Baulcombe, D.C. (2011). An antiviral defense role of AGO2 in plants. *PLoS One 6*, e14639.

Hashimi, S.T., Fulcher, J.A., Chang, M.H., Gov, L., Wang, S., and Lee, B. (2009). MicroRNA profiling identifies miR-34a and miR-21 and their target genes JAG1 and WNT1 in the coordinate regulation of dendritic cell differentiation. *Blood 114*, 404–414.

Hauptmann, J., Dueck, A., Harlander, S., Pfaff, J., Merkl, R., and Meister, G. (2013). Turning catalytically inactive human Argonaute proteins into active slicer enzymes. *Nature Structural & Molecular Biology 20*, 814–817.

Hauptmann, J., Kater, L., Löffler, P., Merkl, R., and Meister, G. (2014). Generation of catalytic human Ago4 identifies structural elements important for RNA cleavage. *RNA 20*, 1532–1538.

Hauptmann, J., Schraivogel, D., Bruckmann, A., Manickavel, S., Jakob, L., Eichner, N., Pfaff, J., Urban, M., Sprunck, S., Hafner, M., et al. (2015). Biochemical isolation of Argonaute protein complexes by Ago-APP. *Proc Natl Acad Sci U S A 112*, 11841–11845.

Hawn, T.R., Verbon, A., Lettinga, K.D., Zhao, L.P., Li, S.S., Laws, R.J., Skerrett, S.J., Beutler, B., Schroeder, L., Nachman, A., et al. (2003). A Common Dominant TLR5 Stop Codon Polymorphism Abolishes Flagellin Signaling and Is Associated with Susceptibility to Legionnaires' Disease. *J Exp Med 198*, 1563–1572.

Hawn, T.R., Smith, K.D., Aderem, A., and Skerrett, S.J. (2006). Myeloid differentiation primary response gene (88)- and toll-like receptor 2-deficient mice are susceptible to infection with aerosolized *Legionella pneumophila. J Infect Dis 193*, 1693–1702.

Hayashi, T., Miyake, M., Fukui, T., Sugaya, N., Daimon, T., Itoh, S., Oku, T., Tsuji, T., Toyoshima, S., and Imai, Y. (2008). Exclusion of actin-binding protein p57/coronin-1 from bacteria-containing phagosomes in macrophages infected with *Legionella. Biol Pharm Bull 31*, 861–865.

Hayashi, Y., Tsujii, M., Wang, J., Kondo, J., Akasaka, T., Jin, Y., Li, W., Nakamura, T., Nishida, T., Iijima, H., et al. (2013). CagA mediates epigenetic regulation to attenuate let-7 expression in Helicobacter pylori-related carcinogenesis. *Gut 62*, 1536–1546.

Hellmich, K.A., Levinsohn, J.L., Fattah, R., Newman, Z.L., Maier, N., Sastalla, I., Liu, S., Leppla, S.H., and Moayeri, M. (2012). Anthrax Lethal Factor Cleaves Mouse Nlrp1b in Both Toxin-Sensitive and Toxin-Resistant Macrophages. *PLOS ONE 7*, e49741.

Helwak, A., Kudla, G., Dudnakova, T., and Tollervey, D. (2013). Mapping the Human miRNA Interactome by CLASH Reveals Frequent Noncanonical Binding. *Cell 153*, 654–665.

Hempstead, A.D., and Isberg, R.R. (2013). Host signal transduction and protein kinases implicated in *Legionella* infection. *Curr Top Microbiol Immunol 376*, 249–269.

Herkt, C.E., Caffrey, B.E., Surmann, K., Blankenburg, S., Gesell Salazar, M., Jung, A.L., Herbel, S.M., Hoffmann, K., Schulte, L.N., Chen, W., et al. (2020). A MicroRNA Network Controls *Legionella pneumophila* Replication in Human Macrophages via LGALS8 and MX1. *MBio 11*.

Hervet, E., Charpentier, X., Vianney, A., Lazzaroni, J.-C., Gilbert, C., Atlan, D., and Doublet, P. (2011). Protein kinase LegK2 is a type IV secretion system effector involved in endoplasmic reticulum recruitment and intracellular replication of *Legionella pneumophila. Infect Immun 79*, 1936–1950.

Heyam, A., Lagos, D., and Plevin, M. (2015). Dissecting the roles of TRBP and PACT in double-stranded RNA recognition and processing of noncoding RNAs. *WIREs RNA 6*, 271–289.

Hicks, J.A., Li, L., Matsui, M., Chu, Y., Volkov, O., Johnson, K.C., and Corey, D.R. (2017). Human GW182 Paralogs are the Central Organizers for RNA-Mediated Control of Transcription. *Cell Rep 20*, 1543–1552.

Hilbi, H., Segal, G., and Shuman, H.A. (2001). Icm/dot-dependent upregulation of phagocytosis by *Legionella pneumophila. Mol Microbiol 42*, 603–617.

Hinas, A., Reimegård, J., Wagner, E.G.H., Nellen, W., Ambros, V.R., and Söderbom, F. (2007). The small RNA repertoire of Dictyostelium discoideum and its regulation by components of the RNAi pathway. *Nucleic Acids Res 35*, 6714–6726.

Hoeke, L., Sharbati, J., Pawar, K., Keller, A., Einspanier, R., and Sharbati, S. (2013). Intestinal *Salmonella typhimurium* infection leads to miR-29a induced caveolin 2 regulation. *PLoS ONE 8*, e67300.

Hoffmann, C., Harrison, C.F., and Hilbi, H. (2014). The natural alternative: protozoa as cellular models for *Legionella* infection. *Cell Microbiol 16*, 15–26.

Hoorn, R.A.L. van der, and Kamoun, S. (2008). From Guard to Decoy: A New Model for Perception of Plant Pathogen Effectors. *The Plant Cell 20*, 2009–2017.

Horman, S.R., Janas, M.M., Litterst, C., Wang, B., MacRae, I.J., Sever, M.J., Morrissey, D.V., Graves, P., Luo, B., Umesalma, S., et al. (2013). Akt-mediated phosphorylation of Argonaute 2 down-regulates cleavage and up-regulates translational repression of microRNA targets. *Mol Cell 50*, 356–367.

Hornung, V., Ablasser, A., Charrel-Dennis, M., Bauernfeind, F., Horvath, G., Caffrey, D.R., Latz, E., and Fitzgerald, K.A. (2009). AIM2 recognizes cytosolic dsDNA and forms a caspase-1-activating inflammasome with ASC. *Nature 458*, 514–518.

Horwitz, M. (1984). Phagocytosis of the legionnaires' disease bacterium (l*egionella pneumophila*) occurs by a novel mechanism: Engulfment within a Pseudopod coil. *Cell 36*, 27–33.

Horwitz, M.A. (1983a). The Legionnaires' disease bacterium (*Legionella pneumophila*) inhibits phagosome-lysosome fusion in human monocytes. *J Exp Med 158*, 2108–2126.

Horwitz, M.A. (1983b). Formation of a novel phagosome by the Legionnaires' disease bacterium (*Legionella pneumophila*) in human monocytes. *J Exp Med 158*, 1319–1331.

Hou, J., Wang, P., Lin, L., Liu, X., Ma, F., An, H., Wang, Z., and Cao, X. (2009). MicroRNA-146a feedback inhibits RIG-I-dependent Type I IFN production in macrophages by targeting TRAF6, IRAK1, and IRAK2. *J Immunol 183*, 2150–2158.

Hou, Y., Zhai, Y., Feng, L., Karimi, H.Z., Rutter, B.D., Zeng, L., Choi, D.S., Zhang, B., Gu, W., Chen, X., et al. (2019). A Phytophthora Effector Suppresses Trans-Kingdom RNAi to Promote Disease Susceptibility. *Cell Host & Microbe 25*, 153-165.e5.

Huang, J., and Brumell, J.H. (2014). Bacteria-autophagy interplay: a battle for survival. *Nat Rev Microbiol 12*, 101–114.

Huang, C.-Y., Wang, H., Hu, P., Hamby, R., and Jin, H. (2019). Small RNAs – Big Players in Plant-Microbe Interactions. *Cell Host & Microbe 26*, 173–182.

Hubber, A., and Roy, C.R. (2010). Modulation of host cell function by *Legionella pneumophila* type IV effectors. *Annu Rev Cell Dev Biol 26*, 261–283.

Hudzik, C., Hou, Y., Ma, W., and Axtell, M.J. (2020). Exchange of Small Regulatory RNAs between Plants and Their Pests1[OPEN]. *Plant Physiol 182*, 51–62.

Huntzinger, E., and Izaurralde, E. (2011). Gene silencing by microRNAs: contributions of translational repression and mRNA decay. *Nat. Rev. Genet. 12*, 99–110.

Huntzinger, E., Braun, J.E., Heimstädt, S., Zekri, L., and Izaurralde, E. (2010). Two PABPC1-binding sites in GW182 proteins promote miRNA-mediated gene silencing. *EMBO J 29*, 4146–4160.

Huntzinger, E., Kuzuoğlu-Öztürk, D., Braun, J.E., Eulalio, A., Wohlbold, L., and Izaurralde, E. (2013). The interactions of GW182 proteins with PABP and deadenylases are required for both translational repression and degradation of miRNA targets. *Nucleic Acids Res 41*, 978–994.

Hutvágner, G., McLachlan, J., Pasquinelli, A.E., Bálint, E., Tuschl, T., and Zamore, P.D. (2001). A cellular function for the RNA-interference enzyme Dicer in the maturation of the let-7 small temporal RNA. *Science 293*, 834–838.

Iliopoulos, D., Hirsch, H.A., and Struhl, K. (2009). An Epigenetic Switch Involving NF-κB, Lin28, Let-7 MicroRNA, and IL6 Links Inflammation to Cell Transformation. *Cell 139*, 693–706.

Inohara, N., Chamaillard, M., McDonald, C., and Nuñez, G. (2005). NOD-LRR proteins: role in host-microbial interactions and inflammatory disease. *Annu. Rev. Biochem. 74*, 355–383.

Isberg, R.R., O'Connor, T.J., and Heidtman, M. (2009). The *Legionella pneumophila* replication vacuole: making a cosy niche inside host cells. *Nat Rev Microbiol 7,* 13–24.

Iwakawa, H.-O., and Tomari, Y. (2015). The Functions of MicroRNAs: mRNA Decay and Translational Repression. *Trends Cell Biol. 25*, 651–665.

Iwasaki, S., Kobayashi, M., Yoda, M., Sakaguchi, Y., Katsuma, S., Suzuki, T., and Tomari, Y. (2010). Hsc70/Hsp90 chaperone machinery mediates ATP-dependent RISC loading of small RNA duplexes. *Mol. Cell 39*, 292–299.

Jacob, F., Vernaldi, S., and Maekawa, T. (2013). Evolution and Conservation of Plant NLR Functions. *Front. Immunol. 4*.

Janeway, C.A. (1989). Approaching the asymptote? Evolution and revolution in immunology. *Cold Spring Harb Symp Quant Biol 54 Pt 1*, 1–13.

Jia, Y., McAdams, S.A., Bryan, G.T., Hershey, H.P., and Valent, B. (2000). Direct interaction of resistance gene and avirulence gene products confers rice blast resistance. *EMBO J 19*, 4004–4014.

Jin, W., Ibeagha-Awemu, E.M., Liang, G., Beaudoin, F., Zhao, X., and Guan, L.L. (2014). Transcriptome microRNA profiling of bovine mammary epithelial cells challenged with *Escherichia coli* or *Staphylococcus aureusbacteria* reveals pathogen directed microRNA expression profiles. *BMC Genomics 15*, 181.

Jin, Y., Zhao, J.-H., and Guo, H.-S. (2021). Recent advances in understanding plant antiviral RNAi and viral suppressors of RNAi. *Curr Opin Virol 46*, 65–72.

Jo, M.H., Shin, S., Jung, S.-R., Kim, E., Song, J.-J., and Hohng, S. (2015). Human Argonaute 2 Has Diverse Reaction Pathways on Target RNAs. *Mol Cell 59*, 117–124.

Johnnidis, J.B., Harris, M.H., Wheeler, R.T., Stehling-Sun, S., Lam, M.H., Kirak, O., Brummelkamp, T.R., Fleming, M.D., and Camargo, F.D. (2008). Regulation of progenitor cell proliferation and granulocyte function by microRNA-223. *Nature 451*, 1125–1129.

Jonas, S., and Izaurralde, E. (2015). Towards a molecular understanding of microRNA-mediated gene silencing. *Nat. Rev. Genet*. *16*, 421–433.

Jones, J.D.G., Vance, R.E., and Dangl, J.L. (2016). Intracellular innate immune surveillance devices in plants and animals. *Science 354*.

Joseph, A.M., and Shames, S.R. (2021). Affecting the Effectors: Regulation of *Legionella pneumophila* Effector Function by Metaeffectors. *Pathogens 10*.

Joshi, A.D., and Swanson, M.S. (2011). Secrets of a Successful Pathogen: *Legionella* Resistance to Progression Along the Autophagic Pathway. *Front Microbiol 2*, 138.

Jovanovic, M., and Hengartner, M.O. (2006). miRNAs and apoptosis: RNAs to die for. *Oncogene 25*, 6176–6187.

Jung, A.L., Stoiber, C., Herkt, C.E., Schulz, C., Bertrams, W., and Schmeck, B. (2016). *Legionella pneumophila*-Derived Outer Membrane Vesicles Promote Bacterial Replication in Macrophages. *PLoS Pathog 12*, e1005592.

Kagan, J.C., and Roy, C.R. (2002). *Legionella* phagosomes intercept vesicular traffic from endoplasmic reticulum exit sites. *Nat Cell Biol 4*, 945–954.

Kagan, J.C., Stein, M.-P., Pypaert, M., and Roy, C.R. (2004). *Legionella* Subvert the Functions of Rab1 and Sec22b to Create a Replicative Organelle. *J Exp Med 199*, 1201–1211.

Kahvejian, A., Svitkin, Y.V., Sukarieh, R., M'Boutchou, M.-N., and Sonenberg, N. (2005). Mammalian poly(A)-binding protein is a eukaryotic translation initiation factor, which acts via multiple mechanisms. *Genes Dev 19*, 104–113.

Kakumani, P.K., Ponia, S.S., S, R.K., Sood, V., Chinnappan, M., Banerjea, A.C., Medigeshi, G.R., Malhotra, P., Mukherjee, S.K., and Bhatnagar, R.K. (2013). Role of RNA interference (RNAi) in dengue virus replication and identification of NS4B as an RNAi suppressor. *J. Virol. 87*, 8870–8883.

Kakumani, P.K., Rajgokul, K.S., Ponia, S.S., Kaur, I., Mahanty, S., Medigeshi, G.R., Banerjea, A.C., Chopra, A.P., Malhotra, P., Mukherjee, S.K., et al. (2015). Dengue NS3, an RNAi suppressor, modulates the human miRNA pathways through its interacting partner. *Biochem J 471*, 89–99.

Kamenska, A., Simpson, C., Vindry, C., Broomhead, H., Bénard, M., Ernoult-Lange, M., Lee, B.P., Harries, L.W., Weil, D., and Standart, N. (2016). The DDX6–4E-T interaction mediates translational repression and P-body assembly. *Nucleic Acids Research 44*, 6318–6334.

Karjee, S., Minhas, A., Sood, V., Ponia, S.S., Banerjea, A.C., Chow, V.T.K., Mukherjee, S.K., and Lal, S.K. (2010). The 7a accessory protein of severe acute respiratory syndrome coronavirus acts as an RNA silencing suppressor. *J. Virol. 84*, 10395–10401.

Kasschau, K.D., Xie, Z., Allen, E., Llave, C., Chapman, E.J., Krizan, K.A., and Carrington, J.C. (2003). P1/HC-Pro, a viral suppressor of RNA silencing, interferes with *Arabidopsis* development and miRNA unction. *Dev Cell 4*, 205–217.

Kawasaki, T., and Kawai, T. (2014). Toll-like receptor signaling pathways. *Front Immunol 5*, 461.

Keestra, A.M., Winter, M.G., Auburger, J.J., Fräßle, S.P., Xavier, M.N., Winter, S.E., Kim, A., Poon, V., Ravesloot, M.M., Waldenmaier, J.F.T.(2013). Manipulation of small Rho GTPases is a pathogen-induced process detected by NOD1. *Nature 496*, 233–237.

Keestra-Gounder, A.M., Byndloss, M.X., Seyffert, N., Young, B.M., Chávez-Arroyo, A., Tsai, A.Y., Cevallos, S.A., Winter, M.G., Pham, O.H., Tiffany, C.R., et al. (2016). NOD1 and NOD2 signalling links ER stress with inflammation. *Nature 532*, 394–397.

Kennedy, E.M., Whisnant, A.W., Kornepati, A.V.R., Marshall, J.B., Bogerd, H.P., and Cullen, B.R. (2015). Production of functional small interfering RNAs by an amino-terminal deletion mutant of human Dicer. *Proc. Natl. Acad. Sci. U.S.A. 112*, E6945-6954.

Khelef, N., Shuman, H.A., and Maxfield, F.R. (2001). Phagocytosis of wild-type *Legionella pneumophila* occurs through a wortmannin-insensitive pathway. *Infect Immun 69*, 5157–5161.

Kiga, K., Mimuro, H., Suzuki, M., Shinozaki-Ushiku, A., Kobayashi, T., Sanada, T., Kim, M., Ogawa, M., Iwasaki, Y.W., Kayo, H. (2014). Epigenetic silencing of miR-210 increases the proliferation of gastric epithelium during chronic Helicobacter pylori infection. *Nat Commun 5*, 4497.

Kim, J.K., Lee, H.-M., Park, K.-S., Shin, D.-M., Kim, T.S., Kim, Y.S., Suh, H.-W., Kim, S.Y., Kim, I.S., Kim, J.-M. (2017). MIR144* inhibits antimicrobial responses against Mycobacterium tuberculosis in human monocytes and macrophages by targeting the autophagy protein DRAM2. *Autophagy 13*, 423–441.

Kim, M.G., da Cunha, L., McFall, A.J., Belkhadir, Y., DebRoy, S., Dangl, J.L., and Mackey, D. (2005). Two *Pseudomonas syringae* type III effectors inhibit RIN4-regulated basal defense in *Arabidopsis. Cell 121*, 749–759.

Kim, S.H., Qi, D., Ashfield, T., Helm, M., and Innes, R.W. (2016). Using decoys to expand the recognition specificity of a plant disease resistance protein. *Science 351*, 684–687.

Kim, V.N., Han, J., and Siomi, M.C. (2009). Biogenesis of small RNAs in animals. *Nat Rev Mol Cell Biol 10*, 126–139.

King, C.H., Fields, B.S., Shotts, E.B., and White, E.H. (1991). Effects of cytochalasin D and methylamine on intracellular growth of *Legionella pneumophila* in amoebae and human monocyte-like cells. *Infect Immun 59*, 758–763.

Kirby, J.E., Vogel, J.P., Andrews, H.L., and Isberg, R.R. (1998). Evidence for pore-forming ability by *Legionella pneumophila. Mol Microbiol 27*, 323–336.

Koeppen, K., Nymon, A., Barnaby, R., Bashor, L., Li, Z., Hampton, T.H., Liefeld, A.E., Kolling, F.W., LaCroix, I.S., Gerber, S.A., et al. (2021). Let-7b-5p in vesicles secreted by human airway cells reduces biofilm formation and increases antibiotic sensitivity of *P. aeruginosa. Proc Natl Acad Sci U S A 118*, e2105370118.

Kok, K.-H., Lui, P.-Y., Ng, M.-H.J., Siu, K.-L., Au, S.W.N., and Jin, D.-Y. (2011). The double-stranded RNA-binding protein PACT functions as a cellular activator of RIG-I to facilitate innate antiviral response. *Cell Host Microbe 9*, 299–309.

van der Krol, A.R., Mur, L.A., Beld, M., Mol, J.N., and Stuitje, A.R. (1990). Flavonoid genes in petunia: addition of a limited number of gene copies may lead to a suppression of gene expression. *Plant Cell 2*, 291–299.

Kubori, T., Shinzawa, N., Kanuka, H., and Nagai, H. (2010). *Legionella* metaeffector exploits host proteasome to temporally regulate cognate effector. *PLoS Pathog 6*, e1001216.

Kufer, T.A., Creagh, E.M., and Bryant, C.E. (2019). Guardians of the Cell: Effector-Triggered Immunity Steers Mammalian Immune Defense. *Trends Immunol 40*, 939–951.

Kühn, S., Bergqvist, J., Gil, M., Valenzuela, C., Barrio, L., Lebreton, S., Zurzolo, C., and Enninga, J. (2020). Actin Assembly around the *Shigella*-Containing Vacuole Promotes Successful Infection. *Cell Rep 31*, 107638.

Kumar, M., Sahu, S.K., Kumar, R., Subuddhi, A., Maji, R.K., Jana, K., Gupta, P., Raffetseder, J., Lerm, M., Ghosh, Z., et al. (2015). MicroRNA let-7 Modulates the Immune Response to Mycobacterium tuberculosis Infection via Control of A20, an Inhibitor of the NF-κB Pathway. *Cell Host & Microbe 17*, 345–356.

Kumar, R., Sahu, S.K., Kumar, M., Jana, K., Gupta, P., Gupta, U.D., Kundu, M., and Basu, J. (2016). MicroRNA 17-5p regulates autophagy in Mycobacterium tuberculosis-infected macrophages by targeting Mcl-1 and STAT3. *Cellular Microbiology 18*, 679–691.

Kuzuoğlu-Öztürk, D., Bhandari, D., Huntzinger, E., Fauser, M., Helms, S., and Izaurralde, E. (2016). miRISC and the CCR4–NOT complex silence mRNA targets independently of 43S ribosomal scanning. *The EMBO Journal 35*, 1186–1203.

La Rocca, G., Olejniczak, S.H., González, A.J., Briskin, D., Vidigal, J.A., Spraggon, L., DeMatteo, R.G., Radler, M.R., Lindsten, T., Ventura, A., et al. (2015). In vivo, Argonaute-bound microRNAs exist predominantly in a reservoir of low molecular weight complexes not associated with mRNA. *Proc Natl Acad Sci U S A 112*, 767–772.

Lazzaretti, D., Tournier, I., and Izaurralde, E. (2009). The C-terminal domains of human TNRC6A, TNRC6B, and TNRC6C silence bound transcripts independently of Argonaute proteins. *RNA 15*, 1059–1066.

Lecellier, C.-H., Dunoyer, P., Arar, K., Lehmann-Che, J., Eyquem, S., Himber, C., Saïb, A., and Voinnet, O. (2005). A cellular microRNA mediates antiviral defense in human cells. *Science 308*, 557–560.

Lee, A.J., and Ashkar, A.A. (2018). The Dual Nature of Type I and Type II Interferons. *Front Immunol 9*, 2061.

Lee, P.-C., and Machner, M.P. (2018). The *Legionella* Effector Kinase LegK7 Hijacks the Host Hippo Pathway to Promote Infection. *Cell Host Microbe 24*, 429-438.e6.

Lee, P.-C., Beyrakhova, K., Xu, C., Boniecki, M.T., Lee, M.H., Onu, C.J., Grishin, A.M., Machner, M.P., and Cygler, M. (2020). The *Legionella* kinase LegK7 exploits the Hippo pathway scaffold protein MOB1A for allostery and substrate phosphorylation. *Proc Natl Acad Sci U S A 117*, 14433–14443.

Lee, R.C., Feinbaum, R.L., and Ambros, V. (1993). The *C. elegans* heterochronic gene lin-4 encodes small RNAs with antisense complementarity to lin-14. *Cell 75*, 843–854.

Lee, Y., Ahn, C., Han, J., Choi, H., Kim, J., Yim, J., Lee, J., Provost, P., Rådmark, O., Kim, S., et al. (2003). The nuclear RNase III Drosha initiates microRNA processing. *Nature 425*, 415–419.

Lee, Y., Kim, M., Han, J., Yeom, K.-H., Lee, S., Baek, S.H., and Kim, V.N. (2004). MicroRNA genes are transcribed by RNA polymerase II. *EMBO J. 23*, 4051–4060.

Leung, A.K.L., Calabrese, J.M., and Sharp, P.A. (2006). Quantitative analysis of Argonaute protein reveals microRNA-dependent localization to stress granules. *Proc Natl Acad Sci U S A 103*, 18125–18130.

Leuschner, P.J.F., Ameres, S.L., Kueng, S., and Martinez, J. (2006). Cleavage of the siRNA passenger strand during RISC assembly in human cells. *EMBO Reports 7*, 314–320.

Levinsohn, J.L., Newman, Z.L., Hellmich, K.A., Fattah, R., Getz, M.A., Liu, S., Sastalla, I., Leppla, S.H., and Moayeri, M. (2012). Anthrax Lethal Factor Cleavage of Nlrp1 Is Required for Activation of the Inflammasome. *PLOS Pathogens 8*, e1002638.

Li, H., Li, W.X., and Ding, S.W. (2002). Induction and suppression of RNA silencing by an animal virus. *Science 296*, 1319–1321.

Li, H.W., Lucy, A.P., Guo, H.S., Li, W.X., Ji, L.H., Wong, S.M., and Ding, S.W. (1999). Strong host resistance targeted against a viral suppressor of the plant gene silencing defence mechanism. *EMBO J 18*, 2683–2691.

Li, L., Chen, X.-P., and Li, Y.-J. (2010a). MicroRNA-146a and human disease. *Scand J Immunol 71*, 227–231.

Li, M., Ma, X., Chiang, Y.-H., Yadeta, K.A., Ding, P., Dong, L., Zhao, Y., Li, X., Yu, Y., Zhang, L., et al. (2014). Proline isomerization of the immune receptor-interacting protein RIN4 by a cyclophilin inhibits effector-triggered immunity in *Arabidopsis. Cell Host Microbe 16*, 473–483.

Li, W.-X., Li, H., Lu, R., Li, F., Dus, M., Atkinson, P., Brydon, E.W.A., Johnson, K.L., García-Sastre, A., Ball, L.A., et al. (2004). Interferon antagonist proteins of *influenza* and *vaccinia* viruses are suppressors of RNA silencing. *Proc. Natl. Acad. Sci. U.S.A. 101*, 1350–1355.

Li, X., Wang, X., Cheng, Z., and Zhu, Q. (2020). AGO2 and its partners: a silencing complex, a chromatin modulator, and new features. *Crit Rev Biochem Mol Biol 55*, 33–53.

Li, Y., Zhang, Q., Zhang, J., Wu, L., Qi, Y., and Zhou, J.-M. (2010b). Identification of MicroRNAs Involved in Pathogen-Associated Molecular Pattern-Triggered Plant Innate Immunity. *Plant Physiology 152*, 2222–2231.

Li, Y., Lu, J., Han, Y., Fan, X., and Ding, S.-W. (2013). RNA Interference Functions as an Antiviral Immunity Mechanism in Mammals. *Science 342*.

Li, Y., Basavappa, M., Lu, J., Dong, S., Cronkite, D.A., Prior, J.T., Reinecker, H.-C., Hertzog, P., Han, Y., Li, W.-X., et al. (2016). Induction and suppression of antiviral RNA interference by *influenza A* virus in mammalian cells. *Nat Microbiol 2*, 16250.

Li, Z., Dugan, A.S., Bloomfield, G., Skelton, J., Ivens, A., Losick, V., and Isberg, R.R. (2009). The amoebal MAP kinase response to *Legionella pneumophila* is regulated by DupA. *Cell Host Microbe 6*, 253–267.

Lian, S.L., Li, S., Abadal, G.X., Pauley, B.A., Fritzler, M.J., and Chan, E.K.L. (2009). The C-terminal half of human Ago2 binds to multiple GW-rich regions of GW182 and requires GW182 to mediate silencing. *RNA 15*, 804–813.

Liao, Z., Kjellin, J., Hoeppner, M.P., Grabherr, M., and Söderbom, F. (2018). Global characterization of the Dicer-like protein DrnB roles in miRNA biogenesis in the social amoeba *Dictyostelium discoideum. RNA Biol 15*, 937–954.

Lichner, Z., Silhavy, D., and Burgyán, J. (2003). Double-stranded RNA-binding proteins could suppress RNA interference-mediated antiviral defences. *J. Gen. Virol. 84*, 975–980.

Lightfield, K.L., Persson, J., Brubaker, S.W., Witte, C.E., von Moltke, J., Dunipace, E.A., Henry, T., Sun, Y.-H., Cado, D., Dietrich, W.F., et al. (2008). Critical function for Naip5 in inflammasome activation by a conserved carboxy-terminal domain of flagellin. *Nat Immunol 9*, 1171–1178.

Lightfield, K.L., Persson, J., Trinidad, N.J., Brubaker, S.W., Kofoed, E.M., Sauer, J.-D., Dunipace, E.A., Warren, S.E., Miao, E.A., and Vance, R.E. (2011). Differential requirements for NAIP5 in activation of the NLRC4 inflammasome. *Infect Immun 79*, 1606–1614.

Lippmann, J., Rothenburg, S., Deigendesch, N., Eitel, J., Meixenberger, K., van Laak, V., Slevogt, H., N'guessan, P.D., Hippenstiel, S., Chakraborty, T., et al. (2008). IFNbeta responses induced by intracellular bacteria or cytosolic DNA in different human cells do not require ZBP1 (DLM-1/DAI). *Cell Microbiol 10*, 2579–2588.

Lippmann, J., Müller, H.C., Naujoks, J., Tabeling, C., Shin, S., Witzenrath, M., Hellwig, K., Kirschning, C.J., Taylor, G.A., Barchet, W., et al. (2011). Dissection of a type I interferon pathway in controlling bacterial intracellular infection in mice. *Cell Microbiol 13*, 1668–1682.

Liston, A., and Masters, S.L. (2017). Homeostasis-altering molecular processes as mechanisms of inflammasome activation. *Nature Reviews Immunology 17*, 208–214.

Liu, C., Xin, Y., Xu, L., Cai, Z., Xue, Y., Liu, Y., Xie, D., Liu, Y., and Qi, Y. (2018). Arabidopsis ARGONAUTE 1 Binds Chromatin to Promote Gene Transcription in Response to Hormones and Stresses. *Dev Cell 44*, 348-361.e7.

Liu, J., Carmell, M.A., Rivas, F.V., Marsden, C.G., Thomson, J.M., Song, J.-J., Hammond, S.M., Joshua-Tor, L., and Hannon, G.J. (2004). Argonaute2 Is the Catalytic Engine of Mammalian RNAi. *Science 305*, 1437–1441.

Liu, J., Rivas, F.V., Wohlschlegel, J., Yates, J.R., Parker, R., and Hannon, G.J. (2005). A role for the P-body component, GW182, in microRNA function. *Nat Cell Biol 7*, 1261–1266.

Liu, J., Elmore, J.M., Lin, Z.-J.D., and Coaker, G. (2011). A Receptor-like Cytoplasmic Kinase Phosphorylates the Host Target RIN4, Leading to the Activation of a Plant Innate Immune Receptor. *Cell Host & Microbe 9*, 137–146.

Liu, P.T., Wheelwright, M., Teles, R., Komisopoulou, E., Edfeldt, K., Ferguson, B., Mehta, M.D., Vazirnia, A., Rea, T.H., Sarno, E.N., et al. (2012). MicroRNA-21 targets the vitamin D-dependent antimicrobial pathway in leprosy. *Nat Med 18*, 267–273.

Liu, S., da Cunha, A.P., Rezende, R.M., Cialic, R., Wei, Z., Bry, L., Comstock, L.E., Gandhi, R., and Weiner, H.L. (2016). The Host Shapes the Gut Microbiota via Fecal MicroRNA. *Cell Host & Microbe 19*, 32–43.

Liu, Y.-C., Chen, W.L., Kung, W.-H., and Huang, H.-D. (2017). Plant miRNAs found in human circulating system provide evidences of cross kingdom RNAi. *BMC Genomics 18*, 112.

Lolle, S., Stevens, D., and Coaker, G. (2020). Plant NLR-triggered immunity: from receptor activation to downstream signaling. *Curr Opin Immunol 62*, 99–105.

Lomma, M., Dervins-Ravault, D., Rolando, M., Nora, T., Newton, H.J., Sansom, F.M., Sahr, T., Gomez-Valero, L., Jules, M., Hartland, E.L., et al. (2010). The *Legionella pneumophila* F-box protein Lpp2082 (AnkB) modulates ubiquitination of the host protein parvin B and promotes intracellular replication. *Cell Microbiol 12*, 1272–1291.

Lopes Fischer, N., Naseer, N., Shin, S., and Brodsky, I.E. (2020). Effector-triggered immunity and pathogen sensing in metazoans. *Nat Microbiol 5*, 14–26.

Lopez-Orozco, J., Pare, J.M., Holme, A.L., Chaulk, S.G., Fahlman, R.P., and Hobman, T.C. (2015). Functional analyses of phosphorylation events in human Argonaute 2. *RNA 21*, 2030–2038.

Losick, V.P., and Isberg, R.R. (2006). NF-kappaB translocation prevents host cell death after low-dose challenge by *Legionella pneumophila. J Exp Med 203*, 2177–2189.

Losick, V.P., Haenssler, E., Moy, M.-Y., and Isberg, R.R. (2010). LnaB: a *Legionella pneumophila* activator of NF-κB. *Cell Microbiol 12*, 1083–1097.

Lou, J., Wang, Y., Zhang, Z., and Qiu, W. (2017). MiR-20b inhibits mycobacterium tuberculosis induced inflammation in the lung of mice through targeting NLRP3. *Experimental Cell Research 358*, 120–128.

Lou, Q., Hu, Y., Ma, Y., and Dong, Z. (2019). RNA interference may suppress stress granule formation by preventing argonaute 2 recruitment. *Am J Physiol Cell Physiol 316*, C81–C91.

Lu, H., and Clarke, M. (2005). Dynamic properties of *Legionella*-containing phagosomes in *Dictyostelium amoebae. Cell Microbiol 7*, 995–1007.

Lu, S., and Cullen, B.R. (2004). Adenovirus VA1 noncoding RNA can inhibit small interfering RNA and MicroRNA biogenesis. *J. Virol. 78*, 12868–12876.

Lu, L.-F., Thai, T.-H., Calado, D.P., Chaudhry, A., Kubo, M., Tanaka, K., Loeb, G.B., Lee, H., Yoshimura, A., Rajewsky, K., et al. (2009). Foxp3-dependent microRNA155 confers competitive fitness to regulatory T cells by targeting SOCS1 protein. *Immunity 30*, 80–91.

Lu, R., Maduro, M., Li, F., Li, H., Broitman-Maduro, G., Li, W., and Ding, S. (2005). Animal virus replication and RNAi-mediated antiviral silencing in *C elegans*. *Nature 436*, 1040–1043.

Lund, E., Güttinger, S., Calado, A., Dahlberg, J.E., and Kutay, U. (2004). Nuclear export of microRNA precursors. *Science 303*, 95–98.

Luo, Y., Na, Z., and Slavoff, S.A. (2018). P-Bodies: Composition, Properties, and Functions. *Biochemistry 57*, 2424–2431.

Lurie-Weinberger, M.N., Gomez-Valero, L., Merault, N., Glöckner, G., Buchrieser, C., and Gophna, U. (2010). The origins of eukaryotic-like proteins in *Legionella pneumophila. Int J Med Microbiol 300*, 470–481.

Ma, E., MacRae, I.J., Kirsch, J.F., and Doudna, J.A. (2008). Autoinhibition of human dicer by its internal helicase domain. *J. Mol. Biol. 380*, 237–243.

Ma, F., Xu, S., Liu, X., Zhang, Q., Xu, X., Liu, M., Hua, M., Li, N., Yao, H., and Cao, X. (2011). The microRNA miR-29 controls innate and adaptive immune responses to intracellular bacterial infection by targeting interferon-γ. *Nat Immunol 12*, 861–869.

Mackey, D., Holt, B.F., Wiig, A., and Dangl, J.L. (2002). RIN4 Interacts with Pseudomonas syringae Type III Effector Molecules and Is Required for RPM1-Mediated Resistance in Arabidopsis. *Cell 108*, 743–754.

Maillard, P.V., Ciaudo, C., Marchais, A., Li, Y., Jay, F., Ding, S.W., and Voinnet, O. (2013a). Antiviral RNA Interference in Mammalian Cells. *Science 342*.

Maillard, P.V., Ciaudo, C., Marchais, A., Li, Y., Jay, F., Ding, S.W., and Voinnet, O. (2013b). Antiviral RNA interference in mammalian cells. *Science 342*, 235–238.

Maillard, P.V., Van der Veen, A.G., Deddouche-Grass, S., Rogers, N.C., Merits, A., and Reis e Sousa, C. (2016). Inactivation of the type I interferon pathway reveals long double-stranded RNA-mediated RNA interference in mammalian cells. *The EMBO Journal 35*, 2505–2518.

Maillard, P.V., van der Veen, A.G., Poirier, E.Z., and Reis e Sousa, C. (2019). Slicing and dicing viruses: antiviral RNA interference in mammals. *EMBO J. 38*.

Mallory, A.C., Reinhart, B.J., Bartel, D., Vance, V.B., and Bowman, L.H. (2002). A viral suppressor of RNA silencing differentially regulates the accumulation of short interfering RNAs and micro-RNAs in tobacco. *PNAS 99*, 15228–15233.

Marcais, A., Blevins, R., Graumann, J., Feytout, A., Dharmalingam, G., Carroll, T., Amado, I.F., Bruno, L., Lee, K., Walzer, T., et al. (2014). microRNA-mediated regulation of mTOR complex components facilitates discrimination between activation and anergy in CD4 T cells. *J Exp Med 211*, 2281–2295.

Marra, A., Blander, S.J., Horwitz, M.A., and Shuman, H.A. (1992). Identification of a *Legionella pneumophila* locus required for intracellular multiplication in human macrophages. *Proc Natl Acad Sci U S A 89*, 9607–9611.

Martinez, J., and Tuschl, T. (2004). RISC is a 5′ phosphomonoester-producing RNA endonuclease. *Genes Dev 18*, 975–980.

Martinez-Nunez, R.T., Louafi, F., Friedmann, P.S., and Sanchez-Elsner, T. (2009). MicroRNA-155 modulates the pathogen binding ability of dendritic cells (DCs) by down-regulation of DC-specific intercellular adhesion molecule-3 grabbing non-integrin (DC-SIGN). *J. Biol. Chem. 284*, 16334–16342.

Mascarenhas, D.P.A., and Zamboni, D.S. (2017). Inflammasome biology taught by *Legionella pneumophila. J Leukoc Biol 101*, 841–849.

Massis, L.M., and Zamboni, D.S. (2011). Innate immunity to legionella pneumophila. *Front Microbiol 2*, 109.

Mathonnet, G., Fabian, M.R., Svitkin, Y.V., Parsyan, A., Huck, L., Murata, T., Biffo, S., Merrick, W.C., Darzynkiewicz, E., Pillai, R.S., et al. (2007). MicroRNA inhibition of translation initiation in vitro by targeting the cap-binding complex eIF4F. *Science 317*, 1764–1767.

Mathys, H., Basquin, J., Ozgur, S., Czarnocki-Cieciura, M., Bonneau, F., Aartse, A., Dziembowski, A., Nowotny, M., Conti, E., and Filipowicz, W. (2014). Structural and biochemical insights to the role of the CCR4-NOT complex and DDX6 ATPase in microRNA repression. *Mol. Cell 54*, 751–765.

Matranga, C., Tomari, Y., Shin, C., Bartel, D.P., and Zamore, P.D. (2005). Passenger-Strand Cleavage Facilitates Assembly of siRNA into Ago2-Containing RNAi Enzyme Complexes. *Cell 123*, 607–620.

Matzinger, P. (1994). Tolerance, danger, and the extended family. *Annu Rev Immunol 12*, 991–1045.

Maudet, C., Mano, M., and Eulalio, A. (2014a). MicroRNAs in the interaction between host and bacterial pathogens. *FEBS Letters 588*, 4140–4147.

Maudet, C., Mano, M., Sunkavalli, U., Sharan, M., Giacca, M., Förstner, K.U., and Eulalio, A. (2014b). Functional high-throughput screening identifies the miR-15 microRNA family as cellular restriction factors for *Salmonella* infection. *Nature Communications 5.*

McDade, J.E., Shepard, C.C., Fraser, D.W., Tsai, T.R., Redus, M.A., and Dowdle, W.R. (1977). Legionnaires' disease: isolation of a bacterium and demonstration of its role in other respiratory disease. *N. Engl. J. Med. 297*, 1197–1203.

McDade, J.E., Brenner, D.J., and Bozeman, F.M. (1979). Legionnaires' disease bacterium isolated in 1947. *Ann Intern Med 90*, 659–661.

Meier, D., Kruse, J., Buttlar, J., Friedrich, M., Zenk, F., Boesler, B., Förstner, K.U., Hammann, C., and Nellen, W. (2016). Analysis of the Microprocessor in Dictyostelium: The Role of RbdB, a dsRNA Binding Protein. *PLOS Genetics 12*, e1006057.

Meister, G. (2013). Argonaute proteins: functional insights and emerging roles. *Nature Reviews Genetics 14*, 447–459.

Meister, G., Landthaler, M., Patkaniowska, A., Dorsett, Y., Teng, G., and Tuschl, T. (2004). Human Argonaute2 mediates RNA cleavage targeted by miRNAs and siRNAs. *Mol. Cell 15*, 185–197.

Mellouk, N., Weiner, A., Aulner, N., Schmitt, C., Elbaum, M., Shorte, S.L., Danckaert, A., and Enninga, J. (2014). *Shigella* subverts the host recycling compartment to rupture its vacuole. *Cell Host Microbe 16*, 517–530.

Mercante, J.W., and Winchell, J.M. (2015). Current and emerging *Legionella* diagnostics for laboratory and outbreak investigations. *Clin Microbiol Rev 28*, 95–133.

Michaeli, S., Clavel, M., Lechner, E., Viotti, C., Wu, J., Dubois, M., Hacquard, T., Derrien, B., Izquierdo, E., Lecorbeiller, M., et al. (2019). The viral F-box protein P0 induces an ER-derived autophagy degradation pathway for the clearance of membrane-bound AGO1. *PNAS 116*, 22872–22883.

Michard, C., Sperandio, D., Baïlo, N., Pizarro-Cerdá, J., LeClaire, L., Chadeau-Argaud, E., Pombo-Grégoire, I., Hervet, E., Vianney, A., Gilbert, C., et al. (2015). The *Legionella* Kinase LegK2 Targets the ARP2/3 Complex To Inhibit Actin Nucleation on Phagosomes and Allow Bacterial Evasion of the Late Endocytic Pathway. *MBio 6*, e00354-00315.

Mishra, R., Kumar, A., Ingle, H., and Kumar, H. (2020). The Interplay Between Viral-Derived miRNAs and Host Immunity During Infection. *Front. Immunol. 10*.

Miyamoto, M., and Komuro, A. (2017). PACT is required for MDA5-mediated immunoresponses triggered by Cardiovirus infection via interaction with LGP2. *Biochem Biophys Res Commun 494*, 227–233.

Molmeret, M., Bitar, D.M., Han, L., and Kwaik, Y.A. (2004). Disruption of the phagosomal membrane and egress of *Legionella pneumophila* into the cytoplasm during the last stages of intracellular infection of macrophages and *Acanthamoeba polyphaga. Infect Immun 72*, 4040–4051.

Molmeret, M., Horn, M., Wagner, M., Santic, M., and Kwaik, Y.A. (2005). Amoebae as Training Grounds for Intracellular Bacterial Pathogens. *Appl. Environ. Microbiol. 71*, 20–28.

Molofsky, A.B., and Swanson, M.S. (2004). Differentiate to thrive: lessons from the *Legionella pneumophila* life cycle. *Mol Microbiol 53*, 29–40.

Mondino, S., Schmidt, S., Rolando, M., Escoll, P., Gomez-Valero, L., and Buchrieser, C. (2020a). Legionnaires' Disease: State of the Art Knowledge of Pathogenesis Mechanisms of *Legionella*. *Annual Review of Pathology: Mechanisms of Disease 15*, 439–466.

Mondino, S., Schmidt, S., and Buchrieser, C. (2020b). Molecular Mimicry: a Paradigm of Host-Microbe Coevolution Illustrated by Legionella. *MBio 11*, e01201-20.

Monroe, K.M., McWhirter, S.M., and Vance, R.E. (2009). Identification of host cytosolic sensors and bacterial factors regulating the type I interferon response to Legionella pneumophila. *PLoS Pathog 5*, e1000665.

Montavon, T.C., Baldaccini, M., Lefèvre, M., Girardi, E., Chane-Woon-Ming, B., Messmer, M., Hammann, P., Chicher, J., and Pfeffer, S. (2021). Human DICER helicase domain recruits PKR and modulates its antiviral activity. *PLoS Pathog 17*, e1009549.

Morel, J.-B., Godon, C., Mourrain, P., Béclin, C., Boutet, S., Feuerbach, F., Proux, F., and Vaucheret, H. (2002). Fertile Hypomorphic ARGONAUTE (ago1) Mutants Impaired in Post-Transcriptional Gene Silencing and Virus Resistance. *Plant Cell 14*, 629–639.

Moretti, F., Kaiser, C., Zdanowicz-Specht, A., and Hentze, M.W. (2012). PABP and the poly(A) tail augment microRNA repression by facilitated miRISC binding. *Nat Struct Mol Biol 19*, 603–608.

Moss, S.M., Taylor, I.R., Ruggero, D., Gestwicki, J.E., Shokat, K.M., and Mukherjee, S. (2019). A *Legionella pneumophila* Kinase Phosphorylates the Hsp70 Chaperone Family to Inhibit Eukaryotic Protein Synthesis. *Cell Host Microbe 25*, 454-462.e6.

Mu, J., Xu, J., Zhang, L., Shu, T., Wu, D., Huang, M., Ren, Y., Li, X., Geng, Q., Xu, Y., et al. (2020a). SARS-CoV-2-encoded nucleocapsid protein acts as a viral suppressor of RNA interference in cells. S*ci China Life Sci* 1–4.

Mu, J., Zhang, H., Li, T., Shu, T., Qiu, Y., and Zhou, X. (2020b). The 3A protein of coxsackievirus B3 acts as a viral suppressor of RNA interference. *J Gen Virol 101*, 1069–1078.

Muder, R.R., and Yu, V.L. (2002). Infection due to *Legionella* species other than *L. pneumophila. Clin Infect Dis 35*, 990–998.

Muder, R.R., Yu, V.L., and Woo, A.H. (1986). Mode of transmission of *Legionella pneumophila.* A critical review. *Arch Intern Med 146*, 1607–1612.

Mukherjee, T., Hovingh, E.S., Foerster, E.G., Abdel-Nour, M., Philpott, D.J., and Girardin, S.E. (2019). NOD1 and NOD2 in inflammation, immunity and disease. *Arch Biochem Biophys 670*, 69–81.

Mukhopadhyay, U., Chanda, S., Patra, U., Mukherjee, A., Komoto, S., and Chawla-Sarkar, M. (2019). Biphasic regulation of RNA interference during rotavirus infection by modulation of Argonaute2. *Cell Microbiol 21*, e13101.

Mulero, M.C., Huxford, T., and Ghosh, G. (2019). NF-κB, IκB, and IKK: Integral Components of Immune System Signaling. *Adv Exp Med Biol 1172*, 207–226.

Muñoz-Planillo, R., Kuffa, P., Martínez-Colón, G., Smith, B.L., Rajendiran, T.M., and Núñez, G. (2013). K^+ efflux is the common trigger of NLRP3 inflammasome activation by bacterial toxins and particulate matter. *Immunity 38*, 1142–1153.

Nakanishi, K. (2016). Anatomy of RISC: how do small RNAs and chaperones activate Argonaute proteins? *WIREs RNA 7*, 637–660.

Nakata, K., Sugi, Y., Narabayashi, H., Kobayakawa, T., Nakanishi, Y., Tsuda, M., Hosono, A., Kaminogawa, S., Hanazawa, S., and Takahashi, K. (2017). Commensal microbiota-induced microRNA modulates intestinal epithelial permeability through the small GTPase ARF4. *J. Biol. Chem. 292*, 15426–15433.

Napoli, C., Lemieux, C., and Jorgensen, R. (1990). Introduction of a Chimeric Chalcone Synthase Gene into Petunia Results in Reversible Co-Suppression of Homologous Genes in trans. *The Plant Cell 2*, 279–289.

Naujoks, J., Tabeling, C., Dill, B.D., Hoffmann, C., Brown, A.S., Kunze, M., Kempa, S., Peter, A., Mollenkopf, H.-J., Dorhoi, A., et al. (2016). IFNs Modify the Proteome of *Legionella*-Containing Vacuoles and Restrict Infection Via IRG1-Derived Itaconic Acid. *PLoS Pathog 12*.

Naujoks, J., Lippmann, J., Suttorp, N., and Opitz, B. (2018). Innate sensing and cell-autonomous resistance pathways in Legionella pneumophila infection. International Journal of Medical *Microbiology 308*, 161–167.

Navarro, L., Jay, F., Nomura, K., He, S.Y., and Voinnet, O. (2008). Suppression of the microRNA pathway by bacterial effector proteins. *Science 321*, 964–967.

Neild, A.L., Shin, S., and Roy, C.R. (2005). Activated macrophages infected with *Legionella* inhibit T cells by means of MyD88-dependent production of prostaglandins. *J Immunol 175*, 8181–8190.

Nejad, C., Stunden, H.J., and Gantier, M.P. (2018). A guide to miRNAs in inflammation and innate immune responses. *The FEBS Journal 285*, 3695–3716.

Newton, H.J., Ang, D.K.Y., van Driel, I.R., and Hartland, E.L. (2010). Molecular pathogenesis of infections caused by *Legionella pneumophila. Clin Microbiol Rev 23*, 274–298.

Ngou, B.P.M., Ahn, H.-K., Ding, P., and Jones, J.D.G. (2021). Mutual potentiation of plant immunity by cell-surface and intracellular receptors. *Nature 592*, 110–115.

Nguyen, Q.-M., Iswanto, A.B.B., Son, G.H., and Kim, S.H. (2021). Recent Advances in Effector-Triggered Immunity in Plants: New Pieces in the Puzzle Create a Different Paradigm. *Int J Mol Sci 22*.

Nguyen, T.A., Jo, M.H., Choi, Y.-G., Park, J., Kwon, S.C., Hohng, S., Kim, V.N., and Woo, J.-S. (2015). Functional Anatomy of the Human Microprocessor. *Cell 161*, 1374–1387.

Ngwaga, T., Chauhan, D., and Shames, S.R. (2021). Mechanisms of Effector-Mediated Immunity Revealed by the Accidental Human Pathogen *Legionella pneumophila. Front Cell Infect Microbiol 10.*

Ni, W.-J., and Leng, X.-M. (2015). Dynamic miRNA–mRNA paradigms: New faces of miRNAs. *Biochemistry and Biophysics Reports 4*, 337–341.

Niaz, S., and Hussain, M.U. (2018). Role of GW182 protein in the cell. T*he International Journal of Biochemistry & Cell Biology 101*, 29–38.

Niu, D., Lii, Y.E., Chellappan, P., Lei, L., Peralta, K., Jiang, C., Guo, J., Coaker, G., and Jin, H. (2016). miRNA863-3p sequentially targets negative immune regulator ARLPKs and positive regulator SERRATE upon bacterial infection. *Nat Commun 7*, 1–13.

Noutoshi, Y., Ito, T., Seki, M., Nakashita, H., Yoshida, S., Marco, Y., Shirasu, K., and Shinozaki, K. (2005). A single amino acid insertion in the WRKY domain of the Arabidopsis TIR-NBS-LRR-WRKY-type disease resistance protein SLH1 (sensitive to low humidity 1) causes activation of defense responses and hypersensitive cell death. *Plant J 43*, 873–888.

O'Brien, J., Hayder, H., Zayed, Y., and Peng, C. (2018). Overview of MicroRNA Biogenesis, Mechanisms of Actions, and Circulation. *Front Endocrinol* (Lausanne) *9*, 402.

O'Carroll, D., Mecklenbrauker, I., Das, P.P., Santana, A., Koenig, U., Enright, A.J., Miska, E.A., and Tarakhovsky, A. (2007). A Slicer-independent role for Argonaute 2 in hematopoiesis and the microRNA pathway. *Genes Dev 21*, 1999–2004.

O'Connell, R.M., Chaudhuri, A.A., Rao, D.S., and Baltimore, D. (2009). Inositol phosphatase SHIP1 is a primary target of miR-155. *Proc. Natl. Acad. Sci. U.S.A. 106*, 7113–7118.

Olejniczak, S.H., La Rocca, G., Gruber, J.J., and Thompson, C.B. (2013). Long-lived microRNA–Argonaute complexes in quiescent cells can be activated to regulate mitogenic responses. *Proc Natl Acad Sci U S A 110*, 157–162.

Oliva, G., Sahr, T., and Buchrieser, C. (2018). The Life Cycle of *L. pneumophila*: Cellular Differentiation Is Linked to Virulence and Metabolism. *Front Cell Infect Microbiol 8*.

O'Neill, L.A., Sheedy, F.J., and McCoy, C.E. (2011). MicroRNAs: the fine-tuners of Toll-like receptor signalling. *Nature Reviews Immunology 11*, 163–175.

Opitz, B., Vinzing, M., van Laak, V., Schmeck, B., Heine, G., Günther, S., Preissner, R., Slevogt, H., N'Guessan, P.D., Eitel, J., et al. (2006). *Legionella pneumophila* induces IFNbeta in lung epithelial cells via IPS-1 and IRF3, which also control bacterial replication. *J Biol Chem 281*, 36173–36179.

Orban, T.I., and Izaurralde, E. (2005). Decay of mRNAs targeted by RISC requires XRN1, the Ski complex, and the exosome. *RNA 11*, 459–469.

Orth, K., Xu, Z., Mudgett, M.B., Bao, Z.Q., Palmer, L.E., Bliska, J.B., Mangel, W.F., Staskawicz, B., and Dixon, J.E. (2000). Disruption of signaling by Yersinia effector YopJ, a ubiquitin-like protein protease. *Science 290*, 1594–1597.

Ota, H., Sakurai, M., Gupta, R., Valente, L., Wulff, B.-E., Ariyoshi, K., Iizasa, H., Davuluri, R.V., and Nishikura, K. (2013). ADAR1 forms a complex with Dicer to promote microRNA processing and RNA-induced gene silencing. *Cell 153*, 575–589.

Paddison, P.J., Caudy, A.A., and Hannon, G.J. (2002). Stable suppression of gene expression by RNAi in mammalian cells. *Proc. Natl. Acad. Sci. U.S.A. 99*, 1443–1448.

Pagliari, M., Munari, F., Toffoletto, M., Lonardi, S., Chemello, F., Codolo, G., Millino, C., Della Bella, C., Pacchioni, B., Vermi, W., et al. (2017). *Helicobacter pylori* Affects the Antigen Presentation Activity of Macrophages Modulating the Expression of the Immune Receptor CD300E through miR-4270. *Front Immunol 8*, 1288.

Parameswaran, P., Sklan, E., Wilkins, C., Burgon, T., Samuel, M.A., Lu, R., Ansel, K.M., Heissmeyer, V., Einav, S., Jackson, W., et al. (2010). Six RNA viruses and forty-one hosts: viral small RNAs and modulation of small RNA repertoires in vertebrate and invertebrate systems. *PLoS Pathog. 6*, e1000764.

Pare, J.M., Tahbaz, N., López-Orozco, J., LaPointe, P., Lasko, P., and Hobman, T.C. (2009). Hsp90 regulates the function of argonaute 2 and its recruitment to stress granules and P-bodies. *Mol Biol Cell 20*, 3273–3284.

Park, J.M., Ghosh, S., and O'Connor, T.J. (2020a). Combinatorial selection in amoebal hosts drives the evolution of the human pathogen *Legionella pneumophila. Nat Microbiol 5*, 599–609.

Park, M.S., Phan, H.-D., Busch, F., Hinckley, S.H., Brackbill, J.A., Wysocki, V.H., and Nakanishi, K. (2017). Human Argonaute3 has slicer activity. *Nucleic Acids Res. 45*, 11867–11877.

Park, M.S., Sim, G., Kehling, A.C., and Nakanishi, K. (2020b). Human Argonaute2 and Argonaute3 are catalytically activated by different lengths of guide *RNA*. PNAS *117*, 28576–28578.

Parker, R., and Sheth, U. (2007). P bodies and the control of mRNA translation and degradation. *Mol. Cell 25*, 635–646.

Patel, R.C., and Sen, G.C. (1998). PACT, a protein activator of the interferon-induced protein kinase, PKR. *EMBO J 17*, 4379–4390.

Payne, N.R., and Horwitz, M.A. (1987). Phagocytosis of *Legionella pneumophila* is mediated by human monocyte complement receptors. *J Exp Med 166*, 1377–1389.

Pazhouhandeh, M., Dieterle, M., Marrocco, K., Lechner, E., Berry, B., Brault, V., Hemmer, O., Kretsch, T., Richards, K.E., Genschik, P., et al. (2006). F-box-like domain in the polerovirus protein P0 is required for silencing suppressor function. *Proc Natl Acad Sci U S A 103*, 1994–1999.

Pedro-Botet, L., and Yu, V.L. (2006). *Legionella*: macrolides or quinolones? *Clin Microbiol Infect 12 Suppl 3*, 25–30.

Peracino, B., Balest, A., and Bozzaro, S. (2010). Phosphoinositides differentially regulate bacterial uptake and Nramp1-induced resistance to *Legionella* infection in *Dictyostelium. J Cell Sci 123*, 4039–4051.

Pereira, M.S.F., Morgantetti, G.F., Massis, L.M., Horta, C.V., Hori, J.I., and Zamboni, D.S. (2011). Activation of NLRC4 by flagellated bacteria triggers caspase-1-dependent and -independent responses to restrict *Legionella pneumophila* replication in macrophages and in vivo. *J Immunol 187*, 6447–6455.

Pfaff, J., Hennig, J., Herzog, F., Aebersold, R., Sattler, M., Niessing, D., and Meister, G. (2013). Structural features of Argonaute-GW182 protein interactions. *Proc Natl Acad Sci U S A 110*, E3770-3779.

Pfeffer, S., Zavolan, M., Grässer, F.A., Chien, M., Russo, J.J., Ju, J., John, B., Enright, A.J., Marks, D., Sander, C., et al. (2004). Identification of virus-encoded microRNAs. *Science 304*, 734–736.

Phukan, U.J., Jeena, G.S., and Shukla, R.K. (2016). WRKY Transcription Factors: Molecular Regulation and Stress Responses in Plants. *Front Plant Sci 7*, 760.

Piatek, M.J., and Werner, A. (2014). Endogenous siRNAs, regulators of internal affairs. *Biochem Soc Trans 42*, 1174–1179.

Pillai, R.S., Bhattacharyya, S.N., Artus, C.G., Zoller, T., Cougot, N., Basyuk, E., Bertrand, E., and Filipowicz, W. (2005). Inhibition of translational initiation by Let-7 MicroRNA in human cells. *Science 309*, 1573–1576.

Plumlee, C.R., Lee, C., Beg, A.A., Decker, T., Shuman, H.A., and Schindler, C. (2009). Interferons direct an effective innate response to *Legionella pneumophila* infection. *J Biol Chem 284*, 30058–30066.

Poirier, E.Z., Buck, M.D., Chakravarty, P., Carvalho, J., Frederico, B., Cardoso, A., Healy, L., Ulferts, R., Beale, R., and Reis E Sousa, C. (2021). An isoform of Dicer protects mammalian stem cells against multiple RNA viruses. *Science 373*, 231–236.

Ponia, S.S., Arora, S., Kumar, B., and Banerjea, A.C. (2013). Arginine rich short linear motif of HIV-1 regulatory proteins inhibits Dicer dependent RNA interference. *Retrovirology 10*, 97.

Popoff, M.R. (2014). Bacterial factors exploit eukaryotic Rho GTPase signaling cascades to promote invasion and proliferation within their host. *Small GTPases 5*, e28209.

Pradeu, T., Jaeger, S., and Vivier, E. (2013). The speed of change: towards a discontinuity theory of immunity? *Nat Rev Immunol 13*, 764–769.

Prashar, A., Ortiz, M.E., Lucarelli, S., Barker, E., Tabatabeiyazdi, Z., Shamoun, F., Raju, D., Antonescu, C., Guyard, C., and Terebiznik, M.R. (2018). Small Rho GTPases and the Effector VipA Mediate the Invasion of Epithelial Cells by Filamentous *Legionella pneumophila. Front Cell Infect Microbiol 8*, 133.

Principe, L., Tomao, P., and Visca, P. (2017). Legionellosis in the occupational setting. *Environ Res 152*, 485–495.

Protter, D.S.W., and Parker, R. (2016). Principles and Properties of Stress Granules. *Trends in Cell Biology 26*, 668–679.

Qian, Q., Zhou, H., Shu, T., Mu, J., Fang, Y., Xu, J., Li, T., Kong, J., Qiu, Y., and Zhou, X. (2020). The Capsid Protein of Semliki Forest Virus Antagonizes RNA Interference in Mammalian Cells. *J Virol 94*.

Qin, T., Zhou, H., Ren, H., and Liu, W. (2017). Distribution of Secretion Systems in the *Genus Legionella* and Its Correlation with Pathogenicity. *Front Microbiol 8*.

Qiu, J., and Luo, Z.-Q. (2017). Hijacking of the Host Ubiquitin Network by *Legionella pneumophila*. *Front Cell Infect Microbiol 7*.

Qiu, Y., Xu, Y., Zhang, Y., Zhou, H., Deng, Y.-Q., Li, X.-F., Miao, M., Zhang, Q., Zhong, B., Hu, Y., et al. (2017). Human Virus-Derived Small RNAs Can Confer Antiviral Immunity in Mammals. *Immunity 46*, 992-1004.e5.

Qiu, Y., Xu, Y., Zhang, Y., Zhou, H., Deng, Y.-Q., Li, X.-F., Miao, M., Zhang, Q., Zhong, B., Hu, Y., et al. (2018). Human Virus-Derived Small RNAs Can Confer Antiviral Immunity in Mammals. *Immunity 49*, 780–781.

Qiu, Y., Xu, Y.-P., Wang, M., Miao, M., Zhou, H., Xu, J., Kong, J., Zheng, D., Li, R.-T., Zhang, R.-R., et al. (2020). Flavivirus induces and antagonizes antiviral RNA interference in both mammals and mosquitoes. *Science Advances 6*, eaax7989.

Quévillon Huberdeau, M., Zeitler, D.M., Hauptmann, J., Bruckmann, A., Fressigné, L., Danner, J., Piquet, S., Strieder, N., Engelmann, J.C., Jannot, G., et al. (2017). Phosphorylation of Argonaute proteins affects mRNA binding and is essential for microRNA-guided gene silencing *in vivo*. *The EMBO Journal 36*, 2088–2106.

Quiat, D., and Olson, E.N. (2013). MicroRNAs in cardiovascular disease: from pathogenesis to prevention and treatment. *J Clin Invest 123*, 11–18.

Rajaram, M.V.S., Ni, B., Morris, J.D., Brooks, M.N., Carlson, T.K., Bakthavachalu, B., Schoenberg, D.R., Torrelles, J.B., and Schlesinger, L.S. (2011). Mycobacterium tuberculosis lipomannan blocks TNF biosynthesis by regulating macrophage MAPK-activated protein kinase 2 (MK2) and microRNA miR-125b. *Proc Natl Acad Sci U S A 108*, 17408–17413.

Ray, S.K., Macoy, D.M., Kim, W.-Y., Lee, S.Y., and Kim, M.G. (2019). Role of RIN4 in Regulating PAMP-Triggered Immunity and Effector-Triggered Immunity: Current Status and Future Perspectives. *Mol Cells 42*, 503–511.

Rebane, A., and Akdis, C.A. (2013). MicroRNAs: Essential players in the regulation of inflammation. *Journal of Allergy and Clinical Immunology 132*, 15–26.

Rechnitzer, C., and Blom, J. (1989). Engulfment of the Philadelphia strain of *Legionella pneumophila* within pseudopod coils in human phagocytes. Comparison with other *Legionella* strains and species. *APMIS 97*, 105–114.

Reinhart, B.J., Slack, F.J., Basson, M., Pasquinelli, A.E., Bettinger, J.C., Rougvie, A.E., Horvitz, H.R., and Ruvkun, G. (2000). The 21-nucleotide let-7 RNA regulates developmental timing in *Caenorhabditis elegans*. *Nature 403*, 901–906.

Ren, B., Wang, X., Duan, J., and Ma, J. (2019). Rhizobial tRNA-derived small RNAs are signal molecules regulating plant nodulation. *Science 365*, 919–922.

Ricci, E.P., Limousin, T., Soto-Rifo, R., Rubilar, P.S., Decimo, D., and Ohlmann, T. (2013). miRNA repression of translation *in vitro* takes place during 43S ribosomal scanning. *Nucleic Acids Res 41*, 586–598.

van Rij, R.P., Saleh, M.-C., Berry, B., Foo, C., Houk, A., Antoniewski, C., and Andino, R. (2006). The RNA silencing endonuclease Argonaute 2 mediates specific antiviral immunity in *Drosophila melanogaste*r. *Genes Dev 20*, 2985–2995.

Rittig, M.G., Jagoda, J.C., Wilske, B., Murgia, R., Cinco, M., Repp, R., Burmester, G.R., and Krause, A. (1998). Coiling phagocytosis discriminates between different spirochetes and is enhanced by phorbol myristate acetate and granulocyte-macrophage colony-stimulating factor. *Infect Immun 66*, 627–635.

Roberts, T.L., Idris, A., Dunn, J.A., Kelly, G.M., Burnton, C.M., Hodgson, S., Hardy, L.L., Garceau, V., Sweet, M.J., Ross, I.L., et al. (2009). HIN-200 proteins regulate caspase activation in response to foreign cytoplasmic DNA. *Science 323*, 1057–1060.

Robertson, K.A., Hsieh, W.Y., Forster, T., Blanc, M., Lu, H., Crick, P.J., Yutuc, E., Watterson, S., Martin, K., Griffiths, S.J., et al. (2016). An Interferon Regulated MicroRNA Provides Broad Cell-Intrinsic Antiviral Immunity through Multihit Host-Directed Targeting of the Sterol Pathway. *PLoS Biol. 14*, e1002364.

Rodriguez, A., Vigorito, E., Clare, S., Warren, M.V., Couttet, P., Soond, D.R., van Dongen, S., Grocock, R.J., Das, P.P., Miska, E.A., et al. (2007). Requirement of bic/microRNA-155 for Normal Immune Function. *Science 316*, 608–611.

Rodriguez-Gil, A., Ritter, O., Hornung, J., Stekman, H., Krüger, M., Braun, T., Kremmer, E., Kracht, M., and Schmitz, M.L. (2016). HIPK family kinases bind and regulate the function of the CCR4-NOT complex. *Mol Biol Cell 27*, 1969–1980.

Rolando, M., Sanulli, S., Rusniok, C., Gomez-Valero, L., Bertholet, C., Sahr, T., Margueron, R., and Buchrieser, C. (2013). *Legionella pneumophila* effector RomA uniquely modifies host chromatin to repress gene expression and promote intracellular bacterial replication. *Cell Host Microbe 13*, 395–405.

Rothmeier, E., Pfaffinger, G., Hoffmann, C., Harrison, C.F., Grabmayr, H., Repnik, U., Hannemann, M., Wölke, S., Bausch, A., Griffiths, G., et al. (2013). Activation of Ran GTPase by a *Legionella* effector promotes microtubule polymerization, pathogen vacuole motility and infection. *PLoS Pathog 9*, e1003598.

Rouya, C., Siddiqui, N., Morita, M., Duchaine, T.F., Fabian, M.R., and Sonenberg, N. (2014). Human DDX6 effects miRNA-mediated gene silencing via direct binding to CNOT1. *RNA 20*, 1398–1409.

Roy, B.C., Subramaniam, D., Ahmed, I., Jala, V.R., Hester, C.M., Greiner, K.A., Haribabu, B., Anant, S., and Umar, S. (2015). Role of bacterial infection in the epigenetic regulation of Wnt antagonist WIF1 by PRC2 protein EZH2. *Oncogene 34*, 4519–4530.

Ruby, J.G., Jan, C.H., and Bartel, D.P. (2007). Intronic microRNA precursors that bypass Drosha processing. *Nature 448*, 83–86.

Ruda, V.M., Chandwani, R., Sehgal, A., Bogorad, R.L., Akinc, A., Charisse, K., Tarakhovsky, A., Novobrantseva, T.I., and Koteliansky, V. (2014). The roles of individual mammalian argonautes in RNA interference in vivo. *PLoS One 9*, e101749.

Rüdel, S., Wang, Y., Lenobel, R., Körner, R., Hsiao, H.-H., Urlaub, H., Patel, D., and Meister, G. (2011). Phosphorylation of human Argonaute proteins affects small RNA binding. *Nucleic Acids Res 39*, 2330–2343.

Sahu, S.K., Kumar, M., Chakraborty, S., Banerjee, S.K., Kumar, R., Gupta, P., Jana, K., Gupta, U.D., Ghosh, Z., Kundu, M., et al. (2017). MicroRNA 26a (miR-26a)/KLF4 and CREB-C/EBPβ regulate innate immune signaling, the polarization of macrophages and the trafficking of Mycobacterium tuberculosis to lysosomes during infection. *PLOS Pathogens 13*, e1006410.

Samuel, G.H., Wiley, M.R., Badawi, A., Adelman, Z.N., and Myles, K.M. (2016). Yellow fever virus capsid protein is a potent suppressor of RNA silencing that binds double-stranded RNA. *Proc Natl Acad Sci U S A 113*, 13863–13868.

Sandstrom, A., Mitchell, P.S., Goers, L., Mu, E.W., Lesser, C.F., and Vance, R.E. (2019). Functional degradation: A mechanism of NLRP1 inflammasome activation by diverse pathogen enzymes. *Science 364*.

Schirle, N.T., and MacRae, I.J. (2012). The Crystal Structure of Human Argonaute2. *Science 336*, 1037–1040.

Schlee, M., and Hartmann, G. (2016). Discriminating self from non-self in nucleic acid sensing. *Nat. Rev. Immunol. 16*, 566–580.

Schneider, W.M., Chevillotte, M.D., and Rice, C.M. (2014). Interferon-Stimulated Genes: A Complex Web of Host Defenses. *Annual Review of Immunology 32*, 513–545.

Schroeder, G.N. (2018). The Toolbox for Uncovering the Functions of Legionella Dot/Icm Type IVb Secretion System Effectors: Current State and Future Directions. *Front Cell Infect Microbiol 7*.

Schuelein, R., Spencer, H., Dagley, L.F., Li, P.F., Luo, L., Stow, J.L., Abraham, G., Naderer, T., Gomez-Valero, L., Buchrieser, C., et al. (2018). Targeting of RNA Polymerase II by a nuclear *Legionella pneumophila* Dot/Icm effector SnpL. *Cell Microbiol 20*, e12852.

Schulte, L.N., Eulalio, A., Mollenkopf, H.-J., Reinhardt, R., and Vogel, J. (2011). Analysis of the host microRNA response to *Salmonella* uncovers the control of major cytokines by the *let-7* family: MicroRNA and bacterial infection. *The EMBO Journal 30*, 1977–1989.

Schulte, L.N., Westermann, A.J., and Vogel, J. (2013). Differential activation and functional specialization of miR-146 and miR-155 in innate immune sensing. *Nucleic Acids Res. 41*, 542–553.

Schürmann, N., Trabuco, L.G., Bender, C., Russell, R.B., and Grimm, D. (2013). Molecular dissection of human Argonaute proteins by DNA shuffling. *Nat Struct Mol Biol 20*, 818–826.

Schuster, S., Miesen, P., and van Rij, R.P. (2019). Antiviral RNAi in Insects and Mammals: Parallels and Differences. *Viruses 11*.

Sebé-Pedrós, A., de Mendoza, A., Lang, B.F., Degnan, B.M., and Ruiz-Trillo, I. (2011). Unexpected repertoire of metazoan transcription factors in the unicellular holozoan Capsaspora owczarzaki. Mol *Biol Evol 28*, 1241–1254.

Segal, G., and Shuman, H.A. (1998). How is the intracellular fate of the *Legionella pneumophila* phagosome determined? Trends Microbiol *6*, 253–255.

Seo, J.-K., Wu, J., Lii, Y., Li, Y., and Jin, H. (2013). Contribution of Small RNA Pathway Components in Plant Immunity. *Mol Plant Microbe Interact 26*, 617–625.

Shapiro, J.S., Varble, A., Pham, A.M., and tenOever, B.R. (2010). Noncanonical cytoplasmic processing of viral microRNAs. *RNA 16*, 2068–2074.

Sheedy, F.J. (2015). Turning 21: Induction of miR-21 as a Key Switch in the Inflammatory Response. *Front. Immunol. 6*.

Sheedy, F.J., Palsson-McDermott, E., Hennessy, E.J., Martin, C., O'Leary, J.J., Ruan, Q., Johnson, D.S., Chen, Y., and O'Neill, L.A.J. (2010). Negative regulation of TLR4 via targeting of the proinflammatory tumor suppressor PDCD4 by the microRNA miR-21. *Nat. Immunol. 11*, 141–147.

Sheu-Gruttadauria, J., and MacRae, I.J. (2018). Phase transitions in the assembly and function of human miRISC. *Cell 173*, 946-957.e16.

Shim, H.K., Kim, J.Y., Kim, M.J., Sim, H.S., Park, D.W., Sohn, J.W., and Kim, M.J. (2009). *Legionella* lipoprotein activates toll-like receptor 2 and induces cytokine production and expression of costimulatory molecules in peritoneal macrophages. *Exp Mol Med 41*, 687–694.

Shin, S., Case, C.L., Archer, K.A., Nogueira, C.V., Kobayashi, K.S., Flavell, R.A., Roy, C.R., and Zamboni, D.S. (2008). Type IV Secretion-Dependent Activation of Host MAP Kinases Induces an Increased Proinflammatory Cytokine Response to *Legionella pneumophila. PLoS Pathog 4*, e1000220.

Siddle, K.J., Tailleux, L., Deschamps, M., Loh, Y.-H.E., Deluen, C., Gicquel, B., Antoniewski, C., Barreiro, L.B., Farinelli, L., and Quintana-Murci, L. (2015). Bacterial Infection Drives the Expression Dynamics of microRNAs and Their isomiRs. *PLOS Genetics 11*, e1005064.

Silwal, P., Kim, Y.S., Basu, J., and Jo, E.-K. (2020). The roles of microRNAs in regulation of autophagy during bacterial infection. *Seminars in Cell & Developmental Biology 101*, 51–58.

Singh, N., Shirdel, E.A., Waldron, L., Zhang, R.-H., Jurisica, I., and Comelli, E.M. (2011). The *Murine Caecal* MicroRNA Signature Depends on the Presence of the Endogenous Microbiota. *Int J Biol Sci 8*, 171–186.

Snyder, D.T., Hedges, J.F., and Jutila, M.A. (2017). Getting "Inside" Type I IFNs: Type I IFNs in Intracellular Bacterial Infections. *J Immunol Res 2017*, 9361802.

Sohn, K.H., Segonzac, C., Rallapalli, G., Sarris, P.F., Woo, J.Y., Williams, S.J., Newman, T.E., Paek, K.H., Kobe, B., and Jones, J.D.G. (2014). The nuclear immune receptor RPS4 is required for RRS1SLH1-dependent constitutive defense activation in *Arabidopsis thaliana*. *PLoS Genet 10*, e1004655.

Soldan, S.S., Plassmeyer, M.L., Matukonis, M.K., and González-Scarano, F. (2005). La Crosse Virus Nonstructural Protein NSs Counteracts the Effects of Short Interfering RNA. *Journal of Virology 79*, 234–244.

Speir, M., Vince, J.E., and Naderer, T. (2014). Programmed cell death in *Legionella* infection. *Future Microbiol 9*, 107–118.

Spörri, R., Joller, N., Albers, U., Hilbi, H., and Oxenius, A. (2006). MyD88-dependent IFN-gamma production by NK cells is key for control of *Legionella pneumophila* infection. *J Immunol 176*, 6162–6171.

Stalder, L., Heusermann, W., Sokol, L., Trojer, D., Wirz, J., Hean, J., Fritzsche, A., Aeschimann, F., Pfanzagl, V., Basselet, P., et al. (2013). The rough endoplasmatic reticulum is a central nucleation site of siRNA-mediated RNA silencing. *EMBO J 32*, 1115–1127.

Stoecklin, G., and Kedersha, N. (2013). Relationship of GW/P-Bodies with Stress Granules. *Adv Exp Med Biol*, 197–211.

Stone, B.J., and Abu Kwaik, Y. (1998). Expression of multiple pili by *Legionella pneumophila*: identification and characterization of a type IV pilin gene and its role in adherence to mammalian and protozoan cells. *Infect Immun 66*, 1768–1775.

Subtelny, A.O., Eichhorn, S.W., Chen, G.R., Sive, H., and Bartel, D.P. (2014). Poly(A)-tail profiling reveals an embryonic switch in translational control. *Nature 508*, 66–71.

Sullivan, C.S., and Ganem, D. (2005). A virus-encoded inhibitor that blocks RNA interference in mammalian cells. *J. Virol*. *79*, 7371–7379.

Sullivan, C.S., Grundhoff, A.T., Tevethia, S., Pipas, J.M., and Ganem, D. (2005). SV40-encoded microRNAs regulate viral gene expression and reduce susceptibility to cytotoxic T cells. *Nature 435*, 682–686.

Sun, H., Kamanova, J., Lara-Tejero, M., and Galán, J.E. (2018). *Salmonella* stimulates pro-inflammatory signaling through p21-activated kinases bypassing innate immune receptors. *Nat Microbiol 3*, 1122–1130.

Sun, Y., Zhu, Y.-X., Balint-Kurti, P.J., and Wang, G.-F. (2020). Fine-Tuning Immunity: Players and Regulators for Plant NLRs. *Trends Plant Sci 25*, 695–713.

Sundaram, K., Miller, D.P., Kumar, A., Teng, Y., Sayed, M., Mu, J., Lei, C., Sriwastva, M.K., Zhang, L., Yan, J., et al. (2019). Plant-Derived Exosomal Nanoparticles Inhibit Pathogenicity of Porphyromonas gingivalis. *IScience 21*, 308–327.

Sunkavalli, U., Aguilar, C., Silva, R.J., Sharan, M., Cruz, A.R., Tawk, C., Maudet, C., Mano, M., and Eulalio, A. (2017). Analysis of host microRNA function uncovers a role for miR-29b-2-5p in *Shigella* capture by filopodia. *PLoS Pathog 13*.

Taganov, K.D., Boldin, M.P., Chang, K.-J., and Baltimore, D. (2006). NF-kappaB-dependent induction of microRNA miR-146, an inhibitor targeted to signaling proteins of innate immune responses. *Proc. Natl. Acad. Sci. U.S.A. 103*, 12481–12486.

Takahashi, T., and Ui-Tei, K. (2020). Mutual Regulation of RNA Silencing and the IFN Response as an Antiviral Defense System in Mammalian Cells. I*nt J Mol Sci 21*.

Takahashi, T., Nakano, Y., Onomoto, K., Murakami, F., Komori, C., Suzuki, Y., Yoneyama, M., and Ui-Tei, K. (2018). LGP2 virus sensor regulates gene expression network mediated by TRBP-bound microRNAs. *Nucleic Acids Res. 46*, 9134–9147.

Takahashi, T., Nakano, Y., Onomoto, K., Yoneyama, M., and Ui-Tei, K. (2020). LGP2 virus sensor enhances apoptosis by upregulating apoptosis regulatory genes through TRBP-bound miRNAs during viral infection. *Nucleic Acids Res 48*, 1494–1507.

Takimoto, K., Wakiyama, M., and Yokoyama, S. (2009). Mammalian GW182 contains multiple Argonaute-binding sites and functions in microRNA-mediated translational repression. *RNA 15*, 1078–1089.

Tam, O.H., Aravin, A.A., Stein, P., Girard, A., Murchison, E.P., Cheloufi, S., Hodges, E., Anger, M., Sachidanandam, R., Schultz, R.M., et al. (2008). Pseudogene-derived small interfering RNAs regulate gene expression in mouse oocytes. *Nature 453*, 534–538.

Tang, B., Xiao, B., Liu, Z., Li, N., Zhu, E.-D., Li, B.-S., Xie, Q.-H., Zhuang, Y., Zou, Q.-M., and Mao, X.-H. (2010). Identification of MyD88 as a novel target of miR-155, involved in negative regulation of *Helicobacter pylori*-induced inflammation. *FEBS Lett 584*, 1481–1486.

Tarver, J.E., Donoghue, P.C.J., and Peterson, K.J. (2012). Do miRNAs have a deep evolutionary history? *BioEssays 34*, 857–866.

Taylor, M., Ross, K., and Bentham, R. (2009). *Legionella, protozoa*, and biofilms: interactions within complex microbial systems. *Microb Ecol 58*, 538–547.

Teng, G., Wang, W., Dai, Y., Wang, S., Chu, Y., and Li, J. (2013). Let-7b Is Involved in the Inflammation and Immune Responses Associated with *Helicobacter pylori* Infection by Targeting Toll-Like Receptor 4. *PLoS One 8*.

Teng, Y., Miao, J., Shen, X., Yang, X., Wang, X., Ren, L., Wang, X., Chen, J., Li, J., Chen, S., et al. (2016). The modulation of MiR-155 and MiR-23a manipulates *Klebsiella pneumoniae* Adhesion on Human pulmonary Epithelial cells via Integrin α5β1 Signaling. Sci Rep *6*.

Teng, Y., Ren, Y., Sayed, M., Hu, X., Lei, C., Kumar, A., Hutchins, E., Mu, J., Deng, Z., Luo, C., et al. (2018). Plant-Derived Exosomal MicroRNAs Shape the Gut Microbiota. *Cell Host Microbe 24*, 637-652.e8.

Thai, T.-H., Calado, D.P., Casola, S., Ansel, K.M., Xiao, C., Xue, Y., Murphy, A., Frendewey, D., Valenzuela, D., Kutok, J.L. (2007). Regulation of the Germinal Center Response by MicroRNA-155. *Science 316*, 604–608.

Thi, E.P., and Reiner, N.E. (2012). Phosphatidylinositol 3-kinases and their roles in phagosome maturation. *J Leukoc Biol 92*, 553–566.

Thiébeauld, O., Meenu Singla Rastogi, Magali Charvin, Fan Yang, Dominique Pontier, Cécile Pouzet, Laure Bapaume, Delase Amesefe, Guangyong Li, Laurent Deslandes (2021). A bacterial GW-effector directly targets Arabidopsis Argonaute 1 to suppress PAMP-triggered immunity and cause disease. *BioRxiv.*

Thiébeauld, O., Singla Rastogi, M., Charvin, M., Perez Quintero, A., and Navarro, L. The Pseudomonas syringae type III effector HopT1-1 is sensed by host cells, which leads to a potent NLR-mediated immune signaling activation. *In Preparation.*

Thurston, T.L.M., Wandel, M.P., von Muhlinen, N., Foeglein, Á., and Randow, F. (2012). Galectin-8 targets damaged vesicles for autophagy to defend cells against bacterial invasion. Nature *482*, 414–418.

Tili, E., Michaille, J.-J., Cimino, A., Costinean, S., Dumitru, C.D., Adair, B., Fabbri, M., Alder, H., Liu, C.G., Calin, G.A., et al. (2007). Modulation of miR-155 and miR-125b levels following lipopolysaccharide/TNF-alpha stimulation and their possible roles in regulating the response to endotoxin shock. *J. Immunol. 179*, 5082–5089.

Till, S., Lejeune, E., Thermann, R., Bortfeld, M., Hothorn, M., Enderle, D., Heinrich, C., Hentze, M.W., and Ladurner, A.G. (2007). A conserved motif in Argonaute-interacting proteins mediates functional interactions through the Argonaute PIWI domain. *Nature Structural & Molecular Biology 14*, 897–903.

Tilney, L.G., Harb, O.S., Connelly, P.S., Robinson, C.G., and Roy, C.R. (2001). How the parasitic bacterium *Legionella pneumophila* modifies its phagosome and transforms it into rough ER: implications for conversion of plasma membrane to the ER membrane. *J Cell Sci 114*, 4637–4650.

Ting, J.P.Y., Duncan, J.A., and Lei, Y. (2010). How the noninflammasome NLRs function in the innate immune system. *Science 327*, 286–290.

Trobaugh, D.W., and Klimstra, W.B. (2017). MicroRNA Regulation of RNA Virus Replication and Pathogenesis. *Trends Mol Med 23*, 80–93.

Udeshi, N.D., Svinkina, T., Mertins, P., Kuhn, E., Mani, D.R., Qiao, J.W., and Carr, S.A. (2013). Refined preparation and use of anti-diglycine remnant (K-ε-GG) antibody enables routine quantification of 10,000s of ubiquitination sites in single proteomics experiments. *Mol Cell Proteomics 12*, 825–831.

Umbach, J.L., Kramer, M.F., Jurak, I., Karnowski, H.W., Coen, D.M., and Cullen, B.R. (2008). MicroRNAs expressed by herpes simplex virus 1 during latent infection regulate viral mRNAs. *Nature 454*, 780–783.

UniProt Consortium, T. (2018). UniProt: the universal protein knowledgebase. *Nucleic Acids Res 46*, 2699.

Urwyler, S., Nyfeler, Y., Ragaz, C., Lee, H., Mueller, L.N., Aebersold, R., and Hilbi, H. (2009). Proteome analysis of *Legionella vacuoles* purified by magnetic immunoseparation reveals secretory and endosomal GTPases. *Traffic 10*, 76–87.

Vaccaro, L., Izquierdo, F., Magnet, A., Hurtado, C., Salinas, M.B., Gomes, T.S., Angulo, S., Salso, S., Pelaez, J., Tejeda, M.I., et al. (2016). First Case of Legionnaire's Disease Caused by *Legionella anisa* in Spain and the Limitations on the Diagnosis of *Legionella* non-pneumophila Infections. *PLoS One 11*, e0159726.

Valencia-Gallardo, C.M., Carayol, N., and Tran Van Nhieu, G. (2015). Cytoskeletal mechanics during *Shigella* invasion and dissemination in epithelial cells. *Cell Microbiol 17*, 174–182.

Vance, R.E., Isberg, R.R., and Portnoy, D.A. (2009). Patterns of pathogenesis: discrimination of pathogenic and nonpathogenic microbes by the innate immune system. *Cell Host Microbe 6*, 10–21.

Varble, A., Chua, M.A., Perez, J.T., Manicassamy, B., García-Sastre, A., and tenOever, B.R. (2010). Engineered RNA viral synthesis of microRNAs. *Proc. Natl. Acad. Sci. U.S.A. 107*, 11519–11524.

van der Veen, A.G., Maillard, P.V., Schmidt, J.M., Lee, S.A., Deddouche-Grass, S., Borg, A., Kjær, S., Snijders, A.P., and Reis e Sousa, C. (2018). The RIG-I-like receptor LGP2 inhibits Dicer-dependent processing of long double-stranded RNA and blocks RNA interference in mammalian cells. *EMBO J. 37*.

Venkataraman, C., Haack, B.J., Bondada, S., and Abu Kwaik, Y. (1997). Identification of a Gal/GalNAc lectin in the protozoan *Hartmannella vermiformis* as a potential receptor for attachment and invasion by the Legionnaires' disease bacterium. *J Exp Med 186*, 537–547.

Verma, S., Mohapatra, G., Ahmad, S.M., Rana, S., Jain, S., Khalsa, J.K., and Srikanth, C.V. (2015). *Salmonella* Engages Host MicroRNAs To Modulate SUMOylation: a New Arsenal for Intracellular Survival. *Mol Cell Biol 35*, 2932–2946.

Vigorito, E., Perks, K.L., Abreu-Goodger, C., Bunting, S., Xiang, Z., Kohlhaas, S., Das, P.P., Miska, E.A., Rodriguez, A., Bradley, A., et al. (2007). microRNA-155 Regulates the Generation of Immunoglobulin Class-Switched Plasma Cells. *Immunity 27*, 847–859.

Vinzing, M., Eitel, J., Lippmann, J., Hocke, A.C., Zahlten, J., Slevogt, H., N′Guessan, P.D., Günther, S., Schmeck, B., Hippenstiel, S., et al. (2008). NAIP and Ipaf Control *Legionella pneumophila* Replication in Human Cells. *The Journal of Immunology 180*, 6808–6815.

Vogel, J.P., Andrews, H.L., Wong, S.K., and Isberg, R.R. (1998). Conjugative transfer by the virulence system of Legionella pneumophila. Science *279*, 873–876.

Voinnet, O., Pinto, Y.M., and Baulcombe, D.C. (1999). Suppression of gene silencing: A general strategy used by diverse DNA and RNA viruses of plants. *PNAS 96*, 14147–14152.

Vojtechova, Z., and Tachezy, R. (2018). The Role of miRNAs in Virus-Mediated Oncogenesis. *Int J Mol Sci 19*, 1217.

Wahle, E., and Winkler, G.S. (2013). RNA decay machines: deadenylation by the Ccr4-not and Pan2-Pan3 complexes. Biochim. *Biophys. Acta 1829*, 561–570.

Wakiyama, M., Takimoto, K., Ohara, O., and Yokoyama, S. (2007). Let-7 microRNA-mediated mRNA deadenylation and translational repression in a mammalian cell-free system. *Genes Dev. 21*, 1857–1862.

Wang, B., Li, S., Qi, H.H., Chowdhury, D., Shi, Y., and Novina, C.D. (2009). Distinct passenger strand and mRNA cleavage activities of human Argonaute proteins. *Nat Struct Mol Biol 16*, 1259–1266.

Wang, F., Liu, J., Zou, Y., Jiao, Y., Huang, Y., Fan, L., Li, X., Yu, H., He, C., Wei, W., et al. (2017). MicroRNA-143-3p, up-regulated in H. pylori-positive gastric cancer, suppresses tumor growth, migration and invasion by directly targeting AKT2. *Oncotarget 8*, 28711–28724.

Wang, M., Weiberg, A., Lin, F.-M., Thomma, B., Huang, H.-D., and Jin, H. (2016). Bidirectional cross-kingdom RNAi and fungal uptake of external RNAs confer plant protection. *Nat Plants 2*, 16151.

Wang, X.-H., Aliyari, R., Li, W.-X., Li, H.-W., Kim, K., Carthew, R., Atkinson, P., and Ding, S.-W. (2006a). RNA interference directs innate immunity against viruses in adult *Drosophila*. *Science 312*, 452–454.

Wang, X.-H., Aliyari, R., Li, W.-X., Li, H.-W., Kim, K., Carthew, R., Atkinson, P., and Ding, S.-W. (2006b). RNA Interference Directs Innate Immunity Against Viruses in Adult *Drosophila*. *Science 312*, 452–454.

Wang, Y., Kato, N., Jazag, A., Dharel, N., Otsuka, M., Taniguchi, H., Kawabe, T., and Omata, M. (2006c). Hepatitis C virus core protein is a potent inhibitor of RNA silencing-based antiviral response. *Gastroenterology 130*, 883–892.

Warburg, O. (1956). On the origin of cancer cells. *Science 123*, 309–314.

Watanabe, T., Totoki, Y., Toyoda, A., Kaneda, M., Kuramochi-Miyagawa, S., Obata, Y., Chiba, H., Kohara, Y., Kono, T., Nakano, T., et al. (2008). Endogenous siRNAs from naturally formed dsRNAs regulate transcripts in mouse oocytes. *Nature 453*, 539–543.

Watarai, M., Derre, I., Kirby, J., Growney, J.D., Dietrich, W.F., and Isberg, R.R. (2001). *Legionella pneumophila* Is Internalized by a Macropinocytotic Uptake Pathway Controlled by the Dot/Icm System and the Mouse Lgn1 Locus✪. *J Exp Med 194*, 1081–1096.

Watt, L.G., Crawshaw, S., Rhee, S.-J., Murphy, A.M., Canto, T., and Carr, J.P. (2020). The cucumber mosaic virus 1a protein regulates interactions between the 2b protein and ARGONAUTE 1 while maintaining the silencing suppressor activity of the 2b protein. *PLoS Pathog 16*, e1009125.

Weber, S., Wagner, M., and Hilbi, H. (2014). Live-cell imaging of phosphoinositide dynamics and membrane architecture during *Legionella* infection. *MBio 5*, e00839-00813.

Weick, E.-M., and Miska, E.A. (2014). piRNAs: from biogenesis to function. *Development 141*, 3458–3471.

Weiner, A., Mellouk, N., Lopez-Montero, N., Chang, Y.-Y., Souque, C., Schmitt, C., and Enninga, J. (2016). Macropinosomes are Key Players in Early *Shigella* Invasion and Vacuolar Escape in Epithelial Cells. *PLoS Pathog 12*, e1005602.

Welsh, C.T., Summersgill, J.T., and Miller, R.D. (2004). Increases in c-Jun N-Terminal Kinase/Stress-Activated Protein Kinase and p38 Activity in Monocyte-Derived Macrophages following the Uptake of *Legionella pneumophila. Infect Immun 72*, 1512–1518.

Wen, Q., Zhou, C., Xiong, W., Su, J., He, J., Zhang, S., Du, X., Liu, S., Wang, J., and Ma, L. (2016). MiR-381-3p Regulates the Antigen-Presenting Capability of Dendritic Cells and Represses Antituberculosis Cellular Immune Responses by Targeting CD1c. *The Journal of Immunology 197*, 580–589.

Wianny, F., and Zernicka-Goetz, M. (2000). Specific interference with gene function by double-stranded RNA in early mouse development. *Nat. Cell Biol. 2*, 70–75.

Wu, X., Valli, A., García, J.A., Zhou, X., and Cheng, X. (2019). The Tug-of-War between Plants and Viruses: Great Progress and Many Remaining Questions. *Viruses 11*.

Wu, X.-Y., Fan, W.-D., Fang, R., and Wu, G.-F. (2014). Regulation of microRNA-155 in endothelial inflammation by targeting nuclear factor (NF)-κB P65. *J Cell Biochem 115*, 1928–1936.

Wu, Z., Lu, H., Sheng, J., and Li, L. (2012). Inductive microRNA-21 impairs anti-mycobacterial responses by targeting IL-12 and Bcl-2. *FEBS Lett 586*, 2459–2467.

Xu, H., Yang, J., Gao, W., Li, L., Li, P., Zhang, L., Gong, Y.-N., Peng, X., Xi, J.J., Chen, S., et al. (2014). Innate immune sensing of bacterial modifications of Rho GTPases by the Pyrin inflammasome. *Nature 513*, 237–241.

Xu, J., Kong, J., Lyu, B., Wang, X., Qian, Q., Zhou, X., and Qiu, Y. (2021). The Capsid Protein of *Rubella* Virus Antagonizes RNA Interference in Mammalian Cells. *Viruses 13*.

Xu, L., Shen, X., Bryan, A., Banga, S., Swanson, M.S., and Luo, Z.-Q. (2010). Inhibition of host vacuolar H+-ATPase activity by a *Legionella pneumophila* effector. *PLoS Pathog 6*, e1000822.

Xu, Y.-P., Qiu, Y., Zhang, B., Chen, G., Chen, Q., Wang, M., Mo, F., Xu, J., Wu, J., Zhang, R.-R., et al. (2019). *Zika* virus infection induces RNAi-mediated antiviral immunity in human neural progenitors and brain organoids. *Cell Res. 29*, 265–273.

Yamashita, A., Chang, T.-C., Yamashita, Y., Zhu, W., Zhong, Z., Chen, C.-Y.A., and Shyu, A.-B. (2005). Concerted action of poly(A) nucleases and decapping enzyme in mammalian mRNA turnover. *Nat Struct Mol Biol 12*, 1054–1063.

Yang, J.-S., Maurin, T., Robine, N., Rasmussen, K.D., Jeffrey, K.L., Chandwani, R., Papapetrou, E.P., Sadelain, M., O'Carroll, D., and Lai, E.C. (2010). Conserved vertebrate mir-451 provides a platform for Dicer-independent, Ago2-mediated microRNA biogenesis. *Proc Natl Acad Sci U S A 107*, 15163–15168.

Yang, S., Tutton, S., Pierce, E., and Yoon, K. (2001). Specific double-stranded RNA interference in undifferentiated mouse embryonic stem cells. *Mol. Cell. Biol. 21*, 7807–7816.

Yao, B., Li, S., Jung, H.M., Lian, S.L., Abadal, G.X., Han, F., Fritzler, M.J., and Chan, E.K.L. (2011). Divergent GW182 functional domains in the regulation of translational silencing. *Nucleic Acids Res 39*, 2534–2547.

Ye, X., Huang, N., Liu, Y., Paroo, Z., Huerta, C., Li, P., Chen, S., Liu, Q., and Zhang, H. (2011). Structure of C3PO and Mechanism of Human RISC Activation. *Nat Struct Mol Biol 18*, 650–657.

Yi, H., Park, J., Ha, M., Lim, J., Chang, H., and Kim, V.N. (2018). PABP Cooperates with the CCR4-NOT Complex to Promote mRNA Deadenylation and Block Precocious Decay. *Mol Cell 70*, 1081-1088.e5.

Yi, R., Qin, Y., Macara, I.G., and Cullen, B.R. (2003). Exportin-5 mediates the nuclear export of pre-microRNAs and short hairpin RNAs. *Genes Dev. 17*, 3011–3016.

Yu, N.Y., Wagner, J.R., Laird, M.R., Melli, G., Rey, S., Lo, R., Dao, P., Sahinalp, S.C., Ester, M., Foster, L.J., *et al.* (2010). PSORTb 3.0: improved protein subcellular localization prediction with refined localization subcategories and predictive capabilities for all prokaryotes. *Bioinformatics 26*, 1608–1615.

Yu, V.L., Plouffe, J.F., Pastoris, M.C., Stout, J.E., Schousboe, M., Widmer, A., Summersgill, J., File, T., Heath, C.M., Paterson, D.L., *et al.* (2002). Distribution of *Legionella* species and serogroups isolated by culture in patients with sporadic community-acquired legionellosis: an international collaborative survey. *J Infect Dis 186*, 127–128.

Yuan, M., Ngou, B.P.M., Ding, P., and Xin, X.-F. (2021a). PTI-ETI crosstalk: an integrative view of plant immunity. *Curr Opin Plant Biol 62*, 102030.

Yuan, M., Jiang, Z., Bi, G., Nomura, K., Liu, M., Wang, Y., Cai, B., Zhou, J.-M., He, S.Y., and Xin, X.-F. (2021b). Pattern-recognition receptors are required for NLR-mediated plant immunity. *Nature 592*, 105–109.

Yue, J.-X., Meyers, B.C., Chen, J.-Q., Tian, D., and Yang, S. (2012). Tracing the origin and evolutionary history of plant nucleotide-binding site-leucine-rich repeat (NBS-LRR) genes. *New Phytol 193*, 1049–1063.

Zamboni, D.S., Kobayashi, K.S., Kohlsdorf, T., Ogura, Y., Long, E.M., Vance, R.E., Kuida, K., Mariathasan, S., Dixit, V.M., Flavell, R.A., et al. (2006). The Birc1e cytosolic pattern-recognition receptor contributes to the detection and control of *Legionella pneumophila* infection. *Nat Immunol 7*, 318–325.

Zekri, L., Kuzuoğlu-Öztürk, D., and Izaurralde, E. (2013). GW182 proteins cause PABP dissociation from silenced miRNA targets in the absence of deadenylation. *EMBO J. 32*, 1052–1065.

Zeng, J., Gupta, V.K., Jiang, Y., Yang, B., Gong, L., and Zhu, H. (2019). Cross-Kingdom Small RNAs among Animals, Plants and Microbes. *Cells 8*, 371.

Zhan, S., Wang, Y., and Chen, X. (2020). RNA virus-encoded microRNAs: biogenesis, functions and perspectives on application. *ExRNA 2*, 15.

Zhang, H., Kolb, F.A., Jaskiewicz, L., Westhof, E., and Filipowicz, W. (2004). Single Processing Center Models for Human Dicer and Bacterial RNase III. *Cell 118*, 57–68.

Zhang, H., Ehrenkaufer, G.M., Pompey, J.M., Hackney, J.A., and Singh, U. (2008). Small RNAs with 5'-polyphosphate termini associate with a Piwi-related protein and regulate gene expression in the single-celled eukaryote *Entamoeba histolytica*. *PLoS Pathog 4*, e1000219.

Zhang, H., Pompey, J.M., and Singh, U. (2011). RNA interference in *Entamoeba histolytica*: implications for parasite biology and gene silencing. *Future Microbiol 6*, 103–117.

Zhang, Q., Lenardo, M.J., and Baltimore, D. (2017). 30 Years of NF-κB: A Blossoming of Relevance to Human Pathobiology. *Cell 168*, 37–57.

Zhang, T., Yu, J., Zhang, Y., Li, L., Chen, Y., Li, D., Liu, F., Zhang, C.-Y., Gu, H., and Zen, K. (2014). *Salmonella enterica serovar enteritidis* modulates intestinal epithelial miR-128 levels to decrease macrophage recruitment via macrophage colony-stimulating factor. *J. Infect. Dis. 209*, 2000–2011.

Zhang, X., Yuan, Y.-R., Pei, Y., Lin, S.-S., Tuschl, T., Patel, D.J., and Chua, N.-H. (2006). Cucumber mosaic virus-encoded 2b suppressor inhibits Arabidopsis Argonaute1 cleavage activity to counter plant defense. *Genes Dev 20*, 3255–3268.

Zhang, Y., Li, Z., Ye, Z., Xu, Y., Wang, B., Wang, C., Dai, Y., Lu, J., Lu, B., Zhang, W., et al. (2020). The activation of antiviral RNA interference not only exists in neural progenitor cells but also in somatic cells in mammals. *Emerg Microbes Infect 9*, 1580–1589.

Zhao, C., Zhou, Z., Zhang, T., Liu, F., Zhang, C.-Y., Zen, K., and Gu, H. (2017). *Salmonella* small RNA fragment Sal-1 facilitates bacterial survival in infected cells via suppressing iNOS induction in a microRNA manner. *Sci Rep 7*, 1–11.

Zhou, H., Huang, X., Cui, H., Luo, X., Tang, Y., Chen, S., Wu, L., and Shen, N. (2010). miR-155 and its star-form partner miR-155* cooperatively regulate type I interferon production by human plasmacytoid dendritic cells. *Blood 116*, 5885–5894.

Zhou, X., Li, X., and Wu, M. (2018). miRNAs reshape immunity and inflammatory responses in bacterial infection. *Signal Transduct Target Ther 3*.

Zielezinski, A., and Karlowski, W.M. (2015). Integrative data analysis indicates an intrinsic disordered domain character of Argonaute-binding motifs. *Bioinformatics 31*, 332–339.

Zielezinski, A., and Karlowski, W.M. (2017). Identification and Analysis of WG/GW ARGONAUTE-Binding Domains. *Plant Argonaute Proteins* 241–256.

Zipprich, J.T., Bhattacharyya, S., Mathys, H., and Filipowicz, W. (2009). Importance of the C-terminal domain of the human GW182 protein TNRC6C for translational repression. *RNA 15*, 781–793.

Zwack, E.E., Snyder, A.G., Wynosky-Dolfi, M.A., Ruthel, G., Philip, N.H., Marketon, M.M., Francis, M.S., Bliska, J.B., and Brodsky, I.E. (2015). Inflammasome activation in response to the *Yersinia* type III secretion system requires hyperinjection of translocon proteins YopB and YopD. *MBio 6*, e02095-02014.

Zwack, E.E., Feeley, E.M., Burton, A.R., Hu, B., Yamamoto, M., Kanneganti, T.-D., Bliska, J.B., Coers, J., and Brodsky, I.E. (2017). Guanylate Binding Proteins Regulate Inflammasome Activation in Response to Hyperinjected *Yersinia* Translocon Components. *Infect Immun 85*.

ANNEX

Pathogen	Protein	Average of W-Scores
Acinetobacter baumannii	RTX toxin	22.3
Bartonella henselae	BepB	6.8
Bordetella pertussis	Pertussis toxin S1 (PT)	12.5
Burkholderia pseudomallei	BapA	10.5
Chlamydia trachomatis	Tarp	21.8
Clostridium difficile	CdtB	9.8
Enterobacter aerogenes	Hcp1	15.3
Enterobacter cloacae	Hcp1	8.9
Enterococcus faecalis	SalA	11.7
Escherichia coli O157:H7	NleH1	10.0
Helicobacter pylori	VacA	14.9
Klebsiella pneumoniae	S-type pyocin	23.5
Legionella pneumophila	Lpp1439 (LegK1)	13.5
Legionella pneumophila	Lpp2474	9.1
Listeria monocytogenes	Listeriolysin O (LLO)	17.7
Mycobacterium tuberculosis	RipA	17.7
Mycobacterium tuberculosis	RpfB	14.8
Neisseria meningitidis B	Ribonuclease HI	18.9
Proteus mirabilis	Autotransporteur	28.4
Pseudomonas aeruginosa	ExoY	7.8
Pseudomonas aeruginosa	Hcp1	10.2
Shigella flexneri	IpgD	6.8
Staphylococcus aureus	α-hemolysin (HLA)	17.5
Stenotrophomonas maltophilia	Autotransporteur	11.4
Yersinia pestis	YopM	9.0

Table S2.1. Scores of predicted W-motifs on a selection of bacterial candidate proteins.
The Wsearch score average of the predicted W-motifs from each human bacterial protein was determined using the animal (AGO-Animals) matrice of the Wsearch algorithm (Zielezinski and Karlowski, 2015, 2017). Wsearch uses Position-specific Scoring Matrices (PSSM) to score Tryptophan (W)-containing sequences. This matrice reflects experimental observations that tryptophan residues are crucial for the interaction with Ago proteins, and that specific composition of W-surrounding residues is necessary for such interaction to occur (Zielezinski and Karlowski, 2015, 2017). The source sequence dataset consists of experimentally validated W-rich protein domains. The animal matrice was generated from the orthologous sequences of TNRC6A, TNRC6B, TNRC6C (TNRC6 from mammals), GAWKY (from fruit fly), AIN1, AIN2 (AIN from worm) and PrP.

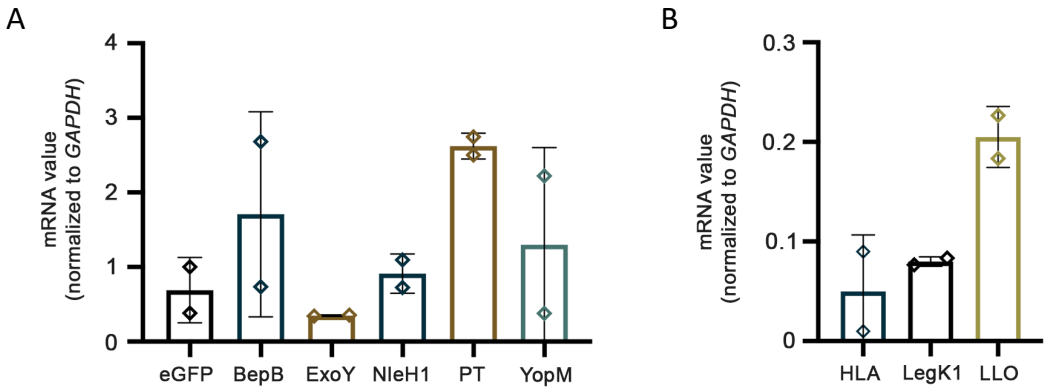

Figure S2.1. Transcript levels of each candidate bacterial genes after their transfection in human cells.
(A) mRNA value of candidate bacterial genes transiently expressed in human cells. HeLa cells were transfected with plasmid expressing each candidate bacterial gene or the control eGFP. After 48h, total RNAs were extracted from the transfected cells, and the mRNA value for each of the indicated candidate genes were determined by RT-qPCR. The data represent absolute values that were normalized to the absolute value of the constitutively expressed *GAPDH* gene. Error bars indicate the standard deviations (SD) from duplicate experiments. **(B)** As in (A) excepts that low expressed candidate bacterial genes are shown in the same graph.

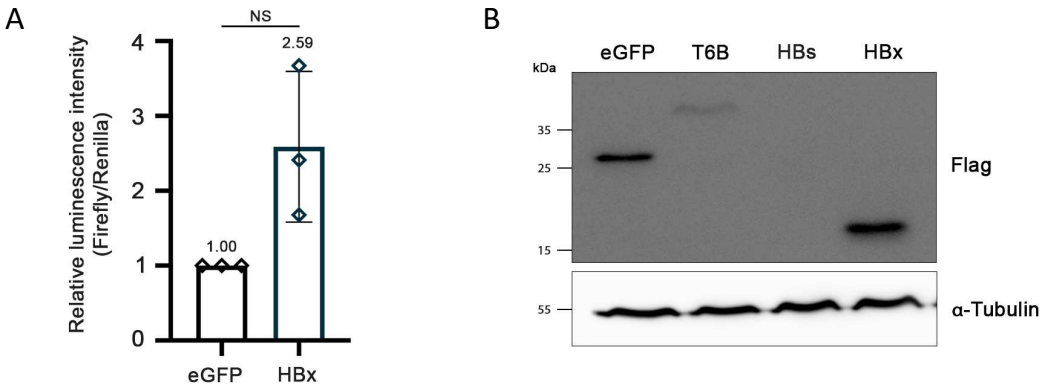

Figure S2.2. The VSR HBx suppresses siRNA-directed silencing of the CXCR4-2p reporter system in HeLa cells.
(A) Luciferase-based siRNA report assay in the presence of the VSR HBx in HeLa cells. HeLa cells were co-transfected with expression vectors for *firefly luciferase*, *renilla luciferase*, CXCR4 siRNA duplexes and vectors expressing either HBx or eGFP. The luciferase activity was measured at 48h post-transfection. The luminescence intensity of Firefly luciferase relative to the one of Renilla was calculated and further normalized to the eGFP condition. Error bars indicate the standard deviations (SD) from three independent experiments. P-values were calculated using unpaired student t-test. NS, not significant. **(B)** Both the control eGFP and the HBx proteins are detected in HeLa cells by immunoblot. HeLa cells were transiently transfected with vectors expressing either Flag-eGFP, Flag-T6B or 3xFlag-HBx constructs and samples were collected at 48 hours after transfection. The protein levels were determined by Western Blot analysis using anti-Flag antibodies. α-Tubulin was used as a loading control. The results shown are representative of three independent experiments.

Matrice / Name	AGO-Animals		SD-GW182	
	Motif	W-score	Motif	W-score
W41	NDNDSPGAWNNNQG	11.56	DSPGAWNNN	6.87
W283	DVWSTG	-0.15	VWSTGR	-0.97
W293	LWGD	1.93	LWG	3.96
W473	LWLVA	-6.48	LWLVAELST	-0.67

Table S2.2. Wsearch scores of W-motifs present in the LegK1 protein sequence.
The score of each predicted W-motif of LegK1 protein sequence was determined using either the animal (AGO-Animals) or GW182 (Silencing Domain (SD)-GW182) matrices from the Wsearch algorithm (Zielezinski and Karlowski, 2015, 2017). Wsearch uses Position-specific Scoring Matrices (PSSM) to score Tryptophan (W)-containing sequences. These matrices reflect experimental observations that tryptophan residues are crucial for the interaction with Ago proteins, and that specific composition of W-surrounding residues is necessary for such interaction to occur (Zielezinski and Karlowski, 2015, 2017). The source sequence dataset consists of experimentally validated W-rich protein domains. The animal matrix was generated from the orthologous sequences of TNRC6A, TNRC6B, TNRC6C (TNRC6 from mammals), GAWKY (from fruit fly), AIN1, AIN2 (AIN from worm) and PrP, while the GW182 matrice is based on the orthologous sequences of TNRC6A, TNRC6B, TNRC6C, GAWKY, 8x4Wmer and 4x4Wmer (synthetic).

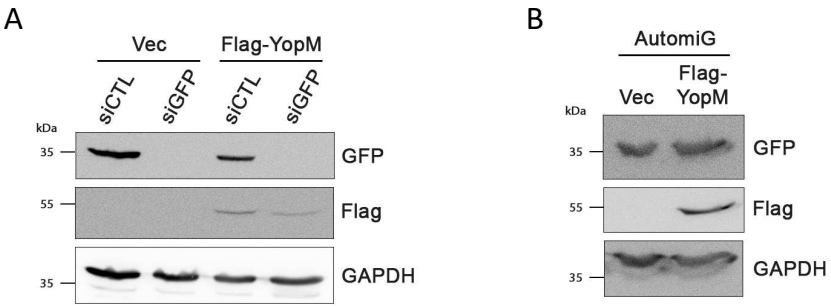

Figure S2.3. YopM does not suppress RNAi.
(A) *eGFP*-based siRNA silencing reporter assay in the presence of YopM. HEK293T cells were co-transfected with vectors expressing eGFP, *GFP* RNA duplexes (siGFP) or AllStars negative control siRNAs (siCTL) and empty vector pFlag-HA (Vec) or vector expressing Flag-HA-YopM recombinant protein. At 48h post-transfection, cell lysates were subjected to Western Blot analysis using indicated antibodies. GAPDH was used as a loading control. The results shown are representative of three independent experiments. **(B)** AutomiG silencing reporter assay in the presence of YopM. HEK293T cells were co-transfected with AutomiG vector and empty vector pFlag-HA (Vec) or Flag-HA-YopM recombinant protein. At 48h post-transfection, cell lysates were subjected to Western Blot analysis using indicated antibodies. GAPDH was used as a loading control. The results shown are representative of three independent experiments.

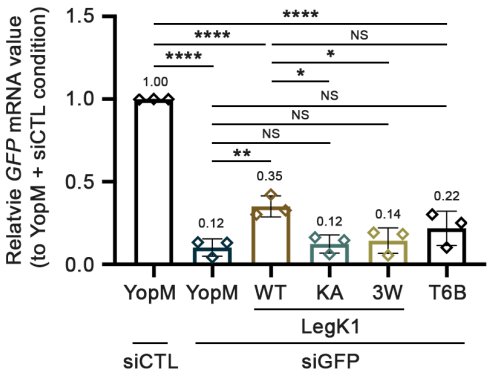

Figure S2.4. The predicted Ago-binding platform of LegK1 dampens siRNA-directed destabilization of *eGFP* mRNAs from the *eGFP*-based siRNA silencing reporter assay.

Fold change of *eGFP* mRNA accumulation levels on *eGFP*-based siRNA silencing assay in the presence of either LegK1 WT, kinase-dead or the triple W-motif mutants. HEK293T cells were co-transfected with expression vectors for eGFP, *GFP* RNA duplexes (siGFP) or AllStars negative control siRNAs (siCTL) and vector expressing Flag-HA-YopM, 2xFlag-HA-LegK1 (WT), 2xFlag-HA-LegK1-KA (kinase dead), 2xFlag-HA-LegK1-3W (three W-motifs mutant) or Flag-HA-T6B recombinant proteins. At 48h post-transfection, total RNAs were extracted from the transfected cells and subjected to RT-qPCR. The *eGFP* mRNA values are relative to the *GAPDH* mRNA values and further normalized to the YopM control condition (with siCTL). P-values were calculated using ordinary one-way ANOVA (Dunnett's multiple comparisons test). *; *P*< 0.05, **; P< 0,005, ***; *P*< 0.001, ****; *P*< 0.0001, NS, not significant.

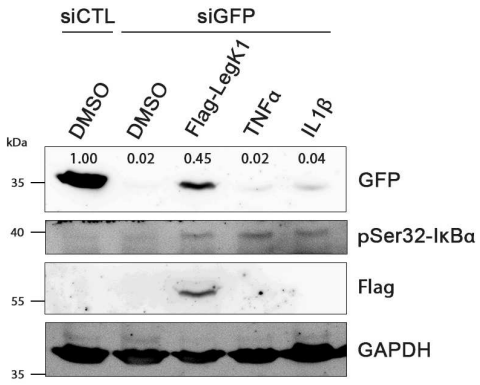

Figure S2.5. TNFα and IL1β treatments do not alter siRNA-guided gene silencing activity.
eGFP-based siRNA silencing reporter assay in HEK293T cell line treated with TNFα or IL1β. The HEK293T cell line was co-transfected with vectors expressing *eGFP*, *GFP* RNA duplexes (siGFP) or AllStars negative control siRNAs (siCTL) and the empty vector p2xFlag or vector expressing 2xFlag-HA-LegK1. Cells were treated for 1h with 10 ng/ml of TNFα or for 4h with 20 ng/µl of IL1β or DMSO, as negative control. At 48h post-transfection, cell lysates were subjected to Western Blot analysis with indicated antibodies. The phosphorylation of the serine 32 of IκB-α was used as a marker for the activation of the NF-κB signaling and GAPDH as a loading control. The eGFP protein levels are relative to the ones of GAPDH and further normalized to the YopM control condition (with siCTL). The relative values are indicated at the top of the GFP immunoblot. Quantification was carried out using the ImageJ software. The results shown are representative of three independent experiments.

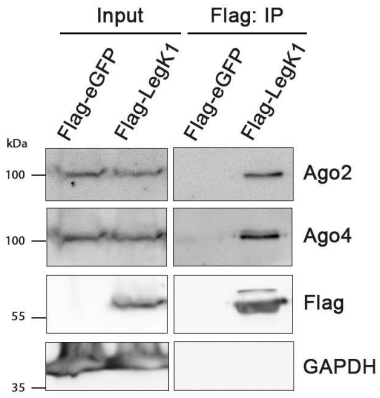

Figure S2.6. LegK1 interacts with human Ago4 in HEK293T cells.
Co-immunoprecipitation of LegK1 in human cells. HEK293T cells were transfected with vector expressing Flag-eGFP or 2xFlag-HA-LegK1 (WT). At 48h post-transfection, cells were lysed and proteins were immunoprecipitated using an anti-Flag antibody. Total cell lysates (input) and the immunoprecipitates were analyzed by Western blot using indicated antibodies. GAPDH was used as a loading control. The results shown are representative of one experiment.

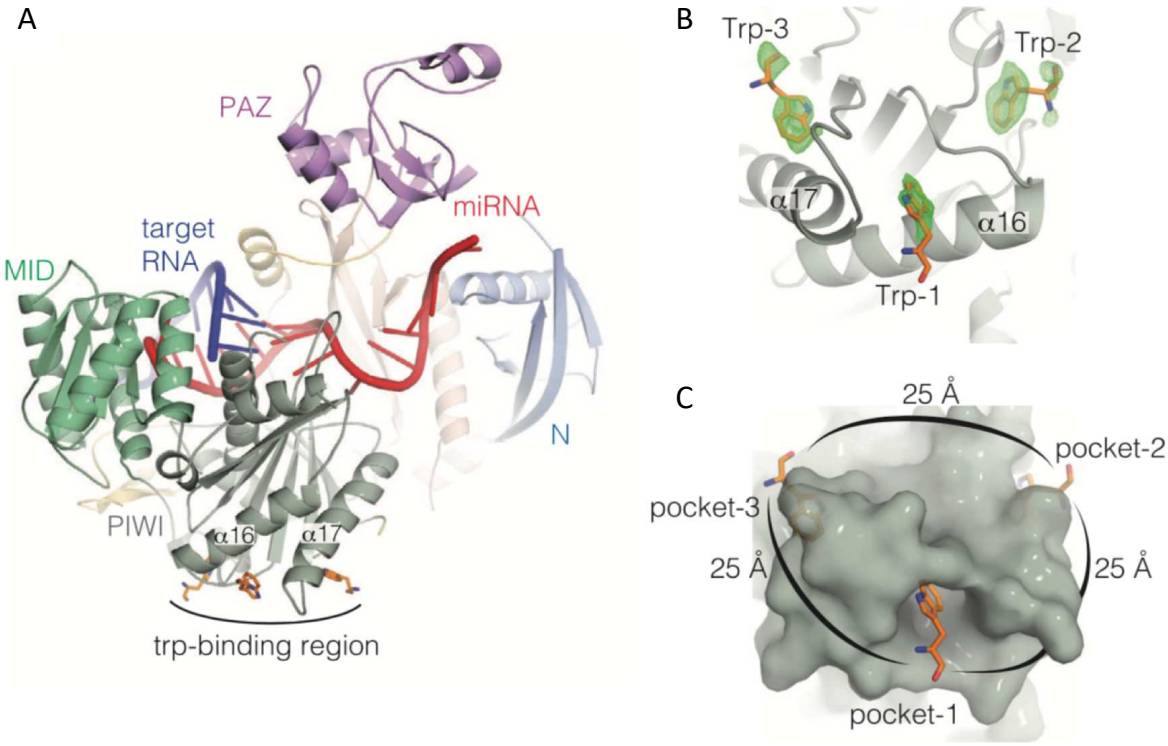

Figure S2.7. Positions of the W-binding pockets in the structure of human Ago2.
(A) Schematic structure of human Ago2 illustrating the position of the W-binding regions in the PIWI domain of Ago2. **(B)** Close up view of the W-binding region depicting the three W-binding pockets. Fo-Fc tryptophan omit map, contoured at 2.5 σ, (green mesh) shows well-ordered indole side chains of three linked tryptophan molecules. **(C)** Surface representation of the W-binding regions illustrating the three W-binding pockets (pockets-1-3). The approximative distances between adjacent pockets are indicated by curved lines. Derived from Sheu Gruttadauria and MacRae, 2018.

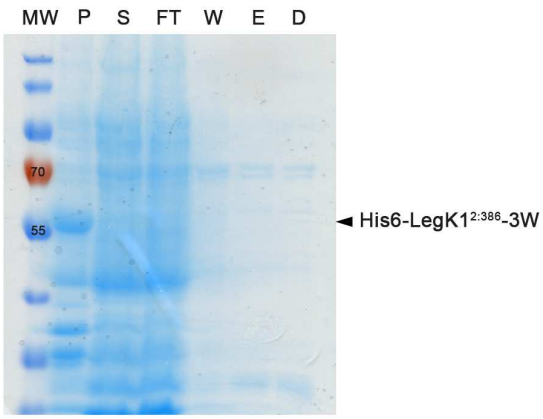

Figure S2.8. Coomassie Blue stained analytical SDS-PAGE showing expression of the LegK1-3W recombinant protein in *E. coli*.
His-LegK1-3W (a.a. 2:386) recombinant protein expression in *E. coli* strain BL21(DE3) codon plus were induced with IPTG, followed by overnight growth. Bacterial cells were collected by centrifugation, resuspended and lysed by sonication. Lysate was clarified by high-speed centrifugation in order to separate the pellet (P) from the supernatant (S). The supernatant was incubated with resin for 2h, subsequently the flow-through was removed (FT). The protein-bound resin was washed (W) and proteins were eluted from the beads (E). Excess imidazole was removed by overnight dialysis (D).

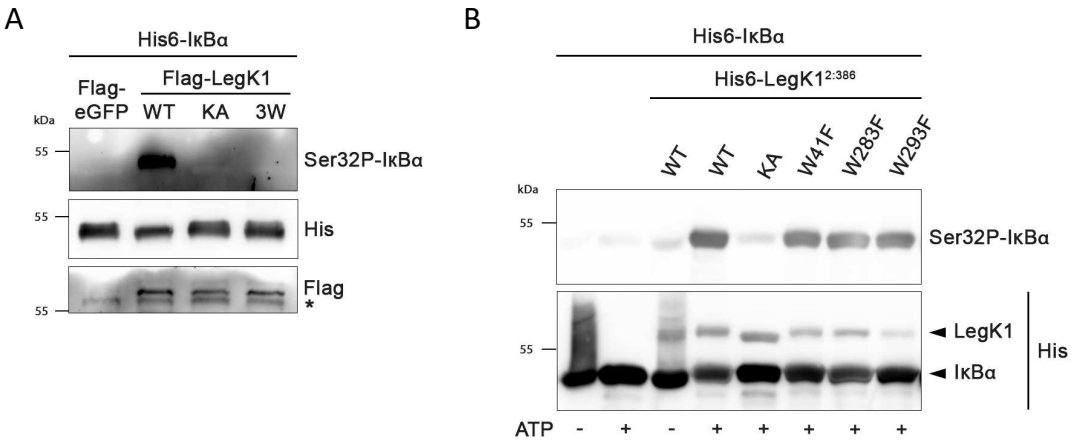

Figure S2.9. Mutations in the three W-motifs of LegK1 abolish its catalytic activity, while single mutations in the W-motif of LegK1 do not alter its catalytic activity.

(A) Kinase assay in the presence of LegK1 mutants. HEK293T cells were co-transfected with expression vectors for *eGFP*, 2xFlag-HA-LegK1 (WT), 2xFlag-HA-LegK1-KA (kinase-dead mutant) or 2xFlag-HA-LegK1-3W (three putative W-motifs mutant). At 48h post-transfection, cells were lysed and subjected to a Flag immunoprecipitation. The resulting immunoprecipitates were incubated with purified His6-IκBα recombinant protein. The phosphorylation of the serine 32 of IκBα was analyzed by Western blot using a specific antibody. GAPDH was used as a loading control. The results shown are representative of two independent experiments. **(B)** *In vitro* kinase assay in the presence of LegK1 mutants. His6-LegK1-WT, KA (kinase-dead mutant), -W41F, -W283F, -W293F (a.a. 2:386) were incubated in the presence or absence of ATP and His6-IκBα. The phosphorylation of the serine 32 of IκBα was analyzed by Western blot using a specific antibody. GAPDH was used as a loading control. The results shown are representative of three independent experiments.

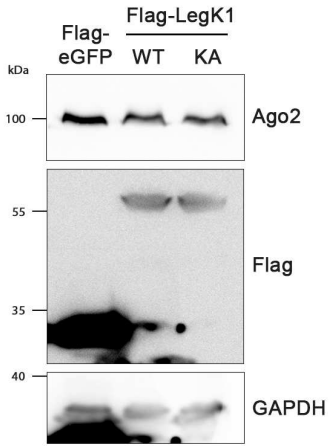

Figure S2.10. HeLa cells expressing LegK1 wild-type or kinase-dead mutant (used for mass spectrometry analyses).
HeLa cells were transfected with vectors expressing Flag-HA-eGFP, 2xFlag-HA-LegK1 or 2xFlag-HA-LegK1-KA (kinase-dead mutant). At 24h post-transfection, total cell were lysed (input) and were analyzed by Western blot using indicated antibodies. GAPDH was used as a loading control. The shown is representative of five independent experiments.

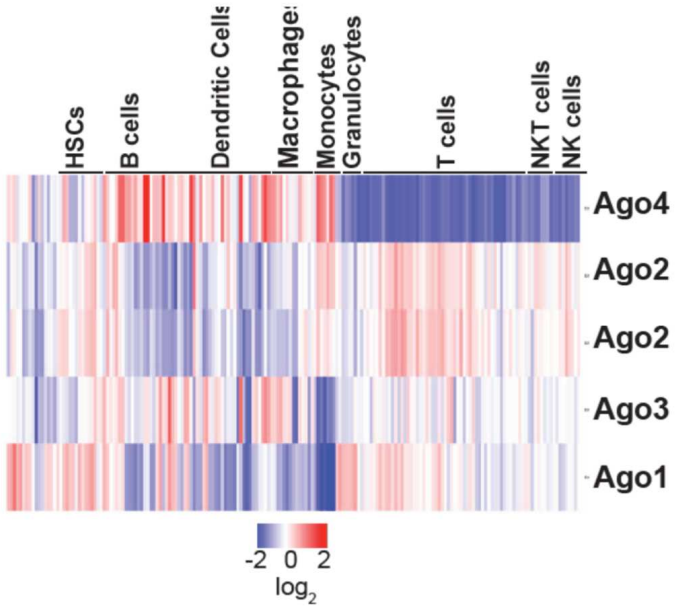

Figure S2.11. *Ago4* transcripts are abundant in innate immune cells.
Heatmap of *Ago1*, *Ago2*, *Ago3* and *Ago4* transcript levels in indicated immune cell types, obtained from www.immgen.org. Color scale is z-score. Two different microarray probes against Ago2 were used. Derived from Adiliaghdam *et al*., 2020.

A

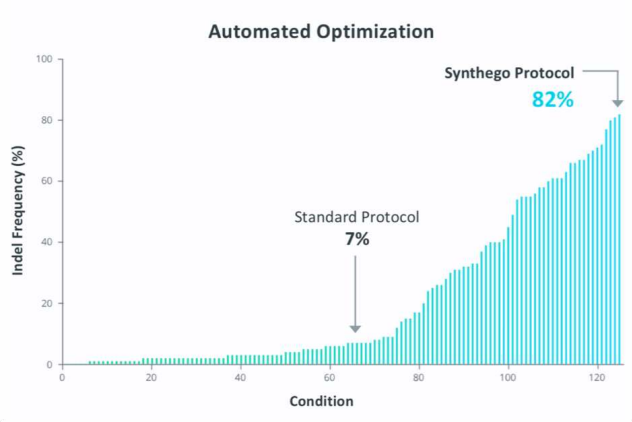

B

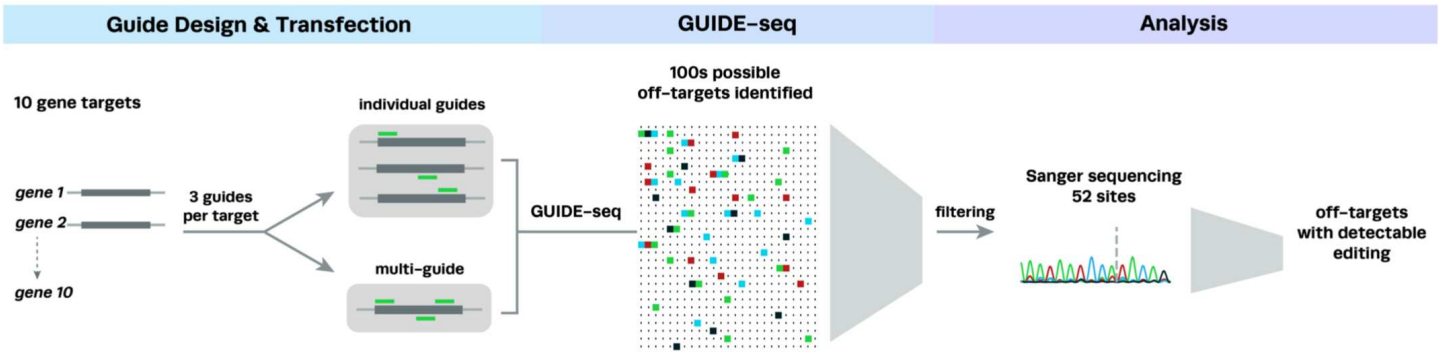

C

D

Figure S2.12. Characterization of THP-1 *ago2*$^{-/-}$ and *ago4*$^{-/-}$ cell lines from CRISPR/Cas9-based knockout pools.
(A) Histogram showing the optimized efficiency of THP-1 cell line transfection protocol from Synthego. The indel frequency includes all detected sequences that are different from wild-type, such as insertions or deletions present in the sample, to estimate the editing efficiency 3 days post-transfection. Derived from https://www.synthego.com/platforms. **(B)** Strategy employed by Synthego to obtain CRISPR/Cas9-based Knockout cell pools. Derived from https://www.synthego.com/platforms. **(C-D)** RNA sequencing analysis from *ago2* $^{-/-}$ **(C)** and *ago4* $^{-/-}$ **(D)** THP-1 cell lines isolated from THP-1 CRISPR/Cas9-based cell knockout pools. The analysis was obtained from Inference of CRISPR Edits (ICE) software of Synthego. The guide RNAs used for editing of the cell pools are indicated. The protospacer adjacent motif (PAM) is the short DNA sequence that follows the DNA region targeted for cleavage by the CRISPR/Cas9 system. The indel percentage includes all detected sequences that are different from wild-type, such as insertions or deletions. The Model Fit (R^2) score corresponds to Pearson correlation coefficient (r) on the ICE linear regression. The Knockout-Score only includes sequences that have either a frameshift mutation or a fragment deletion of more than 21 bp.

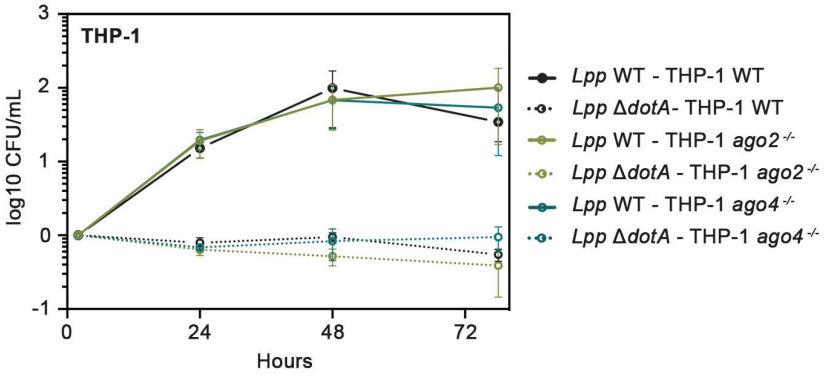

Figure S2.13. The intracellular replication of the wild-type and the *dotA*-defective *L. pneumophila* strains is not altered in human macrophages depleted of Ago2 or Ago4.

Intracellular replication of the WT or the *dotA*-deleted *L. pneumophila* strains in human macrophages depleted of Ago2 or Ago4. *WT, ago2*$^{-/-}$ and *ago4*$^{-/-}$ THP-1 cells were infected with WT (Paris) or Δ*dotA* mutant *L. pneumophila* strain at a multiplicity of infection (MOI) of 10. Intracellular growth was determined by recording the number of colony-forming units (CFU) through plating on buffered charcoal yeast extract (BCYE) agar at the indicated time points after infection. Results shown are log10 ratio CFU/mL, where CFU were normalized with the associated condition at 2h post-infection, corresponding to the entry of bacteria in the host cell. Error bars indicate the mean and standard error of mean (± SEM) from three independent experiments.